

INTEGRATED ECOTOXICOLOGICAL ASSESSMENT OF THE
ENGINEERED NANOPARTICLES, C₆₀ FULLERENES IN
DIFFERENT LIFE STAGES OF MARINE MUSCLE,
MYTILUS EDULIS

SHERAIN NASER AL-SUBIALI

Ph.D

2011

Dedicated to my husband

Copyright Statement

This copy of the thesis has been supplied on the condition that anyone who consults it is understood to recognise that its copyright rests with its author and that no quotation from the thesis and no information derived from it may be published without the author's prior consent.

**AN INTEGRATED ECOTOXICOLOGICAL ASSESSMENT OF THE
ENGINEERED NANOPARTICLES, C₆₀ FULLERENES IN
DIFFERENT LIFE STAGES OF MARINE MUSSELS, *MYTILUS
EDULIS***

by

SHERAIN NASER AL-SUBIAI

A thesis submitted to the University of Plymouth in
partial fulfilment for the degree of

DOCTOR OF PHILOSOPHY

School of Biomedical and Biological Sciences
Faculty of Science

July 2011

**AN INTEGRATED ECOTOXICOLOGICAL ASSESSMENT OF THE
ENGINEERED NANOPARTICLES, C₆₀ FULLERENES IN
DIFFERENT LIFE STAGES OF MARINE MUSSELS, *MYTILUS
EDULIS***

SHERAIN N. AL-SUBIAI

Abstract

Studies were undertaken to determine ecotoxicological effects of model manufactured or engineered nanoparticles (ENPs), either alone or in combination with a representative polycyclic aromatic hydrocarbon (i.e. PAHs: fluoranthene) at different levels of biological organisation (viz. biochemical, histological and behavioural levels) in a sentinel, widely distributed marine invertebrate species, *Mytilus edulis*. With the current and predicted levels of pollution in the marine and coastal environment, there is an urgent need to establish the potential effects of persistent and emerging contaminants which includes ENPs and PAHs, to protect human and environmental health. In this study, initially, it was aimed to optimise the induction of biotransformation enzyme P-450 as a robust biochemical tool and good progress (chapter 3) was made to standardise P-450 in mussel. Due to certain technical and logistic limitations however we could not apply measurement of P-450 as potential biochemical biomarkers in this species. The possibility of using glutathione levels instead in the cell-free component of haemolymph samples as an indicator of oxidative stress, in an analogous way to that used in mammals was evaluated (chapter 4). The evidence suggested that cell-free haemolymph samples collected from adductor muscle of *Mytilus edulis* may be significantly contaminated with intracellular contents of myocytes of this organ (i.e. adductor muscle) and adductor muscle tissue is more generally useful to determine glutathione system responses.

The validation study of different assays using copper as a relevant environmental contaminant (chapter 5) suggested the existence of clear relationships between genotoxic (as determined by induction of DNA strand breaks using the Comet assay) and higher level effects. The results further

suggested the feasibility of adoption of an integrated approach and robustness of selected biomarkers to evaluate short and long-term toxic effects of pollutants. A multiple biomarker approach was then used to determine the potential interactive effect of C₆₀ fullerenes in combination with fluoranthene. Where appropriate analytical tools (i.e. ICP-MS, GC-MS) were used to determine the levels of contaminant exposure and characterise the properties of the ENPs. The combined exposure of fluoranthene and C₆₀ fullerenes produced enhanced biological damage at approximately at an- "additive" rather than synergistic level, which appeared to be as a result of oxidative stress (chapter 6).

The final experiments were carried out in both the early and adult life stages to test the potential toxicity resulting from photochemical transformation of C₆₀ fullerenes in *Mytilus edulis* (chapter 7). In general, the results showed, for the first time, genotoxic and developmental impact of the photochemically transformed C₆₀ fullerenes at different life stages of marine mussel. Further research is required to identify the degraded products of C₆₀ fullerenes and to understand the mechanism by which fresh and aged C₆₀ fullerenes induces biological responses including oxidative stress and affect ecologically relevant aquatic organisms at different life stages. The thesis has taken the opportunity to discuss (chapter 8) the importance of applications of biological responses in hazard and risk assessment posed by anthropogenic chemicals in a broader context.

List of contents

List of contents	6
List of Figures	12
List of tables	17
List of Plates	18
1. Introduction.....	3
1.1 <i>Marine pollution</i>	3
1.2 <i>Manufactured or engineered nanoparticles (ENPs): a potential environmental pollutant</i>	5
1.2.1 <i>Types of engineered nanoparticles (ENPs)</i>	6
1.2.2 <i>Major fate of engineered nanoparticles (ENPs) in aquatic environment</i> ...	7
1.2.3 <i>Metabolic activation of engineered nanoparticles (ENPs)</i>	10
1.3 <i>Polycyclic Aromatic Hydrocarbons (PAHs) as environmental pollutant</i>	11
1.3.1 <i>Major fate of PAHs in aquatic environment</i>	16
1.3.2 <i>Metabolic activation of PAHs</i>	17
1.4 <i>Bivalve mussels, Mytilus edulis as a model species in ecotoxicology</i>	18
1.4.1 <i>Biotransformation enzymes in Mussels</i>	23
1.4.2 <i>Cytochrome P-450 induction</i>	25
1.5 <i>Oxidative stress</i>	27
1.6 <i>Antioxidant defence</i>	29
1.7 <i>Damage caused by the oxidative stress</i>	30
1.8 <i>Interactive effect of contaminants</i>	32
1.9 <i>Application of biomarkers in ecotoxicology</i>	34
1.9.1 <i>Glutathione level</i>	35
1.9.2 <i>Lipid peroxidation</i>	36
1.9.3 <i>Measurement of DNA strand breaks using the Comet Assay</i>	36
1.9.4 <i>Histopathology</i>	38
1.9.5 <i>Feeding Rate</i>	38
1.10 <i>Aims and objectives</i>	40
2.1 <i>Animals collection</i>	44
2.2 <i>Experimental design</i>	48
2.3 <i>Sample preparation</i>	48
2.3.1 <i>Collection of haemolymph samples</i>	48
2.3.2 <i>Preparation of adductor muscle extract</i>	49
2.4 <i>Determination of DNA strand breaks using the Comet assay</i>	51
2.4.1 <i>Cell viability</i>	51
2.4.2 <i>Slide preparation</i>	51

2.4.3	Cell lysis	52
2.4.4	Alkaline unwinding of DNA and electrophoresis	52
2.4.5	Neutralisation and staining	52
2.5	Determination of total glutathione level in adductor muscle extract	54
2.6	Histological preparation for different organs	54
2.6.1	Tissues processing and paraffin embedding	54
2.6.2	Slide staining	55
2.7	Clearance rate	58
2.8	Analysis of C_{60} in tissue samples	60
2.8.1	Tissue sample preparation for HPLC analysis	60
2.8.2	HPLC analysis	60
2.9	Statistical analyses	63
3.1	Introduction	65
3.2	Materials and Methods	70
3.2.1	Microsome preparation	70
3.2.2	Gel electrophoresis	72
3.2.2.1	Glass plates assemblage and gel preparation	72
3.2.2.2	Sample preparation	74
3.2.2.3	Fixing, staining and destaining	75
3.2.3	Measurement of P-450 by western blot assay	78
3.2.3.1	Blotting	78
3.2.3.2	Blocking	79
3.2.3.3	Incubation with primary antibody	79
3.2.3.4	Incubation with secondary antibody and development of colour	80
3.2.4	Measurement of 'cytochrome P-450 reductase' activity	80
3.2.5	Measurement of P-450 activity by bioluminescence assay	81
3.3	Results & Discussion	83
3.3.1	Standardizing the isolation of the microsomal fraction	83
3.3.2	Measurement of P-450 by western blot	87
3.3.3	Measurement of 'cytochrome P-450 reductase' activity	90
3.3.4	Measurement of P-450 activity by bioluminescence assay	93
3.4	Conclusion	98
4.1	Introduction	102
4.2.1	Animal collection and maintenance	104
4.2.2	Extraction of haemolymph	104
4.2.2.1	Extraction of haemolymph: method 1	104
4.2.2.2	Extraction of haemolymph: method 2	104

4.2.3	<i>Preparation of adductor muscle extract</i>	105
4.2.4	<i>Exposure of mussels to copper</i>	105
4.2.5	<i>Measurement of biochemical parameters</i>	106
4.2.5.1	<i>Measurement of total glutathione</i>	106
4.2.5.2	<i>Measurement of opine dehydrogenase (ODH) activity</i>	106
4.2.5.3	<i>Measurement of glutathione peroxidase (GPx) activity</i>	108
4.2.5.4	<i>Measurement of acetylcholinesterase (AChE) activity</i>	109
4.2.5.5	<i>Determination of protein</i>	109
4.3	<i>Results</i>	110
4.4	<i>Discussion</i>	120
	<i>Hypothesis: Copper induce responses at different levels of biological organisation</i> ..	126
	<i>Abstract</i>	126
5.1	<i>Introduction</i>	128
5.2	<i>Materials & Methods</i>	131
5.2.1	<i>Chemicals and animal collection</i>	131
5.2.2	<i>Experimental design</i>	131
5.2.3	<i>Sample preparation</i>	134
5.2.3.1	<i>Collection of haemolymph samples from M. edulis</i>	134
5.2.3.2	<i>Preparation of adductor muscle extract</i>	134
5.2.4	<i>Cell viability</i>	134
5.2.5	<i>Determination of DNA strand breaks using the Comet assay</i>	134
5.2.6	<i>Measurement of total glutathione</i>	135
5.2.7	<i>Determination of histopathological changes</i>	135
5.2.8	<i>Analysis of copper concentrations in the tissues</i>	135
5.2.9	<i>Determination of clearance rate</i>	136
5.2.10	<i>Statistical analyses</i>	137
5.3	<i>Results</i>	138
5.3.1	<i>Determination of MTC</i>	138
5.3.2	<i>Determination of clearance rate</i>	138
5.3.3	<i>Determination of DNA strand breaks</i>	140
5.3.4	<i>Total glutathione levels in adductor muscle</i>	140
5.3.5	<i>Determination of histopathological effects</i>	143
5.3.5.1	<i>Posterior adductor muscle</i>	143
5.3.5.2	<i>Gills</i>	143
5.3.5.3	<i>Digestive gland</i>	143
5.3.6	<i>Analysis of copper accumulation</i>	144
5.3.7	<i>Correlation between genotoxicity and higher level biological responses</i> ..	147

5.4	Discussion.....	149
5.5	Conclusions	154
	<i>Hypothesis: C₆₀ fullerenes enhances the toxic impact of a model PAHs, fluoranthene.</i>	155
	Abstract	156
6.1	Introduction	158
6.2	Materials & Methods	161
6.2.1	<i>Chemicals</i>	161
6.2.2	<i>Solution preparation</i>	161
6.2.3	<i>Animals collection and maintenance</i>	161
6.2.4	<i>Exposure condition</i>	162
6.2.4.1	<i>Fluoranthene exposure</i>	162
6.2.4.2	<i>C₆₀ exposure</i>	164
6.2.4.3	<i>Combined exposures of C₆₀ fullerenes and fluoranthene</i>	164
6.2.4.4	<i>Collection of haemolymph samples and preparation of adductor muscle extract</i> 167	
6.2.5	<i>Determination of DNA strand breaks using the Comet assay</i>	167
6.2.6	<i>DNA adduct analysis</i>	167
6.2.6.1	<i>DNA extraction</i>	167
6.2.6.2	<i>DNA ³²P-post labelling</i>	170
6.2.7	<i>Determination of total glutathione level in adductor muscle extract</i>	171
6.2.8	<i>Histological preparation for adductor muscle, digestive gland and gills</i> ...	171
6.2.9	<i>Clearance rate</i>	171
6.2.10	<i>Chemical analysis of fluoranthene and C₆₀ using analytical techniques</i> ...	172
6.2.10.1	<i>GC-analysis of fluoranthene in water samples</i>	172
6.2.10.2	<i>HPLC-analysis of C₆₀ in tissue samples</i>	174
6.2.11	<i>Statistical analyses</i>	174
6.3	Results.....	176
6.3.1	<i>Characterisation of C₆₀ nanoparticle</i>	176
6.3.2	<i>Determination of DNA damage</i>	178
6.3.2.1	<i>Combined exposures of C₆₀ and fluoranthene</i>	178
6.3.2.2	<i>Determination of DNA adduct</i>	179
	The main radioactive	179
6.3.3	<i>Determination of total Glutathione level in adductor muscle</i>	182
6.3.4	<i>Histological studies</i>	184
6.3.4.1	<i>Posterior adductor muscle</i>	184
6.3.4.2	<i>Gills</i>	184

6.3.4.3	<i>Digestive gland</i>	185
6.3.5	<i>C₆₀ accumulation</i>	187
6.3.5.1	<i>C₆₀ exposure</i>	187
6.3.5.2	<i>Combined exposures of C₆₀ and fluoranthene</i>	187
6.3.6	<i>Clearance rate (CR)</i>	191
6.4	<i>Discussion</i>	193
6.5	<i>Conclusions</i>	198
	<i>Hypothesis: C₆₀ fullerenes suspension in seawater exposed to sunlight are more toxic to marine mussel, Mytilus edulis.</i>	200
	<i>Abstract</i>	200
7.1	<i>Introduction</i>	202
7.2	<i>Materials and Methods</i>	205
7.2.1	<i>C₆₀ preparation</i>	205
7.2.2	<i>Mussels collection and experimental design</i>	206
7.2.3	<i>In vitro exposure</i>	206
7.2.4	<i>In vivo exposure</i>	216
7.2.4.1	<i>Collection of haemolymph samples and preparation of adductor muscle extract</i> 216	
7.2.4.2	<i>Determination of DNA strand breaks using the Comet assay in haemocytes</i>	217
7.2.4.3	<i>Determination of total glutathione level in adductor muscle extract</i>	217
7.2.4.5	<i>Histological preparation for adductor muscle, digestive gland and gills</i> 219	
7.2.4.6	<i>Clearance rate</i>	219
7.2.5	<i>HPLC-analysis of C₆₀ in tissue samples</i>	219
7.2.6	<i>C₆₀ characterisation</i>	220
7.2.6.1	<i>Dynamic Light Scattering (DLS) and zeta potential</i>	220
7.2.6.2	<i>Transmission electron microscopy (TEM) and energy-dispersive X-ray spectrometry (EDX)</i>	222
7.2.6.3	<i>Atomic force microscopy (AFM)</i>	225
7.2.6.4	<i>X-ray diffraction (XRD)</i>	228
7.2.8	<i>Statistical analyses</i>	229
7.3	<i>Results</i>	230
7.3.1	<i>C₆₀ characterisation</i>	230
7.3.2	<i>In vitro exposure</i>	235
7.3.2.1	<i>Determination of sperm viability by AFC</i>	235
7.3.2.2	<i>Sperm DNA damage assessment</i>	238
7.3.2.3	<i>Determination of fertilization success</i>	240
7.3.2.4	<i>Embryo development assessment</i>	240

7.3.3	<i>In vivo</i> exposure.....	244
7.3.3.1	Determination of DNA damage.....	244
7.3.3.2	Determination of total glutathione level in adductor muscle.....	246
7.3.3.3	Histological studies.....	246
7.3.3.4	C_{60} accumulation.....	250
7.3.3.5	Clearance rate (CR).....	253
7.4	Discussion.....	255
7.4.1	Studies with <i>in vitro</i> exposure of sperms.....	256
7.4.2	Studies with <i>in vivo</i> exposure of adult mussels.....	259
7.5	Conclusions.....	263
8.1	Discussion.....	265
8.1.1	Environmental pollution-current and future prospect.....	266
8.1.2	Environmental risk assessment (ERA).....	267
8.1.3	Validation and robustness of the biomarkers.....	270
8.1.4	Model organisms for biomarker responses.....	271
8.1.5	Application of integrated approach.....	273
	References.....	278

List of Figures

Chapter 1: Introduction

Fig. 1.1 A model of fate and transformations of ENPs in the environment (modified from Simonet and Valcárcel (2009)).	9
Fig. 1.2 Possible mechanisms of interaction of ENPs with cellular system leading to oxidative stress.	10
Fig. 1.3 Activation of B(a)P via dihydrodiol epoxide by cytochrome P-450 (Xue and Warshawsky 2005).	20
Fig. 1.4 Activation of B(a)P via formation of radical cations (Xue and Warshawsky 2005).	21
Fig. 1.5 Activation of B(a)P via formation of o-quinones catalyzed by dihydrodiol dehydrogenases (Xue and Warshawsky 2005).	22
Fig. 1.6 Biochemical indicators of oxidative stress and oxidative damage at the cellular level (adapted from Prof. Galloway, T).	39
Fig. 1.7 Thesis outline and research hypothesis tested in each experimental chapter.	42

Chapter 2: Materials and Methods

Fig. 2.1 Map of south-west, UK showing mussel collection sites at Cornwall. PQ = Port Quin; TS = Trebarwith Strand.	47
Fig. 2.2 Major steps involved in standard single cell gel electrophoresis (SCEG) or the Comet assay procedure.	53
Fig. 2.3 A standard curve for C_{60} analysis by HPLC using different concentrations ranging from 0.125 and 2.0 $mg\ l^{-1}$ using Elite C18.	62

Chapter 3: Optimisation of P-450 induction in *Mytilus edulis*

Fig. 3.1 Carbon monoxide difference spectra of digestive gland cytosolic/microsomal fraction. (A) dithionite-reduced sample. (B) The content of the sample cell was then saturated with CO, (C) the difference spectrum was calculated.	68
Fig. 3.2 P-420 levels in the digestive gland of <i>Mytilus edulis</i> . Exposure was only carried over days 4, 5 and 6. Data represent mean \pm S.E.	69
Fig. 3.3 Preparation of microsomal fraction from <i>Mytilus edulis</i> digestive gland using ultracentrifuge and freeze & thaw methods.	71
Fig. 3.4 Casting the gel. Slowly, the syringe was grabbed by thumb over the plunger and loaded with gel solution, by using small tip (5-200 μ l) connected to glass syringe and fixed to 5 cm length of tubing (1 mm diameter).	73
Fig. 3.5 Plot of the relative mobility of protein standards against the log of their molecular weight. Relative mobility, R_f , is the distance the protein has migrated from its point of origin.	77
Fig. 3.6 Conversion of luciferin-PFBE (P-450-Glo substrate) by P-450. CYP3A4 enzyme act on luminogenic luciferin-PFBE substrate to produce a luciferin product that generates light with luciferin detection reagent.	82
Fig. 3.7 Protein yield in the cytosolic and microsomal fractions of mussel digestive gland from differential centrifugation and freeze and thaw methods. The data shown are means \pm SE; n = 3. U = differential centrifugation; FT = freeze and thaw; U total = microsome + cytosol from differential centrifugation method; FT total = microsome + cytosol from freeze and thaw method.	86
Fig. 3.8 Purification of <i>Mytilus edulis</i> microsomes. SDS-PAGE analysis using 8% polyacrylamide-SDS gel. 1 and 2, microsomal fractions (15 and 30 μ l were loaded respectively), prepared by ultracentrifuge method. 3, molecular weight marker. 4 and 5,	

microsomal fractions (15 and 30 μ l were loaded respectively), prepared by freeze and thaw method. Dashed circle showing 54 kDa band.	88
Fig. 3.9 Dot blot test showing the efficiency of the western blot procedure and the binding of the primary antibody to the PVDF membrane (inset) by Ponceau S stain.....	89
Fig. 3.10 P-450 luminescence activity in digestive gland microsomal fraction with different volume of samples and incubation times; (A) 10 min, (B) 30 min and (C) 45 min.....	94
Fig. 3.11 P-450 luminescence activities in different dilution of digestive gland microsomal fraction.....	95
Fig. 3.12 P-450 luminescence in microsomal fraction of <i>Mytilus edulis</i> digestive gland following 3 days <i>in vivo</i> exposure to ASW, FC ₆₀ and AC ₆₀ (details available in chapter 7). (A) 2-fold dilution; (B) 10-fold dilution; (C) P-450 luminescence in 10-fold diluted sample calculated between 20-40 min. The data shown in panel (C) are means \pm S.E., n = 3. Bars with the same letters are not significantly different according to the multiple range test (LSD). ASW = aged seawater, FC ₆₀ = fresh C ₆₀ , AC ₆₀ = aged C ₆₀	97

Chapter 4: Validation and optimisation of total glutathione content in *Mytilus edulis*

Fig. 4.1 Relative opine dehydrogenase activity in extracts from posterior adductor muscle. Activities are expressed as percentages relative to the activity with lysine as substrate (i.e. lysopine dehydrogenase activity) for the same extract. The data shown are means \pm S.E., n = 4. In each case the activity in the absence of the amino acid substrate (1.5 ± 0.4 nmol NADH oxidised $\text{min}^{-1} \text{mg}^{-1}$ protein) was subtracted. Lysopine dehydrogenase activity was 27.2 ± 5.5 nmol NADH oxidised $\text{min}^{-1} \text{mg}^{-1}$ protein. Same letters denote significant differences between data sets.....	111
Fig. 4.2 Relationship between the glutathione content of cell-free haemolymph and lysopine dehydrogenase activity. The solid line is a linear regression, and the dashed lines represent 95% confidence limits. Each point represents an individual cell-free haemolymph sample; the error bars indicate the variability of the measurements (\pm S.E., n = 3).	112
Fig. 4.3 Relationship between the glutathione content of cell-free haemolymph and lysopine dehydrogenase activity in mussels either exposed to $40 \mu\text{g l}^{-1}$ Cu (O) or not (●). The lines show linear regressions derived from GLM analysis of the data where the model included the effects of LyDH ($P < 0.00005$) and the interaction between LyDH and Cu on total glutathione ($P = 0.0001$). The effect of Cu was omitted from the model because it was not significant (see text).....	116
Fig. 4.4 (A) relationship between the GPx activity and LyDH activity in cell-free haemolymph. (B) relationships between GPx and LyDH activities and the protein content of cell-free haemolymph; the solid line is a mutual best fit linear regression, and the dashed line is a mutual best fit non-linear regression (quadratic). (O) GPx and LyDH; (●) protein.	118
Fig. 4.5(A) relationship between AChE activity and LyDH activity in cell-free haemolymph from <i>Mytilus edulis</i> ; the solid line is a non-linear regression (rectangular hyperbola, two parameter; $P = 0.0004$). The Pearson product moment and Spearman rank correlation coefficients for AChE versus LyDH are 0.509 ($P = 0.0068$) and 0.537 ($P = 0.0062$), respectively. (B) relationship between AChE activity and the protein content of cell-free haemolymph; the solid line is a non-linear regression (logistic sigmoidal, three parameter). The Pearson product moment correlation coefficients for AChE versus protein and LyDH versus protein are 0.736 ($P < 0.0001$) and 0.711 ($P < 0.0001$), respectively.	119

Chapter 5: Validation of biochemical, histological and behavioural responses in *Mytilus edulis*

- Fig. 5.1 Flow chart illustrating integrated experimental design adopted in the study to evaluate genotoxicological, biochemical, structural and behavioural effects in *M. edulis*. AM = adductor muscle; DG = digestive gland; G = gills. 133
- Fig. 5.2 Clearance rates of *M. edulis* following 5 days *in vivo* exposure to copper. The values are means \pm S.E ($n = 4$). Different letters denote significant differences between data sets. 139
- Fig. 5.3 DNA damage in *Mytilus edulis* haemocytes following 5 days *in vivo* exposure to copper. Different letters denote significant differences between data sets. 141
- Fig. 5.4 Levels of total glutathione content in adductor muscle following 5 days *in vivo* exposure to copper. Different letters denote significant differences between data sets. 142
- Fig. 5.5 Light micrographs of sections (5-8 μm thickness, stained with H & E) through adductor muscle (A & B), gills (C & D) & digestive gland (E & F) of control and Cu-exposed mussels. (A, C & E) control; (B, D & F) exposed to $32 \mu\text{g l}^{-1}$. mc = myocytes; ct = connective tissue; dt = digestive tubule; fc = frontal cilia; lc = lateral cilia; ge = gill epithelium; dt = digestive tubules; N = necrosis; HI = haemocyte infiltration. Scale bar: 100 μm 145
- Fig. 5.6 Copper concentrations in adductor muscle, digestive gland and gills. Data are means \pm S.E.M., $n = 4$ mussel per treatment after 5 days of exposure. Different letters denote significant differences between data sets. 146
- Fig. 5.7 Linear regression analysis illustrating correlations for genotoxic effects with (A) total glutathione level, (B) Cu accumulation in gills and (C) clearance rate in *Mytilus edulis* following 5 d exposure to Cu. The solid line is a linear regression and the dashed lines represent 95% confidence limits. 148

Chapter 6: Interactive toxic effects of C_{60} fullerenes and fluoranthene in adult marine mussels, *Mytilus edulis*

- Fig. 6.1 Fluoranthene exposure experimental design. AM = adductor muscle; DG = digestive gland; G = gills. 163
- Fig. 6.2 C_{60} , fullerenes exposure experimental design. AM = adductor muscle; DG = digestive gland; G = gills. 165
- Fig. 6.3 Experimental design for C_{60} , fluoranthene & binary exposure of C_{60} + fluoranthene. AM = adductor muscle; DG = digestive gland; G = gills. 166
- Fig. 6.4 DNA purity and concentrations data from different tissues of *Mytilus edulis*. Highlighted number is DNA concentration in 2 μl of the sample. 169
- Fig. 6.5 Total ion current GC-MS chromatograms of standard compounds (1 = Phen d_{10} ; 2 = fluoranthene. 173
- Fig. 6.6 A standard curve for C_{60} (dissolved in toluene) using different concentrations dissolved in toluene ranging from 0.125 and 2 mg l^{-1} using (A) Elite C18 and (B) Plgel 5 μm 50 \AA . . 175
- Fig. 6.7 Representative of TEM image of C_{60} (inset) and histogram of C_{60} particles diameter determined by TEM. 177
- Fig. 6.8 Induction of DNA strand breaks, represented as %Tail DNA in *Mytilus edulis* haemocytes following 3 days *in vivo* exposure to: (A) fluoranthene (32, 56 and 100 $\mu\text{g l}^{-1}$); (B) C_{60} (0.1 and 1.0 mg l^{-1}); and (C) C_{60} + fluoranthene (0.1 mg l^{-1} C_{60} and 32 $\mu\text{g l}^{-1}$ fluoranthene). The values are mean \pm S.E. Bars with the same letters are not significantly different according to the multiple range test (LSD). 180
- Fig. 6.9 ^{32}P -post labelling analysis of DNA from cells exposed to C_{60} , fluoranthene and C_{60} + fluoranthene. DNA adduct profiles measured in digestive gland. Same results were obtained with gills and adductor muscle. 181
- Fig. 6.10 Total glutathione levels in the adductor muscle extract following 3 days *in vivo* exposure to: (A) C_{60} ; and (B) mixture of C_{60} + fluoranthene (0.1 mg l^{-1} C_{60} and 32 $\mu\text{g l}^{-1}$

	fluoranthene). The values are mean \pm S.E. Bars with the same letters are not significantly different according to the multiple range test (LSD).....	183
Fig. 6. 11	Light micrographs of sections through adductor muscle, gills & digestive gland of <i>M. edulis</i> showing histological structure of control and treated mussels stained with H & E at 5-8 μm thickness. (A, D & G) control; (B, E & H) exposed to C_{60} . (C, F & I) exposed to C_{60} + fluoranthene. mc = myocyte cell; si = sinus; dc = digestive cell; pbc = pyramidal basophilic secretory cell; dd = digestive diverticula; gf = gill filaments; fc = frontal cilia; lc = lateral cilia; ge = gill epithelium; dt = digestive tubules; at = atrophy; n = necrosis; hypo = hypoplasia; e = erosion. Scale bar: 100 μm	186
Fig. 6. 12	C_{60} concentrations in <i>Mytilus edulis</i> tissues. (A) accumulation of C_{60} in adductor muscle, digestive gland and gills after exposure to 0.1 & 1.0 mg l^{-1} . (B, C & D) accumulation of C_{60} after exposure to mixture of C_{60} + fluoranthene (adductor muscle, digestive gland and gills, respectively). Data are mean \pm S.E., n = 3 mussel per treatment after 3 days of exposure. Bars with the same letters are not significantly different according to the multiple range test (LSD).....	190
Fig. 6. 13	Clearance rate (represent as liter h^{-1}) in <i>Mytilus edulis</i> following 3 days <i>in vivo</i> exposure to: (A) C_{60} (0.1 & 1.0 mg l^{-1}), and (B) mixture of C_{60} + fluoranthene (0.1 mg l^{-1} C_{60} and 32 $\mu\text{g l}^{-1}$ fluoranthene). The values are mean \pm S.E. Bars with the same letters are not significantly different according to the multiple range test (LSD).....	192

Chapter 7: Investigation of the toxic effect of aged C_{60} in different life stages of *Mytilus edulis*

Fig. 7.1	Experimental design for <i>in vitro</i> sperm exposure and embryo development assay. ...	210
Fig. 7.2	Flow cytometry of control <i>Mytilus</i> spermatozoa stained with Sytox Green. Density plots for control samples of side versus forward light scatter; (a and b) side scatter versus green fluorescence in control samples (i.e. unexposed sperm); (c and d) sperm exposed to CuSO_4 (1.0 $\mu\text{g l}^{-1}$). An approximate region (R1) was placed around sperm identified from their light scattering properties (a and c) and then the data within R1 were re-analysed to observe the side scatter and Sytox Green fluorescence properties of the samples (b and d), and to discriminate between live and dead sperm.....	212
Fig. 7.3	The effect of unwinding time (A-C) negative control; (D-F) positive control- 50 μM H_2O_2 . (A & D) 20 min electrophoresis (B & E) 30 min electrophoresis (C & F) 40 min electrophoresis; n = 3.	215
Fig. 7.4	Transmission electron microscopy (TEM) micrograph showing (A) large aggregates of FC_{60} particles and (B) aggregates with smaller size particles of AC_{60}	231
Fig. 7.5	X-Ray diffraction pattern (diffractogram) of C_{60} crystallites powder.....	232
Fig. 7.6	EDX analysis of (A) fresh and (B) aged C_{60} -fullerene suspensions on the TEM grid..	233
Fig. 7.7	Characterisation of FC_{60} versus AC_{60} particles using AFM; (A) partially representative AFM image; (B) 3-D AFM image; (C) particle size-distribution.....	234
Fig. 7.8	Flow cytometric analysis of sperms viability following 2 h exposure to range of CuSO_4 concentrations (0.1-1.0 $\mu\text{g l}^{-1}$). (A) %dead sperm; (B) ratio of live to dead sperm.....	236
Fig. 7.9	The effect of <i>in vitro</i> exposure of different agents on sperm viability as determined by analytical flow cytometry (AFC). (A) Sperm exposed to different concentration (0.1, 0.5 and 1.0 $\mu\text{g l}^{-1}$) of CuSO_4 ; (B) sperm exposed to 1.0 mg l^{-1} FC_{60} and AC_{60} . Vertical bars represent mean \pm S.E percentage of dead cell counts from the total counts per second using AFC. Bars with the same letters are not significantly different according to the multiple range test (LSD).....	237
Fig. 7.10	DNA single strand breaks in sperm cells after 2 h exposure to (A) different concentrations of CuSO_4 and (B) 1.0 mg l^{-1} FC_{60} and AC_{60} fullerenes. Vertical bars represent mean \pm S.E. Bars with the same letters are not significantly different according to the multiple range test (LSD).....	239

- Fig. 7.11 The effect of FC_{60} and AC_{60} on fertilisation capability of sperm. Vertical bars represent mean \pm S.E percentage of dividing cells within 2 h from *in vitro* fertilisation of eggs by pre-exposed (2 h) sperm. Bars with the same letters are not significantly different according to the multiple range test (LSD)..... 241
- Fig. 7.12 Light-microscopy photographs of the typical early developmental stages of *Mytilus edulis* at 48 h (at 15 °C). (A) normal egg; (B) abnormal egg; (C) normal 'D-shell' stage; (D) delayed trochophore; (E) abnormal D-shell with protruding mantle; (F) cell debris and decaying materials..... 242
- Fig. 7.13 The effect of FC_{60} and AC_{60} fullerenes on embryo development. Vertical bars represent mean \pm S.E percentage of normal D-shell stage larvae after 48 h from *in vitro* fertilisation of eggs by pre-exposed sperm. Bars with the same letters are not significantly different according to the multiple range test (LSD). 243
- Fig. 7.14 DNA single strand breaks as determined by the comet assay in haemocytes of mussels after 3 days exposure and post-exposure to aged seawater (ASW), C_{60} in fresh seawater (FC_{60}) and aged seawater (AC_{60}). Vertical bars represent mean \pm S.E. percentage of tail DNA. Bars with the same letters are not significantly different according to the multiple range test (LSD)..... 245
- Fig. 7.15 Total glutathione levels in the adductor muscle extract following 3 days *in vivo* exposure and post-exposure in the clean seawater to ASW, FC_{60} and AC_{60} (1.0 mg l^{-1}). The values are mean \pm S.E. Bars with the same letters are not significantly different according to the multiple range test (LSD)..... 247
- Fig. 7.16 Light micrographs of sections through adductor muscle, digestive gland & gills showing histological structure of control and treated mussels stained with H & E at 5-8 μm thickness. (A, D & G) control; (B, E & H) exposed to FC_{60} . (C, F & I) exposed to AC_{60} . mc = myocyte; dt = digestive tubules; fc = frontal cilia; lc = lateral cilia; ge = gill epithelium; at = atrophy; n = necrosis; hypo = hypoplasia. Scale bar: 100 μm 249
- Fig. 7.17 C_{60} fullerenes accumulation pattern in *Mytilus edulis* tissues as analysed by (HPLC) (A) adductor muscle, (B) digestive gland and (C) gills after exposure to aged seawater (ASW), C_{60} fullerenes in fresh seawater (FC_{60}) and aged seawater (AC_{60}). Data are mean \pm S.E., $n = 5$. Bars with the same letters are not significantly different ($P < 0.05$) according to the multiple range test (LSD). White colour represent chromatogram peak at 3.5 min; grey colour represent chromatogram peak at 3.2 min. 252
- Fig. 7.18 Clearance rate in *Mytilus edulis* following 3 days *in vivo* exposure and post-exposure to ASW, FC_{60} and AC_{60} . The values are mean \pm S.E. Bars with the same letters are not significantly different ($P < 0.05$) according to the multiple range test (LSD). 254

Chapter 8: General discussion

- Fig. 8.1 The generalised diagram showing key steps in environmental risk assessment process for chemical substances (modified from IPCS (2001))..... 269
- Fig. 8.2 Diagram showing different levels of biological organisation at which potential toxic exposure could affect natural ecosystem. 275

List of tables

Chapter 1: Introduction

Table 1.1 Structures for the 16 priority PAHs in the environment, arrangement based on their molecular weight (USEPA 2001).....	13
Table 1.2 Major biotransformation enzymes in phase I and II.....	24
Table 1.3 Examples of field studies employing CYP 1A-immunoidentified protein as a biomarker for pollution.....	28
Table 1.4 Examples of different types of reactive oxygen species (ROS).....	31
Table 1.5 Examples of different types of antioxidant defence present in the cellular system.	31

Chapter 3: Optimisation of P-450 induction in *Mytilus edulis*

Table 3.1 Different assays to demonstrate cytochrome P-450 induction.....	66
Table 3.2 Stock buffer solution for SDS-PAGE.....	76
Table 3.3 Composition of separating and stacking gel.....	76
Table 3.4 Stock solutions for fixing, staining and destaining.....	76
Table 3.5 Protein recovery in microsomal fraction by using differential centrifugation and freeze and thaw methods, n =3.....	85
Table 3.6 Cytochrome P-450 reductase' activity. The data shown are means \pm S.E.; n = 3.	92

Chapter 4: Validation and optimisation of total glutathione content in *Mytilus edulis*

Table 4.1 Opine dehydrogenase (ODH) rate in fresh and frozen haemolymph samples.....	107
--	-----

Chapter 5: Validation of biochemical, histological and behavioural responses in *Mytilus edulis*

Table 5.1 Copper concentrations determined for exposure solutions at each of the nominal Cu concentrations. Data are means \pm S.E, n = 3.	132
---	-----

Chapter 7: Investigation of the toxic effect of aged C₆₀ in different life stages of *Mytilus edulis*

Table 7.1 Results showing characterisation measurements of fresh (F ₆₀) and aged C ₆₀ (AC ₆₀) using different techniques. Values are mean \pm S.E; n=3.	231
---	-----

List of Plates

Chapter 2: Materials and Methods

Plate 2.1 Mussel beds on rocky outcrops.	45
Plate 2.2 Photographic image of collection sites. (A) Port Quin; (B) Trebarwith Strand.	46
Plate 2.3 Extraction of haemolymph from the posterior adductor muscle.	49
Plate 2.4 The internal view of dissected adult <i>M.edulis</i> , showing position of the posterior adductor muscle and the internal organs.	50
Plate 2.5 Mussel dissection procedure (A-I) and dissected organs (J).	57
Plate 2.6 The Beckman Coulter counter (Z2) counting algal cells in seawater.	59
Plate 2.7 The HPLC UV-Vis spectrophotometer.	61

Chapter 6: Interactive toxic effects of C₆₀ fullerenes and fluoranthene in adult marine mussels, *Mytilus edulis*

Plate 6. 1 HPLC chromatogram results.(A-D): C ₆₀ standard; (F-H): C ₆₀ exposed mussels. (E): blank (toluene); AM= adductor muscle; DG = digestive gland; G = gill.	189
--	-----

Chapter 7: Investigation of the toxic effect of aged C₆₀ in different life stages of *Mytilus edulis*

Plate 7.1 C ₆₀ fullerene solutions in seawater at concentration of 1.0 mg l ⁻¹ ; (A) fresh C ₆₀ 'FC ₆₀ ', (B) Aged C ₆₀ 'AC ₆₀ ' stored at room temperature exposed to natural sunlight light for 30 days.	205
Plate 7.2 Photomicrographs showing the mussels releasing the gametes, (A) male with released sperms (B) female with released eggs.	207
Plate 7.3 Experimental setup for a short-term (3 d) exposure of <i>Mytilus edulis</i> to FSW, ASW, FC ₆₀ and AC ₆₀ in individual 5 L aerated tanks.	218
Plate 7.4 Malvern Zetasizer (model ZEN3600) used for DLS analysis.	221
Plate 7.5 TEM drop deposition procedure steps.	223
Plate 7.6 Phillips Technai F20 used for TEM analysis.	224
Plate 7.7 AFM drop deposition procedure steps.	226
Plate 7.8 XE-100 microscope used for AFM analysis.	227
Plate 7.9 Bruker AX D8 used for XRD analysis.	228
Plate 7.10 Typical Comets for: (a) control sperm in natural seawater showing nuclei with no DNA migrating into the tail; (b-d) sperm exposed to 0.1, 0.5 and 1.0 µg l ⁻¹ CuSO ₄ , respectively, showing a head with DNA fragments migrating into the tail region as a result of strand break.	238
Plate 7.11 HPLC chromatogram results. (A-C): C ₆₀ standard; (D-F): FC ₆₀ exposed mussels. (G-I): AC ₆₀ exposed mussels; AM= adductor muscle; DG = digestive gland; G = gill.	251

Acknowledgements

I am deeply grateful to Prof. Awadhesh Jha for his kind support and advice throughout the duration of this research even in his very busy time. A huge thanks to Dr. John Moody; his words of intelligence have helped greatly in the *production of this thesis*. Thanks to Prof. James Readman for his contributions of time, ideas, and support during these studies. A enormous thanks to Dr. Eniko Kadar for her help and guidance during the spawning experiment. I would also like to thank Dr. William Langston (MBA) and Sean O'Hara for laboratory help with ultracentrifuge. I am grateful to the Kuwait Institute for Scientific Research (KISR) for the financial support which made this PhD possible. I cannot forget to express appreciation to all the technical staff who have helped me along the way; in particular, thanks to Andy Attifield and William Vevers. Also, thank you to Dr. Bjorn Stolpe and Prof. Jamie Lead at University of Brimingham for their kind assistance with nanoparticles characterisation.

I am especially grateful to my best friend Sanaa Mustafa for her constant and interminable support throughout everything I have ever undertaken. Huge thanks go to many student colleagues Sherin Sheir, Sahar Kareeb, Christopher Ramsden, Helena Reinaardy and Yanan Di for providing unwavering support, kind words, welcome distractions, chocolates and fun when I needed it most.

Last but not the least I owe my loving thanks to my husband Ameen Al Douser, my son Eisa and my daughters Juood and Mesk. They have missed and lost a lot due to my research. Without their encouragement and understanding, it would have been impossible for me to finish this work. My special gratitude is due to Dad, Mum, Sisters (Shimaa, Asmaa, Eman and Maha) and brothers (Bader, Mohamed and Abdul-aziz) for their loving support. Hope I have made you proud.

Author's Declaration

At no time during the registration for the degree of Doctor of Philosophy has the author been registered for any other University award without prior agreement of the Graduate Committee. This study was financed with the aid of Kuwait Institute for Scientific Research (KISR). Relevant scientific seminars and conferences were attended at which work was presented and papers have been prepared for publication:

Publications (please refer to Appendix I for the full manuscripts)

Al-Subiai, S.N., Jha, A.N. and Moody, A.J., 2009. Contamination of bivalve haemolymph samples by adductor muscle components: implications for biomarker studies, *Ecotoxicology* 18, 334-342.

Beg, M.U., **Al-Subiai, S.N.**, Beg, K.R., Butt, S.A., Al-Jandal, N., Al-Hasan, E., Al-Hussaini, M. 2010. Seasonal effect on heat shock proteins in fish from Kuwait bay. *Bulletin of Environmental Contamination and Toxicology* 84, 91-95.

Kadar, E., Tarran, G.A., Jha, A.N. and **Al-Subiai, S.N.**, 2011. Stabilization of engineered zero-valent nanoiron with Na-acrylic copolymer enhances spermotoxicity. *Environmental Science and Technology* 45, 3245–3251.

Al-Subiai, S.N., Mustafa, S.A., Moody, A.J. and Jha, A.N., In press. A multiple-biomarker approach to investigate the effects of copper on the marine bivalve mollusc, *Mytilus edulis*. *Ecotoxicology and Environmental Safety*.

Mustafa, S.A., **Al-Subiai, S.N.**, Davies, S.J. and Jha, A.N., In press. Hypoxia-induced oxidative DNA damage links with higher level biological effects including specific growth rate in common carp, *Cyprinus carpio* L. *Ecotoxicology*.

Kadar, E., **Al-Subiai, S.N.**, Dyson, O. and Handy, R.D. Are reproduction impairments of free spawning marine invertebrates exposed to zero-valent nano iron associated with dissolution of nanoparticles? Submitted to *Nanotoxicology* (under review).

Platform presentations

Interactive Toxic Effects of C₆₀ fullerenes and fluoranthene in the common blue mussel, *Mytilus edulis*. University of Plymouth, Plymouth, UK, Nov 2010.

Poster presentations (please refer to Appendix II)

The level of glutathione in the cell-free haemolymph of the blue mussel, *Mytilus edulis*. SETAC 2006 Scientific Conference, Liverpool, UK, Sep 2006.

Contamination of bivalve haemolymph samples by adductor muscle components: implications for biomarker studies. SETAC Congress 2008, Sydney, Australia, Aug 2008.

An integrated approach to determine effects of copper in bivalve mollusc, *Mytilus edulis*. Plymouth Marine Sciences Partnership Symposium: Marine Science for a Changing World, Plymouth, UK, April 2009.

An integrated approach to determine oxidative stress in mirror carp *Cyprinus carpio*. 15th International Symposium on Pollutant in Marine Organisms. Bordeaux, France, May 2009.

Interactive toxic effect of C₆₀ fullerenes and fluoranthene at different levels of biological organisation in *Mytilus edulis*. Annual Meeting of the European Environmental Mutagen Society (EEMS), Oslo, Norway Sept 2010.

Photo-induced toxicity of aged C₆₀ in a marine invertebrate model. 21st SETAC Europe annual meeting, Milan, Italy, May 2011

Word count of main body of thesis: 43 404

Signed 
Date 25.7.11

Abbreviations

%	Percent
µg	microgram (10^{-6})
µm	micrometer
µl	microliter
Abs	absorbance
ANOVA	analysis of variance
APS	ammonium persulfate
B(a)P	benzo(a)pyrene
BSA	bovine serum albumin
CAT	catalase
C ₆₀	fullerenes (buckyballs)
DDT	dichlorodiphenyltrichloroethane
DMSO	dimethyl sulfoxide
DNA	deoxyribonucleic acid
DTNB	5,5'-dithiobis(2-nitrobenzoic acid)
Dw	dry weight
EDTA	ethylenediamine tetra acetic acid
EndoIII	endonucleases III
ENPs	engineered nanoparticles
EROD	7-ethoxyresorufin O-deethylase
F	fluoranthene
Fisher's LSD	fisher's least significant difference
FMO	flavoprotein monooxygenase system
FSW	filtered seawater
FPG	formamidopyrimidine glycosylase
<i>g_{ve}</i>	standard gravity
GC/MS	gas chromatography mass spectrometry
GR	glutathione reductase
GSH	glutathione (reduced)
GSSG	glutathione (oxidised)
GST	glutathione S- transferase
H & E	hematoxylin and eosin stain
HEPES	<i>N</i> -2-hydroxyethylpiperazine- <i>N'</i> -2-ethanesulphonic acid
HMP	high melting point agarose
H ₂ O ₂	hydrogen peroxide
ICES	International Council for the Exploration of Sea
ICP-MS	inductively coupled plasma mass spectrometry
IMS	Industrial methylated spirit
K _{ow}	octanol-water partition coefficient
LMP	low melting point agarose
LyDH	lysopine dehydrogenase
MDA	malondialdehyde
MFO	mixed function oxygenase
MTC	maximum tolerance concentration
NADH	reduced β nicotinamide adenine dinucleotide
NADPH	reduced nicotinamide adenine dinucleotide phosphate
nm	nanometre
NRR	neutral red retention
OECD	<i>Organisation for Economic Cooperation and Development</i>
<i>P</i>	statistical probability

P-450	cytochrome P 450
PAHs	polycyclic aromatic hydrocarbons
PBS	phosphate buffered saline
PCBs	polychlorinated biphenyls
PCDDs	polychlorinated dibenzo- <i>p</i> -dioxins
PUFA	poly-unsaturated fatty acids
SCGE	single cell gel electrophoresis
SE	standard error
SOD	superoxide dismutase
$^1\text{O}_2$	singlet oxygen
TBA	Tris buffered saline
TBARS	thiobarbituric Acid Reactive Substances
TEMED	<i>N,N,N,N'</i> -Tetramethylethylenediamine
US EPA	United States Environmental Protection Agency
w/v	weight/volume
ww	wet weight

Chapter 1

Introduction

1. Introduction

1.1 *Marine pollution*

In the recent decades, human activities have influenced the structure of ecosystems more rapidly and extensively than in any similar period of time in the geological past. Aquatic environment covers more than 2/3rd of our planet. As a result of anthropogenic activities, aquatic environment and aquatic organisms have been increasingly exposed to a variety of chemicals that could be potentially toxic (Jha 2004). It is well documented that the human population is heavily dependent on marine resources and around 70% of world's population live within 100 Km of the coastal regions (Knap et al. 2002). The marine and coastal environment therefore has direct implications for human health through different interconnected processes. This has resulted in a considerable irreparable loss in the biodiversity in the marine environment. The effects of the contamination by these chemicals might be chronic or acute, depending on the intensity of the exposures and the amount received by the organism. These chemicals produce a variety of detrimental effects, some of these pollutants or their transformed products are potentially carcinogenic or mutagenic (Ariese et al. 2001). These included chemicals such as: polycyclic aromatic hydrocarbons (PAHs), polychlorinated biphenyls (PCBs), dichlorodiphenyltrichloroethane (DDT), polychlorinated dibenzo-*p*-dioxins (PCDDs), heavy metals (Hg, Cd, Cu, Pb), etc. Among all these agents, petroleum products are becoming the major threat to the health of organisms inhabiting the marine environment as well as to the organisms which depend on them as a result of food chain interaction. Contamination of the marine environment by oil has occurred due to natural sources such as, oil leakage in

the field or, more likely due to human activities such as oil exploration, transport (oil leakage and spills), industry and processing. Traditionally, pollution levels and types of specific compounds present in the marine environment are monitored using analytical techniques. However, measuring all chemicals that comprise a complex material like crude oil is becoming more and more difficult and expensive. Also, measurements of these chemicals in the environment do not reflect whether they have induced adverse effects on the biota or not. Since contaminants occur in all probable combinations and their detection if they occur in low concentrations might not be possible by analytical techniques, another approach is needed to assess their potential impact on the environment. In recent years, increasing concern for public health and environmental problems have resulted in a considerable interest in monitoring the biological effects of the pollutants, although depending upon the exposure conditions environmental impact could be a slow process resulting in biological responses to be measured particularly for chronic low level exposures. The consideration of organism health, whether of human beings or other species, is essential in the overall quality of the ecosystem (Schwarzenbach et al. 2006).

Among different types of contaminants in recent years emphasis is given to the potential detrimental effects of the manufactured or engineered nanoparticles (ENPs) and PAHs exposure, either alone or in combination on the biological responses or biomarkers i.e., a measurable biochemical, physiological or other alteration within an organism that can be recognized as a potential health impairment or disease.

1.2 *Manufactured or engineered nanoparticles (ENPs): a potential environmental pollutant*

A nanometre scale is 1×10^{-9} m (i.e. 1 billionth of a metre), to give a sense of this scale, a human sperm has length of around 46,000,000 nm, bacteria typically have a maximum dimension of around 5,000 to 500 nm, and viruses normally have a dimension range from 10 to 100 nm. Worldwide there are many definitions of engineered nanoparticles (ENPs) which are generally in agreement. The Organisation for Economic Co-operation, Development (OECD), Environmental Protection Agency (EPA), EU Scientific Committee on Emerging and Newly Identified Health Risks (SCENIHR), and Nanotechnology Industrial Association (NIA) indicated that nanoparticles are particles with sizes between about 1 and 100 nm that show properties that are not found in bulk samples of the same material. Such a small size (i.e. very large surface area to volume ratio) give rise to distinctive electrical, thermal, mechanical, and imaging properties in some of these ENPs from their bulk material (Royal Society 2004).

The production of ENPs has shown a massive increase since their discovery in the 1980's. ENPs have been used in a wide range of applications from medicine to electronics. It is estimated that by 2015, nanotechnology will value \$1 trillion on the consumer products world market (Schmidt 2009). It is therefore likely that, in common with other contaminants, the aquatic environment will ultimately get contaminated by these nanoparticles in the near as a result of industrial and human activities (Moore 2006). Currently there are two main challenges to scientists. The first challenge is to detect manufactured or engineered nanomaterials in the environmental compartments. This challenge comes up because at present different varieties of ENPs exist and their numbers are

increasing. The second challenge is to monitor their fate, movement and transformation in the environment which is still poorly understood (USEPA 2010).

1.2.1 Types of engineered nanoparticles (ENPs)

There are several ways of classification of ENPs, but a broad classification can be based on size, shape and composition. The three main groups which form the basis of their chemical composition are: metallic and metallic oxide nanoparticles, carbon based nanoparticles and quantum dots (fluorescent semiconductor). Metal ENPs (i.e. Au, Pt, Fe, Co, CdS, Pd, Cu, etc) are clusters containing from a few tens to several thousand metal atoms. Their sizes, morphology and coating could vary their physical properties. Metallic oxide nanoparticles also have extensive applications in a wide range of fields such as fuel additive (cerium dioxide (CeO_2)); cosmetics (titanium dioxide (TiO_2) and zinc oxide (ZnO)) and manufacturing pigments (Iron oxide (Fe_3O_4 and Fe_2O_3)) (Ju-Nam and Lead 2008). The carbon based group is subdivided into carbon nanotubes which are composed of single (SWCNT) and multiwalled carbon nanotubes (MWCNT), and spherical (fullerenes) (Sloan et al. 2000). The last category of ENPs is the quantum dots, tiny fluorescence-emitting nanoparticles, which have unique optical and electrical features. Such properties gave quantum dots ENPs potential application in biomedical imaging and in the electronics industries (Moore 2006). An example for quantum dots: cadmium/selenide (CdSe) core with a zinc sulfide (ZnS) or a cadmium sulfide (CdS).

1.2.2 Major fate of engineered nanoparticles (ENPs) in aquatic environment

Most research on ENPs has focused on their toxicity, but there are very few studies conducted on their environmental fate. The transport and fate of ENPs in the environment is one of the main complications facing scientists, which could be due to the difficulty to identify and quantify ENPs in complex matrices such as aquatic environment. ENPs can reach the aquatic environment through different sources, industrial waste or human activities. Once into the environment, ENPs can be transported directly to water and soil or indirectly through air phase which end up in soil and water. In the environment, fate of ENPs could be influenced by a number of abiotic (e.g. pH, ionic strength, hardness temperature or organic ligands) and biotic (e.g. microorganisms) factors, as illustrated in **Fig. 1.1**. These interactions may lead to chemical modifications (i.e. change surface coating) or degradation which could strongly affect ENPs behaviour in the water column by changing their nature (i.e. size distribution, state of aggregation, charge and solubility) (Nowack and Bucheli 2007). For example, Baalousha et al., (2008) reported that the degree of iron oxide nanoparticles aggregation is dependent on the concentration of humic substance (natural organic colloids), where 1 nm humic substance surface coating on iron oxide nanoparticles induced greater stability, but iron oxides were shown to form increasingly large aggregates with higher concentration of humic substance. Also they found by dynamic light scattering (DLS) analysis that high aggregation of ENPs began at approximately pH 5 to 6 and reached a maximum at approximately pH 8.5. Baun et al., (2008) also showed that the toxicity of phenanthrene, in fresh water flea, *Daphnia magna* was enhanced by 60% in the presence of C₆₀ fullerenes. This effect highlights the role of ENPs in

enhancing the toxic effect of the pollutants in the environment. Another possible reaction that could occur in the environment is photochemical transformation in the presence of the sunlight (i.e. UV) and water. Some ENPs (e.g. C₆₀ fullerenes) possess strong light absorptive properties, where absorbed light of certain wavelengths results in photoexcitation (release electron) of the ground-state of the ENPs, which then transfer energy to the oxygen (O₂) to produce singlet oxygen (¹O₂) (Lee et al. 2009a). Taken together, the current scientific uncertainties surrounding the complex chemical and physical interactions of these nanoparticles continue. Fundamental understanding of interaction of ENPs with other anthropogenic and natural compounds present in the environment is essential. In addition, the potential effect of ageing process of ENPs in various environmental media is needed.

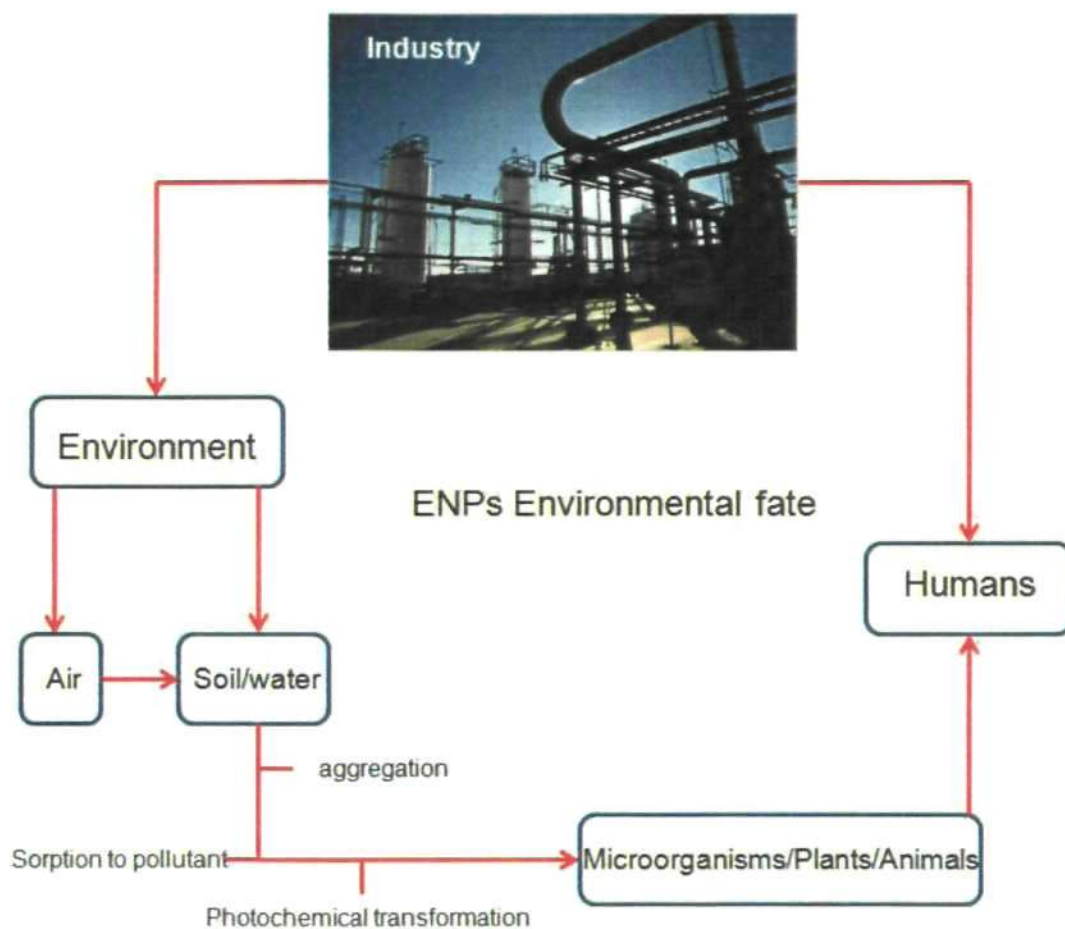


Fig. 1.1 A model of fate and transformations of ENPs in the environment (modified from Simonet and Valcárcel (2009)).

1.2.3 Metabolic activation of engineered nanoparticles (ENPs)

There is agreement that the unique property (large surface area) of ENPs plays an important role in the interaction within cell and should therefore be considered when evaluating their risk on living organisms. ENPs can be uptaken by the cells by two ways: (1) penetration through cell membrane (either directly or through transporters) or (2) phagocytosis by certain cells (macrophages) (Singh et al. 2009). Once ENPs get inside the cell, it triggers the formation of ROS which have the ability to react with cellular biomolecules. The high production of reactive oxygen species (ROS) can cause mechanical damage within the cell (**Fig. 1.2**) and therefore induces oxidative stress (as discussed in details in section 1.5).

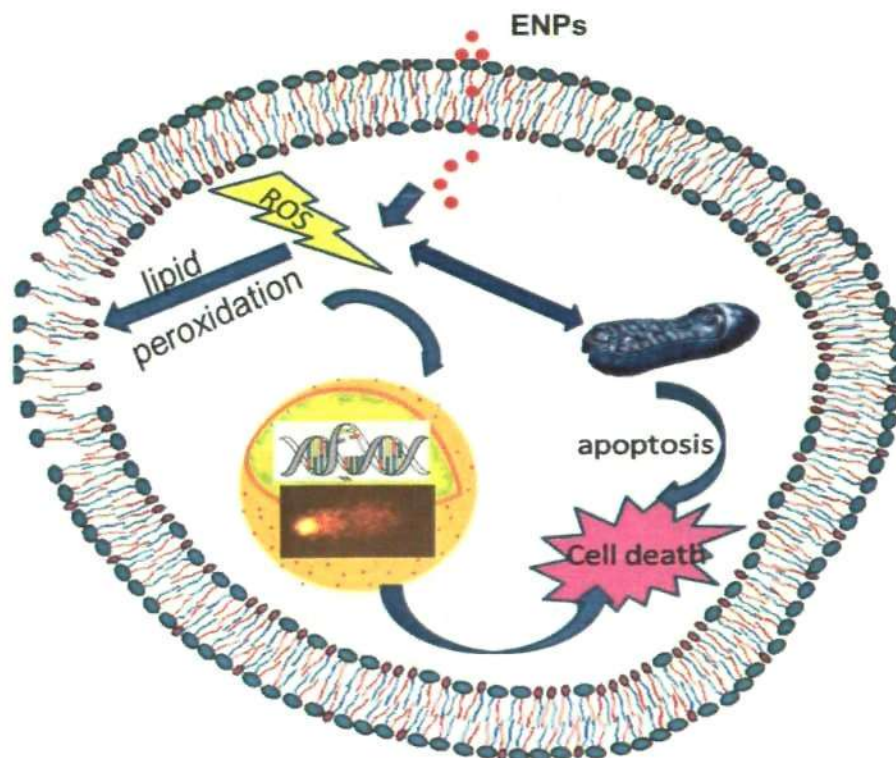


Fig. 1.2 Possible mechanisms of interaction of ENPs with cellular system leading to oxidative stress.

1.3 Polycyclic Aromatic Hydrocarbons (PAHs) as environmental pollutant

Polycyclic aromatic hydrocarbons (PAHs) are organic chemical compounds composed of hydrogen and carbon comprising two or more fused benzene rings (Wild and Jones 1995). Indeed, the widespread occurrence of PAHs in the environment is mainly due to their formation and release during the incomplete combustion of oil, petrol, wood, coal, cigarette and even grilled or fried food (Walker et al. 2001). Anthropogenic PAHs are divided into two main groups based on their source. The first group is pyrolytic PAHs which are formed as a result of incomplete combustion, and characterised by (relative) high molecular weight. Examples of pyrolytic PAHs include: benzo(a)pyrene and pyrene. Petrogenic group, however, result from petroleum products, and are characterised by (relative) low molecular weight such as: naphthalene and phenanthrene. USEPA (2001) has selected 16 priority toxic PAHs list (**Table 1.1**). Individual PAHs differ substantially in their chemical and physical properties. There is an inverse relationship between Octanol–Water coefficient (K_{ow}) and water solubility of the compound. Generally, PAHs with low water solubility are marked with high K_{ow} , high lipophilicity, and high molecular weight.

PAHs, components of crude and refined oil, are one of several classes of potential organic pollutants that are released into the environment in large quantities which tend to accumulate in sediments and in the organisms at different trophic levels. These compounds are known to cause a range of damages which include oxidative damage in aquatic organisms effecting nucleic acid, proteins, lipids and carbohydrates resulting in disturbance in normal metabolic function with potential for long-term consequences for ecosystem

health and sustainability (Beg et al. 2003). Estimation of the quantity of petroleum hydrocarbons products entering the sea over the year is varied and difficult to determine. According to GESAMP (2007), 1.5 billion tons yr^{-1} of oil are transported over the sea, and about 6.19 million t yr^{-1} of petroleum hydrocarbons products is released to the aquatic environment. Crude oil is a complex mixture of many thousands of organic compounds. Hydrocarbons usually represent 75% of the weight with 0.2 to more than 7% being PAHs (Neff 1985).

Table 1.1 Structures for the 16 priority PAHs in the environment, arrangement based on their molecular weight (USEPA 2001).

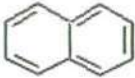
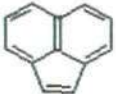
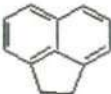


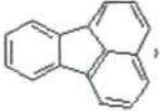
Chemical	Structure	Molecular weight (g mol ⁻¹)	Water solubility (mg l ⁻¹)
Naphthalene		128.2	31
Acenaphthylene		152.2	16.1
Acenaphthene		154.2	3.8
Fluorene		166.2	1.9
Phenanthrene		178.2	1.1
Anthracene		202.3	0.26

Table 1 continue



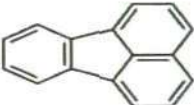

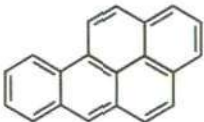
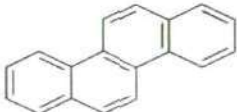
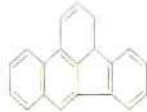
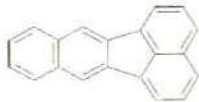


Chemical	Structure	Molecular weight (g mol ⁻¹)	Water solubility (mg l ⁻¹)
Pyrene		202.3	0.132
Indeno[1,2,3cd]pyrene		276.3	0.062
Fluoranthene		178.2	0.045
Benzo[a]anthracene		228.3	0.011
Benzo[a]pyrene		252.32	0.0038
Chrysene		228.3	0.0015

Table 1 continue

Chemical	Structure	Molecular weight (g mol ⁻¹)	Water solubility (mg l ⁻¹)
Benzo[b]fluoranthene		252.3	0.0015
Benzo(k)fluoranthene		252.31	0.0008
Dibenz[ah]anthracene		266.3	0.0005
Benzo[ghi]perylene		276.4	0.00026

1.3.1 Major fate of PAHs in aquatic environment

PAHs entering the aquatic environment tend to associate with the sediment, due to their hydrophobic nature. Adequate qualitative and quantitative characterizations of the toxic effects of PAHs on aquatic organisms require an understanding of the fate of PAHs in the aquatic environment. In marine organisms, PAHs are absorbed in several ways: the direct one is the absorption of compounds present in the water phase through the gills, and the indirect one is the absorption of PAHs adsorbed on the food through the digestive process. The uptake of PAHs in marine invertebrates is being dependent on a number of variables, including route of uptake, time of exposure, exogenous and endogenous factors (Livingstone 1991a). The fate of PAHs in an organism could be divided into four stages: Absorption, Distribution, Biotransformation and Excretion. Absorption of PAHs depends on molecular properties (lipophilicity, size, polarity/charge) and the features of the organism. For example, the main absorption mechanism in aquatic invertebrate and fish is passive diffusion through gills, digestive tract and also through body surface. Distribution of PAHs is mainly determined by the route of uptake and tissue lipid levels (same principles as absorption). Lipophilic compound are readily taken up into the tissues of living organism and accumulate in those tissues (bioaccumulation). Generally, the bioaccumulation increases as tissue lipid levels increase in organism. After, PAHs have been distributed among the tissues, metabolic reactions are initiated by enzymes. These enzymes have a wide tissue distribution but the highest activities are generally found in tissues concerned with the food processing (Sjolin and Livingstone 1997). Different biotransformational enzymes can have different tissue, cellular and subcellular distributions. For example, cytochrome P-450, flavoprotein monooxygenase

system (FMO), flavoprotein reductase, epoxide hydratase and UDP-glucuronyl transferases can be found in the endoplasmic reticulum (microsomes) compartment while other enzymes are mainly cytosolic. The biotransformational enzymes have a wide range of substrate specificities enabling them to metabolise most of the chemicals (but not all) (Rand 1995). They exist in multiple forms as: isoforms and isoenzymes, with different substrate specificities. Inducibility of biotransformation enzymes may vary with exogenous (e.g. temperature, salinity, oxygen) and endogenous factors (e.g. sex, size, age, life stage, nutritional status, and season). Most of the enzymes are inducible (i.e. more enzymes are synthesised) in response to exposure to a particular xenobiotic. Time-course and duration of induction of biotransformation enzyme activities varies with enzyme and the nature of the pollutants (Livingstone and Pipe 1992). The role of biotransformation enzymes for the metabolism of PAHs has been discussed in more details in section 1.4.1. Finally, the chemical is going through an excretion step where waste products of the metabolism and other non-useful materials are eliminated from the body. The higher molecular weight PAHs (less water soluble) are normally eliminated at lower rate (Juhász and Naidu 2000).

1.3.2 Metabolic activation of PAHs

Once the PAHs enter the biological system, there are three main metabolic pathways for activation of PAHs that have been reported with laboratory evidence: (a) *via* dihydrodiol epoxide by cytochrome P-450. This has been extensively established by researchers in this field as the main mechanism of chemical carcinogenesis of PAHs, **Fig. 1.3**, (Hall and Grover 1990), (b) *via* formation of radical cations of PAHs, where one-electron oxidation catalyzed by

P-450 peroxidase, **Fig. 1.4**, (Cavalieri and Rogan 1995) and (c) *via* formation of *o*-quinones of PAHs catalyzed by dihydrodiol dehydrogenases, **Fig. 1.5**, (Penning et al. 1999).

1.4 Bivalve mussels, *Mytilus edulis* as a model species in ecotoxicology

Biological systems are targets for the action of environmental contaminants and many aquatic organisms are used to evaluate their potential effects. In this context, bivalve mussels are widely used for ecotoxicological and environmental biomonitoring purposes. In this thesis, the most common, marine mussel species, *Mytilus edulis*, widely distributed along European shore has been selected as a model organism for the study. Mussels are found in high population densities forming extensive mats on solid substrate. They are also valued seafood and have a commercial importance in aquaculture. Mussels are among the most efficient filter feeders of all shellfish and can filter litres of water per hour (van Duren et al. 2006), consuming virtually everything in it. *Mytilus edulis* is known to accumulate high levels of organic compounds and trace metals in their tissues, providing a time-integrated indication of environmental contamination with observable cellular and physiological responses. For low or moderately polluted aquatic systems, biochemical parameters in mussels may be useful for monitoring the pollution level. These features in mussels make them a well-known and extensively used "sentinel" organism in environmental monitoring programme worldwide including for the 'mussel watch' programme (Livingstone et al. 2000; Ramu et al. 2007). For the advantages mentioned above, we decided to select blue mussel, *Mytilus edulis* as a sentinel, experimental organism in our project. Different life stages (i.e. embryo-larvae

and adult) of this species have been used extensively in our laboratory condition to determine different biomarkers following a range of environmental contaminants (Cheung et al. 2006; Hagger et al. 2005; Jha et al. 2000; Jha et al. 2005). The mussels could be collected from different reference or pristine sites from the region and could be maintained relatively easily under laboratory condition in well defined conditions.

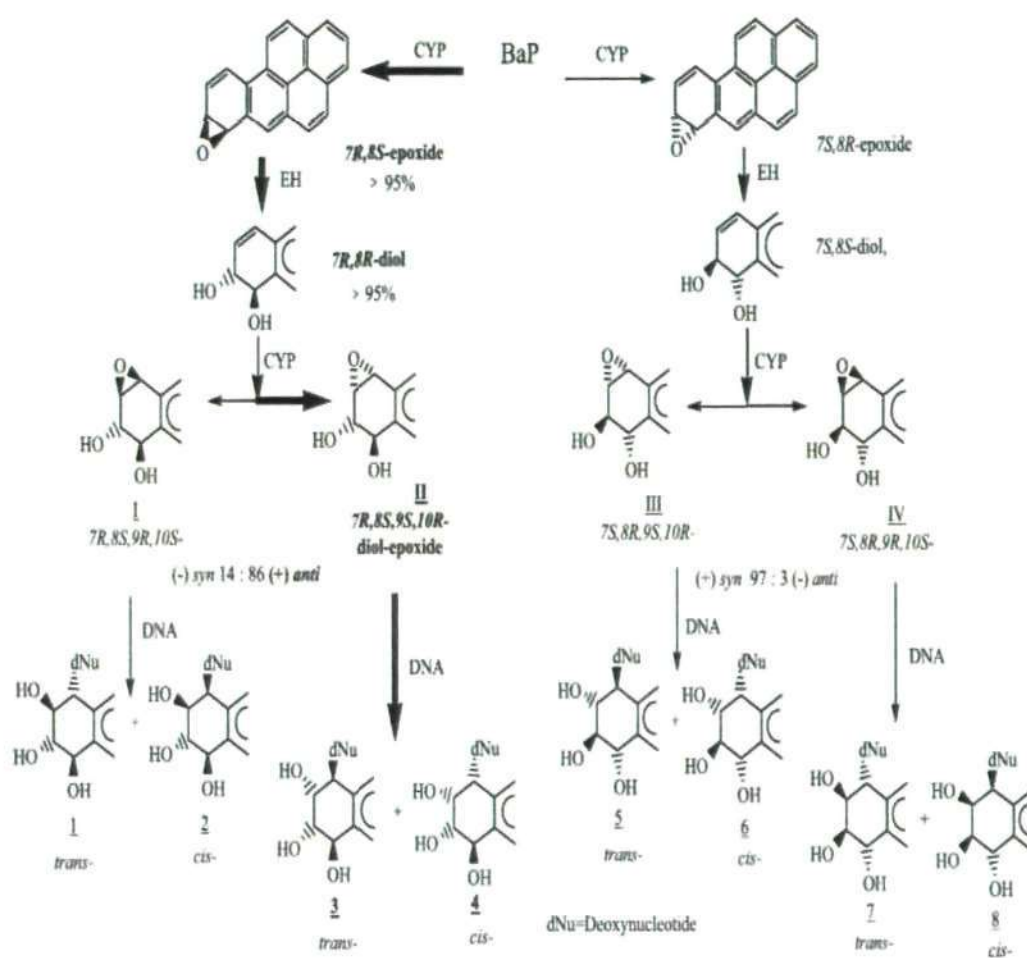


Fig. 1.3 Activation of B(a)P via dihydrodiol epoxide by cytochrome P-450 (Xue and Warshawsky 2005).

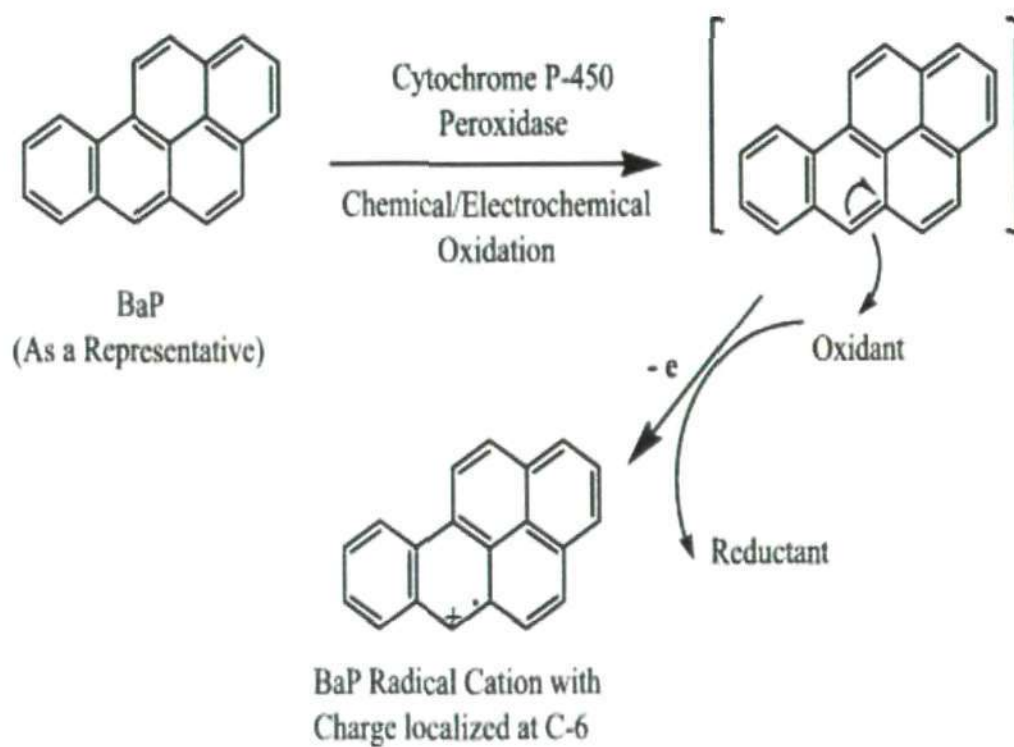


Fig. 1.4 Activation of B(a)P via formation of radical cations (Xue and Warshawsky 2005).

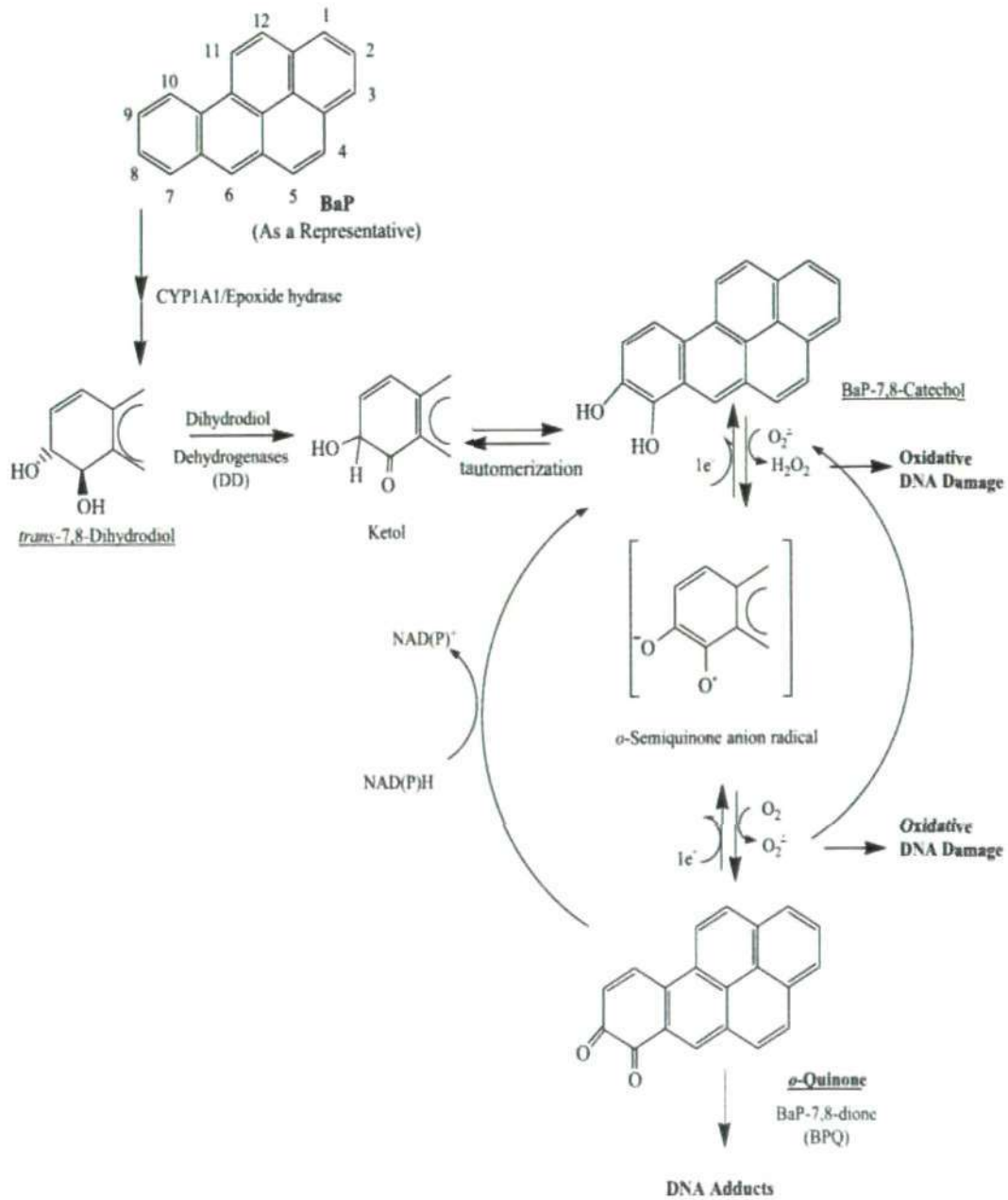


Fig. 1.5 Activation of B(a)P via formation of o-quinones catalyzed by dihydrodiol dehydrogenases (Xue and Warshawsky 2005).

1.4.1 Biotransformation enzymes in Mussels

Mussels like all organisms possess a suite of biotransformation enzymes for the metabolism of the toxic chemicals, usually present in highest levels in the digestive gland, equivalent to liver in higher organisms (main organ for food processing). The major function of these enzymes is to alter the biological activity of PAHs by converting them to water-soluble excretable metabolites. The biotransformation of PAHs is usually divided into phase I and phase II metabolism, as summarized in **Table 1.2**, (Livingstone 1991b). Phase I, functionalization metabolism, is the alteration of the original toxic compound, so as enzymes catalyse virtually every reaction that a compound can undergo (oxidation, reduction, hydration, hydrolysis) and introduce a functional group, e.g. -OH, -COOH or modifies an existing functional group, e.g. -NO₂ reduced to -NH₂, which can then be conjugated in phase II. Phase II enzymes, conjugative metabolism, utilize a variety of endogenous molecules (glutathione, sugars, amino acid, sulphate, etc.) to attach polar moieties to the functional groups to produce water-soluble compound which are generally non-toxic and easily hydrolyzed to other products (Timbrell 2000). Most types of biotransformation enzymes for phase I and phase II metabolism in mammals have also been identified in marine invertebrates (Livingstone 1991b) including cytochrome P-450, FMO, flavoprotein reductase, epoxide hydratase and phase II Glutathione S-transferase (GST). In higher organisms, a phase III enzyme system exists in which the xenobiotic conjugates may be further hydrolysed or remetabolised.

Table 1.2 Major biotransformation enzymes in phase I and II.

Phase	Reaction	Enzyme	Substrate
Phase I	Oxidation	CYP* (EC 1.14.14.1) FMO* (EC 1.14.13.8)	Many structurally diverse compounds Amines & many sulphur compounds
	Reduction	DT-diaphorase (EC 1.6.99.2)	Quinones
	Hydrolysis	Esterases (EC 3.1)	Esters & amides
	Hydration	Epoxide hydratase (EC 4.2.1.64)	Epoxides
Phase II	Sulphation	Sulphotransferase (EC 2.8.2.1)	Phenols, alcohols, amines & thiols
	Glutathione conjugation	Glutathione-S-transferase (EC 2.5.1.18)	Epoxides, haloalkanes, nitroalkanes, alkenes, aromatic halo & nitro compounds
	Glucuronidation	UDP-glucuronyltransferase (EC 2.4.1.17)	Phenols, alcohols, amines, amides & thiols
	Glycosidation	UDP-glucosyltransferase (EC 2.4.1.81)	Phenols, alcohols, amines, amides & thiols

* CYP = cytochrome P-450, FMO = mixed-function oxygenase system.

1.4.2 Cytochrome P-450 induction

When concentration of PAHs exceeds beyond a certain level in the cell, it may trigger responses designed to protect the organism against potential toxic effects. Very commonly, this response is an increase in the level of biotransformational enzymes (Peters et al. 1999). A number of enzymes are induced which can increase the rate of biotransformation of the molecule to water-soluble metabolites and readily excretable conjugates (Timbrell 2000). The cytochrome P-450 (EC 1.14.14.1) (systematic name: heme-thiolate protein) is a highly diversified set (more than 1500 known sequences) of heme-containing proteins. The P-450 superfamily is regarded as one of the most sensitive and specific enzyme systems induced in response to environmentally relevant concentration of PAHs. No other enzyme system can lodge the variety of substrates that are metabolised by the P-450 system, ranging from small molecules such as methanol (MW = 42) to large molecular weight compounds such as the immunosuppressant drug cyclosporine (MW = 1203) (Ioannides 2007). Usually, P-450 form part of multi component electron transfer chains, called P450-dependent monooxygenase system (also known as mixed-function oxygenase (MFO) system, or P-450 containing system). MFO reaction requires electrons and molecular oxygen to catalyse the monooxygenation (i.e. insertion of a single atom of oxygen into the organic substrate) reaction:



Where R = organic substrate, R-OH = hydroxylated product

The name cytochrome P-450 is actually derived from the fact that the reduced forms of the cytochromes (cyto: cellular; chrome: colour) bind carbon monoxide

to form a complex that absorbs light strongly at 450 nm wavelength (Nebert et al. 1991). The heme prosthetic group recruited by cytochromes P-450 to affect monooxygenation is also used by these and other proteins for oxygen transport, reduction, dehalogenation, dealkylation, and electron transfer (Sono et al. 1996). Endoplasmic reticulum is especially rich in P-450s, which metabolize a vast number of PAHs. The induction of P-450 is a compulsory first step in the detoxification of contaminants such as PAHs and PCBs. Usually the product of reaction with P-450 is less toxic than the parent compound, but this is not always the case. Sometimes, metabolism *via* P-450 may activate different contaminants which results in an increased formation of reactive oxygen species (ROS) and metabolites that interact with biomolecules including DNA, leading to genotoxicity and carcinogenicity e.g. activation of benzo[a]pyrene to DNA reactive carcinogens (Halliwell 1999).

P-450 induction is either detected by its catalytical activity, e.g., measurement of the elevation in ethoxyresorufin O-deethylase (EROD) or by immunocytochemical methods with antibodies to P450 1A forms such as, Western blots, ELISA (Jonsson et al. 2006; Shaw et al. 2004). Both immunoassay and catalytic assays have been used to demonstrate P-450 induction by environmental contaminants. Although induction of biotransformation enzyme P-450 is routinely used in fish, much less is known about the application of MFO-related measurements in mussels and other marine invertebrates. Existence of P450-dependent activities in mussels is widely used in aquatic ecotoxicology (Akcha et al. 2000; Solé et al. 1998; Stegeman 1985). Nevertheless, molecular evidence of its presence is recent and no sequence data is available up to date. In a laboratory study, Wootton (1995) used cDNA probes (CYP1A1, CYP3A, CYP4A1 and CYP11A1 from

human, rat and fish) to detect P-450 gene subfamilies in mussel. Also, Peters (1998) demonstrated CYP1A, CYP2A, CYP2B, CYP3A and CYP4A-like proteins in the digestive gland microsomes of *Mytilus galloprovincialis* using antibodies from mammals and fish in western blot analysis. Higher levels of P-450 were also reported in mussel from crude oil contaminated sites, **Table 1.3**.

1.5 Oxidative stress

Basic cellular metabolism in aerobic organisms involves the reduction of O₂ to H₂O. However, partial reduction of O₂ in endogenous oxidative reactions in aerobic cells gives rise to oxygen free radicals and non radicals reactive oxygen species (ROS) (summarised in **Table 1.4**). ROS contain one or more unpaired electrons, which enables them to interact with a variety of macromolecules. The toxic effects of ROS are varied including oxidative DNA damage, protein degradation (especially the sulphur containing groups such as, methionine and cysteine residues) (Dean et al. 1993) and lipid peroxidation (Valavanidis et al. 2006). There are many sources for ROS which include: byproduct of the cytochrome P-450 system enzymatic reactions, ionising radiation, non-catalysed reactions between oxygen and metal cations and organic compounds, phagocytic cell activity, hyperoxia and hypoxia. The discovery and elucidation of role of the ROS in normal biological processes has led to much research into prooxidants and antioxidants (Pampanin et al. 2005).

Table 1.3 Examples of field studies employing CYP 1A-immunoidentified protein as a biomarker for pollution.

Organism	Environment	Measurement	Comments	Reference
<i>Mytilus edulis</i> L.	Galicia, Spain (oil spill)	Western blot	X 3.5 higher P-450	Solé et al. 1996
<i>Mytilus edulis</i> L.	Mediterranean sea, UK	Western blot	Elevation of P-4501A levels	Peters et al. 1999
<i>Mytilus edulis</i> L.	North Sea, Skagerrak	Western blot	Induction of P-450 levels	Livingstone et al. 1997
<i>Mytilus galloprovincialis</i> L.	Exposure to 20 ppb PCB	P450A1	Elevation of P-4501A levels	Forlin et al. 1996
<i>C. rupestris</i> & <i>M. edulis</i>	North Sea, Skagerrak	EROD	Induction of P-450 levels	Solé et al. 1998

EROD = 7-ethoxyresorufin O-deethylase.

The extent to which the ROS can cause damage to macromolecules is dependent on the efficiency of organism's antioxidant defences (Barata et al. 2005). Organisms have a battery of enzymatic and non-enzymatic antioxidant defence systems which limit the potential damage caused by ROS (Livingstone 2001). *The antioxidant defences can be induced by pro-oxidant conditions* which may result from many endogenous and exogenous factors. They are not perfect in the sense that some ROS are not inactivated. If the intracellular redox state becomes more pro-oxidant because of the disproportionate generation of ROS, it leads to oxidative stress. On the other hand, inhibition of antioxidant enzymes occur and damage to macromolecules like proteins, lipids and DNA can take place, which may lead to cell and tissue damage and contribute to *aging, cancer and other pathophysiological conditions* (Correia et al. 2003).

1.6 Antioxidant defence

Living organisms have evolved various defence mechanisms to reduce the harmful effects of contaminants including PAHs. Antioxidant defences consist of three general classes including antioxidant enzymes, cytosolic water-soluble free radical scavengers and membrane bound fat-soluble free radical scavengers (Liebler 1993), as summarized in **Table 1.5**. The levels of antioxidant enzyme activities and scavengers vary with endogenous and exogenous factors. Elevations in antioxidant enzyme activities with laboratory exposure to a variety of organic and metal contaminants have been reported but responses are generally temporary, and inconsistent for different species, enzymes and pollutants (Verlecar et al. 2008). One of the most important characteristics of these enzymes is their induction under oxidative stress status,

and such elevation can be an important indicator to pollutant-induced stress. Glutathione peroxidase (GPx) catalyses the reduction of both H_2O_2 and lipid peroxides (Tran et al. 2007); superoxide dismutase (SOD) catalyzes the transformation of superoxide radicals to H_2O_2 and O_2 (Vlahogianni et al. 2007); Catalase (CAT) catalyses the reduction of hydrogen peroxide (H_2O_2) produced and glutathione transferase (GST) which involves in the detoxification of many xenobiotics which trigger oxidative stress condition.

1.7 Damage caused by the oxidative stress

Under normal physiological condition, the ROS generated from metabolism of extraneous chemicals in the body can be removed by the biotransformation metabolism and antioxidant defence system in the bodies of aerobic organisms. But oxidative stress will be potentially experienced by all aerobic life when antioxidant defences are overcome by pro-oxidant forces. In complex environmental conditions (field situations), where contaminants are present as mixture, compounds, such as unsubstituted PAHs can be altered abiotically and biotically, in particular *via* oxygenation, to more toxic compounds that can produce oxidative stress (Hoeger et al. 2004). Many studies have indicated that PAHs toxicity is usually related to a redox cycling phenomenon which promotes the formation of free radicals, that may induce cellular injury due to membrane breakdown creating structural and functional disability in cells (Stephensen et al. 2000). Photomodification of PAHs as well as metabolism of PAHs in fish and other organisms results in compounds such as quinone that can produce reactive oxygen species *via* redox cycling (Livingstone et al. 1990; Peters et al. 1996).

Table 1.4 Examples of different types of reactive oxygen species (ROS).

Reactive oxygen species (ROS)	
Radicals	Non-radicals
Hydroxyl radical (OH \cdot)	Hydrogen peroxide (H ₂ O ₂)
Superoxide radical (O ₂ \cdot^-)	Ozone (O ₃)
Alkoxy radical (RO \cdot)	Hypochlorous acid (HOCl)

Table 1.5 Examples of different types of antioxidant defence present in the cellular system.

Types of antioxidant defence	Examples
Antioxidant enzymes	GST, CAT, GPx, SOD
Water soluble scavengers	GSH, vit C, purines
Fat soluble scavengers	vit A, vit E, carotenoids

Based on the existing knowledge, oxidative stress is thought to be a major contributor to the aging process. The free radical theory is one of various aging theories, suggesting that the structural and metabolic changes which occur in aging cells are mainly related to ROS reaction (Rikans and Hornbrook 1997). Most components of cellular structure and function are likely to be the potential targets of oxidative damage.

The side chain of fatty acids is very susceptible to free radicals attack. Polyunsaturated fatty acids (PUFA) are particularly prone to attack by hydroxyl radicals due to its double bonds between carbon atoms (Marnett 1999). When PUFA are under oxidative stress its configuration may be altered, and they may develop into lipid peroxides. Malondialdehyde (MDA) is considered to be the most important of the aldehydes, which result from reaction with free amino acids, proteins, and nucleic acids (Esterbauer et al. 1991). Lipid peroxidation may result in the alteration of the protein's biochemical properties and membrane fluidity.

1.8 Interactive effect of contaminants

Contaminants occur as a complex mixture, in all probable combinations in the environment. Organisms are therefore usually exposed simultaneously to mixtures of pollutants *via* multiple exposure routes (Feron and Groten 2002). These pollutants can interact in different combinations, where the resulting effects of combined pollutants may be additive (similar) or synergistic (stronger) or antagonistic (weaker) than expected effects from the single exposure (Sterner 1999).

Investigations on the combined toxic effects of multiple chemicals are limited for many reasons. Firstly, there are a huge number of possible pollutant combinations, and most of the time we do not know which exposure ranges should be investigated, or which combination is important, or which biological parameter should be tested. Secondly, it is much easier to study the effect of single toxic compound on an animal (Benedetti et al. 2007). Thirdly, we even have evidence that single compound could also exert its effects through different pathways. For example, PAHs exerts their toxicity directly through metabolic activation of P-450 enzyme, or indirectly by the production of ROS which can affect macromolecules such as DNA (Barouki and Morel 2001).

Besides the toxic effect of PAHs mentioned earlier, heavy metal input is still on the increase in aquatic ecosystems through discharges of domestic sewage, abandoned ships, war materials, catalyst power, use of anti-fouling paints, pesticides and sediment agitation (Biney et al. 1994). Many studies have shown that metals such as Cd, Cu, Cr, Hg and Fe have the ability to produce ROS species resulting in oxidative damage (DNA damage, lipid peroxidation). PAHs and heavy metals represent important classes of aquatic contaminants due to their toxicity and well-documented individual effects (Livingstone 2001). However, only a few recent studies have noted the effect of PAHs-heavy metals complex on marine organisms. The interaction between PAHs and heavy metals represent an interesting area of research that has not yet been adequately addressed to any extent.

1.9 Application of biomarkers in ecotoxicology

In ecotoxicology a biomarker can be defined as a "*biological response to a chemical or chemicals that gives a measure of exposure and sometimes, also, of toxic effect*" (Walker et al. 2001). Biomarkers can help to link the gap between the field and the laboratory by giving reliable evidence of whether or not a particular animal, plant or ecosystem is being affected by pollution. They will often provide more reliable evidence of exposure as their effects (detectable via biomarkers) may exist for much longer duration, whereas measurements of the contaminants themselves in the environment are complex because they are often short-lived and difficult to detect.

International Council for the Exploration of Sea (ICES) recommended biomarkers for monitoring the marine environment. The levels of stress biomarkers in fish or other species will indicate apparent situations of stress in their surrounding environment and help the regulatory authorities in taking appropriate remedial measures. The knowledge of the relationship between the exposure to physical and chemicals stressors and the changes in the biological response of the exposed organisms is growing. This has led to the possibility of the selection of suitable model species or a specific biochemical response serving as a biomarker of environmental stress (Fig. 1.6). The knowledge of biomarkers may be utilized to assess the degree of environmental stress vis-à-vis associated health risk. Thus, the biomarkers may provide sensitive and specific measures of exposure and often the toxic effects. Efforts are going on for further sophistication in biomonitoring and attention is focused on specific biochemical

responses in an organism that can be used as biomarker (an early warning) of environmental exposure to pollutants.

1.9.1 Glutathione level

A major role of glutathione is to provide protection against oxidative stress that is induced both intra- and extra-cellularly (Regoli and Principato 1995). Numerous reactions involve glutathione such as: synthesis of DNA, proteins and enzyme activity and metabolism (Meister and Aderson 1983). Glutathione has also a significant function with reactive molecules such as H_2O_2 and antioxidant metabolism as it is involved in both phases I and II of the *detoxification processes*. *If reactive molecules are present in excess within the cell, the cell's glutathione level can become depleted.* Reactive molecules can oxidize the thiol groups (-SH) in glutathione which could lead to the change in the thiol status of the cell. In order to restore reduced glutathione status in the cell, glutathione reductase (GR) reduces the oxidized glutathione (GSSG) produced by these reactions.

According to our knowledge, total glutathione levels in cell-free haemolymph have not been studied in aquatic invertebrates exposed to pollutants, although a few researchers have studied the effects of PAHs on the glutathione levels of the digestive gland. In these studies (Cheung et al. 2000; Doyotte et al. 1997) they found an increase in glutathione concentrations in mussels exposed at polluted site with PAHs. Deneke and Fanburg (1989) suggested that since most glutathione is synthesized in the liver, a decrease in liver metabolism due to contaminants may result in severe glutathione depletion in other tissues.

1.9.2 Lipid peroxidation

ROS may cause oxidative damage to lipids, proteins and nucleic acids. The side chain of fatty acids is very vulnerable to free radicals. Poly-unsaturated fatty acids (PUFA) are particularly prone to attack by hydroxyl radicals due to its double bonds between carbon atoms. When PUFA are under oxidative stress its configuration may be altered, and they may develop into lipid peroxides. These dismantle to form secondary products such as ethane, pentane, aldehydes (Storey 1996). MDA is considered to be the most important of the aldehydes, by reacting with free amino acids, proteins, and nucleic acids (Marnett 1999). Lipid peroxidation may result in the alteration of the protein's biochemical properties and membrane fluidity.

The recognition of the role of lipid peroxidation in toxicological processes developed more recently. Several methods have been developed for the evaluation of lipid peroxidation. By far the most popular of these methods, in both chemical and biological systems, is the thiobarbituric acid reactive substances (TBARS) test. This method is based on the condensation of one molecule of MDA with two molecules of TBA under acidic condition. The validity of this method rests on the assumptions that MDA formed during the TBAR assay is diagnostic of the presence and amount of peroxides, and that a quantitative relationship exists between the extent of lipid peroxidation and the MDA detected (Shaw et al. 2004).

1.9.3 Measurement of DNA strand breaks using the Comet Assay

The Comet assay, also called single cell gel electrophoresis (SCGE), is a sensitive method for evaluating DNA damage/repair at the level of the individual

eukaryotic cell. It has wide applications in biomonitoring and ecotoxicology (Collins et al. 2004). Swedish researchers (Östling and Johanson 1984) introduced this method under neutral condition in 1984 which measures DNA double breaks. Singh and co-workers in (1989) modified this technique, as the alkaline Comet assay to detect low level of DNA damage mostly single strand breaks and alkali labile sites with high sensitivity. Comet assay has many advantages which include: (a) rapid (few hours), sensitive (1break in 10^{10}) and inexpensive technique. (b) It counts 50-100 cells per replicates/treatments, allowing more robust statistical analyses. (c) It needs small numbers of cells ($>10,000$ / sample). (d) It uses any eukaryotic cell without requiring any specific dividing state.

The Comet assay is based on the migration of negatively charged loops/fragments DNA through the agarose gel in an electric field. Firstly, the cells are mixed with low melting point agarose and embedded on the slide (coated with high melting point agarose gel). Secondly, lysis step in which DNA is unwinded in lysis solution containing high concentration of salt (pH > 13). Thirdly, electrophoresis stage, the electrical charge is applied through the slide and DNA migrates away from the cell, in the direction of the (+) anode, forming a 'comet'. Modified comet assay using bacterial enzymes (e.g. Fpg and Endo III) which specifically recognises oxidised purines and pyrimidines bases are used to specifically determine oxidative DNA damage (Collins et al. 2004). This technique has been applied to a range of aquatic organisms (Jha 2008).

1.9.4 Histopathology

The name histopathology is actually derived from the Greek *histos* (tissue) and *pathos* (suffering). It is a branch of pathological science which deals with microscopic anatomy of cells and tissues (plants/animals) in order to provide information based on tissue diagnosis of disease. The tissue is prepared using histological procedures (fixation, processing, embedding, sectioning and staining) for viewing under a microscope. Histopathology has been employed to investigate the structural changes in a range of aquatic organisms following exposure to heavy metals (Handy et al. 2002), engineered nanoparticles (Federici et al. 2007), PAHs and PCB (Lowe and Pipe 1987). However, little research has been directed towards the invertebrates. Histopathological tool can also give supporting information for other specific biomarkers used to assess contaminant effect.

1.9.5 Feeding Rate

Understanding the physiology of the organism is very important which indicate the overall health of an animal. In this context, feeding behaviour assay is one of the most simple, direct and robust method for assessing organism's healthiness (Widdows et al. 1995). In feeding rate also known as clearance rate assay, the amount of food consumed by the filter-feeding organism is measured in terms of the rate in which given food (or water) is ingested (or cleared) per time unit. Feeding rate assay, either during or after contamination exposure, has been successfully employed by researchers for many years as an *in situ* assay endpoint for bivalves. Honkoop group (2003) found that feeding rates for the mussels collected from contaminated location were affected (i.e. reduced

feeding rate) compared with those at the uncontaminated location. Also another study by Widdows (2001) found that mussels collected from the majority of coastal and estuarine sites in UK do not feed well (do not filter) at their maximum potential. The study suggested that this situation is due the presence of pollutants in their body tissues.

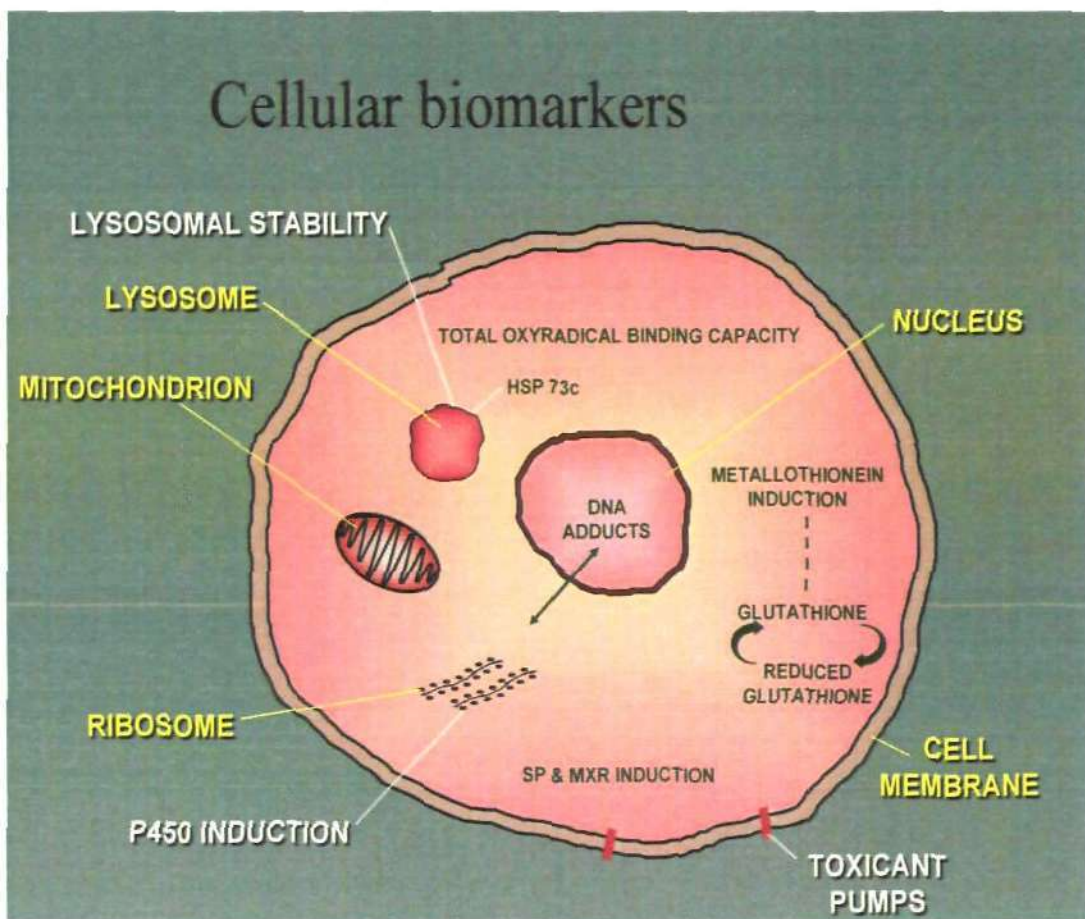


Fig. 1.6 Biochemical indicators of oxidative stress and oxidative damage at the cellular level (adapted from Prof. Galloway, T).

1.10 Aims and objectives

The overall aim of the thesis is to determine potential adverse effects of a representative engineered nanoparticles, C₆₀ fullerenes either in original or in transformed form, either alone or in combination of a representative polycyclic aromatic hydrocarbons on marine mussels, *Mytilus edulis*. To achieve this aim, a suite of biomarker at different levels of biological organisation (i.e. biochemical, DNA, tissue and individual level responses). A schematic outline of the thesis with main research hypotheses to be tested is given in **Fig. 1.7**.

The main objectives of this research were to:

- (i) Determine the relative sensitivity/robustness of different biomarkers and verify if they could be used for environmental risk assessment (chapters 3, 4 and 5).
- (ii) Establish appropriate exposure conditions to evaluate biological responses using fluoranthrene (PAHs) and C₆₀ fullerenes (ENPs) as an emergent contaminant either alone or in combination (chapter 6).
- (iii) Provide an understanding of the toxicity of C₆₀ fullerenes, is in part mediated by oxidative stress and whether the combination with other contaminants could enhance its toxicity (chapter 6).
- (iv) Investigate the impact of the exposure of male gametes (i.e. sperms) to fresh C₆₀ fullerenes (FC₆₀) and aged C₆₀ fullerenes (AC₆₀) on DNA damage and its potential impact on early developmental stages in the marine mussels, *Mytilus edulis* (chapter 7).

- (v) Determine the toxic effects of FC₆₀ and AC₆₀ fullerenes on the adult marine mussels, *Mytilus edulis* to better understand the potential adverse effects of degraded C₆₀ fullerenes (chapter 7).

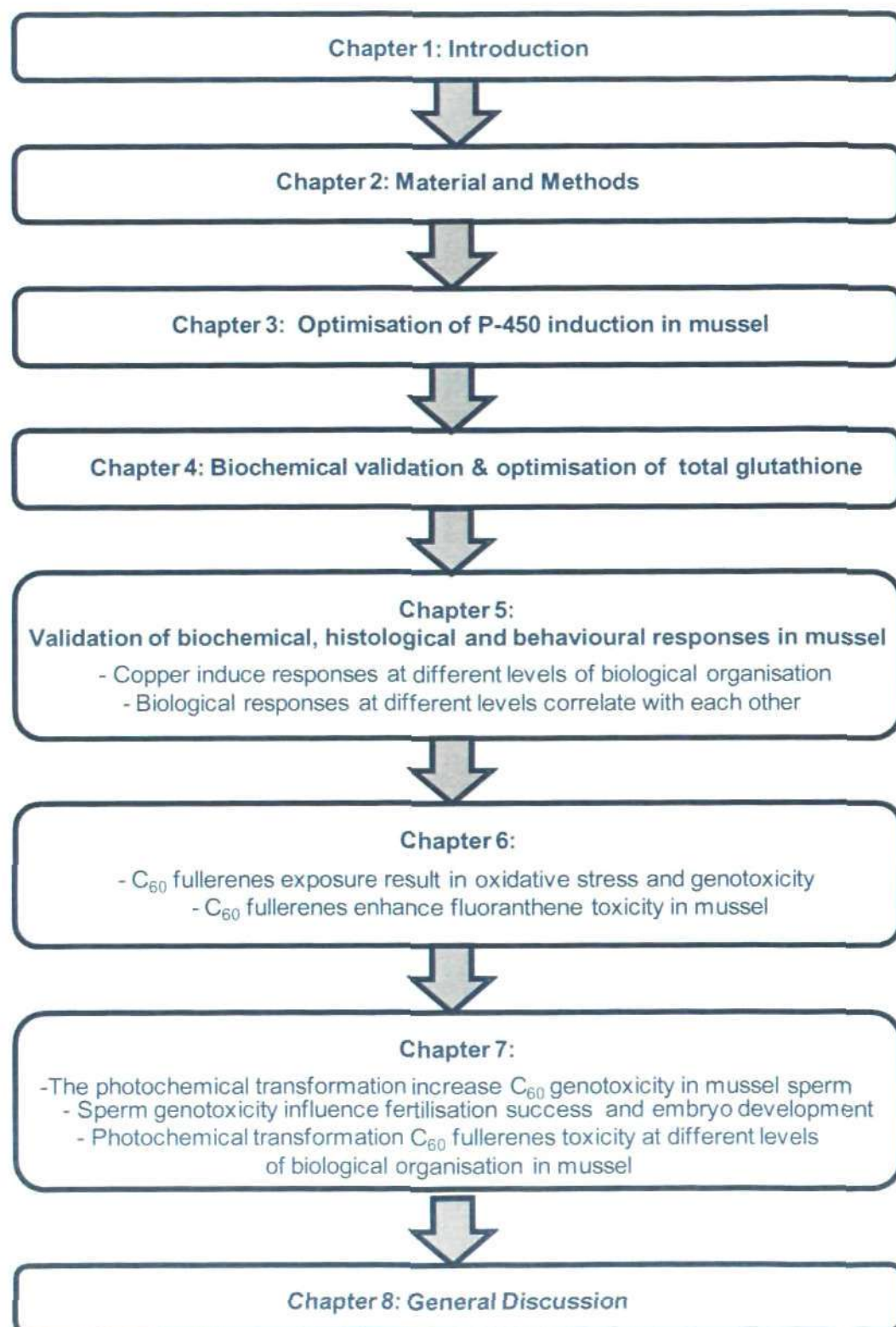


Fig. 1.7 Thesis outline and research hypothesis tested in each experimental chapter.

Chapter 2

Materials and Methods

In the present study, investigations were carried out on the blue marine mussel, *Mytilus edulis*, due to their advantages mentioned earlier in section 1.4. The general methodologies aimed to establish appropriate exposure conditions, and then examine their effects at different levels of biological organisation. End points therefore were chosen to assess oxidative stress status at biochemical, histopathological and behavioural levels. At biochemical level, Comet assay was used to detect DNA damage and glutathione content to assess antioxidant defence. Histopathological studies in target organs were also conducted to evaluate general injury as well as potential inflammation in the tissues. Due to the fact that mussel is an efficient filter feeder, clearance rate was also determined to evaluate physiological behaviour of the animals before and after exposure. All chemicals and reagents were of the highest analytical reagent grade obtained from Sigma-Aldrich (Pool, UK) unless stated otherwise. A series of *in vivo* exposures were conducted to assess the toxicity of C₆₀, fullerenes either alone or in combination. Experimental work then moved to assess the effect of photo-oxidative aging of C₆₀ on adult and early life stages of *Mytilus edulis*.

2.1 Animals collection

Adult mussels (*Mytilus edulis*) of similar shell length (51-58 mm) were collected from their natural beds on rocky outcrops (illustrated in **Plate 2.1**) at low tide from relatively clean sites either from Port Quin (grid reference: SW972 905, **Plate 2.2A**) or Trebarwith Strand (grid reference: SX048 866, **Plate 2.2B**), Cornwall, UK (**Fig. 2.1**). Mussels were removed from their rocky substrates by cutting the byssus threads carefully. After collection, they were immediately transported in cool box to the laboratory (less than 2h) and cleaned of epibionts.

Animals were divided into three groups and placed in highly aerated tanks with filtered ($< 10 \mu\text{m}$) sea water (salinity of 35-37) in ratio of $1.5 \text{ animals l}^{-1}$, with a light: dark cycle of 12 h: 12 h. The mussels were kept under controlled temperature of $15 \pm 1 \text{ }^\circ\text{C}$ and twice a week water was changed to remove faeces and maintain water quality. Mussels were fed twice weekly with microalgae (*Isocrisis galbana*, Liquidfry MarineTM, Interpet, Dorking, UK), $4.6 \times 10^9 \text{ cells l}^{-1}$ seawater, and allowed to acclimatize for at least two weeks before use in experiments. Any animals which did not close their valves on air were considered to be of poor health and removed from the tank to avoid contamination of the remaining group of animals.



Plate 2.1 Mussel beds on rocky outcrops.

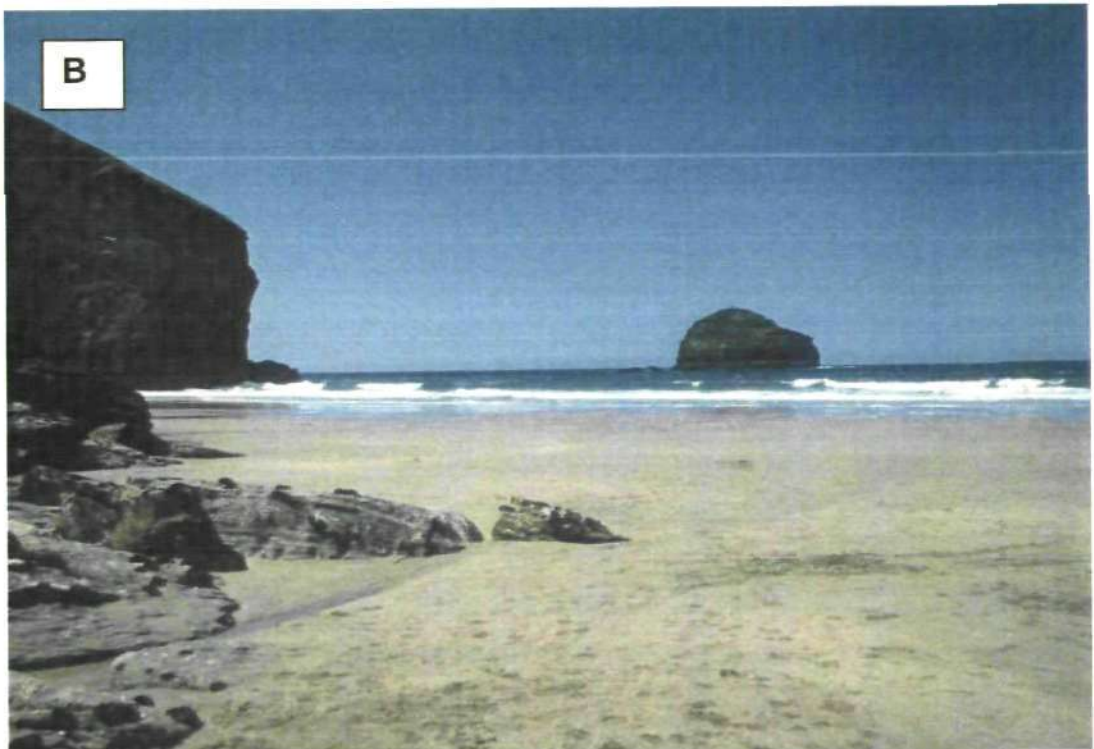


Plate 2.2 Photographic image of collection sites. (A) Port Quin; (B) Trebarwith Strand.

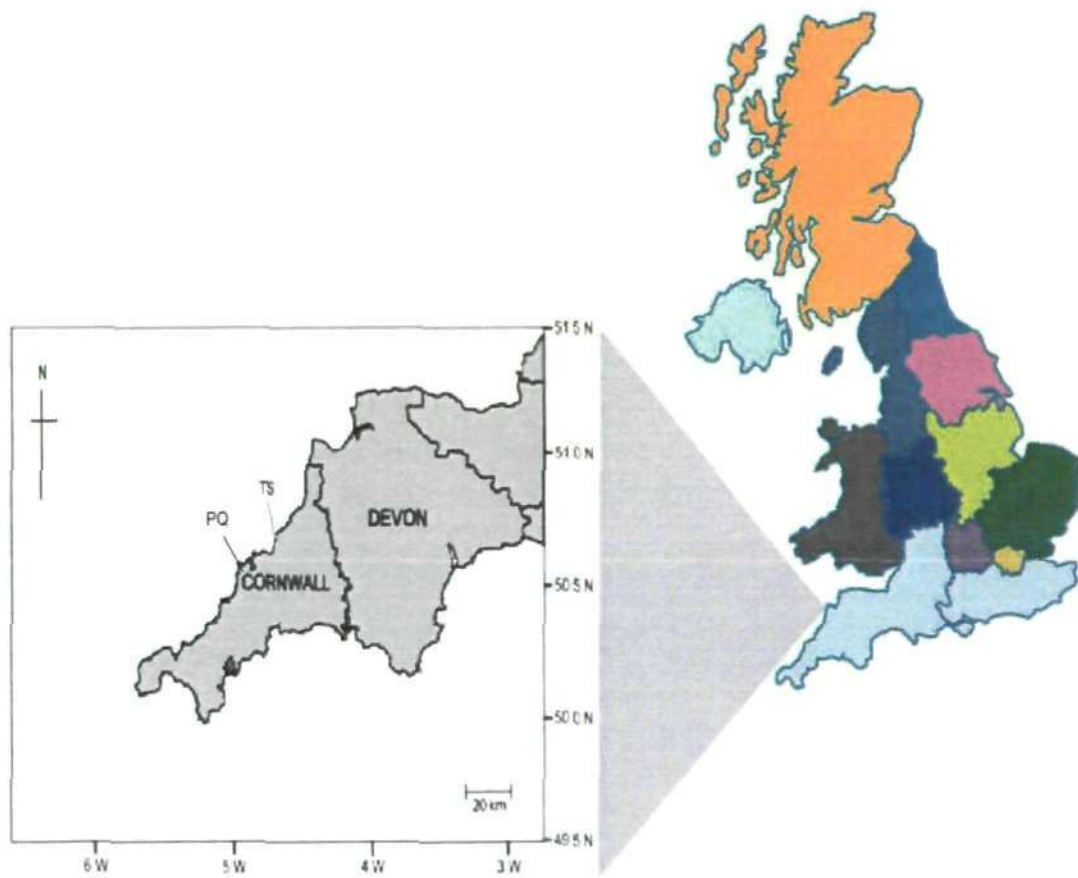


Fig. 2.1 Map of south-west, UK showing mussel collection sites at Cornwall. PQ = Port Quin; TS = Trebarwith Strand.

2.2 *Experimental design*

Each experiment was designed as described separately in each chapter. Seawater quality was confirmed by measuring % dissolved oxygen, pH, total ammonia (mg l^{-1}), temperature ($^{\circ}\text{C}$) and salinity (‰) in each of the experimental tanks using Multi 340i/SET (Germany) on sampling days and during the experiments. Photoperiod 12 light : 12 dark was also maintained after collection and during the experiments.

2.3 *Sample preparation*

2.3.1 *Collection of haemolymph samples*

To access the adductor muscle, the valves were prised apart carefully approximately midway towards the posterior end from the byssus thread by using a pair of scissors (**Plate 2.3**). The excess seawater held within the valves was allowed to drain out. Haemolymph was withdrawn from posterior adductor muscle of mussel *Mytilus edulis* using 1 ml sterilized syringe with a 21 gauge needle. Approximately 0.2 ml haemolymph sample was diluted with an equal volume of physiological saline (0.02 M HEPES pH 7.4, 0.4 M NaCl, 0.1 M MgSO_4 , 0.01M KCl, 0.01 M CaCl_2 , adjusted to pH 7.36). The cell density in the 400 μl haemolymph-physiological saline suspension samples was ~ 20000 cells. Samples were then centrifuged at 60 g_{av} in a microfuge for 2 min to pellet out the haemocytes and then placed on ice until analysis. **Plate 2.4** illustrates the position of the posterior adductor muscle and other organs.

2.3.2 Preparation of adductor muscle extract

The posterior adductor muscles from three mussels (0.2 g ww) were dissected out and were homogenized using the method as described in Al Subiai et al., (2009). Briefly, the tissues were ground with acid-washed sand (0.5 g) using ice-cold extraction buffer (20 mM Tris-chloride, pH 7.6, containing 0.15 M KCl, 0.5 M sucrose and 1 mM EDTA, freshly supplemented with 1 mM DTT and 100 μ l protease inhibitor cocktail (Sigma-P2714; reconstituted according to manufacturer's instructions) using a ratio of 1:3 (w/v). The crude homogenate was centrifuged for 35 min (10,500 g_{av} at 4 °C) after which the supernatant was separated and stored at -80 °C until use.



Plate 2.3 Extraction of haemolymph from the posterior adductor muscle.

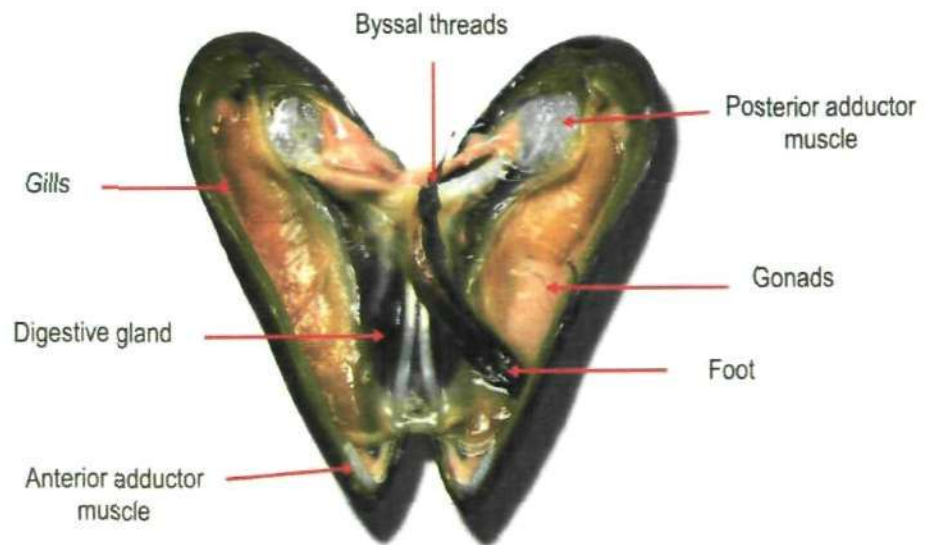


Plate 2.4 The internal view of dissected adult *M. edulis*, showing position of the posterior adductor muscle and the internal organs.

2.4 Determination of DNA strand breaks using the Comet assay

The DNA damage in the haemocytes of mussels was determined using the alkaline Comet assay according to the protocol described by Singh et al., (1988) and adopted for mussels by Jha et al., (2005). The main steps of the assay have been illustrated in **Fig. 2.2**.

2.4.1 Cell viability

Before the use of haemolymph samples for Comet assay, haemocytes viability was assessed using the vital stain Eosin Y. A sub-sample of 40 μl of haemocytes suspended in Tris-buffered saline (TBA) was transferred to a microscope slide and stained with 2 μl of 2 mg ml^{-1} of Eosin Y stock solution. Live cells were stained in green and dead cells as red. The percentage of viability was determined by counting the number of live and dead cells for each treatment. Haemocyte density was also carried out alongside.

2.4.2 Slide preparation

Fully frosted slides were coated with thin base layers of 1% high melting-point agarose (HMP) and then placed for 24 h in 37 °C incubator to allow the base layers of agarose to set on the slides. All the slides were labeled on the underside with a pencil before application of the low melting-point agarose (LMP) with the cells. Following estimation of the cell concentration (number of cells ml^{-1} haemolymph using haemocytometer), cells were pelleted in a microfuge tube and suspended in 180 μl of 0.5% low melting-point agarose (LMP), ensuring the temperature is ~ 35 °C before addition to prevent heat damage of the cells. Two drops (~ 75 μl each) of the cell suspension were placed on the frosted ends of glass slides and covered with a cover slip

(22 mm²). The agarose was allowed to solidify by placing the slides in fridge (4°C) for 15 min.

2.4.3 Cell lysis

While the slides were inside the fridge, the working lysis solution was prepared by adding Triton X-100 and dimethylsulfoxide (DMSO) to the chilled stock lysis solution (2.5 M NaCl, 100 mM EDTA, 10 mM Tris base and 1% *N*-lauroyl-sarcosine; adjusted to pH 10 with 10 M NaOH), to produce a final concentration of 1% and 10%; respectively. The cover slips from the slides were gently removed following which they were placed on the staining tray. The lysis solution was then carefully poured to cover all the slides. The slides immersed in chilled lysing solution at 4 °C for 1 h to remove cellular proteins and cell membrane.

2.4.4 Alkaline unwinding of DNA and electrophoresis

Following lysis step, slides were carefully removed and gently rinsed with chilled distilled water and then placed into an electrophoresis chamber (Pharmacia Biotech, UK) containing electrophoresis buffer (1 M NaOH and 200 mM EDTA, adjusted at pH 13). The slides were completely submerged and left in this solution for 45 min to permit alkaline DNA unwinding. The electrophoresis was carried out for 30 min (400 mA, 30 V) by adjusting the volume of the electrophoresis buffer as necessary.

2.4.5 Neutralisation and staining

Once the electrophoresis had been completed, the slides were removed and rinsed with chilled distilled water, then immersed three times for 5 min in neutralisation buffer (0.4 M Tris–chloride buffer, pH 7.5). Slides were drained of

excess neutralising buffer. The samples were then stained with 20 μl of ethidium bromide (EtBr) ($2 \mu\text{g ml}^{-1}$ in distilled water) and observed under an epifluorescence microscope (Leica, DMR). The Comet 5.0 image-analysis system (Kinetic Imaging, Liverpool, UK) was used to score 100 cells for each slide (50 in each gel from each exposed individual mussel) at a total magnification of $\times 200$. The software was pointed different parameters for the detection of DNA breaks (e.g. olive tail moment, tail length and %tail DNA). Data for percentage tail DNA are presented as a reliable measure of single-strand DNA breaks/alkali labile sites (Kumaravel and Jha 2006).

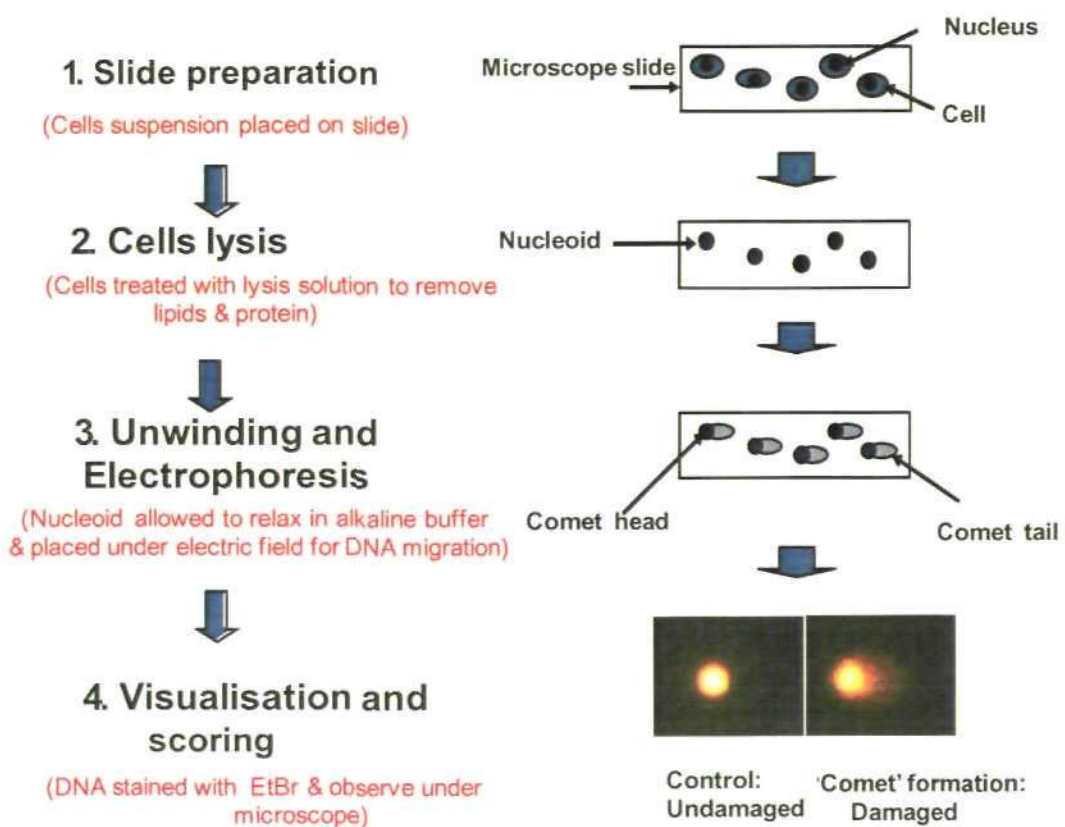


Fig. 2.2 Major steps involved in standard single cell gel electrophoresis (SCEG) or the Comet assay procedure.

2.5 Determination of total glutathione level in adductor muscle extract

The total glutathione (i.e. reduced: GSH, and oxidised: GSSG) content in adductor muscle extract was determined according to the method of Al-Subiai et al., (2009). Samples were treated with DTNB by mixing them at a 1:1 ratio with buffered DTNB (10 mM DTNB in 100 mM potassium phosphate, pH 7.5, containing 5 mM EDTA). One hundred millimolar potassium phosphate (235 μ l), pH 7.5, containing 5 mM EDTA and glutathione reductase (0.6 U, Sigma G-3664 from *Saccharomyces cerevisiae*) and 40 μ l of DTNB-treated samples were mixed. After equilibration for 1 min the reaction was started by the addition of 60 μ l of 1 mM NADPH. The rate of absorbance decrease at 412 nm was measured over 5 min. A 20 μ M GSH standard and a 0 μ M blank were used to calibrate the results. GSH/GSSG contents were measured in triplicate in a microplate reader (Optimax, Molecular Devices, Sunnyvale, CA) using 96 well plates. The assay temperature in each case was 22 °C. Total protein was determined using the biuret method with bovine serum albumin as standard (Gornall 1949).

2.6 Histological preparation for different organs

2.6.1 Tissues processing and paraffin embedding

Animals were examined for histopathology as described elsewhere in details (Sheir et al. 2010). The main target organs (viz, adductor muscle, gills and digestive gland) were carefully removed from each mussel, as illustrated in **Plate 2.5**. Mussel was held with its right valve at the uppermost and the tip of scissors was inserted into the byssal gap and twisted to force the valve to separate completely. Adductor muscle was then scraped away from the shell by using scalpel blade and the whole mussel body was taken out of the shell and

each organ was located. Gills were separated from the mantle tissue, adductor muscle was removed from mussel's body and digestive gland was dissected from other tissues. Following dissection, each organ was placed in buffered formal saline (9 g NaCl, 100 ml of 40% formaldehyde, made to up to 1 L with distilled water, adjusted to pH 7.4) and fixed for at least 48 h. Samples were then dehydrated through an ascending ethanol series (70% (24 h), 90% (2 h) and 100% (2 h) industrial methylated spirit (IMS) to remove excess water). Three changes of xylene were then performed (1h, 30 min and 30 min, respectively) to remove alcohol and also leave tissue transparent, ready for paraffin infiltration. Tissues were transferred to the paraffin oven (58 - 60°C) for 105 min to ensure the tissue was completely permeated with paraffin (except adductor muscle as it required more time ~ 210 min). The paraffin blocks were made manually and then left to harden for 3h. Transverse sections (5-8 μm thickness) were cut and mounted on slides.

2.6.2 Slide staining

Slides were stained with haematoxylin and eosin (Mayer's H and E) following standard protocol with some modifications in staining times to obtain the best cellular details. Slides were first cleared through 3 xylene changes to deparaffinize (2 min each), then dehydrated in 2 changes of absolute alcohol (5 min) and one change in an ascending alcohol series (90%, 70% and 50%) for 2 min each. Tissue sections were stained with alkaline filtered haematoxylin (to remove oxidized particles) for 1 h, followed by wash in running tap water until the water was no longer coloured (~5 min). Slides were blued in alkaline lithium carbonate (LiCO_3) for 4 rinses, then differentiated in acid alcohol for 2 rinse and blued again in LiCO_3 for 4 rinses. All slides were rinsed well in distilled water

and counterstained in acidic eosin for 1 min. Again slides were washed with distilled water and dehydrated in ascending alcohol series (70%, 90% and 100%), 2 min each. Finally, slides were cleared in 3 changes of xylene (2 min each) and covered with clean coverslips making sure that no bubbles trapped underneath it. All tissues from control and treated animals were processed together in batches for histology to eliminate artefacts between treatments. Slides were examined by light microscopy using an Olympus Vanox-T microscope and photographed using a digital camera (Olympus camera C-2020 Z) at total magnifications of x 100 and x 400 (zoom on the camera is x 2.5).

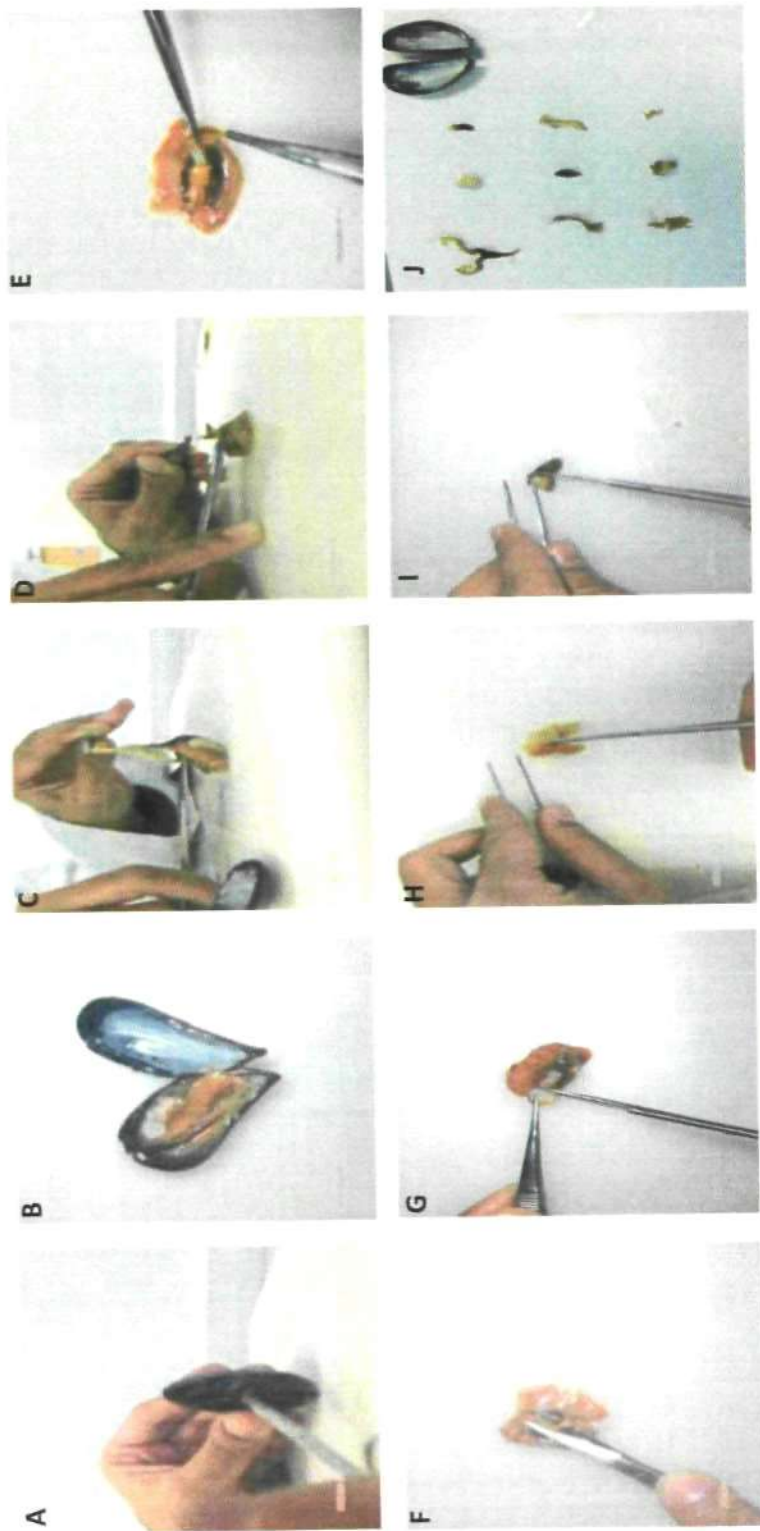


Plate 2.5 Mussel dissection procedure (A-I) and dissected organs (J).

2.7 Clearance rate

Feeding or clearance rate of mussels was determined as described elsewhere (Canty et al. 2009). Individual mussels were gently placed in separate 400 ml glass beakers (using forceps), each containing 350 ml of seawater (15 °C). A 12 x 6 mm magnetic stirrer was added to each beaker. The vessels were placed on 2 separate 15-point magnetic stirrers (RO 15 power, Kika-Werke GmbH & Co, Germany), along with 2 identical beakers without mussels which were used as system controls. The mussels were allowed to acclimatize for 10 min prior to the addition of 500 µl of Isochrysis algal suspension (supplied by Cellpharm Ltd., Malvern, UK), to give a concentration of ~ 20000 algal cells ml⁻¹ in each beaker. The beakers were stirred manually with a glass rod; then a 20 ml aliquot of water was removed using a glass syringe. This procedure was repeated after 20 min, the water samples were analysed on Particle Size and Count Analyser (Beckman Coulter, Z2, USA), as illustrated in **Plate 2.6**, with a 100 µm aperture fitted and set to count particles between 4.0-10.0 µm in diameter. Clearance rate of the mussel is calculated using following equation of Coughlan (1969):

$$\text{Clearance rate (l/h)} = \frac{(v \times 60/t)}{(\ln t_0 - \ln t_2)}$$

Where:

v = volume of water in beaker

t = duration of filtration (min)

t₀ = initial cell count

t₂ = final cell count

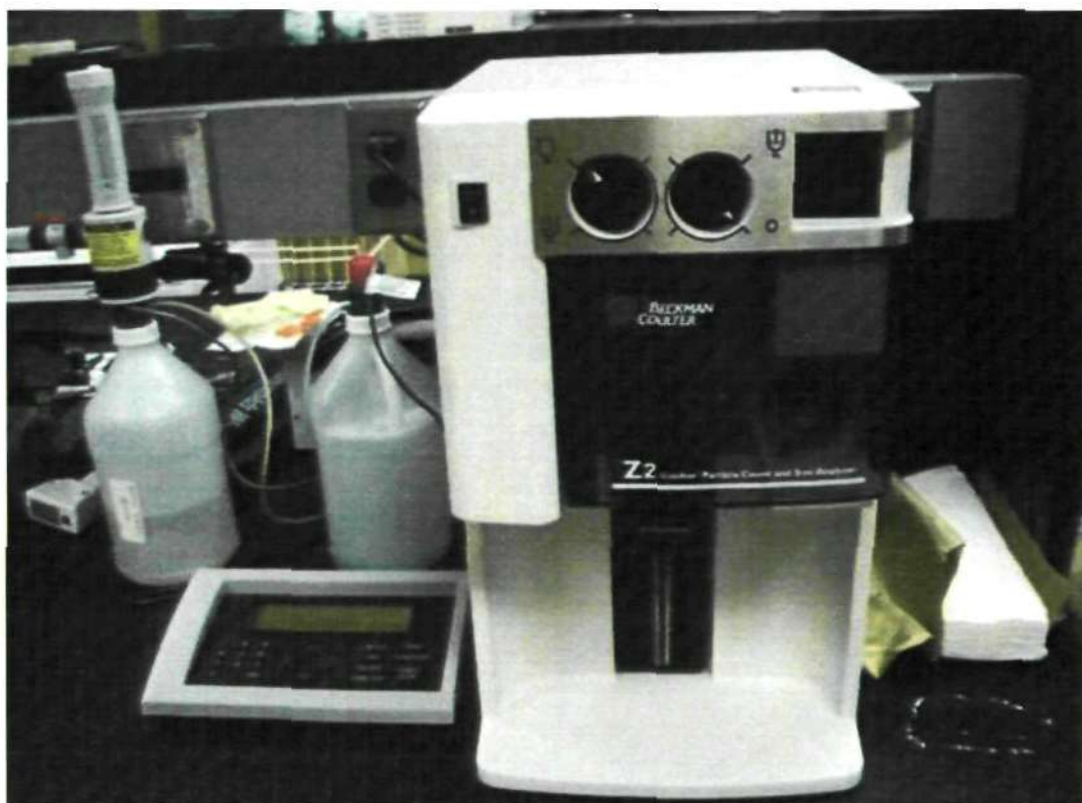


Plate 2.6 The Beckman Coulter counter (Z2) counting algal cells in seawater.

2.8 Analysis of C₆₀ in tissue samples

2.8.1 Tissue sample preparation for HPLC analysis

Adductor muscle, digestive gland and gills were carefully washed with pure toluene to make sure that no C₆₀ particles were adsorbed on the surface of the organs. Then, tissues were extracted in toluene in 1:9 ratio followed by ultrasonication of the homogenates for 15 min and centrifugation at 9,000 g_{av} prior to HPLC analysis.

2.8.2 HPLC analysis

HPLC method was developed for C₆₀ analysis using Hypersil (5 μ) Elite C18 (250 X 4.6 mm I.D.) column. The mobile phase was composed of pure toluene. Mobile phase flow-rate was set at 1.0 ml min⁻¹. Sample injections were performed manually with volumes of 100 μ l. The eluent was monitored at a 330 nm wavelength using a Shimadzu SPD-6 AV UV-Vis spectrophotometer from Shimadzu (**Plate 2.7**). Integration was performed using a Shimadzu-C-R3A chromatopac. For HPLC calibration, a standard curve was generated for C₆₀ concentrations ranging from 0.125 and 2.0 mg l⁻¹ (**Fig. 2.3**). Concentration of test samples was determined by comparison to the standard curve.

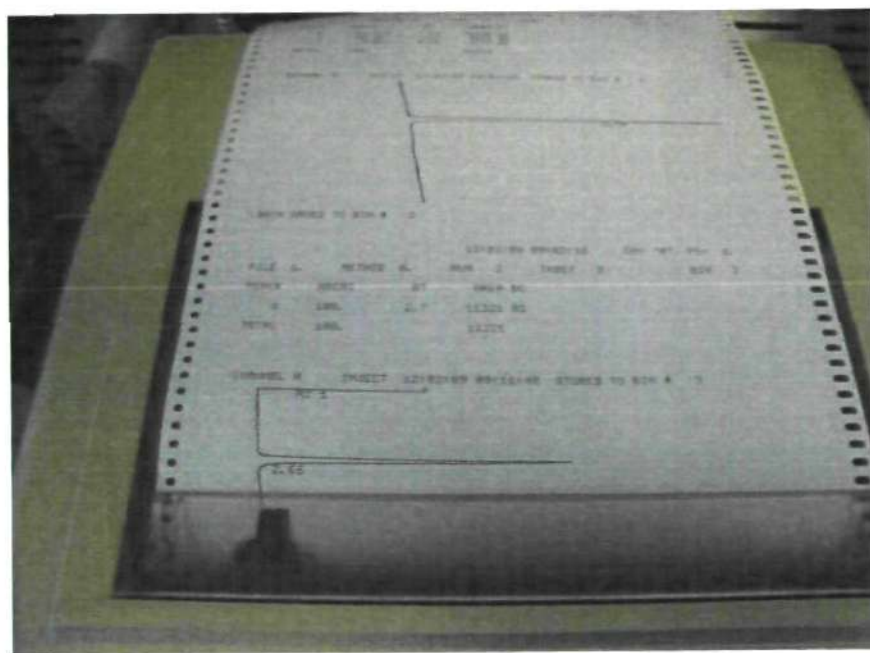


Plate 2.7 The HPLC UV-Vis spectrophotometer.

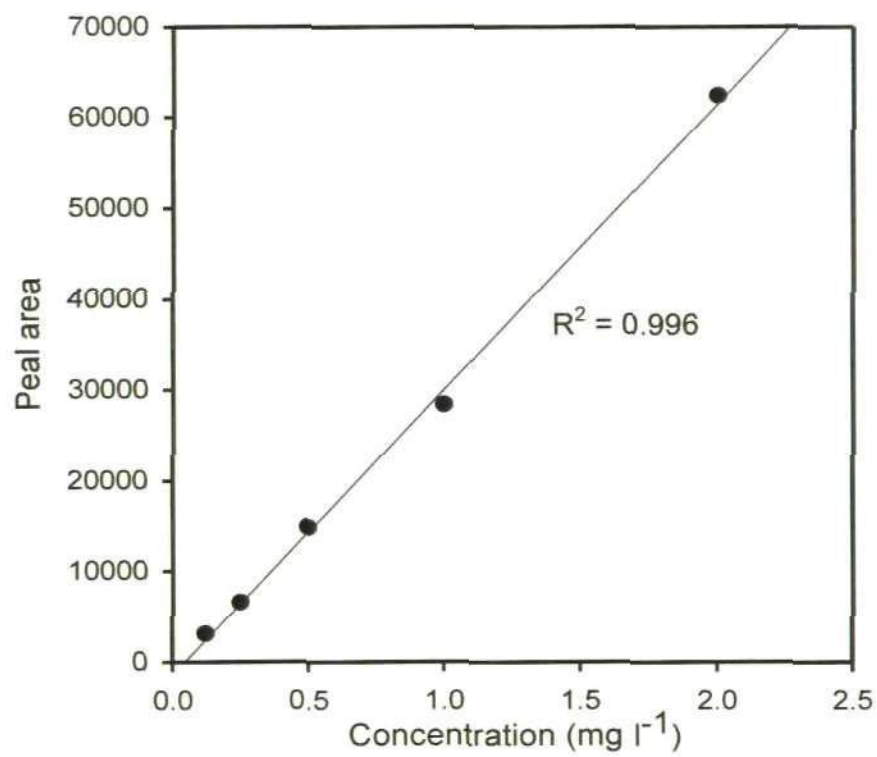


Fig. 2.3 A standard curve for C₆₀ analysis by HPLC using different concentrations ranging from 0.125 and 2.0 mg l⁻¹ using Elite C18.

2.9 *Statistical analyses*

Statistical analyses were performed using statistical package Stat graphics plus version 5.1 (Statistical Graphics Corp, USA). All results are presented as mean \pm S.E. Bartlett's test was applied for variance check. One- way analysis of variance (ANOVA) test was used, wherever the distribution of data was parametric. Non-parametric data were treated with Kurskal Wallis test. Multiple range tests was also used to differentiate between the groups of data, and only $P < 0.05$ was accepted as significant. In some experiment, data were analysed using two-way ANOVA to study the interaction effect between type and time of exposure. Regression analyses were applied wherever dose-response were observed.

Chapter 3

Optimisation of P-450 induction in *Mytilus edulis*

3.1 Introduction

Convincing evidence from many previous studies has shown the interest in use of hepatic microsomal cytochrome P-450 activities as biomarkers of pollution in aquatic species (Grøsvik et al. 2006; Livingstone 1996). Cytochrome P-450 monooxygenases are a family of protein isoenzymes involved in the biotransformation (oxidation) of organic compounds to convert them into less toxic derivatives and more excretable forms (Timbrell 2000). However, there are exceptions, in some cases the transformed chemicals are more toxic than the parent compound (Halliwell 1999). Induction as an environmental monitoring tool appears to have its greatest utility as a general indicator of contamination rather than for identification of specific pollutants.

Several experimental approaches have been used to demonstrate the induction of P-450 activity in several different ways, as described in **Table 3.1**. P-450 activity can be quantified using the carbon monoxide-binding spectra of the CO-P450 complex which produces a unique 450 nm absorption peak. A number of catalysed reactions use synthetic substrates (e.g. ethoxyresorufin for EROD assay or luciferin for luminescence) for measurements of P-450 activity. These activities are usually very low in control (unexposed) individuals. Detection of the presence and activity of P-450 can also be determined by substrates that are converted to a product that has at least one property that can be measured. Immunoquantitation methods such as immunoassays or immunoblotting techniques are very sensitive and simple to carry out once a suitable antibody is available. In addition to catalytic and immunological methods, presence and expression of mRNA level of P-450 genes are maybe investigated by using immunochemistry and Northern blot techniques. It is important to realize that

none of the methods mentioned previously can stand alone in the assessment P-450 and each method has its advantages and disadvantages.

Table 3.1 Different assays to demonstrate cytochrome P-450 induction.

Process	Measurement based on	methods
P-450 reaction	Catalytic rate	EROD fluorescence
		AHH fluorescence
		ECOM fluorescence
		Luciferin luminescence
		CO-binding spectra
P-450 translation	P-450 protein level	ELISA
		Western blot
P-450 transcription	mRNA level	cDNA
		Oligonucleotides
		Immunohistochemistry
		Northern blots

In our preliminary work, we have tested the assumption whether the pattern of P-450 induction with PAHs exposure in mussel is similar to fish (Fent and Bättscher 2000). *In vivo* exposures to benzo(k)fluoranthene (P-450 inducer) and phenanthrene (P-450 non-inducer) were carried out for 3 days, and exposure conditions were designed to stimulate P-450 induction in the digestive gland of *Mytilus edulis*. However, the results were considerably different to those found previously (Al-Subiai 2006), in which the absence of a typical 450 nm peak was reported in all examined microsomal/cytosolic fractions. Nevertheless, another peak was observed near 420 nm in CO-binding spectra (**Fig. 3.1**). There has been much debate about this peak in the literature, some studies have suggested that 420 peak is a degraded product of either P-450 or some other haemo protein (Gilewicz et al. 1984; Stegeman 1985; Yawetz et al. 1992). On the other hand, other studies have suggested that 420 nm peak corresponds to another haeme protein that interferes with detection of the 450 nm peak (Heffernan and Winston 1998; Livingstone et al. 1989). We assumed that P-420 peak is another form of P-450 with a modified active site (Hlavica 2006) and we tried to measure P-420 levels in microsomal/cytosolic sample from the exposure experiment. Spectroscopic measurements showed increases in P-420 level in the first day of the exposure to benzo(k)fluoranthene, however we could not rely on the result due to high variability ($0.007-0.210 \Delta A \text{ mg}^{-1} \text{ l}^{-1}$), as shown graphically in **Fig.3.2**. This led us to investigate P-450 induction in mussel *Mytilus edulis* using different methods to characterize the cytochrome P-450 activity.

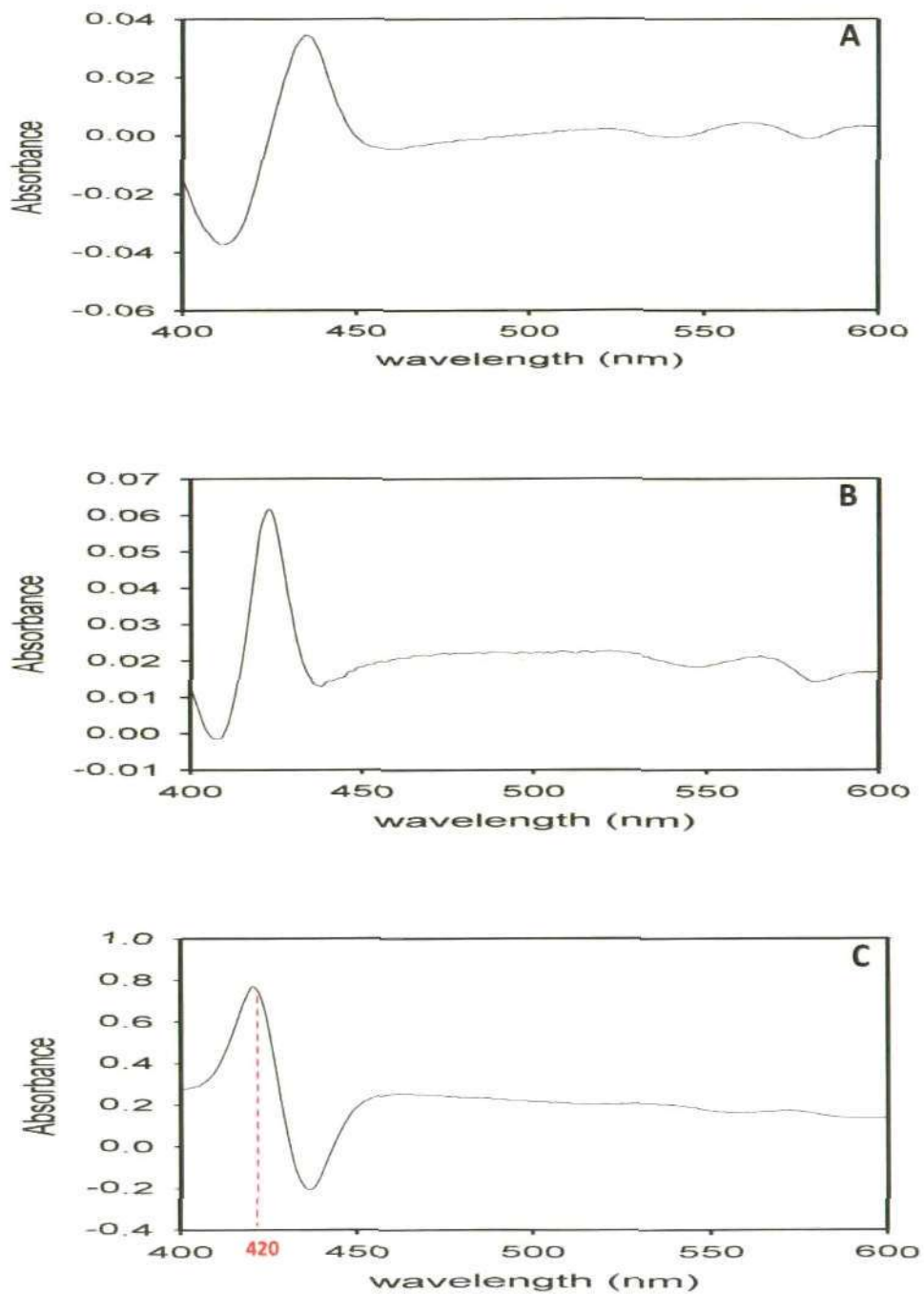


Fig. 3.1 Carbon monoxide difference spectra of digestive gland cytosolic/microsomal fraction. (A) dithionite-reduced sample. (B) The content of the sample cell was then saturated with CO, (C) the difference spectrum was calculated.

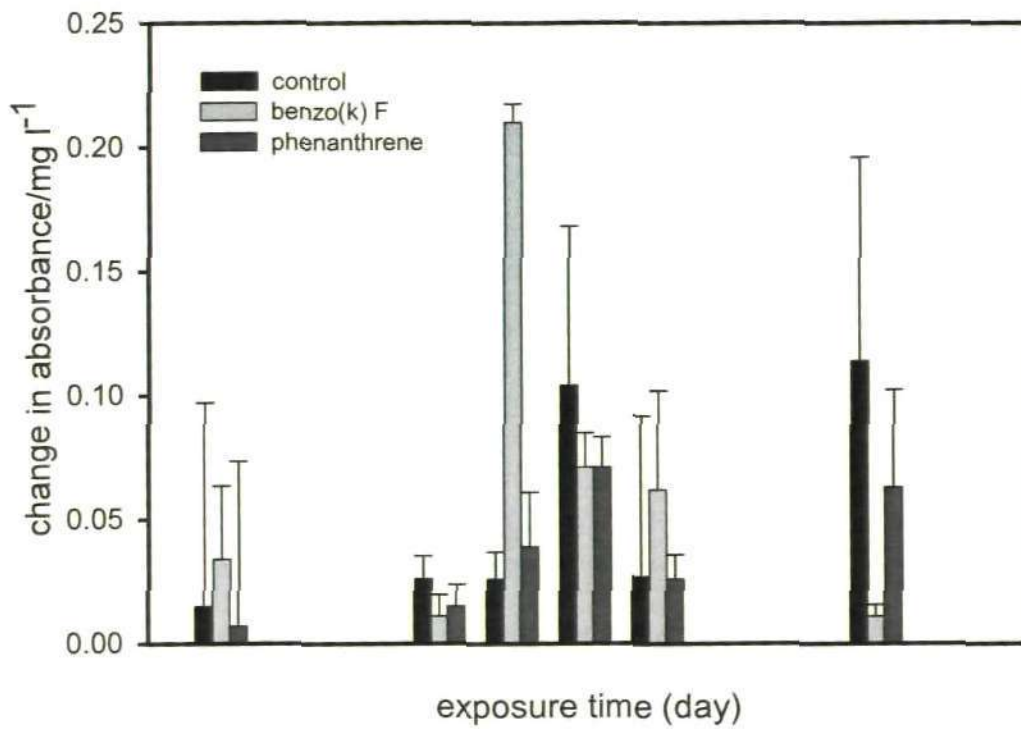


Fig. 3.2 P-420 levels in the digestive gland of *Mytilus edulis*. Exposure was only carried over days 4, 5 and 6. Data represent mean \pm S.E.

3.2 Materials and Methods

3.2.1 *Microsome preparation*

Microsomes were prepared according to the method of Shaw et al., (2004). Briefly, 6 g of pooled digestive glands from *Mytilus edulis* were extracted and homogenized by using mechanical homogenization in extraction buffer containing 10 mM Tris-chloride pH 7.6, 0.15 M KCl, 0.5 M sucrose, in a ratio of 1:4 (w/v). The homogenate was centrifuged at 500 g_{ve} for 15 min at 10 °C to remove cells debris, the supernatant was transferred to new centrifuge tube and centrifuged at 10,000 g_{ve} for 45 min at 4 °C. The post mitochondrial supernatant (PMS) was collected with a pipette carefully avoiding the pellet and the floating lipid layer. The PMS fraction was split equally into two centrifuge tubes, one tube used for ultracentrifugation and the other one used for the freeze and thaw method (Fig. 3.3).

3.2.1.1 *Ultracentrifugation*

The PMS fraction was centrifuged at 100,000 g_{ve} for 90 min at 4 °C (Beckman Coulter, USA). The supernatant was carefully removed to leave microsomal pellet. Microsomes were resuspended in 10 mM Tris-chloride, pH 7.6 containing 20% (v/v) glycerol and stored at -80 °C until analysis.

3.2.1.2 *Freeze and thaw*

Prior to any further centrifugation step, the PMS fraction was frozen at -20 °C and after 24 h the tube was allowed to thaw. Following freeze and thaw, the PMS fraction was centrifuged at 10,000 g_{ve} for 15 min at 4 °C. The supernatant was carefully removed to leave the microsomal pellet. Microsomes were

resuspended in 10 mM Tris-chloride, pH 7.6 containing 20% (v/v) glycerol and stored at -80°C until analysis.

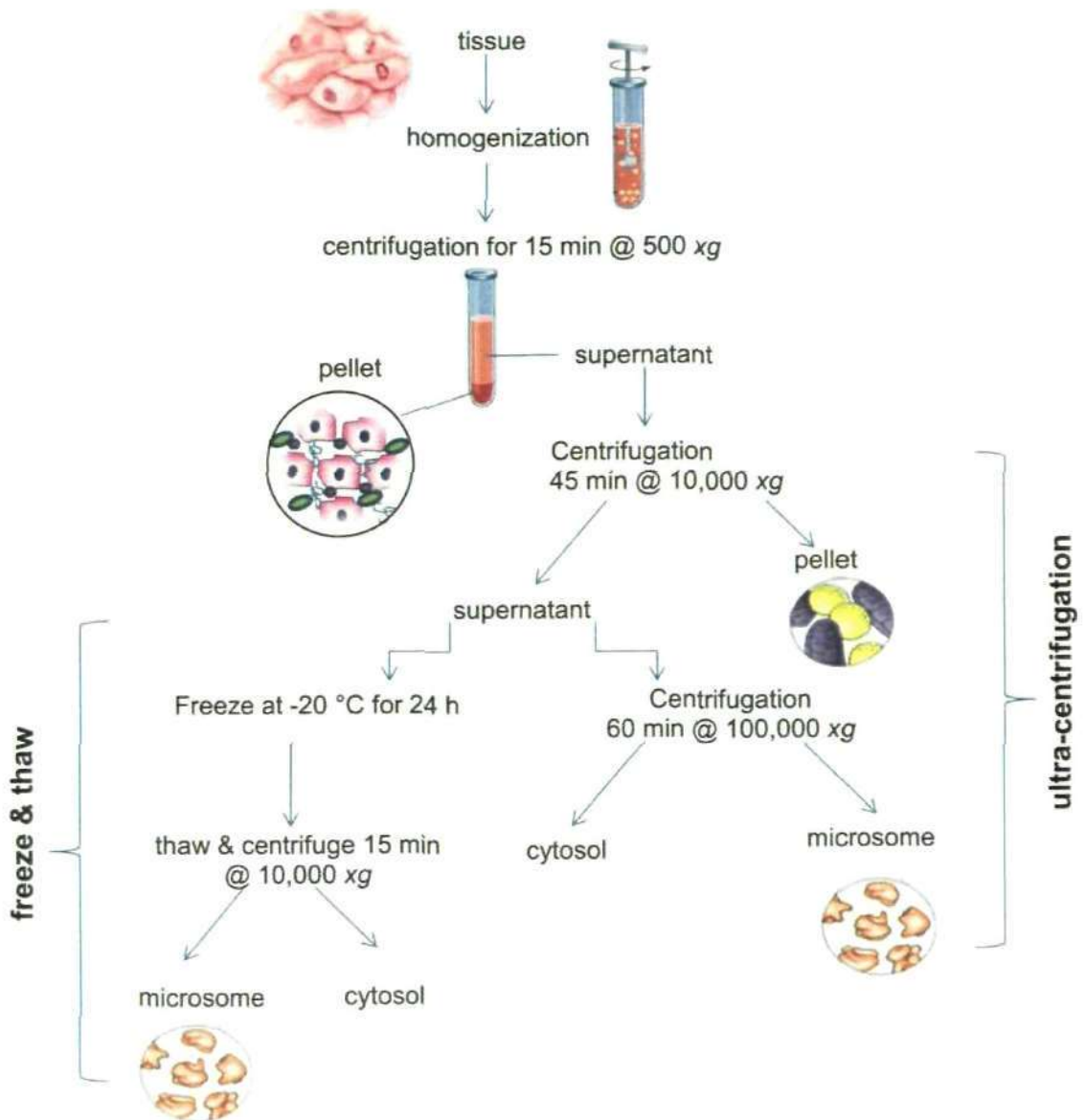


Fig. 3.3 Preparation of microsomal fraction from *Mytilus edulis* digestive gland using ultracentrifuge and freeze & thaw methods.

3.2.2 Gel electrophoresis

Western blotting combines gel electrophoresis to separate the proteins in the microsome fractions with the specificity of immunological detection. Gel electrophoresis was done using 8% sodium dodecyl sulphate-polyacrylamide gels (SDS-PAGE).

3.2.2.1 Glass plates assemblage and gel preparation

SDS-PAGE was carried out according to the method of Schägger (2006). A rubber gasket was fixed on the edge of the glass plate. Spacers were then placed on the plate in which the ridge of the gasket was directed upwards. The second flat glass was placed on top and clipped together.

The stock solutions prepared for gel electrophoresis are given in **Table 3.2**. All solutions were kept at room temperature with the exception of the bis-acrylamide mixture which was stored at 4 °C. The composition of separating and stacking gels is given in **Table 3.3**. The 8% acrylamide (29:1 acrylamide to bis-acrylamide) was used as a uniform separating gel. All the components of the gel were mixing together in Buchner flask and de-gassed, except TEMED and 10% APS (must be fresh) which were added at the end. Gently, the flask was swirled to mix and carefully gel was cast (~ 18 cm x 22 cm plate) by using a glass syringe connected to ~ 1 mm diameter tube to prevent air bubble generation. Ethanol was added (gently) on the top of the separating gel to give a very sharp liquid interface (visible within 10 min), as illustrated in **Fig. 3.4**. The separating gel was left to polymerize for at least 1 h. After termination of the polymerization, the surface of the gel was rinsed with distilled water before pouring of the 3% stacking gel (~1-2 cm). The plate was filled with stacking gel

solution and comb inserted into the gel by taking care not to trap any bubbles below the teeth.

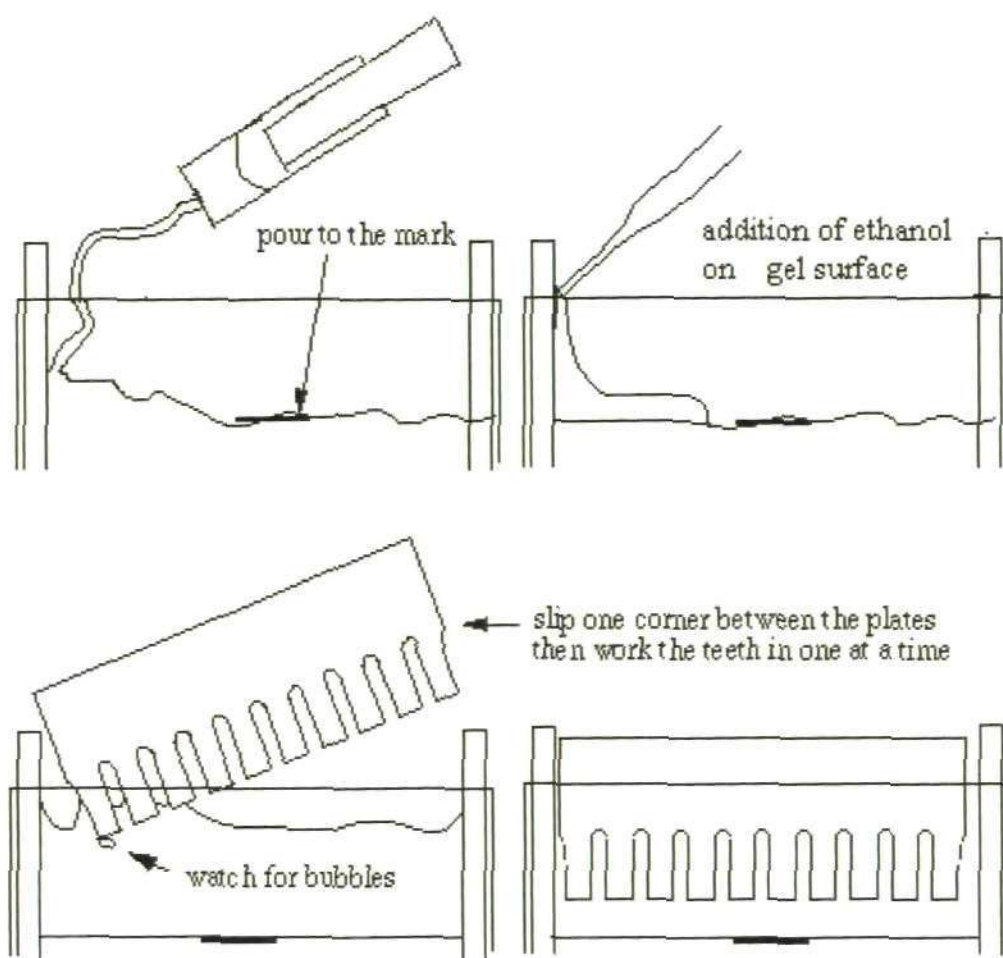


Fig. 3.4 Casting the gel. Slowly, the syringe was grabbed by thumb over the plunger and loaded with gel solution, by using small tip (5-200 μ l) connected to glass syringe and fixed to 5 cm length of tubing (1 mm diameter).

3.2.2.2 *Sample preparation*

The samples were diluted in ratio 1:3 volume of sample buffer (4% SDS, 12% glycerol, 50 mM Tris, 2% mercaptoethanol, 0.01% Bromophenol blue R adjusted with HCl to pH 6.8). The protein samples were then incubated for 30 min at 40 °C.

The comb and rubber gasket spacer were removed from the gel gently and the wells were rinsed with distilled water and the water drained off. The plate set was assembled in the vertical apparatus for running the electrophoresis (Sigma, Z37, 507-1). The upper chamber and the wells were filled with cathode buffer (10 x Tris-tricine-SDS buffer). A sufficient quantity of anode buffer was poured into the lower chamber of the electrophoresis apparatus until the bottom of the gel is immersed in buffer taking care to eliminate bubbles from the bottom of the gel, and the top was covered, while the electrodes reach into the buffer of the upper chamber. The sample was loaded to the bottom of a well. The top of the electrophoresis apparatus was assembled and connected the system to the power source (cathode (+) is connected to the upper buffer chamber). The electrophoresis was performed at room temperature and the run was started at 60 V. After about 30 min, when the sample had completely entered the stacking gel (or left the sample well), the voltage was raised to 140 V for ~ 2.5 h.

The power supply was then turned off and disconnected and the gel apparatus and the glass sandwich were disassembled. Carefully, the sandwich was placed on paper towels and the clamps were removed from the sandwich. Working on one side of the sandwich, the glass plates were gently prised apart by using the spacer as a lever. The bottom glass plate with the gel was lifted and the gel was transferred to an appropriate container filled with fixing buffer.

3.2.2.3 *Fixing, staining and destaining*

The compositions of all the solutions are listed in **Table 3.4**. The protein bands were fixed in a fixing solution for 30 min, before they were stained with staining solution for at least 2 h (or overnight) with shaking with rocker unit. A complete background of the gel was destained into two steps: (1) by shaking the gel in the destain II solution for two hours, the destaining solution being exchanged every half hour, followed by, (2) destaining of the gel in destain I solution, and then storage of the gel in the (3) preservation solution. A plot for molecular weight marker (Sigma-SDS6H2, M.W. 30,000-200,000) is presented in **Fig. 3.5**.

Table 3.2 Stock buffer solution for SDS-PAGE.

Buffers	Tris* (M)	Tricine (M)	pH	SDS (%)
Anode buffer	0.2	-	8.9	-
Cathode buffer	0.1	0.1	8.25	0.1
Separating buffer	3.0	-	8.45	0.3
Stacking buffer	1.64	-	7.5	0.3

(*) adjusted with HCl

Table 3.3 Composition of separating and stacking gel.

Solutions	Separating Gel 8% bis-acrylamide(ml)	Stacking Gel 3% bis-acrylamide(ml)
40% bis-acrylamide	7.0	1.125
gel buffer	11.67	3.72
TEMED	0.015	0.01
10% APS	0.15	0.1
H ₂ O	16.165	10.045

Table 3.4 Stock solutions for fixing, staining and destaining.

Solutions	acetic acid (%)	methanol (%)	H ₂ O	glycerol (%)	brilliantblue R (g)
fixing	7	40	530	-	-
staining	10	45	450	-	1
destain II	10	10	800	-	-
destain I	10	50	400	-	-
preservation	10	-	770	13	-

All solutions made up of 1L.

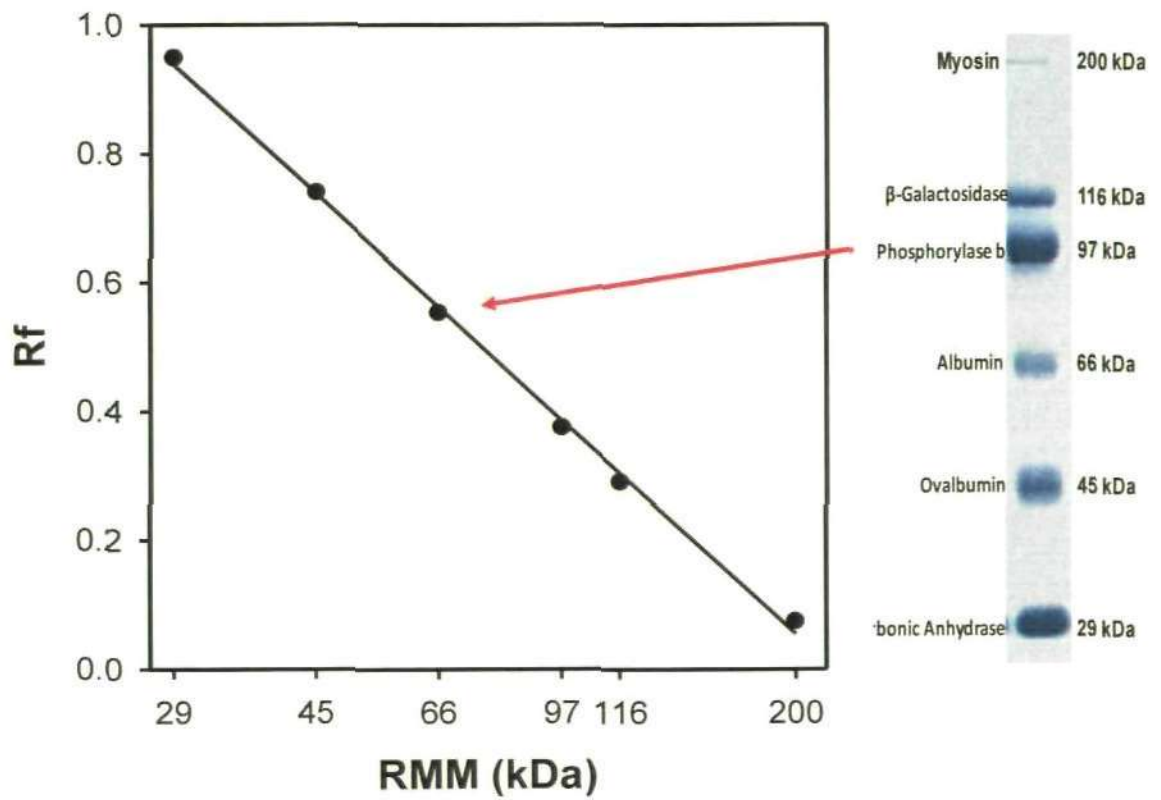


Fig. 3.5 Plot of the relative mobility of protein standards against the log of their molecular weight. Relative mobility, R_f , is the distance the protein has migrated from its point of origin).

3.2.3 Measurement of P-450 by western blot assay

3.2.3.1 Blotting

A previously electrophoresed sodium dodecyl sulphate-polyacrylamide gel containing separated proteins from microsomes (prepared using the ultracentrifuge and freeze & thaw methods, see section 4.2.1) were equilibrated in a tray full of blotting buffer for at least 10 min. The nitrocellulose membrane was cut to the exact size of the gel, wet in methanol for 50 s and equilibrated in the pure water for at least 2 min for activation. Gloves were worn at all times during handling of the membrane and assembling of the membrane gel sandwich. Using a gel holder with sponge supplied with the electroblotting apparatus, a sandwich was assembled as follows:

- One sponge pad was wet and placed on the cathode side of the gel holder.
- Two sheets of filter paper were cut to the size of the gel wet in blotting buffer.
- The pre-equilibrated gel was placed on top of the sponge pad, and the nitrocellulose membrane was placed on top of the gel.
- A clean glass tube was rolled across the membrane to carefully squeeze out any air bubbles trapped between the gel and the membrane.
- The second wet sheet of filter paper was placed on top of the membrane, and then rolled with a clean glass tube to remove air bubbles. The sandwich was completed by placing another sponge pad on top of the filter paper and closing the gel cassette.

- The cassette was placed in the blotting tank filled with blotting buffer, connected to a power supply and run to transfer enzyme protein for 1-2 h at a constant voltage of 100 V that was appropriate for 0.75 mm thick gels (thicker gels may need longer transfer times).

3.2.3.2 Blocking

The PVDA membrane was removed from the sandwich assembly and washed in 1 x PBS/0.05% Tween₂₀ to remove stain for 5 min. Then, the membrane was drained and 25 ml of 5% skimmed milk was added for 1 hour at room temperature on the shaker to block unoccupied sites on the membrane with protein sample. After blocking, the membrane was drained to be ready for primary antibody addition.

3.2.3.3 Incubation with primary antibody

The polyclonal anti-rainbow trout P450 1A1+1A2 antibody was obtained from Abcam laboratories (Cat # ab3713; Cambridge, UK) and diluted in 5% skimmed milk (1:1000 dilution + 0.01% azide). The diluted solution was added to the membrane in a volume sufficient to just cover it. The soaked membrane was then incubated overnight at room temperature with gentle shaking. The membrane was washed 3 times for 10 min each time with PBS/0.05% Tween₂₀.

3.2.3.4 Incubation with secondary antibody and development of colour

The horseradish peroxidase (HRP)-conjugated goat anti-rabbit secondary antibody was purchased from Abcam laboratories (Cat # ab6721; Cambridge, UK) and diluted in PBS/0.05% Tween₂₀ with 5% skimmed milk (1:3000) according to the manufacturer's instructions. Anti-rabbit immunoglobulin of rabbit origin was used as a primary antibody. The diluted antibody was then incubated for 2 h at room temperature with gentle shaking. The membrane was washed three times for 10 min each in PBS/0.05% Tween₂₀ as before. The developing solution (DAB/nickel chloride solution 0.06%: 0.03 w/v) was prepared just prior to use. The two solutions were mixed together and poured immediately over the membrane.

3.2.4 Measurement of 'cytochrome P-450 reductase' activity

'Cytochrome P-450 reductase' activities were measured in the cytosolic and microsomal fractions from mussel digestive gland. Five microliters of sample was incubated for 5 min with 200 μ l of 25 mM potassium HEPES buffer, pH 7.5, containing 3.5 mM NADH or 0.13 mM NADPH. The 'cytochrome P-450 reductase' reaction was then started by addition of the 3 μ l of 0.16 M of cytochrome *c* derived from horse heart (Sigma-C7752), and was monitored by measuring the absorbance change of 'upon reduction of cytochrome *c* absorbance at 550 nm minus the average of the absorbances at 540 and 560 nm (as described by Moody and Rich (1990)) in a diode-array spectrophotometer (WPI Ltd, UK). The initial rate of the reaction was calculated from the slope in the initial rate period.

3.2.5 Measurement of P-450 activity by bioluminescence assay

The catalytic activity of P-450 was measured using the conversion of luminogenic derivatives of luciferin to luciferin which in turn reacts with luciferase to produce light that is directly proportional to the activity of the P450, as illustrated in **Fig. 3.6**. CYP3A4 activity was analyzed in digestive gland microsomes. The assay was performed in triplicate in 96 well white opaque plate using the P450-Glo™ CYP3A4 assay (luciferin-PFBE) according to the manufacturer's protocol (Promega Corporation, Madison, WI, USA). Briefly, 10 μ l of microsomal sample was mixed with 1.25 μ l luminogenic P450 substrate (luciferin-PFBE) and 13.75 μ l of water. After equilibration for 5 min the reaction was started by the addition of 25 μ l of NADPH regeneration system. The assay was carried out for different incubation times (10, 30 and 45 min) at 22 °C to optimise the incubation conditions before adding 50 μ l of luciferin detection reagent. Luminescence measurements were conducted using a microplate reader luminometer (Mithras LB 940, Berthold Technologies GmbH & Co KG, Bad Wildbad, Germany).

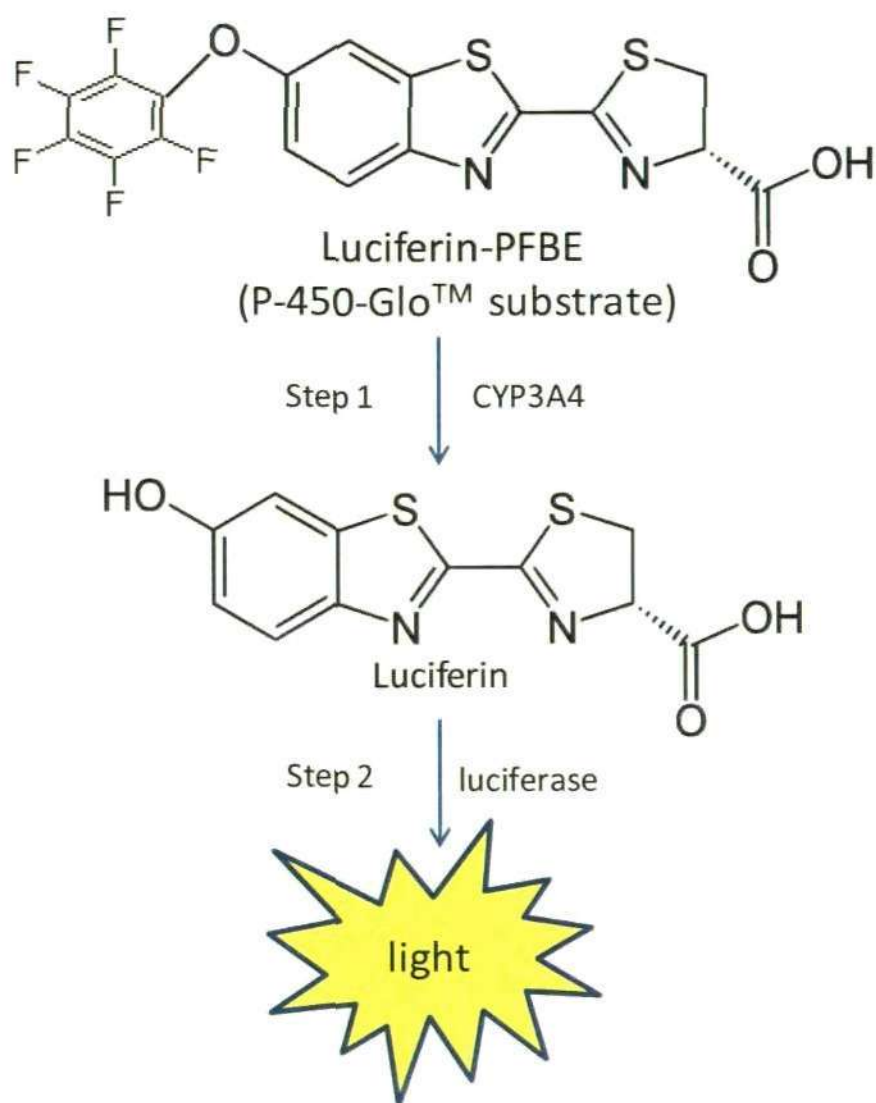


Fig. 3.6 Conversion of luciferin-PFBE (P-450-Glo substrate) by P-450. CYP3A4 enzyme act on luminogenic luciferin-PFBE substrate to produce a luciferin product that generates light with luciferin detection reagent.

3.3 Results & Discussion

3.3.1 *Standardizing the isolation of the microsomal fraction*

In the cell, microsomes are small vesicles that are derived from fragmented smooth endoplasmic reticulum (SER) produced when tissues such as digestive gland are mechanically homogenized. Microsomes are usually considered to contain the cell's cytochrome P450 enzymes which are involved in oxidative metabolism for many xenobiotics (Livingstone 1996; Solé et al. 1998).

At first, it was not possible to obtain microsomal fraction because the ultracentrifuge was broken (in house). For that reason we compromised by using microsomal/cytosolic fraction instead of microsomal fraction. In our preliminary work, cytochrome P-450 protein was determined in *microsomal/cytosolic fractions using CO difference spectra, but we could not depend on the result due to high variability*. We expected based on Livingstone, D.R (personal communication) to be able to detect P-450 when we extracted the microsomal fraction from digestive gland.

We tried to overcome this problem by investigating a new method for microsomal fraction preparation. The aim of this investigation was to modify an existing method of microsomal fraction isolation. Optimal isolation conditions for microsomal fraction were determined in preliminary investigations in which various steps in the isolation procedure were modified. According to Wilson and Walker (2005), the microsomal fraction can be concentrated and isolated from other cellular organelles by using the differential centrifugation method. In general, one can enrich for the following cell components, using increasing centrifugation speeds.

- Whole cells and nuclei at 500 x g
- Mitochondria, lysosomes and peroxisomes at 10,000 x g
- Microsomes and cytosol at 100,000 x g.

At 100,000 xg, ER pellet (reddish brown colour) comes out of suspension and the soluble enzymes remain in the cytosol (supernatant).

Previous experience with mitochondria suggested that a freeze thaw cycle might lead to aggregate of microsomal vesicles and allow them to be pelleted at much lower g values. (Moody, A.J., personal communication). Therefore we expected that after the microsomes-containing supernatant is slowly frozen at – 20 °C, thawed and recentrifuged again on the following day at the same speed the microsomes will be aggregated and therefore it would be possible to isolate them.

We tried the freeze and thaw cycle method and compared it with differential centrifugation method (An ultracentrifuge at the Marine Biological Association was used). The results of freeze and thaw cycle method were promising; although, there was less protein in microsomal fraction prepared using the freeze and thaw cycle method in comparison to that prepared in the conventional way. However, we found by using SDS-PAGE analysis that the freeze and thaw process could separate much of microsomal material. Furthermore, we found evidence that microsomes separated by freeze and thaw are similar (band pattern) to those separated by ultracentrifuge (see **Fig. 3.7**). The amount of protein recovered in the microsomal fractions was measured; **Table 3.5**; 66.7% and 30.2% protein recovery were obtained by freeze and thaw cycle in mussel and fish samples; respectively. The protein yield of digestive gland microsomal from differential centrifugation and freeze

and thaw methods is shown in **Fig. 3.7**. The protein content of microsomal fraction from the differential centrifugation method (338.0 ± 28.73 mg) was about 2.5-fold higher than that from the freeze and thaw method (102.1 ± 18.72 mg), a difference that was significant ($P < 0.05$).

Table 3.5 Protein recovery in microsomal fraction by using differential centrifugation and freeze and thaw methods, n =3.

Method of extraction	Sample	Recovered protein (mg ml⁻¹)*
Differential centrifugation	mussel microsome	3.3 ± 0.67
Freeze and thaw cycle	mussel microsome	2.2 ± 0.45
Differential centrifugation	fish microsome	10.4 ± 1.12
Freeze and thaw cycle	fish microsome	3.1 ± 0.56

*mg recovered protein in pellet per ml of supernatant

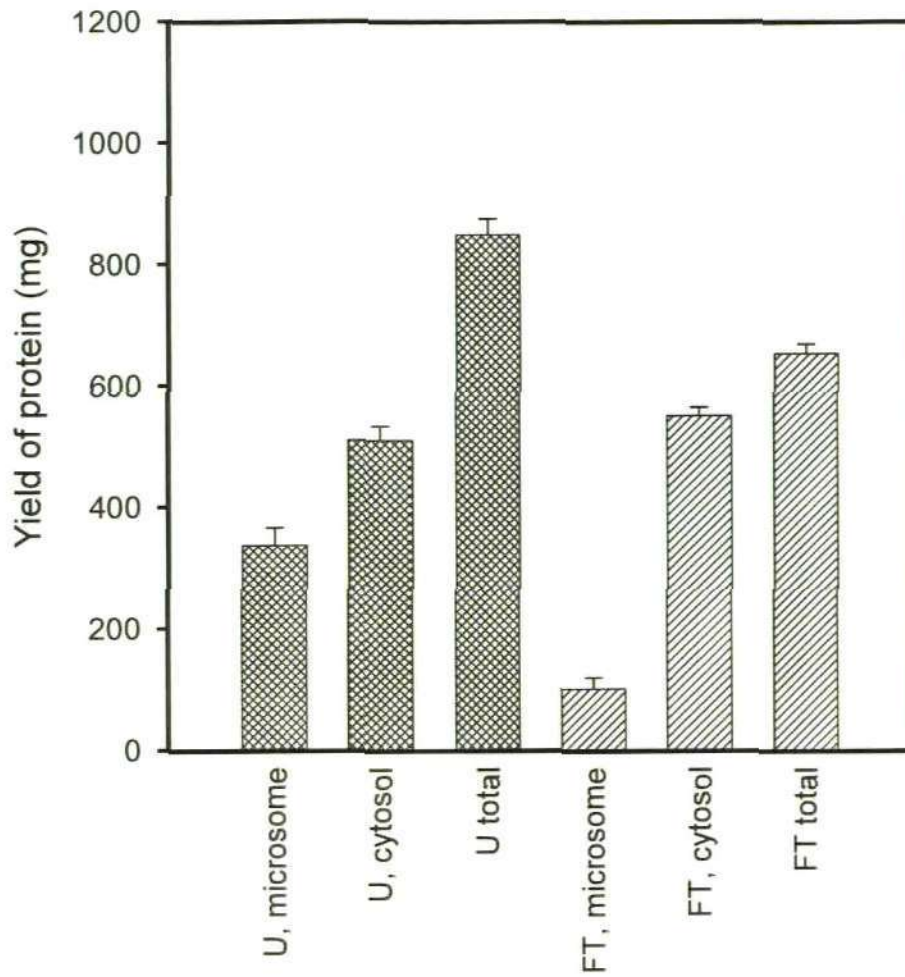


Fig. 3.7 Protein yield in the cytosolic and microsomal fractions of mussel digestive gland from differential centrifugation and freeze and thaw methods. The data shown are means \pm SE; $n = 3$. U = differential centrifugation; FT = freeze and thaw; U total = microsome + cytosol from differential centrifugation method; FT total = microsome + cytosol from freeze and thaw method.

3.3.2 Measurement of P-450 by western blot

We tried to measure P-450 level by immunological method which could measure specific protein (enzyme), section 3.2.2. Cytochrome P-450 1A1 is one of 11,000 different cytochromes P-450 and it is generally presented at very low levels in mussels (Im and Waskell 2011). Grøsvik et al (2006) had indentified CYP1A-immunopositive proteins in bivalves using polyclonal anti-perch CYP1A antibodies and they found two reactive bands of 50 and 75 kDa in digestive gland of *Mytilus edulis*. The immunological method requires the use of specific antibodies which specifically bind the target P450, to do this we tried to measure CYP1A-immunopositive protein using an apparently similar primary antibody (polyclonal anti-rainbow trout CYP1A).

A band at 54 kDa in the microsomal fraction of digestive gland has been observed in the SDS-PAGE (Fig. 3.8), but western blot assay did not show cross reactivity with any band on the PVDF membrane. The transfer process of the protein and antibody activity was checked by dot blot tests to check the efficiency of the western blot procedure. Three tests were carried out to determine if the antibodies and detection system were effective. The first test was run to check the efficiency of the western blot steps, in which the blotted membrane was stained with 0.5% Ponceau-S red solution for 1 min. All bands were detected as shown in Fig. 3.9 indicating that the blotting procedure was effective. To check the binding of the primary antibody to the membrane, 20 μ l of primary antibody (1:1000, diluted in 5% milk) was spotted onto the membrane and incubated for 1 h at room temperature to ensure that the blot was dry before going to the next step. Then the non-specific binding sites on the membrane were blocked with 5% dry skimmed milk in Tween₂₀ buffer for 1 hour

at room temperature and washed 3 times (10 minutes each) in Tween buffer. After washing, the dot was detected by Ponceau S (Fig. 3.9). Again the spot was detected showing that primary antibody was binding to the membrane. In the last test, 1 μ l of secondary antibody-HRP activity was mixed with Dab solution producing the brown colour which confirmed the activity of the conjugate. Therefore from the earlier tests we concluded that there was a problem with the binding between primary and secondary antibodies. It is worth mentioning that the supplier has provided us with new primary and secondary antibody, but it still did not work. With limited budget and time remaining, it was decided to measure P-450 levels with lumigenic substrate technique.

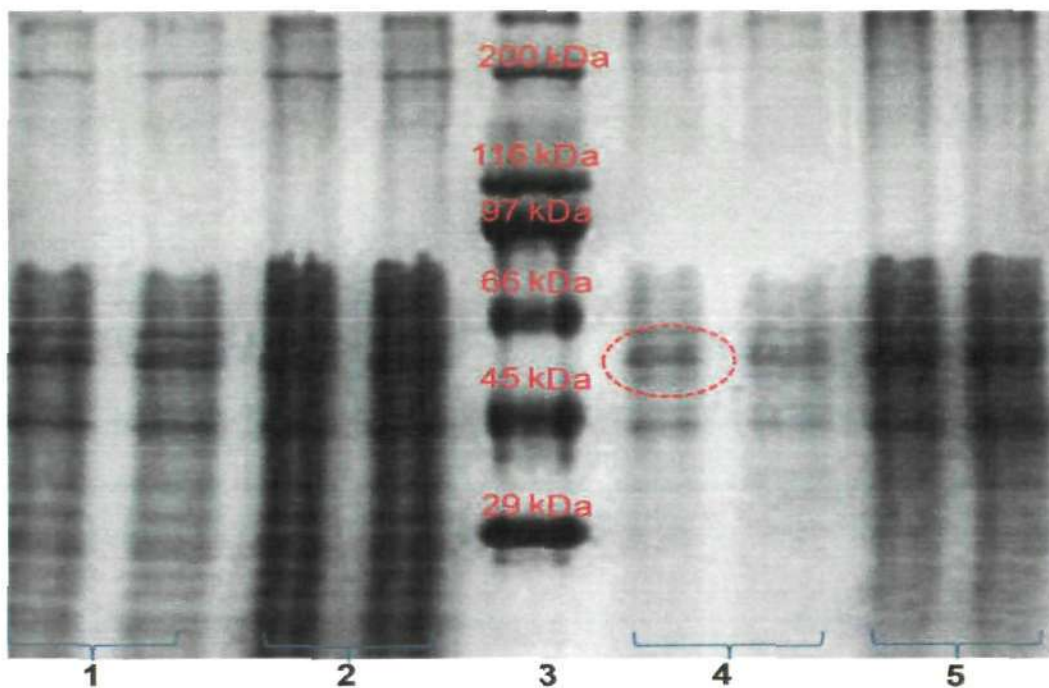


Fig. 3.8 Purification of *Mytilus edulis* microsomes. SDS-PAGE analysis using 8% polyacrylamide-SDS gel. 1 and 2, microsomal fractions (15 and 30 μ l were loaded respectively), prepared by ultracentrifuge method. 3, molecular weight marker. 4 and 5, microsomal fractions (15 and 30 μ l were loaded respectively), prepared by freeze and thaw method. Dashed circle showing 54 kDa band.

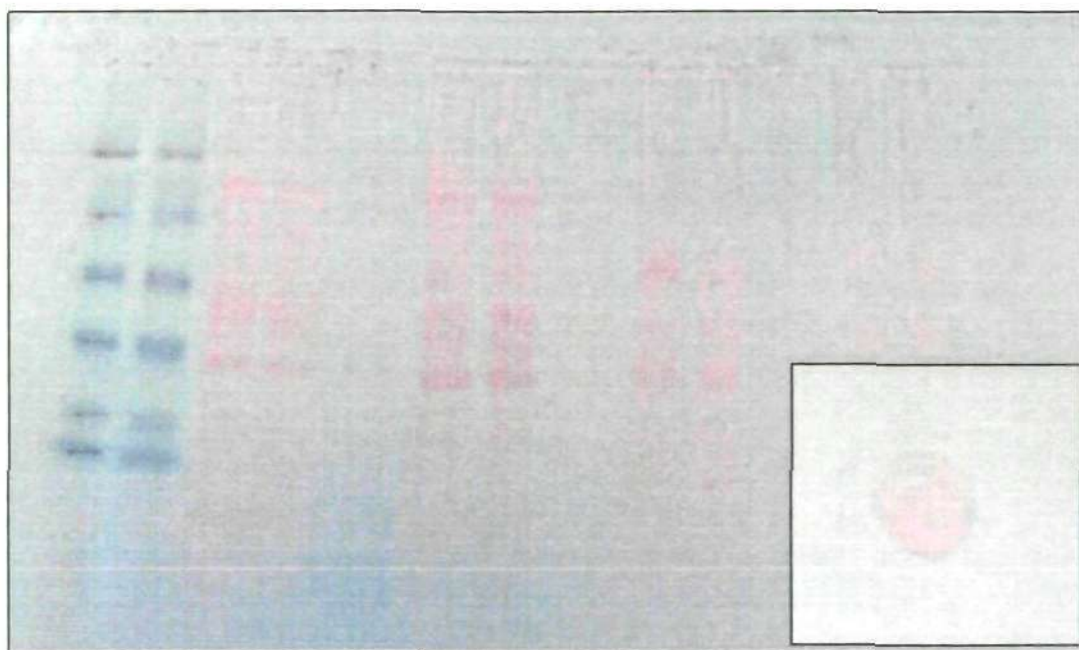


Fig. 3.9 Dot blot test showing the efficiency of the western blot procedure and the binding of the primary antibody to the PVDF membrane (inset) by Ponceau S stain.

3.3.3 Measurement of 'cytochrome P-450 reductase' activity

The P450 monooxygenation system, it is important to consider the role of the protein or proteins involved in electron transfer from a reducing cofactor (NADPH or NADH) to the terminal oxidase enzymes (i.e. P-450) in the electron transport chain (Solé and Livingstone 2005). Thus, any increased 'P-450 reductase activity' could give an indication of increased P-450 catalytic activity. In most eukaryote microsomes, flavin adenine dinucleotide (FAD) and flavin mononucleotide (FMN) could be carriers found as prosthetic groups in a 'P-450 reductase' enzyme (Degtyarenko and Kulikova 2001). As yet, however, cytochrome P-450 reductase activity is poorly defined in invertebrates. However we tried to measure NADPH-dependent and NADH-dependent cytochrome *c* reductase activity as a potential surrogate for cytochrome P-450 activity in digestive gland microsomes (**Table 3.6**) (Osman et al. 2007), section 3.2.3. The spectroscopic data indicate the presence and high activity of NADH-cytochrome P-450 reductase activity in digestive gland microsomes which suggests the presence of cytochrome P-450 like enzymes in mussels (**Fig. 3.10**). The results also demonstrate the existence of two different forms of 'cytochrome P-450 reductase' since activities are additive (**Table 3.6**). Also we noticed a high loss (~ 10-fold) in the total activity from both microsomal and cytosolic fraction in the freeze and thaw method, suggesting that the inactivation of 'cytochrome *c* reductase' in the first cycle of the freeze and thaw. In regard to the presence of the enzyme in cytosolic fraction, NADH-cytochrome *c* reductase activity in cytosol was negligible (1.76% of the total activity), whereas NADPH-cytochrome *c* reductase activity was found to be higher (29.9% of the total activity) indicating the presence of NADPH-dependent cytochrome *c* reductase activity.

We could not confirm P-450 induction in exposed samples since these measurements have been done in microsomal fractions. Our previous results showed the presence of P-450 like enzyme (or P-420) in cytosolic/microsomal, so the use of the microsomal fraction alone could lead to a general underestimation of its significance that could be available in the cytosolic fraction. Unfortunately, samples from the C₆₀ exposure (chapter 7) were lost (or misplaced) during the break down of a -80 °C freezer. Thus, we could not complete the evaluation of cytochrome P-450 reductase to support our findings due to time limitation.

Table 3.6 Cytochrome P-450 reductase' activity. The data shown are means \pm S.E.; n = 3.

Sample	Total yield of protein (mg)	NADH-cytochrome c reductase (nmol min ⁻¹ mg ⁻¹ protein)	NADPH-cytochrome c reductase (nmol min ⁻¹ mg ⁻¹ protein)	NADH/NADPH-cytochrome c reductase (nmol min ⁻¹ mg ⁻¹ protein)	Total NADH-cytochrome c reductase (nmol min ⁻¹)	Total NADPH-cytochrome c reductase (nmol min ⁻¹)
M-U*	338.0 \pm 28.73	31.89 \pm 2.53	3.27 \pm 1.34	35.16 \pm 1.94	10675 \pm 674.0	1091 \pm 432.4
M-FT*	102.2 \pm 18.72	8.30 \pm 2.67	0.99 \pm 0.07	9.29 \pm 1.37	863.4 \pm 292.0	103.3 \pm 26.68
C-U	511.0 \pm 23.46	0.38 \pm 0.08	0.203 \pm 0.09	0.58 \pm 0.09	195.4 \pm 44.00	107.7 \pm 50.58
C-FT	551.7 \pm 13.98	1.142 \pm 0.01	0.43 \pm 0.11	1.57 \pm 0.06	630.3 \pm 19.01	236.8 \pm 59.01

* M-U = microsomal fraction from differential centrifugation method; M-FT = microsomal fraction from freeze and thaw method; C-U = cytosolic fraction from differential centrifugation method; C-FT = cytosolic fraction from freeze and thaw method.

3.3.4 Measurement of P-450 activity by bioluminescence assay

The activity of P-450 was estimated by detecting the light produced from the reaction of luciferin with luciferase, as illustrated in **Fig. 3.6**. We optimised the incubation time with digestive gland microsomes for luciferin-PFBE biotransformation. By comparing the activities of CYP3A4 with different incubation times, we observed low luminescence signals with 10 min incubation in comparison to 30 and 45 min incubation (**Fig. 3.10**). Therefore, 45 min incubation was chosen for the assay as it gave highest luminescence signals. However, with all incubation times, there was a decline in the luminescent intensity after the addition of the luciferin detection reagent. We noticed that the decline started immediately after the luciferase was added to the assay mixture. Also we observed that the luminescence intensity decreased faster with larger sample volumes. The possibility that this was simply caused by interference with the P-450 assay was checked by using a range of different sample dilutions (2-10 fold dilution). It was found that luminescence intensity was dependent of the sample volume used in the assay. In fact, higher luminescence values were found, with more diluted sample (10-fold), as shown in **Fig. 3.11**. The cause of the decline in luminescence 2-fold diluted sample is not yet well understood, but is possibly due to the product inhibition of the light output by oxyluciferin (non-excited state). The more luciferin is oxidised, the more oxyluciferin accumulates in the solution. The decline in the light intensity is observed when an excessively large amount of luciferin is provided, which is assumed to slow down the reaction (Ohmiya et al. 2010).

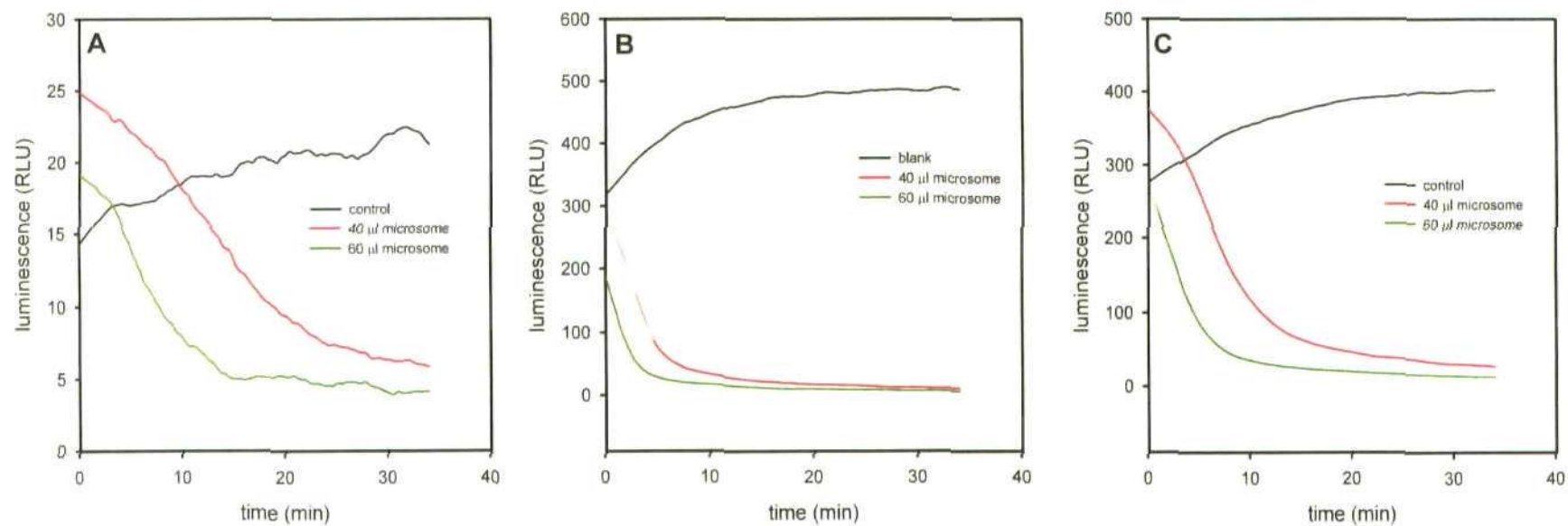


Fig. 3.10 P-450 luminescence activity in digestive gland microsomal fraction with different volume of samples and incubation times; (A) 10 min, (B) 30 min and (C) 45 min.

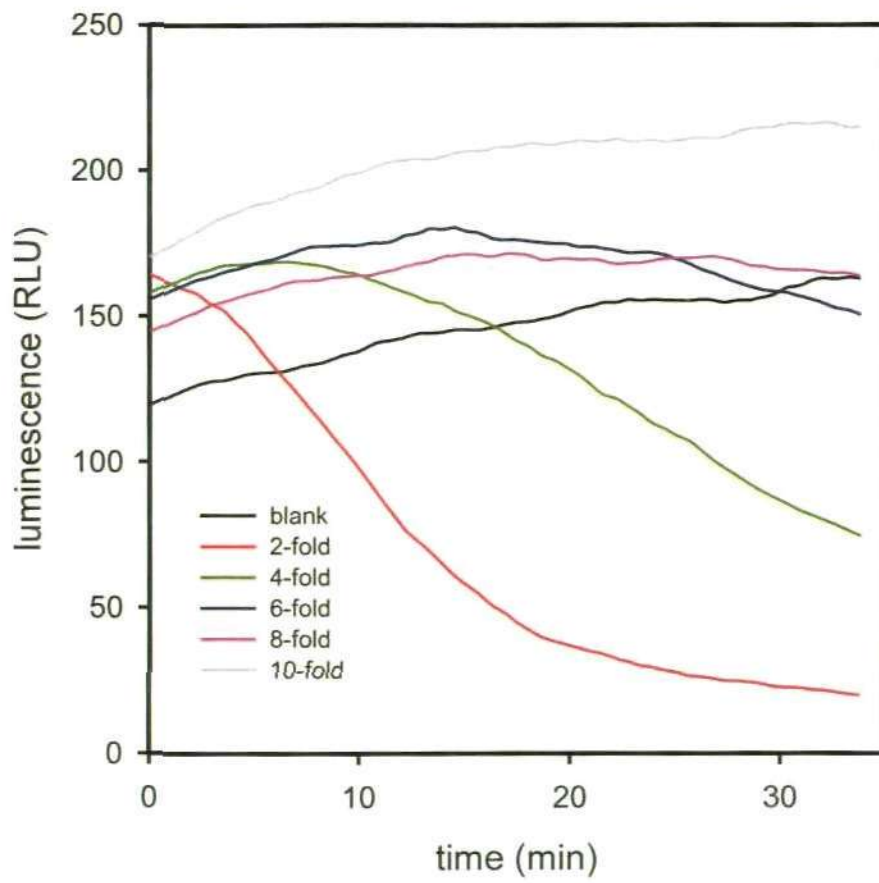


Fig. 3.11 P-450 luminescence activities in different dilution of digestive gland microsomal fraction.

After optimization of assay conditions, the P450-Glo assay held considerable promise to be used as an effective, inexpensive, high-throughput, and sensitive screening assay to measure P450 activity in the digestive gland of mussel from fresh (FC₆₀) and aged C₆₀ (AC₆₀) *in vivo* exposure (chapter 7). Early comparison between 2 and 10-fold diluted samples (digestive gland microsome) confirmed again that luminescence signals in concentrated sample (i.e. 2-fold) is less reproducible compared to 10-fold dilution (**Fig. 3.12**). In 10-fold diluted samples, there was a significant increase in the luminescence in ASW, AC₆₀ and FC₆₀ exposed samples in comparison to the control sample ($P = 0.001$, ANOVA), with highest signal in FC₆₀-exposed sample (14.80 ± 0.31 RLU). However, direct comparison cannot be applied without measuring protein concentration in these samples and due to loss of the samples we could not confirm this activity.

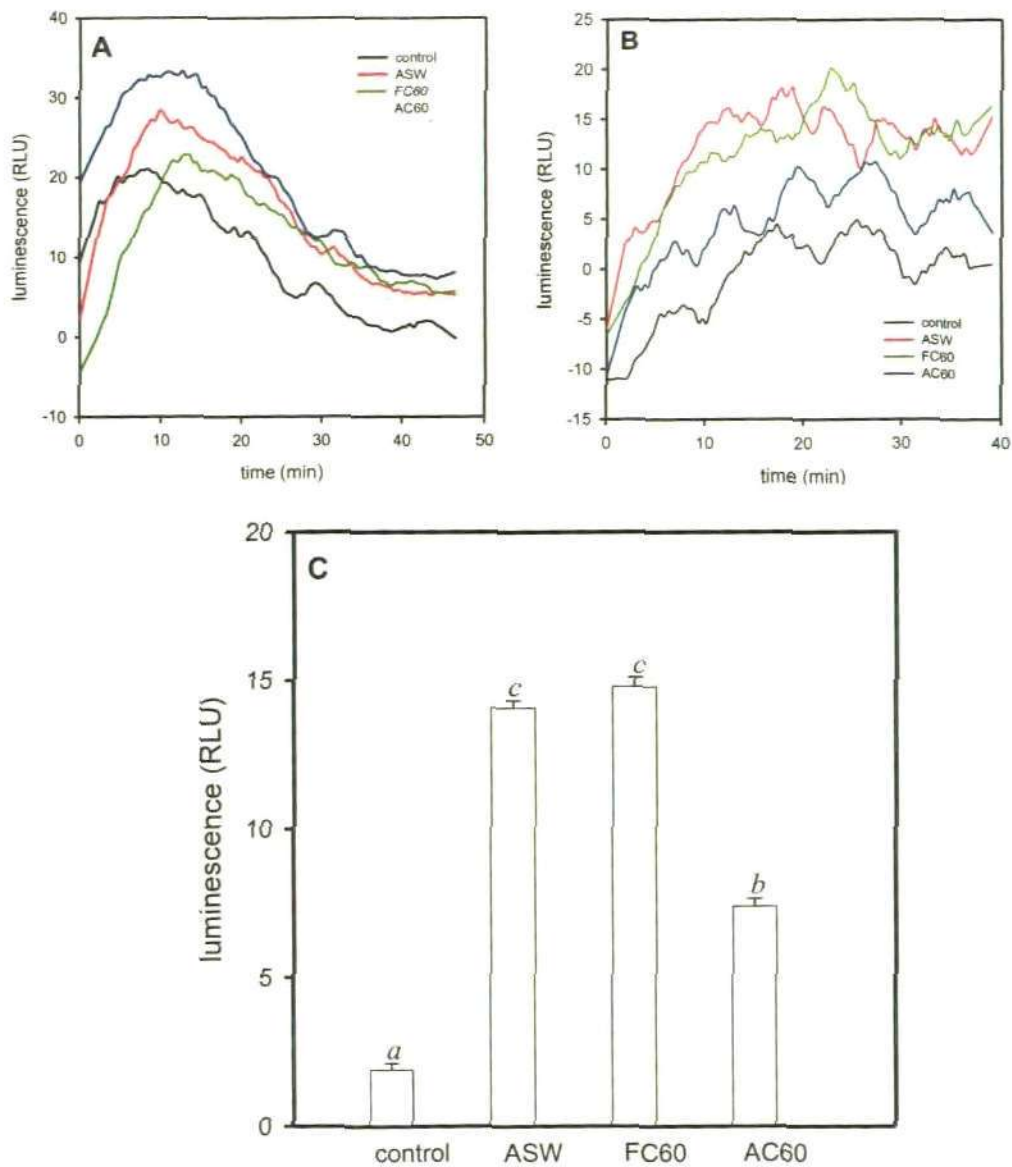


Fig. 3.12 P-450 luminescence in microsomal fraction of *Mytilus edulis* digestive gland following 3 days *in vivo* exposure to ASW, FC₆₀ and AC₆₀ (details available in chapter 7). (A) 2-fold dilution; (B) 10-fold dilution; (C) P-450 luminescence in 10-fold diluted sample calculated between 20-40 min. The data shown in panel (C) are means \pm S.E., $n = 3$. Bars with the same letters are not significantly different according to the multiple range test (LSD). ASW = aged seawater, FC₆₀ = fresh C₆₀, AC₆₀ = aged C₆₀.

3.4 Conclusion

In spite of the lack of evidence of P-450 induction in the present study (due to laboratory, budget and time problems), biomarker tools have been established in the digestive gland of *Mytilus edulis*. Our previous laboratory work demonstrated the presence of P-450-like enzymes i.e. the 'P-420' and spectroscopic signal has been supported with bioluminescence and 'cytochrome P-450 reductase' results. It is important to realise that none of the individual methods used in the present study can stand alone in the assessment of P-450 induction. Further studies, using exposed samples, are needed to more fully understand the mollusc cytochrome P-450 system, including structure-activity relationships for xenobiotic monooxygenation and the role of NADH/NADPH-cytochrome P-450 reductase in cytochrome P-450 system.

Chapter 4

Validation and optimisation of total glutathione content in *Mytilus edulis*

Results from this chapter have been presented at the SETAC 2006 Scientific Conference, Liverpool, UK, Sep 2006 and the SETAC Congress 2008, Sydney, Australia, Aug 2008. The results have also been published in *Ecotoxicology*, 18, 334-342 (Al-Subiai et al., 2009).

Abstract

Haemolymph samples and haemocytes collected via the adductor muscles of bivalve molluscs are extensively used in ecotoxicological studies. Withdrawal of haemolymph from mussels, *Mytilus edulis*, via the posterior adductor muscle, may lead to contamination with the intracellular contents of adductor myocytes. Lysopine dehydrogenase (LyDH) activity, an adductor myocyte marker, was used to investigate the impact of this potential contamination on levels of total glutathione, glutathione peroxidase (GPx) and acetylcholinesterase (AChE) measured in cell-free haemolymph. The mean glutathione content of cell-free haemolymph from 28 mussels was $3.2 \pm 1.8 \mu\text{M}$ (mean \pm S.D.). There was a linear relationship (slope = $0.28 \pm 0.03 \text{ min}$; mean \pm S.E; $P < 0.0001$, $n = 28$) with haemolymph LyDH levels suggesting that at least some of the glutathione measured in cell-free haemolymph had arisen from contamination. Haemolymph LyDH activity was significantly higher in samples extracted using larger diameter needles, and also in samples where there had been some difficulty in the extraction. Exposure of mussels to oxidative stress using $40 \mu\text{g l}^{-1}$ Cu for 5 days resulted in a 1.7-fold increase in glutathione ($P = 0.033$), but no increase ($P = 0.810$) in LyDH activity in adductor muscle. This was reflected in a similar increase in the slope of a plot (**Fig. 4.2**) of cell-free haemolymph glutathione versus LyDH activity ($P = 0.011$), consistent with both of these having originated from the adductor muscle. Cell-free haemolymph GPx and AChE activities also correlated with LyDH activity (Spearman rank correlation coefficients of 0.531 ($P = 0.0068$) and 0.537 ($P = 0.0062$), respectively, $n = 27$) suggesting that these also arise from contamination of the haemolymph. For

GPx there was a significant linear relationship ($P = 0.025$) with haemolymph LyDH levels consistent with both enzymes originating from the myocytes. However, there was hyperbolic relationship ($P = 0.0004$) between haemolymph AChE and LyDH activities. It appears that this is because the AChE originates from a different compartment to the LyDH, i.e. cholinergic neuromuscular junctions in the adductor muscle. We conclude that it would be prudent, when considering the possibility of using a biomarker in cell-free haemolymph from bivalve molluscs, to check whether contamination could be an issue.

4.1 Introduction

The haemolymph of bivalve molluscs, like mammalian blood, is an attractive tissue to use in assessing biochemical and genotoxicological responses to environmental stressors, such as hypoxia (Monari et al., 2005), parasite infestation (Muñoz et al., 2006), radionuclides (Jha et al., 2005), metals (Tran et al., 2007) and organic pollutants (Galloway et al. 2002; Pan et al., 2006; Rickwood and Galloway 2004). Both haemocytes and cell-free haemolymph (plasma) have been used in such investigations, e.g. haemocytes, for the assessment of DNA damage using single cell gel electrophoresis (Comet assay) (Jha et al., 2005) or cell-free haemolymph, for the assessment of acetylcholinesterase levels (Galloway et al., 2002). The advantages of haemocytes over cells from other tissues, such as gill tissue, for genotoxicological studies have been discussed by (Dixon et al. 2002). Haemolymph is simple to extract via either the posterior or anterior adductor muscles, and there is the possibility of non-destructive sequential sampling of haemolymph from the same individuals, at least for some species (Gustafson et al., 2005; Owen et al., 2002).

In rats oxidative stress induced by exposure to reactive oxygen species (ROS) (e.g. *t*-butyl hydroperoxide), or ROS generators (e.g. diquat) causes an increase in plasma glutathione levels through excretion of oxidised glutathione by the liver (Adams et al., 1983). In contrast, acetaminophen or diethyl maleate, which cause oxidative stress by depletion of hepatic glutathione, cause a decrease in plasma glutathione. In mammals, contamination of plasma with glutathione from

the lysis of red blood cells is a potential problem (Giustarini et al., 2007). However, this source of contamination is much less of an issue in bivalve haemolymph, where there is no equivalent to red blood cells, and where the abundance of haemocytes is low (Carballal et al., 1997; Pipe et al., 1997). Hence, the possibility of using glutathione levels in the cell-free component of bivalve haemolymph as an indication of 'global' oxidative stress, in an analogous way to that used by Adams et al., (1983) in rats, is particularly appealing.

However, during preliminary work aimed at testing this idea we found that total glutathione levels in the cell-free haemolymph of the blue mussel, *Mytilus edulis*, were highly variable (>20 fold difference) between highest and lowest concentrations measured. This led us to investigate whether the cell-free haemolymph could be being contaminated with glutathione derived from the adductor muscle through which it was extracted. To address this issue we used an opine dehydrogenase activity (lysopine dehydrogenase) as an intracellular marker that was assumed in this case to be derived from adductor myocytes (Gäde and Grieshaber 1986). Here we report that much of the glutathione detected in cell-free haemolymph is apparently of adductor myocyte origin. Furthermore, we provide evidence that glutathione peroxidase and acetylcholinesterase activities measured in cell-free haemolymph may also arise from contamination of the haemolymph from compartments within the adductor muscle.

4.2 Materials and Methods

All reagents were obtained from Sigma-Aldrich (Poole, UK.) unless otherwise stated.

4.2.1 Animal collection and maintenance

Mussels (*Mytilus edulis*) were collected from their natural beds at low tide (January 2007) from Port Quin (Cornwall, UK), a relatively clean site. Animals were allowed to acclimatise in laboratory conditions for 2 weeks as described in section 2.1 prior to experiments.

4.2.2 Extraction of haemolymph

4.2.2.1 Extraction of haemolymph: method 1

From each mussel, haemolymph was extracted from the posterior adductor muscle, as described in section 2.3.1. Samples were centrifuged for 2 min to remove the haemocytes; the cell-free haemolymph was then either placed on ice until use (for opine dehydrogenase and glutathione peroxidase measurements) or stored at -80 °C (for acetylcholinesterase activity and total glutathione level measurements).

4.2.2.2 Extraction of haemolymph: method 2

An alternative method for extracting haemolymph was also used in which a small notch was made across both valves using a 1 mm wide file. The notch (<1 mm in length) was made adjacent to the location of the posterior adductor, but sufficiently far from it (1–2 mm) so that it was not damaged by the file. Haemolymph was then extracted using a 21 gauge needle as described in section 2.3.1.

4.2.3 Preparation of adductor muscle extract

The posterior adductor muscles from three mussels (0.2 g wet weight) were dissected out and were homogenized using the method in section 2.3.2. The crude homogenate was centrifuged for 35 min (10,500 g_{av} at 4 °C) after which the supernatant was separated and stored at -80 °C until use.

4.2.4 Exposure of mussels to copper

Forty-eight mussels (*Mytilus edulis*) were divided between six 8 l tanks (eight mussels per tank) of sea water. Mussels in three of these tanks were exposed to 40 $\mu\text{g l}^{-1}$ Cu, by adding $\text{CuSO}_4 \cdot 5\text{H}_2\text{O}$; the other three tanks were used as controls. The exposure to copper was maintained for 5 days during which time the water was replaced daily, with the fresh water being re-dosed with $\text{CuSO}_4 \cdot 5\text{H}_2\text{O}$. The water in the control tanks was also replaced daily. Before replacing the water, the tanks were checked for mortalities and any dead animals were removed; there were four dead mussels in the Cu-containing tanks, and none in the control tanks. The mussels were not fed throughout the exposure period. This concentration and duration of exposure were chosen on the basis of published data on the genotoxic (micronucleus and alkaline elution methods) effects of Cu on the closely related species *Mytilus galloprovincialis* (Bolognesi et al., 1999); we have also found that 40 $\mu\text{g l}^{-1}$ Cu is genotoxic (Comet assay) in *M. edulis* (chapter 5). At the end of the exposure, haemolymph was extracted from each mussel using method 1 described above in section 4.2.2.1, and the total glutathione and lysopine dehydrogenase activity in each sample measured (see below), except for two control mussels, where insufficient haemolymph was extracted. The posterior adductor muscle was then dissected from each mussel, and adductor muscle extracts were prepared

as described above. For this, adductor muscles from 3 to 4 mussels were pooled together; this meant that two extracts were prepared per tank. Total glutathione and lysopine dehydrogenase activity were also measured in these extracts.

4.2.5 Measurement of biochemical parameters

All biochemical parameters were measured in triplicate in a microplate reader (Optimax, Molecular Devices, Sunnyvale, CA, USA) using 96 well plates. The assay temperature in each case was 22 °C.

4.2.5.1 Measurement of total glutathione

The total glutathione (i.e. reduced, GSH, and oxidised, GSSG) content of cell-free haemolymph was determined as described in section 2.5. The decrease in absorbance at 412 nm was measured over 5 min. A 20 μ M GSH standard and a 0 μ M blank were used, to calibrate the results.

4.2.5.2 Measurement of opine dehydrogenase (ODH) activity

The activity of ODH was measured essentially as described in the Sigma-Aldrich protocol for octopine dehydrogenase (Gäde and Grieshaber 1975) except that the assay pH was 7.5 rather than 6.5 (to decrease the background rate of autoxidation of NADH) and the L-arginine was replaced with different amino acid substrates. The complete assay mixtures for the opine catabolic reactions were 50 mM potassium HEPES buffer, pH 7.5, containing 4.2 mM NADH; 60 mM amino acid (neutralized) and 60 mM sodium pyruvate. The sample, either 50 μ l of cell-free haemolymph or 50 μ l of adductor muscle extract diluted either 5 or 10-fold with extraction buffer, was added to 250 μ l of assay mixture, and the rate of decrease of absorbance at 340 nm (oxidation of NADH)

was measured for 30 min. It is important to use fresh samples for these measurements as we found that storage at $-80\text{ }^{\circ}\text{C}$ for one week introduced a lag in oxidation of NADH, and even after maximal rates were achieved these were substantially lower (around 9%) than those seen with fresh samples (Table 4.1).

Table 4.1 Opine dehydrogenase (ODH) rate in fresh and frozen haemolymph samples.

sample	LyDH rate in fresh sample (min^{-1})	LyDH rate in frozen sample (min^{-1})	% rate loss	Average rate loss
1	1.101×10^{-4}	2.146×10^{-6}	1.949	
2	1.692×10^{-4}	1.074×10^{-5}	6.348	
3	1.241×10^{-4}	3.829×10^{-6}	3.085	
4	1.781×10^{-4}	2.160×10^{-5}	12.128	8.20 ± 2.17
5	1.327×10^{-4}	8.161×10^{-6}	6.150	
6	3.097×10^{-4}	2.830×10^{-5}	9.138	
7	2.848×10^{-4}	5.303×10^{-5}	18.62	

4.2.5.3 Measurement of glutathione peroxidase (GPx) activity

GPx activity, using H_2O_2 as a substrate, was assayed by following the rate of oxidation of NADPH at 340 nm in the coupled reaction catalysed by glutathione reductase (Lawrence & Burck 1976), as described by Tran et al., (2007), with the exception that cyanide was included here. Just before assay, a mixture containing 50 mM potassium HEPES buffer, pH 7.5, 1 mM EDTA, 0.13 mM NADPH, 0.1 mM sodium cyanide, 1.1 U ml⁻¹ glutathione reductase and 1 mM GSH was prepared; 290 μ l of this mixture and 15 μ l of cell-free haemolymph were mixed and the reaction started by addition of 5 μ l of 12.4 mM H_2O_2 . The absorbance decrease was monitored for 5 min.

4.2.5.4 Measurement of acetylcholinesterase (AChE) activity

The AChE activity was determined in cell-free haemolymph using a modification of the colorimetric method of Ellman et al. (1961) as described by Galloway et al., (2002). Cell-free haemolymph (15 μ l) was incubated for 5 min with 280 μ l of buffered DTNB (270 μ M in 50 mM potassium phosphate, pH 7.5). The AChE-catalysed reaction was then started by addition of the 6 μ l of 3 mM of acetylthiocholine iodide (ATCI), and was monitored by measuring the rate of increase of the absorbance at 412 nm, over 5 min.

4.2.5.5 Determination of protein

The total protein in cell-free haemolymph was determined spectrophotometrically using a commercial kit (BioRad, UK) with bovine serum albumin as the standard.

4.3 Results

4.3.1 Measurements of glutathione levels in cell-free haemolymph

Initial results for the total glutathione (GSH and GSSG) content in mussel haemolymph showed considerable inter-individual variation ($3.2 \pm 1.8 \mu\text{M}$, mean \pm S.D., $n = 28$). A possible explanation for this is that the haemolymph was becoming more or less contaminated with intracellular glutathione depending on the amount of damage caused to the adductor muscle during extraction of the haemolymph. To test this hypothesis, we measured the activity of an opine dehydrogenase, as a marker of cell damage.

4.3.2 Measurements of opine dehydrogenase activity in cell-free haemolymph

An experiment was carried out to find out which of these amino acid substrates gave the highest activity in an adductor muscle extract from *M. edulis*. The activity with the five amino acids tested was ranked as follows: L-lysine > L-arginine >> glycine > L-alanine. No activity was observed with L-histidine (**Fig. 4.1**). We found higher activity with L-lysine than with L-arginine, and it was decided then to use L-lysine as the substrate, i.e., to measure NAD-dependent D-lysopine dehydrogenase (LyDH) activity as a marker to detect intracellular contamination of cell-free haemolymph by intracellular material from myocytes.

In the same haemolymph samples that we measured glutathione levels earlier, we found a significant ($P < 0.0001$) linear relationship (slope = 0.0280 ± 0.0028 min; mean \pm S.E) between glutathione levels and LyDH activity (**Fig. 4.2**). Extrapolation to zero LyDH activity gave a value for cell-free haemolymph

glutathione ($0.74 \pm 0.29 \mu\text{M}$; mean \pm S.E) which though low is significantly greater than zero ($P = 0.0169$) (Fig. 4.2).

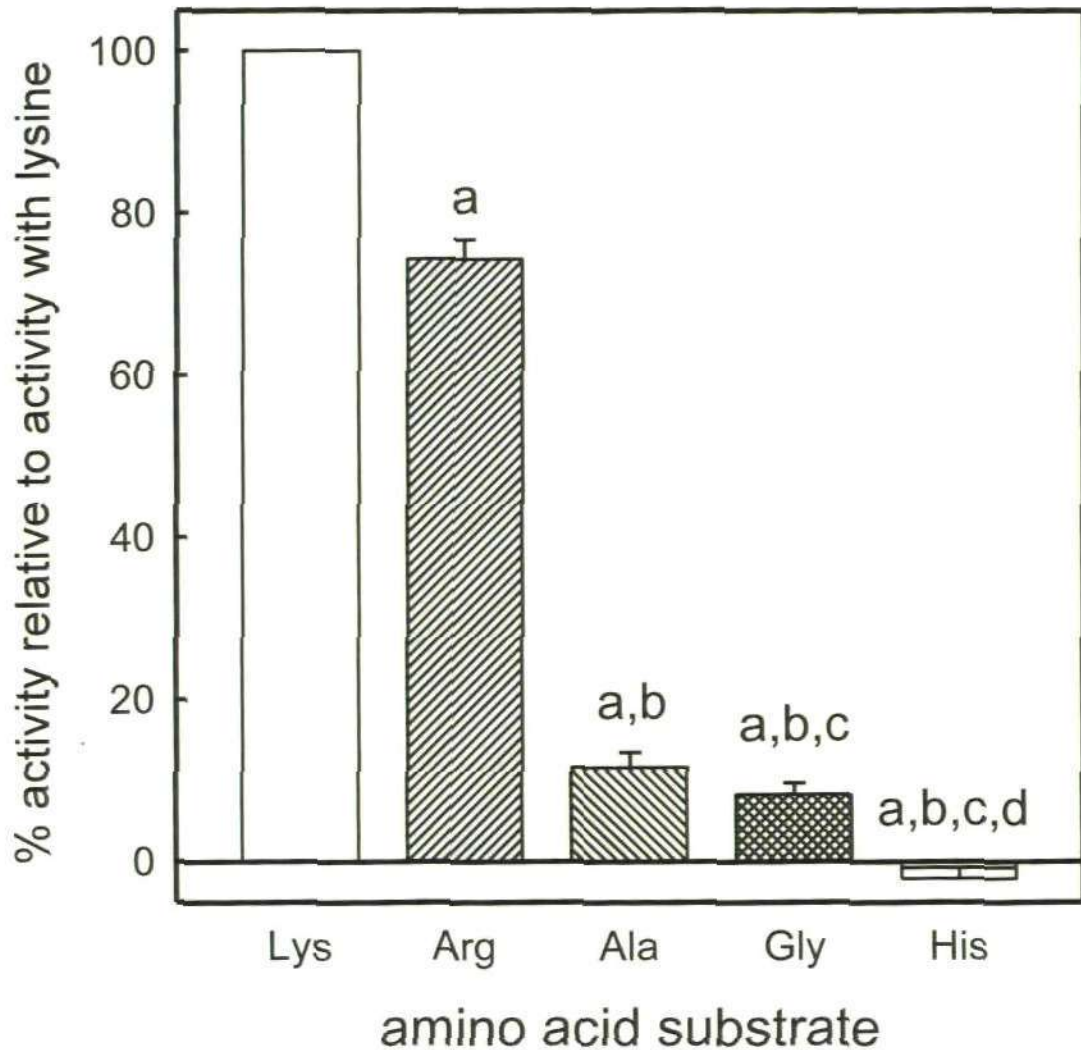


Fig. 4.1 Relative opine dehydrogenase activity in extracts from posterior adductor muscle. Activities are expressed as percentages relative to the activity with lysine as substrate (i.e. lysopine dehydrogenase activity) for the same extract. The data shown are means \pm S.E, $n = 4$. In each case the activity in the absence of the amino acid substrate ($1.5 \pm 0.4 \text{ nmol NADH oxidised min}^{-1} \text{ mg}^{-1} \text{ protein}$) was subtracted. Lysopine dehydrogenase activity was $27.2 \pm 5.5 \text{ nmol NADH oxidised min}^{-1} \text{ mg}^{-1} \text{ protein}$. Same letters denote significant differences between data sets.

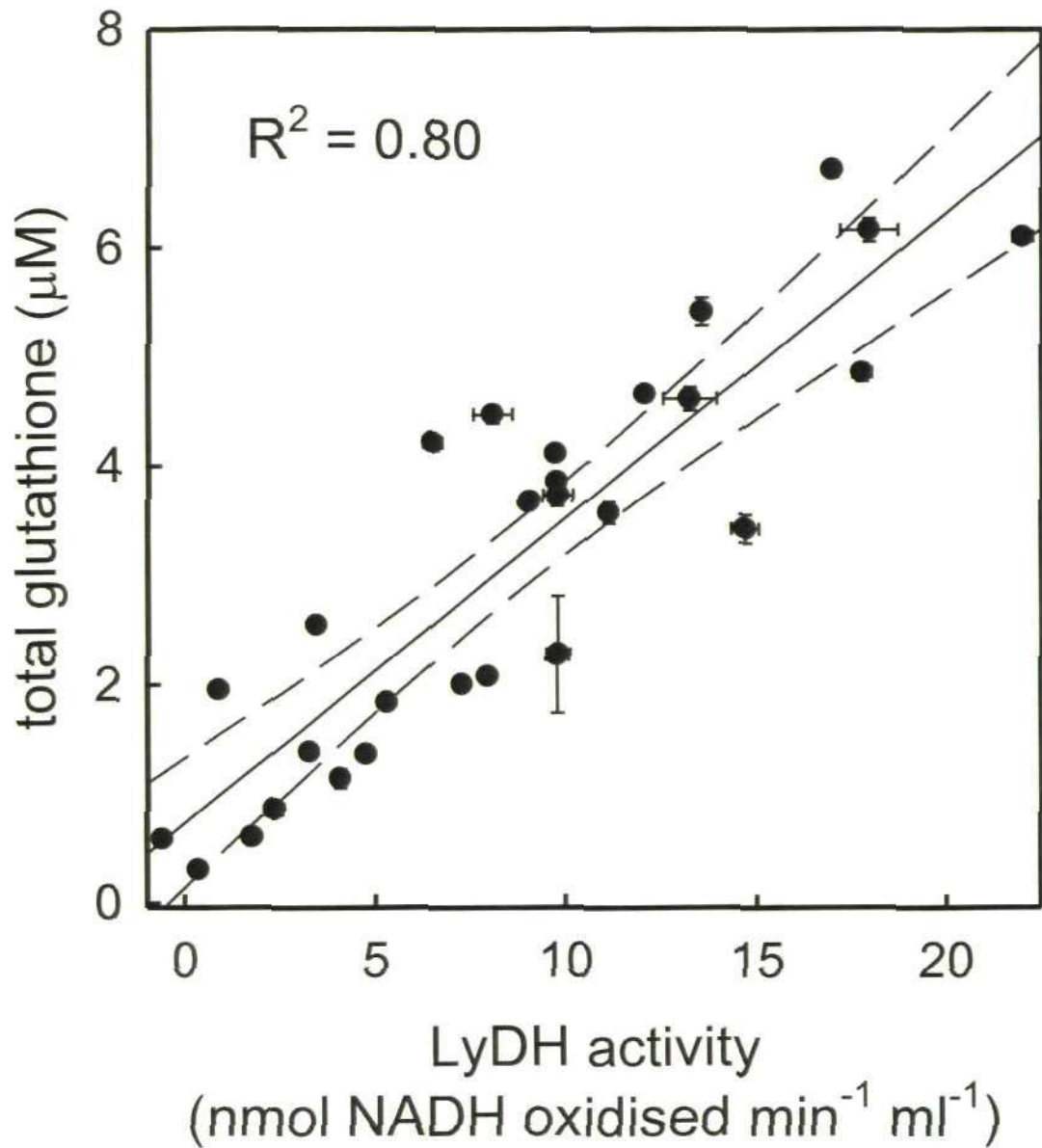


Fig. 4.2 Relationship between the glutathione content of cell-free haemolymph and lysopine dehydrogenase activity. The solid line is a linear regression, and the dashed lines represent 95% confidence limits. Each point represents an individual cell-free haemolymph sample; the error bars indicate the variability of the measurements (\pm S.E., $n = 3$).

4.3.3 Measurements of glutathione and LyDH levels in cell-free haemolymph and adductor muscle extracts

If much of the LyDH activity and glutathione detected in the cell-free haemolymph arises from contamination by the contents of damaged adductor myocytes then LyDH activity and glutathione levels should be much higher in adductor muscle. This was investigated by extracting haemolymph from six mussels, after which the posterior adductor muscle was dissected out and extracts prepared. The total glutathione content and LyDH activities were then measured in both the cell-free haemolymph and the adductor muscle extracts. (N.B. the following experimental values are means \pm S.E, $n = 6$.) The adductor muscle extracts contained $2,353 \pm 278 \text{ nmol min}^{-1} \text{ g}^{-1}$ LyDH activity and $131 \pm 10 \text{ nmol g}^{-1}$ glutathione. These are equivalent to intracellular concentrations in excess of $2,353 \text{ nmol min}^{-1} \text{ ml}^{-1}$ and $131 \mu\text{M}$, respectively, both [100 fold higher than the concentrations, $13.8 \pm 4.0 \text{ nmol min}^{-1} \text{ ml}^{-1}$ and $1.20 \pm 0.31 \mu\text{M}$, respectively, found in cell-free haemolymph from the same mussels. It seems likely that turbulence when extracting the haemolymph might increase the contamination by glutathione and LyDH from adductor myocytes, and that variation in the amount of turbulence might lead to variation in the level of contamination.

In order to investigate these factors we carried out two experiments. In the first, haemolymph was extracted from mussels using different sized hypodermic needles and a record was made of whether or not there was any difficulty in extracting the haemolymph, e.g. a temporary vacuum in the syringe and/ or air bubbles being drawn at the same time as the haemolymph. In the second experiment we tried an alternative method of gaining access to the adductor muscle, i.e. by using a file to make a small notch in the valves rather than

forcing them apart (see section 4.2.2.2). The haemolymph LyDH activity data from the first experiment was analysed using 2-way ANOVA. There was no significant interaction between needle size and difficulty of extraction ($P = 0.160$), so this was omitted from the model. LyDH activities in haemolymph extracted using 19 gauge (outer diameter, 1.07 mm), 21 gauge (outer diameter, 0.82 mm) and 27 gauge (outer diameter, 0.41 mm) needles were 17.9 ± 2.3 , 11.5 ± 2.3 and 11.0 ± 2.3 nmol min⁻¹ ml⁻¹, respectively (mean \pm SE, $n = 8$ in each case). The effect of needle size on haemolymph LyDH was significant at the 90% confidence level ($P = 0.080$); multiple range tests (LSD) showed significant differences at the 95 and 90% confidence levels, respectively, between the LyDH activities in haemolymph extracted using the largest (19 gauge) and smallest (27 gauge) needles, and the largest and middle-sized (21 gauge) needles. LyDH activity was higher (16.8 ± 1.9 nmol min⁻¹ ml⁻¹, $n = 11$) in haemolymph extracted with difficulty (see above) compared to that in haemolymph where there was no difficulty in the extraction (10.1 ± 1.8 nmol min⁻¹ ml⁻¹, $n = 13$). This effect was significant at the 95% confidence level ($P = 0.021$). In the second experiment the LyDH activity obtained using the 'file' method was lower than in cell-free haemolymph obtained using the 'standard' method, on the same day (4.1 ± 0.7 nmol min⁻¹ ml⁻¹, $n = 9$ versus 5.7 ± 0.9 nmol min⁻¹ ml⁻¹, $n = 7$). However, the difference was not statistically significant ($P = 0.169$; Mann-Whitney U test). Overall these data suggest that increased needle size and turbulence during extraction contribute to contamination of the haemolymph with LyDH (and by implication with other adductor muscle components), whereas forcing the valves apart to the limited extent needed for the extraction does not.

4.3.4 *The effect of copper exposure on glutathione levels detected in cell-free haemolymph*

Fig. 4.3 shows the relationship between total glutathione and LyDH activity in cell-free haemolymph from mussels exposed to $40 \mu\text{g l}^{-1}$ Cu compared to that from control mussels. These data were analysed using a general linear model, with glutathione as the dependent variable, presence or absence of Cu as a categorical variable, and LyDH activity as a continuous variable. In graphical terms this analysis shows (a) that there is a significant linear relationship between total glutathione and LyDH activity in the cell-free haemolymph, both from mussels that were exposed to Cu and those that were not ($P < 0.00005$); (b) that there is a significant effect of Cu exposure on the slope of the linear relationship between glutathione and LyDH activity ($P = 0.0111$); and (c) that there is no significant effect of Cu exposure on the value of the y-intercept ($P = 0.466$). In contrast to the data in **Fig. 4.2**, there is no evidence for a 'basal' level of glutathione in the haemolymph, since the y-intercept is not significantly different to zero. However, since Cu exposure affected the slope of the relationship between glutathione and LyDH activity, this suggests that Cu exposure has caused an increase in the levels of glutathione in the adductor muscle (which is, in turn, reflected in an increased level of contamination of the haemolymph samples by glutathione from the adductor myocytes). This was found to be the case: at $169 \pm 13 \mu\text{M}$ (mean \pm SE) the glutathione content of adductor muscle from mussels exposed to Cu was significantly higher ($P = 0.033$, t test) than in control mussels, $101 \pm 17 \mu\text{M}$. In contrast, there was no difference in LyDH activity in adductor muscle from the two groups of mussels ($P = 0.810$, t test): $2.53 \pm 0.32 \mu\text{mol min}^{-1} \text{g}^{-1}$ for Cu exposed mussels, and $2.63 \pm 0.19 \mu\text{mol min}^{-1} \text{g}^{-1}$ for control mussels.

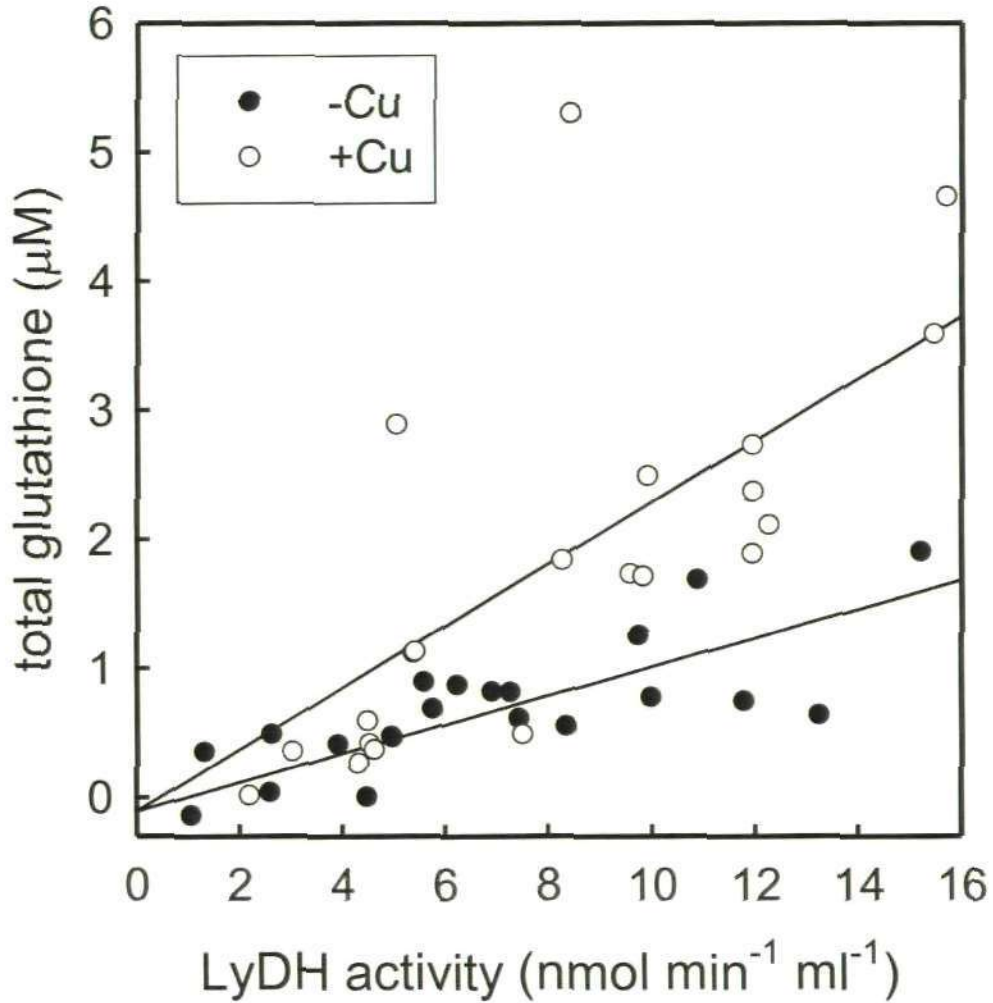


Fig. 4.3 Relationship between the glutathione content of cell-free haemolymph and lysopine dehydrogenase activity in mussels either exposed to $40 \mu\text{g l}^{-1}$ Cu (○) or not (●). The lines show linear regressions derived from GLM analysis of the data where the model included the effects of LyDH ($P < 0.00005$) and the interaction between LyDH and Cu on total glutathione ($P = 0.0001$). The effect of Cu was omitted from the model because it was not significant (see text).

4.3.5 Measurements of biochemical parameters in cell-free haemolymph

Another experiment was undertaken to investigate two enzymes often used in ecotoxicological studies: glutathione peroxidase (GPx) and acetylcholinesterase (AChE). The activities of these enzymes together with LyDH activity and protein content were measured in 27 samples of cell-free haemolymph from *Mytilus edulis*. **Fig. 4.4A**, shows a plot of haemolymph GPx versus LyDH activities. There is a significant linear relationship between these activities ($P = 0.025$). This is further demonstrated in **Fig. 4.4B** where the GPx and LyDH data are plotted against the protein content of the cell-free haemolymph. The Pearson product moment and Spearman rank correlation coefficients for GPx versus LyDH are 0.536 ($P = 0.0040$) and 0.531 ($P = 0.0068$), respectively.

Fig. 4.5A shows a plot of cell-free haemolymph AChE activity against LyDH activity. Although there is clearly a relationship between the two activities, it seems in this case to be non-linear, with AChE activity levelling off at high LyDH activities. The possibility that this was simply caused by interference with the AChE assay was checked. Using a sample with high LyDH activity ($5.4 \text{ nmol min}^{-1} \text{ ml}^{-1}$) it was found that estimates of the AChE activity (in $\text{nmol min}^{-1} \text{ ml}^{-1}$) in the cell-free haemolymph were independent of the sample volume used in the assay (5-30 μl). It is, therefore, unlikely that there was a problem with the AChE assay. When cell-free haemolymph AChE activity is plotted against protein content (**Fig. 4.5B**), there is a significant linear relationship between AChE activity and protein ($P = 0.0136$). The Pearson product moment correlation coefficients for GPx versus protein and LyDH versus protein are 0.681 ($P = 0.0001$) and 0.711 ($P < 0.0001$), respectively. The Spearman rank correlation

coefficients for GPx versus protein and LyDH versus protein are 0.743 ($P = 0.0002$) and 0.738 ($P = 0.0002$), respectively.

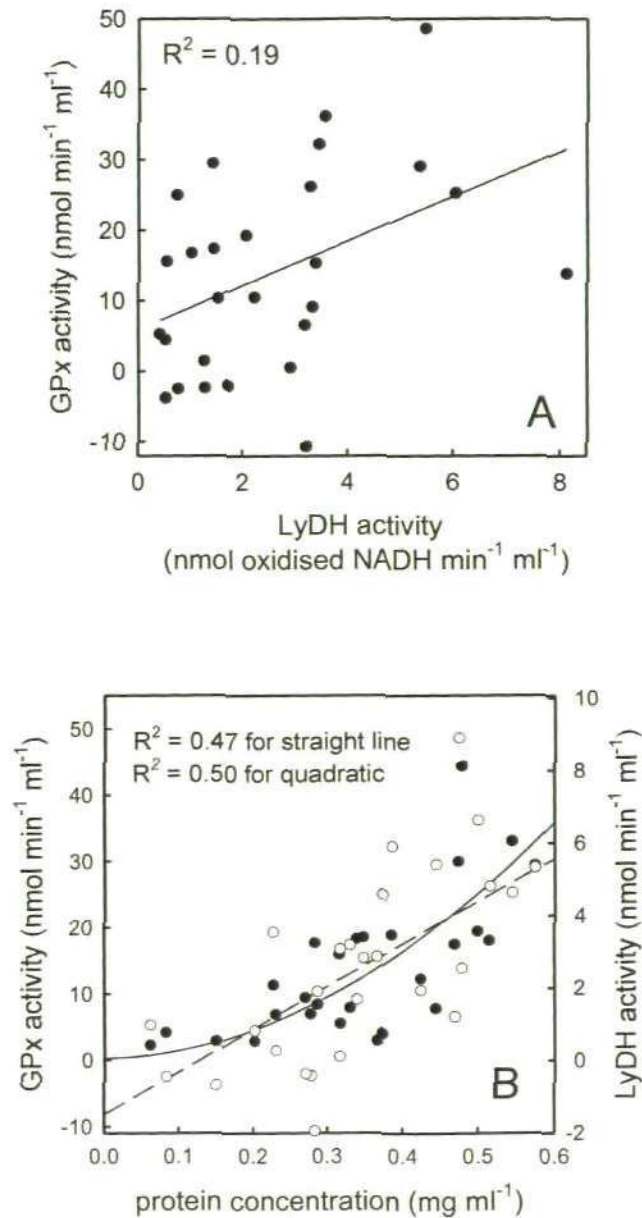


Fig. 4.4 (A) relationship between the GPx activity and LyDH activity in cell-free haemolymph. (B) relationships between GPx and LyDH activities and the protein content of cell-free haemolymph; the solid line is a mutual best fit linear regression, and the dashed line is a mutual best fit non-linear regression (quadratic). (○) GPx and LyDH; (●) protein.

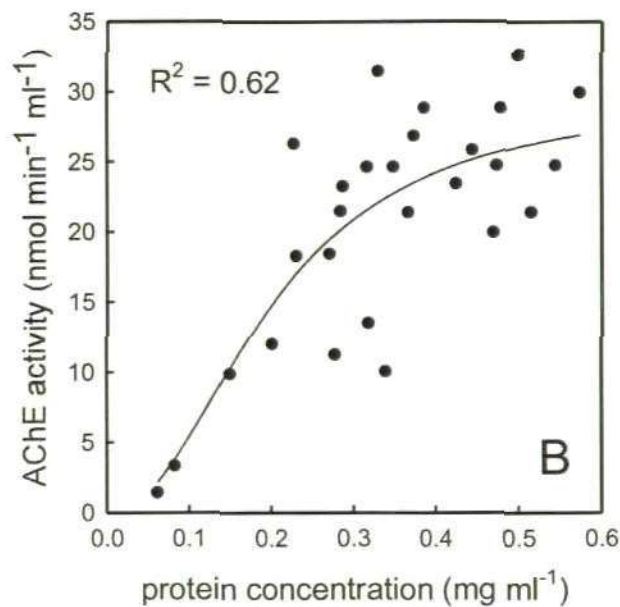
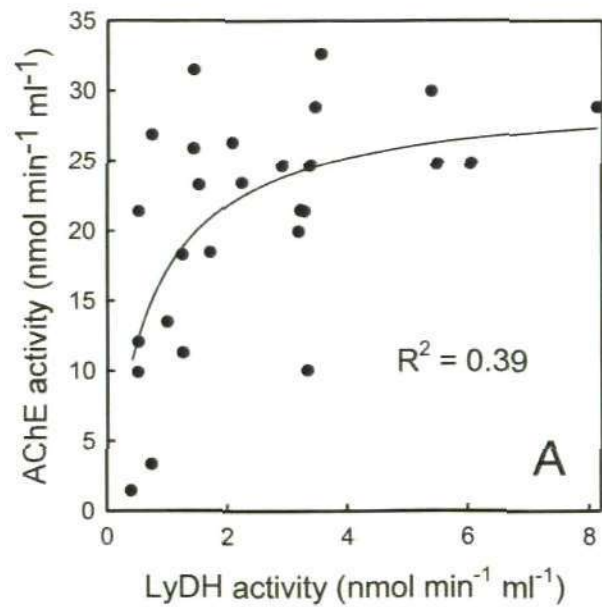
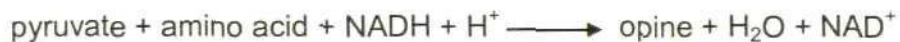


Fig. 4.5 (A) relationship between AChE activity and LyDH activity in cell-free haemolymph from *Mytilus edulis*; the solid line is a non-linear regression (rectangular hyperbola, two parameter; $P = 0.0004$). The Pearson product moment and Spearman rank correlation coefficients for AChE versus LyDH are 0.509 ($P = 0.0068$) and 0.537 ($P = 0.0062$), respectively. (B) relationship between AChE activity and the protein content of cell-free haemolymph; the solid line is a non-linear regression (logistic sigmoidal, three parameter). The Pearson product moment correlation coefficients for AChE versus protein and LyDH versus protein are 0.736 ($P < 0.0001$) and 0.711 ($P < 0.0001$), respectively.

4.4 Discussion

Withdrawal of haemolymph from mussels, *Mytilus edulis*, via the posterior adductor muscle, may lead to contamination with the intracellular contents of adductor myocytes. Opine dehydrogenase was used to investigate the impact of this potential contamination on levels of biochemical parameters measured in cell-free haemolymph. Opine dehydrogenases (also known as pyruvate reductases) are thought to have a similar physiological role to lactate dehydrogenase, which is almost absent in *M. edulis*. They catalyse the reductive condensation of pyruvate with an amino acid to generate an opine (an imino acid derivative) with the concomitant oxidation of NADH.



Several opine dehydrogenase activities have been reported in *M. edulis*. For example, octopine, alanopine and strombine dehydrogenases (Gäde and Grieshaber 1986; Livingstone 1991; Thompson and Donkersloot 1992), where the amino acid substrates are: L-arginine, L-alanine and glycine, respectively; and lysopine dehydrogenase (Coughlan & O'Carra 1996), where the amino acid substrate is L-lysine. Coughlan & O'Carra (Coughlan & O'Carra 1996) found that a single enzyme in *M. edulis* was responsible for both lysopine (L-lysine) and octopine (L-arginine) dehydrogenase activities, and that both substrates gave similar maximal activities. We found higher activity with L-lysine than with L-arginine; this could be attributed to our using different assay conditions (pH and substrate concentrations) to those used by Coughlan and O'Carra (1996).

The strong linear relationship we found between total glutathione with LyDH haemolymph levels suggests two possible explanations: either levels of

glutathione and LyDH activity in cell-free haemolymph are co-regulated, or, more likely, much of the supposed haemolymph glutathione comes, along with LyDH activity, from an intracellular source. Given that the haemolymph was extracted via the posterior adductor muscle, it seems likely that turbulence when extracting the haemolymph might increase the contamination by glutathione and LyDH from adductor myocytes, and that variation in the amount of turbulence might lead to variation in the level of contamination. A more significant factor, however, might be the process of forcing the valves slightly apart in order to gain access to the posterior adductor muscle, given the catch phenomenon shown by mollusc adductor muscles (Funabara et al., 2005). Two experiments were run out to investigate the extraction effect by using different needle size and two different methods for haemolymph extraction. Haemolymph LyDH activity was significantly higher in samples extracted using larger diameter needles, and also in samples where there had been some difficulty in the extraction.

It should be emphasised that the assumption here is that LyDH activity should be absent in mussel haemolymph, in the absence of damage to the adductor muscle. In support of this we have often found cell-free haemolymph samples where LyDH activity is below the detection limit of the assay, consistent with the assumption above that it is normally absent from this compartment. Despite the evidence for contamination of cell-free haemolymph with glutathione from adductor myocytes there was still the possibility that this could be corrected for by also measuring LyDH activity, and hence that the effect of oxidative stress on haemolymph glutathione could be determined. Mussels were therefore exposed to $40 \mu\text{g l}^{-1}$ copper, which is a well known cause of oxidative stress

(e.g. Gaetke and Chow 2003). If oxidative stress were to lead to oxidation of glutathione and excretion of oxidised glutathione into the haemolymph then we might expect that the y-intercept in a plot of total glutathione against LyDH activity would be significantly elevated. The results we found were inconsistent with the idea that 'global' oxidative stress in mussels might lead to excretion of glutathione into the haemolymph. In fact, in this case, in contrast to the data in **Fig. 4.2**, there is no evidence for a 'basal' level of glutathione in the haemolymph, since the y-intercept is not significantly different to zero. However, since Cu exposure affected the slope of the relationship between glutathione and LyDH activity, this suggests that Cu exposure has caused an increase in the levels of glutathione in the adductor muscle (which is, in turn, reflected in an increased level of contamination of the haemolymph samples by glutathione from the adductor myocytes).

Cell-free haemolymph GPx and AChE activities also showed similar, non-linear relationship. A reasonable interpretation of these data is that GPx and LyDH come from the same compartment (presumed to be the cytosol of adductor myocytes) with the implication that much of the GPx activity measured in cell-free haemolymph was artefactual. However, in this case, because of the spread in the data, it is unclear whether there is a basal level of GPx in the cell-free haemolymph. Although extrapolation to zero LyDH activity gives a value of $5.90 \pm 4.21 \text{ nmol min}^{-1} \text{ ml}^{-1}$, statistically this is not significantly greater than zero ($P = 0.1738$).

Once again, the implication of these data is that AChE activity measured in cell-free haemolymph is largely artefactual. Furthermore, the difference in the behaviour of AChE activity compared to GPx activity may reflect its release into

the cell-free haemolymph from a different compartment, one that perhaps is more fragile than the myocyte cytosol. Mollusc adductor muscles show the phenomenon of catch, and are controlled by both cholinergic and serotonergic innervation (Funabara et al., 2005). Given the role of AChE activity in cholinergic neuromuscular junctions, it seems reasonable to suppose that this is the compartment from which this activity is being released during extraction of the haemolymph. However, there is a lack of information relating to the morphology of neuromuscular junctions in *Mytilus edulis*, so it is not possible to judge whether the structure of cholinergic junctions is likely to be particularly fragile in this species. A neuromuscular origin for the AChE activity detected in mussel cell-free haemolymph may account for the variability seen in a previous study where an attempt was made to use mussel haemolymph AChE activity as a biomarker of effect after organophosphorus exposure (Rickwood and Galloway 2004). It is usual practice when comparing tissue enzyme activities to use specific activity, i.e. to express the activity per unit total protein. However, in the case of cell-free haemolymph from mussels, even if the origin of the GPx and AChE activities (and, indeed, of much of the protein) is ignored, the data presented here suggest that the use of specific activities may be problematic since in both cases there is non-linear relationship between enzyme activity and protein content.

4.5 Conclusions

The evidence presented here suggests that cell-free haemolymph from *Mytilus edulis*, and, by extrapolation haemolymph from other bivalve species, may be significantly contaminated by adductor muscle components, e.g. intracellular contents of myocytes and contents of neuromuscular junctions. This can explain

some apparent anomalies in the literature. For example, Brown et al., (2004) expressed doubt about the relevance of measuring AChE activity in mussel haemolymph because of concerns that it might not originate from the nervous system. However, the data presented here (AChE activities) suggest that its origin is the neuromuscular junctions of the adductor muscle.

Despite the likelihood that haemolymph glutathione, and GPx and AChE activities arise from contamination, there are clearly other things in mussel haemolymph, where there are rationales for their presence, that are likely to be bone fide components of that compartment, e.g. phenoloxidase, which has an immune function Muñoz et al., (2006). The implications of the work described here are two fold. First, when using biomarkers in cell-free haemolymph, it may be prudent to check whether contamination is an issue using a myocyte marker such as opine dehydrogenase activity. Second, although the adductor muscle has sometimes been investigated e.g. Dauberschmidt et al., (1997) looked at esterase activity in mussel posterior adductor muscle, it may be a more generally useful tissue in which to determine biomarker responses, e.g. in the glutathione/glutathione peroxidase system.

Chapter 5

Validation of biochemical, histological and behavioural responses in *Mytilus edulis*

The results from this chapter have been presented at the Plymouth Marine Sciences Partnership Symposium 2009, Plymouth, UK, April 2009 (poster presentation). The results have also been published in *Ecotoxicology and Environmental Safety*, (Al-Subiai et al., *In press*).

Hypothesis: *Copper induce responses at different levels of biological organisation*

Abstract

While copper (Cu) is considered to be an essential trace element, its overexposure could induce a wide spectrum of effects including DNA damage. Given that Cu is a highly relevant contaminant in the marine environment, we aimed to evaluate the induction of DNA strand breaks (using the comet assay) in haemocytes, tissue specific accumulation and concurrently determined biological responses at higher levels of biological organisation in bivalve molluscs, *Mytilus edulis*, following exposure for 5 days to a range of environmentally realistic levels of Cu (18-100 $\mu\text{g l}^{-1}$). Prior to evaluation of genetic damage, the maximum tolerated concentration (MTC) was also determined. Complete mortality of the exposed animals was observed at the highest concentration (100 $\mu\text{g l}^{-1}$) tested. In addition to DNA damage, levels of glutathione in adductor muscle extracts were also determined, as were clearance rates for individuals. In addition, various tissues were subjected to histopathological examination and levels of Cu were determined in these tissues using ICP-MS. Cu levels in adductor muscle ($P = 0.012$), digestive gland ($P = 0.008$) and gills ($P = 0.002$) were significantly higher than in the control. There was a strong concentration-dependent induction of DNA damage and total glutathione levels increased by 1.8-fold at 56 $\mu\text{g l}^{-1}$ Cu. Histopathological examination of adductor muscle, digestive gland and gills showed distinct abnormalities. Clearance rate also showed a significant decrease compared to controls even at the lowest concentration of Cu used (18 $\mu\text{g l}^{-1}$; $P = 0.003$). Apart from having differential affinities for tissues, the study suggests that environmentally relevant exposure of Cu is capable of inducing DNA damage

which has different degrees of knock on effects at the higher levels of biological organisation.

5.1 Introduction

The marine environment has long been subject to contamination by heavy metals (e.g. As, Cd, Cr, Co, Cu, Pb, Hg and Ni), either of natural origin, as a result for example of volcanic activity, wind-blown dust, decaying vegetation, or of anthropogenic origin, for example as a result of industrial activities including metal plating, antifouling paints and foundries (Rainbow 2002). Of all these metals, world production of copper (Cu) has expanded in the last few decades and contamination by Cu has become increasingly prevalent in marine environments (WHO 1998) which is likely to increase in coming decades. In relatively unpolluted coastal waters Cu concentrations are less than 5 ppb (Soegianto et al. 1999) but can reach 3 ppm in heavily polluted areas (Parry and Pipe 2004). The increasing Cu concentrations in marine ecosystems are therefore a potential threat to living organisms. Although Cu is essential to the normal function of organisms (e.g. being a cofactor in many enzymes), it can be toxic if present in high levels or if organisms are exposed chronically to low levels in the environment (Gaetke and Chow 2003).

In different groups of organisms, long-term exposure to Cu is typically associated with impairment of feeding mechanisms (Nicholson 2003), growth rates and reproduction (Fitzpatrick et al. 2008), and increased susceptibility to disease and to development of histopathological abnormalities (Zorita et al. 2006). From the regulatory perspective, for example, the water framework directive (WFD; Directive 2000/60/EC) of the EU (Borja et al. 2004) emphasises the need for ecological quality of the hydrosphere in particular, focusing on those contaminants which are carcinogenic, mutagenic or show reproductive toxicity. In ecotoxicological terms, damage to genetic material could lead to

detrimental effects on environmental sustainability (Bickham et al. 2000). Copper-induced toxicity involves both direct and indirect mechanisms. The direct mechanism involves a Fenton-like reaction in which oxidation of Cu^+ drives the conversion of hydrogen peroxide (H_2O_2) to hydroxide (OH^-) and the hydroxyl radical (OH^\bullet) (Gaetke and Chow 2003), which is regarded as the most potent reactive oxygen species (ROS), capable of reacting with every class of biological molecule (Becker et al. 1996; Bremner 1998; Gaetke and Chow 2003). Indirect toxicity of Cu can result from its binding to proteins involved in DNA replication, transcription and repair, leading to impairment of these processes (Nor 1987).

Invertebrates and fish possess complex homeostatic mechanisms that can regulate internal Cu levels in the face of high external inputs (Livingstone 2001). This mainly involves the induction of metallothioneins (MT). In addition, cells contain antioxidant defences, both enzymatic and non-enzymatic, whose function is to maintain low steady-state levels of ROS. Such enzymes include glutathione peroxidase (GPx), catalase (CAT), superoxide dismutase (SOD); non-enzymatic antioxidants include reduced glutathione (GSH) and ascorbic acid (Lopez-Torres et al. 1993). However, during oxidative stress these defences may be overwhelmed leading to covalent modification of proteins, DNA damage, and lipid peroxidation (Barata et al. 2005).

While there is a relatively good understanding of Cu toxicity and bioaccumulation in aquatic organisms from earlier studies, to our knowledge there has been no integrated study where effects at different levels of biological organisation have been concurrently assessed. In particular, tissue-specific affinity, the study of genotoxicity associated with quantitative induction of

glutathione level, potential consequences of genotoxic effects at higher levels of biological organisation has seldom been attempted. Given the context outlined above, the objectives of this chapter were (a) to determine the effects of Cu exposure at different levels of biological organization from biochemical (DNA damage and total glutathione content) to potential tissue specific bioaccumulation and histopathological changes and effects at whole organism level (i.e. clearance rate as a measure of physiological effect) and (b) to test for correlations if any between genotoxicity and higher level biological responses in order to assess how efficiently these biological endpoints could be used as tools to evaluate toxicological responses in the context of pollution monitoring. Among the numerous sessile organisms, bivalves are often used as sentinel organisms to study the biological effects of environmental contaminants (Livingstone et al. 2000). These are filter feeders, which are in direct contact with the contaminated compartments (sediment and water), and so can accumulate high levels of heavy metals in their soft tissues, providing a time-integrated indication of contamination with measurable cellular and physiological responses (van Duren et al. 2006). For the advantages mentioned above, we selected the blue mussel, *Mytilus edulis*, as a model organism in the current study.

5.2 Materials & Methods

5.2.1 Chemicals and animal collection

All chemicals were obtained from Sigma-Aldrich (Poole, UK) unless stated otherwise. Mussels (*Mytilus edulis*) of similar shell length (51-58 mm) were collected at low tide (January, 2008) from Port Quin, Cornwall, UK (grid reference: SW972 905), a relatively clean site (Canty et al. 2009). After collection, animals were kept under controlled laboratory condition as described in section 2.1. Seawater quality was checked during acclimatization and during the experiments by measuring dissolved oxygen ($95.2 \pm 0.2\%$), pH (7.95 ± 0.03), total ammonia ($0.05 \pm 0.01 \text{ mg l}^{-1}$), temperature ($15 \pm 1 \text{ }^\circ\text{C}$) and salinity ($31.3 \pm 0.12 \text{ ‰}$). No spawning or mortality occurred in any of the stock tanks.

5.2.2 Experimental design

The overall experimental design is presented in **Fig. 5.1**. *M. edulis* individuals were exposed to 0, 18, 32, 56 or $100 \text{ } \mu\text{g l}^{-1}$ copper in 2 l glass beakers (3 animals per beaker), with each exposure being carried out in quadruplicate. The concentration range of copper was based on an earlier *in vivo* study (Bolognesi et al. 1999) using *M. galloprovincialis*. However, the concentrations of Cu were slightly modified to fit the semi-logarithmic scale which is widely used in ecotoxicological studies. A primary stock solution of Cu in distilled water was prepared using $\text{CuSO}_4 \cdot 5\text{H}_2\text{O}$ (99% purity). To avoid the confounding effects of general toxicity, the maximum tolerated concentration (MTC) was determined as the highest concentration that elicits a specific toxic effect, mortalities being the final arbiter (Hutchinson et al. 2009). Exposure of *M. edulis* specimens to Cu was carried out over 5 days, with removal of mussels at the end of exposure for

estimation of the DNA damage and histopathology. The 5 day exposure period matched that used in the earlier study by (Bolognesi et al. 1999). During the exposure period, the seawater was changed daily and re-dosed with the appropriate dose of copper. Metal analysis was also carried out in water (**Table 5.1**) and in dissected tissue samples. The highest concentration (i.e. 100 $\mu\text{g l}^{-1}$) the measured concentration was 25% lower than the nominal concentration. This reduction in Cu concentration is in line with observations made previously by other authors using similar analytical techniques (Nadella et al. 2009), and might be due to Cu precipitation in the seawater. Animals were not fed during the experiment.

Table 5.1 Copper concentrations determined for exposure solutions at each of the nominal Cu concentrations. Data are means \pm S.E, n = 3.

Nominal Cu concentration ($\mu\text{g l}^{-1}$)	Measured Cu concentration ($\mu\text{g l}^{-1}$)
0 (control sea water)	1.46 \pm 0.13
18	18.67 \pm 0.12
32	27.63 \pm 0.61
56	52.70 \pm 1.00
100	75.40 \pm 5.20

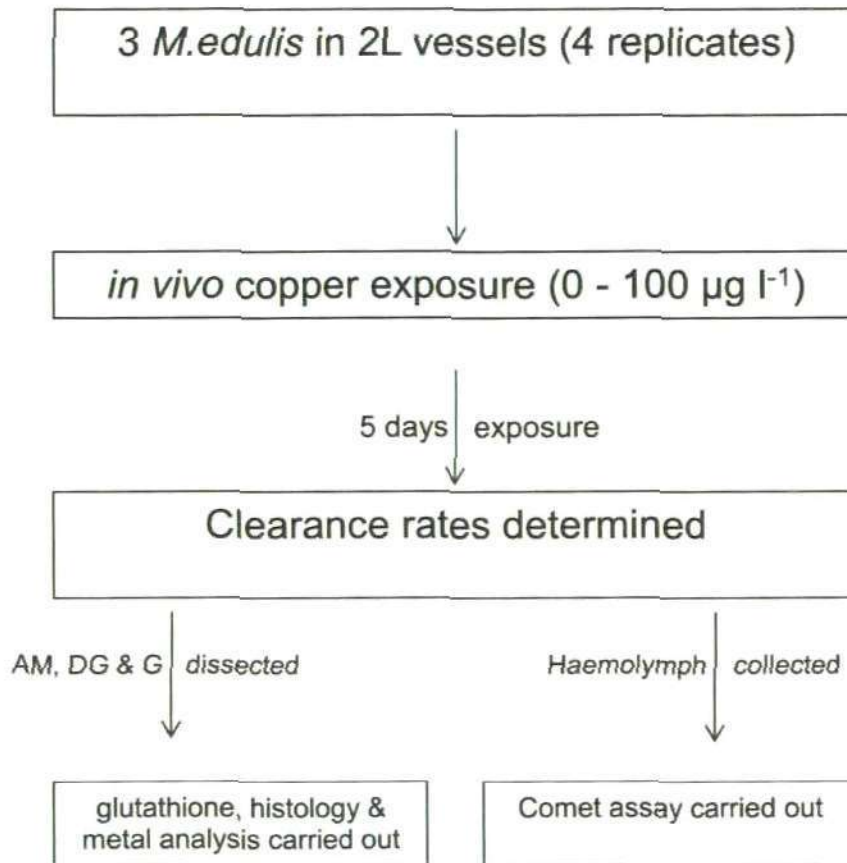


Fig. 5.1 Flow chart illustrating integrated experimental design adopted in the study to evaluate genotoxicological, biochemical, structural and behavioural effects in *M. edulis*. AM = adductor muscle; DG = digestive gland; G = gills.

5.2.3 Sample preparation

5.2.3.1 Collection of haemolymph samples from *M. edulis*

Haemolymph samples were extracted from the posterior adductor muscle into physiological saline as described in section 2.3.1. The samples were then placed on ice until analysis.

5.2.3.2 Preparation of adductor muscle extract

The posterior adductor muscles extracts were prepared described in section 2.3.2. The crude homogenate was centrifuged at 10,500 g_{av} at 4 °C for 35 min. The supernatant was isolated and kept at -80 °C until use. Adductor muscles from pairs of animals were pooled and used for the preparation of extracts. Hence, for each beaker two extracts were prepared, and the total glutathione contents of these determined. These were then averaged to give a single value of glutathione content for mussels from each beaker.

5.2.4 Cell viability

The viability of the haemocytes in each sample was checked using the Eosin Y viability test, prior to Comet assay, as described in section 2.4.1.

5.2.5 Determination of DNA strand breaks using the Comet assay

Determination of induction of DNA strand breaks using *M. edulis* haemocytes was determined as described in section 2.4. The level of DNA damage in 100 cells per sample was measured using Kinetic Imaging, Komet 5.0 image analysis software (Liverpool, UK). The percentage of DNA in the comet tail was used for data analysis. Comet analysis was carried out on samples of haemocytes from individual mussels. These data were then combined by taking

the mean for the three mussels from each of the four replicate beakers for each treatment.

5.2.6 Measurement of total glutathione

Total glutathione content was determined by glutathione reductase cycling assay as described in section 2.5. Both glutathione forms (reduced, GSH + oxidized, GSSG) in the adductor muscle extract were measured in triplicate in a microplate reader (Optimax, Molecular Devices, Sunnyvale, CA) using 96 well plates, and then expressed as $\text{nmol g}^{-1} \text{ ww}$. The assay was conducted at 22 °C.

5.2.7 Determination of histopathological changes

Adductor muscle, gills and digestive gland were dissected out for histopathological examination as described elsewhere in detail in section 2.6. Tissues were dehydrated through series of alcohol and xylene, and embedded in paraffin. Transverse sections were stained with H&E. 48 h. In the present study, following exposure to Cu, a simple histological analysis was carried out on tissues (i.e. adductor muscle, gills and digestive gland) from individual mussels in which the presence or absence of histological changes were determined.

5.2.8 Analysis of copper concentrations in the tissues

The copper concentration was measured according to Federici et al. (2007). The adductor muscle, digestive gland and gills dissected out from each mussel were washed with Milli-Q water, placed on clean individual slides and dried to a constant weight in an oven at 100 °C for 24 h. All glassware was acid-washed (5% Aristar HNO_3 for at least 2 h) to minimise contamination, and then triple rinsed in deionised water. In a fume hood, each piece of dried tissue was

placed in 20 ml polythene screw-top digestion vials (scintillation vials, Simport, Canada) and 1 ml of concentrated Aristar HNO₃ was added. Samples were digested at 70 °C for 2 h in a water bath. Once digestion was completed (no brown fumes evolving), the tubes were allowed to cool, and then the contents were diluted with 4 ml of Milli-Q water. Tissue digests were stored at room temperature. Copper concentrations were measured by using Inductively Coupled Plasma Mass Spectrometry (ICP-MS; Plasma Quad PQ2 Turbo, Thermo Elemental, Winsford, UK; PQ Vision 4.1.2. software). To validate the metal analysis, 0.25 ml of two internal standards was added to all samples. These standards were indium (In) and thallium (Tl). Copper standards were also prepared in order to calibrate the instrument before metal analysis. The standard solutions were made by using 1000 mg l⁻¹ Cu stock solution, diluted using 2% nitric acid. The Cu standards used were 0, 10, 20, 40 ppb. In all standards 0.25 ml of the two internal standards were also added. The isotopes chosen for copper measurements were 63 and 65. Cu analyses were carried on different tissues from individual mussels and then the data were pooled by taking the mean for three mussels from each of the four replicates for each treatment.

5.2.9 Determination of clearance rate

The clearance rate was estimated by measuring the exponential reduction of *Isochrysis* algal particles in glass beaker with known volume of seawater (as previously described in section 2.7). The concentration of the particles was determined by Beckman Coulter, Z2 (USA). Clearance rate data from individuals were then combined by taking the mean for the three mussels from each of the four replicate beakers for each treatment.

5.2.10 Statistical analyses

Statistical analyses were carried out using statistical package Statgraphics Plus version 5.1 (Statistical Graphics Corp). All results are presented as means \pm S.E. Significant differences between groups were determined using either one way ANOVA or the Kruskal-Wallis test, followed by multiple range tests (Fisher's LSD). $P < 0.05$ was accepted as significant. Any correlations between variables were determined using Pearson's correlation coefficient.

5.3 Results

5.3.1 Determination of MTC

Throughout the exposure there was no mortality in the controls or in the 18, 32 and 56 $\mu\text{g l}^{-1}$ Cu treatments. However, by the last day of exposure (day 5) the highest Cu concentration (i.e. 100 $\mu\text{g l}^{-1}$) had caused 100% mortality. Therefore, the MTC was considered to be 56 $\mu\text{g l}^{-1}$ and all the biological responses were determined below this concentration. This mortality may have resulted from the toxicity to the mussels of 100 $\mu\text{g l}^{-1}$ Cu or perhaps from prolonged valve closure by the mussels as an attempt to avoid Cu exposure. Either way, the results from this treatment were excluded.

5.3.2 Determination of clearance rate

The clearance rate data (**Fig. 5.2**) show that Cu exposure caused a significant reduction in clearance rate in comparison to the control (Kruskal-Wallis, $P = 0.003$). The clearance rate reduction ranged from 94% to 96% in groups of animals exposed to different concentrations of Cu, but there were no significant differences between the groups.

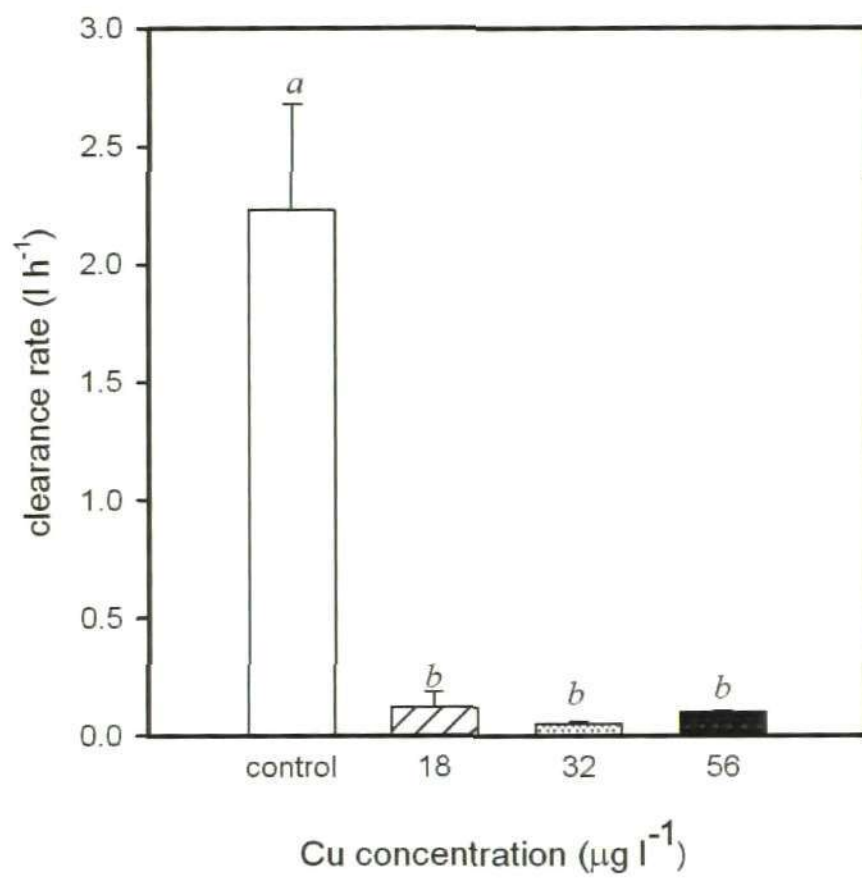


Fig. 5.2 Clearance rates of *M. edulis* following 5 days *in vivo* exposure to copper. The values are means \pm S.E ($n = 4$). Different letters denote significant differences between data sets.

5.3.3 Determination of DNA strand breaks

After the two week acclimatization period, the mussels were tested for baseline levels of DNA damage in their haemocytes using the Comet assay (see Materials and Methods). This batch of collected animals showed low levels of DNA damage (3.05 ± 0.72 % tail DNA, mean \pm S.E., $n = 15$). Before performing the assay cell viability was also assessed using Eosin Y staining; Cell viability was $> 90\%$ in all cases.

Levels of DNA damage in haemocytes from mussels exposed to Cu are shown in **Fig. 5.3**. A strong dose-dependent effect of Cu on DNA damage is evident; a statistically significant increase in % tail DNA compared to the control was found for all Cu treatments. Also, there were significant differences in the level of DNA damage between the different Cu exposures.

5.3.4 Total glutathione levels in adductor muscle

Exposure to Cu caused an increase in total glutathione content in the adductor muscle in all treatments (**Fig. 5.4**). The increase was significant in mussels exposed to 32 and 56 $\mu\text{g l}^{-1}$ Cu, with the highest levels recorded in mussels exposed to 56 $\mu\text{g l}^{-1}$ Cu, where on average total glutathione had increased by 1.83 fold compared to control mussels.

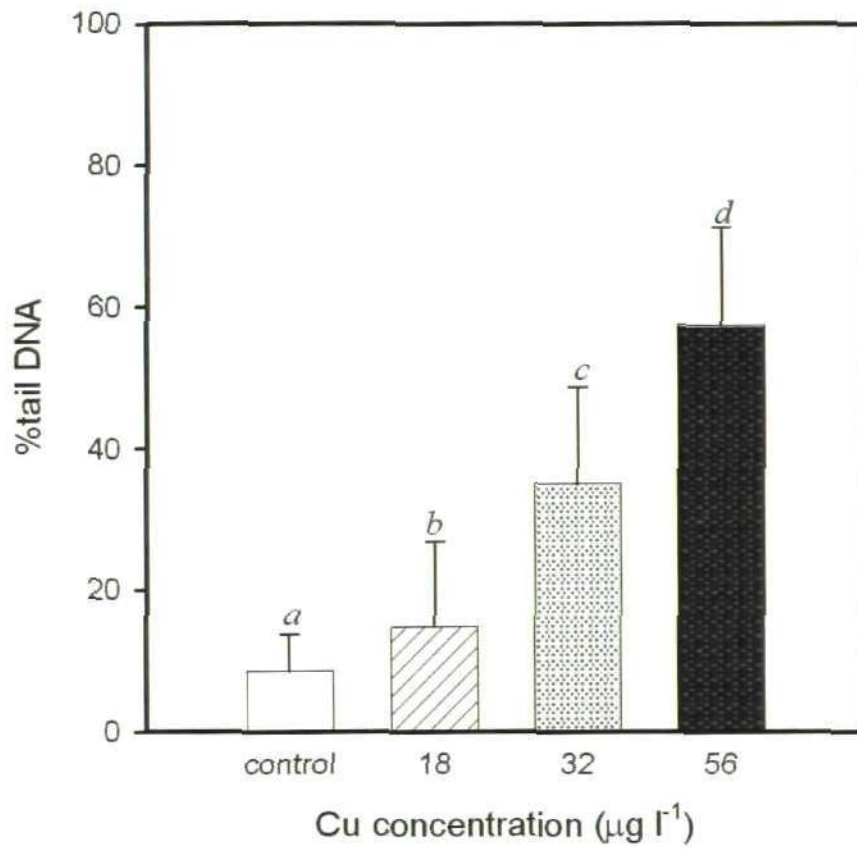


Fig. 5.3 DNA damage in *Mytilus edulis* haemocytes following 5 days *in vivo* exposure to copper. Different letters denote significant differences between data sets.

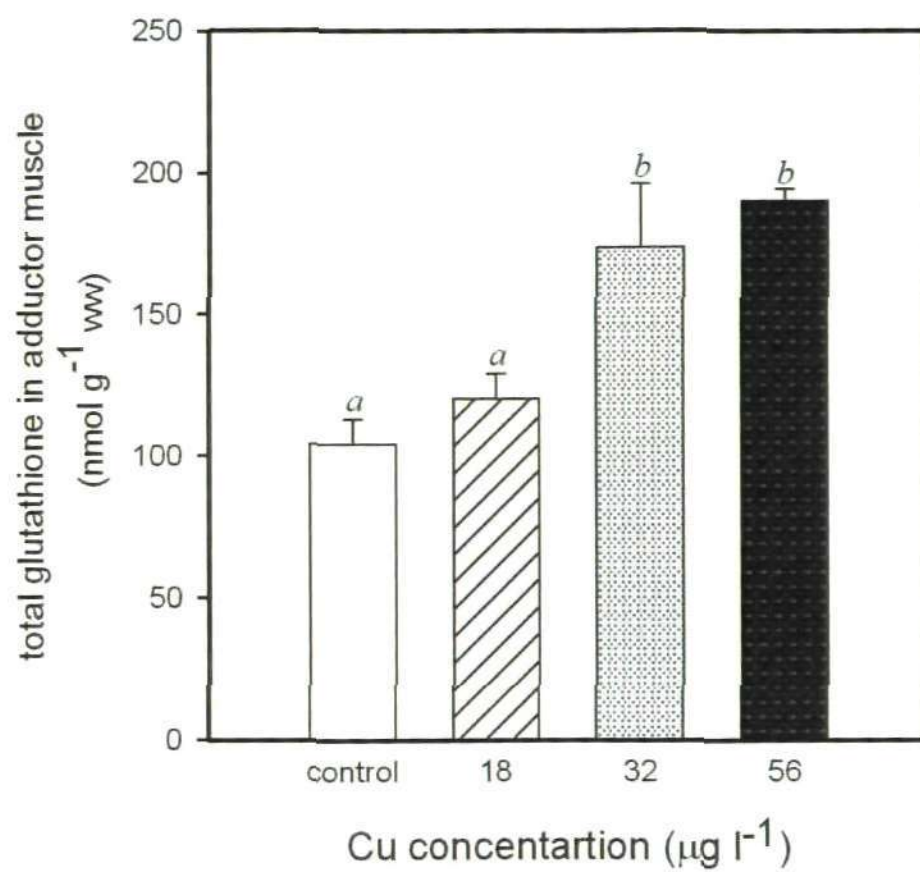


Fig. 5.4 Levels of total glutathione content in adductor muscle following 5 days *in vivo* exposure to copper. Different letters denote significant differences between data sets.

5.3.5 Determination of histopathological effects

5.3.5.1 Posterior adductor muscle

Posterior adductor muscle from control animals showed normal histology with groups of muscle blocks, each made of distinct bundles of muscle fibres. The bundles were surrounded by connective tissue. Myocytes appeared normal, as shown in **Fig. 5.5A**. There was no evidence of haemocyte infiltration, necrosis or other injuries. However, adductor muscle samples from Cu-exposed mussels showed histological abnormalities, e.g. loose structural organization, hydropic changes (swelling) in the myocytes (**Fig. 5.5B**).

5.3.5.2 Gills

Gill histology from control and Cu-exposed mussels is illustrated in **Fig. 5.5C & D**, respectively. In the control group, gills exhibited well-preserved structure; gill filaments are covered with ciliated epithelium on their external surface. The frontal cilia emerge from the frontal epithelium, while the lateral cilia emerge from lateral cells. In contrast, all of the gills from Cu-exposed mussels exhibited histological alterations. Injuries observed include filament necrosis and hypoplasia in the frontal and lateral cilia (**Fig. 5.5D**).

5.3.5.3 Digestive gland

Digestive gland from control mussels showed the normal architecture of digestive tubules, stomach and intestine. Digestive tubules showed normal round/oval structure in all cases lined by columnar epithelium. All the digestive tubules were connected to each other by connective tissue (**Fig. 5.5E**). The stomach had ridges and grooves lined with ciliated epithelium. The stomach

was linked to the primary and secondary digestive tracts and subsequently the digestive tubules. The intestine had more flat ciliated epithelium than the stomach surface. There was no evidence of haemocyte infiltration, necrosis or other injuries in the digestive gland controls (**Fig. 5.5F**). The main change observed after Cu exposure in the digestive tubules tested was necrosis, as indicated by diffuse nuclei and no clear distinction between some epithelial cells. In addition, in some of sections, the stomach was obstructed by haemocyte infiltration.

5.3.6 Analysis of copper accumulation

Copper was analyzed separately in pooled adductor muscle, digestive gland and gill tissues. There was a significant increase in the levels of Cu in *M. edulis* soft tissues after the 5 days of exposure compared to the controls. Gills showed the highest Cu accumulation ($429.2 \pm 50.5 \mu\text{g/g dw}$, at $32 \mu\text{g l}^{-1}$), and the ranking of the organs according to the increase in Cu accumulation was adductor muscle < digestive gland < gills. All treatment groups were significantly different to the control, **Fig. 5.6**. The highest level of copper accumulation was recorded in the gills and digestive gland after exposure to $32 \mu\text{g l}^{-1}$ Cu, whereas, adductor muscle showed similar accumulation with 18 and $32 \mu\text{g l}^{-1}$ Cu. For all tissues there was a decrease in accumulation between 32 and $56 \mu\text{g l}^{-1}$ Cu.

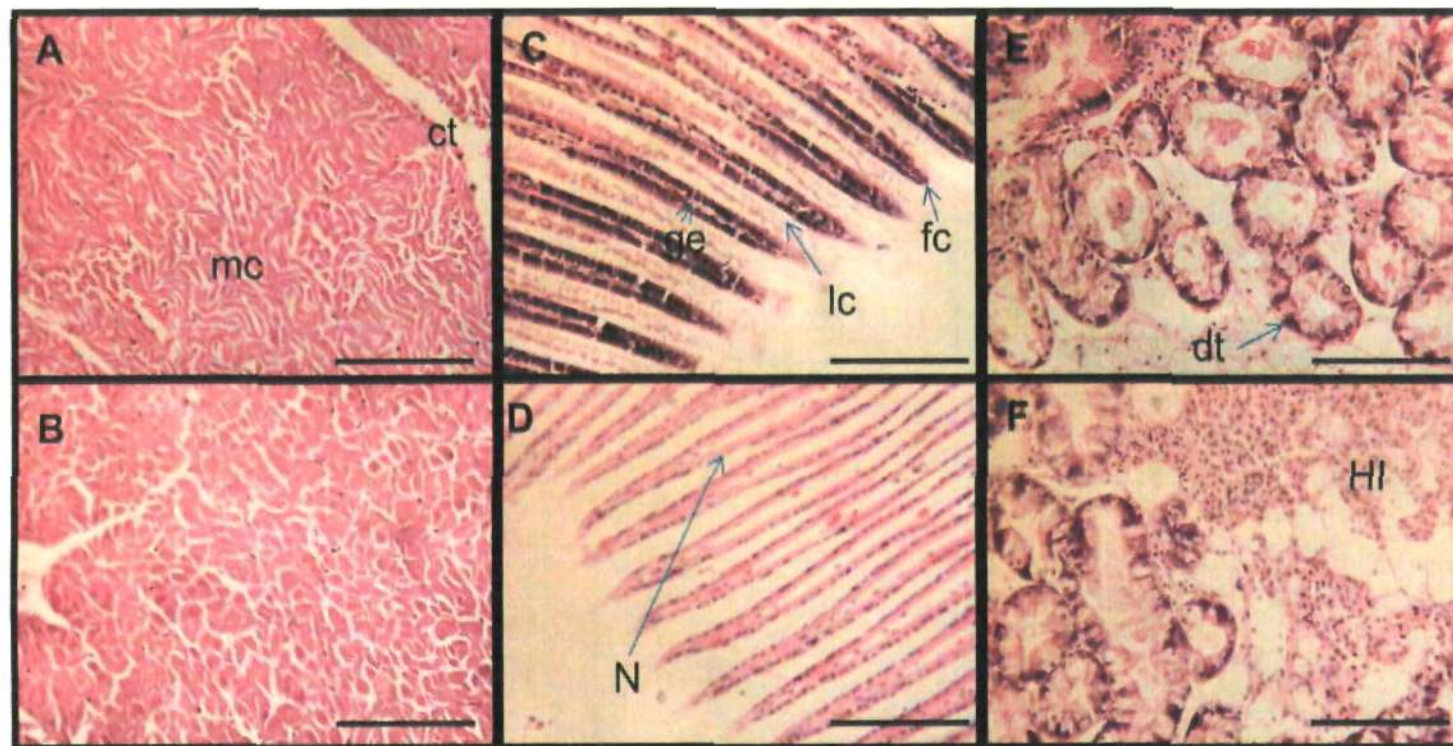


Fig. 5.5 Light micrographs of sections (5-8 μm thickness, stained with H & E) through adductor muscle (A & B), gills (C & D) & digestive gland (E & F) of control and Cu-exposed mussels. (A, C & E) control; (B, D & F) exposed to $32 \mu\text{g l}^{-1}$. mc = myocytes; ct = connective tissue; dt = digestive tubule; fc = frontal cilia; lc = lateral cilia; ge = gill epithelium; N = necrosis; HI = haemocyte infiltration. Scale bar: 100 μm .

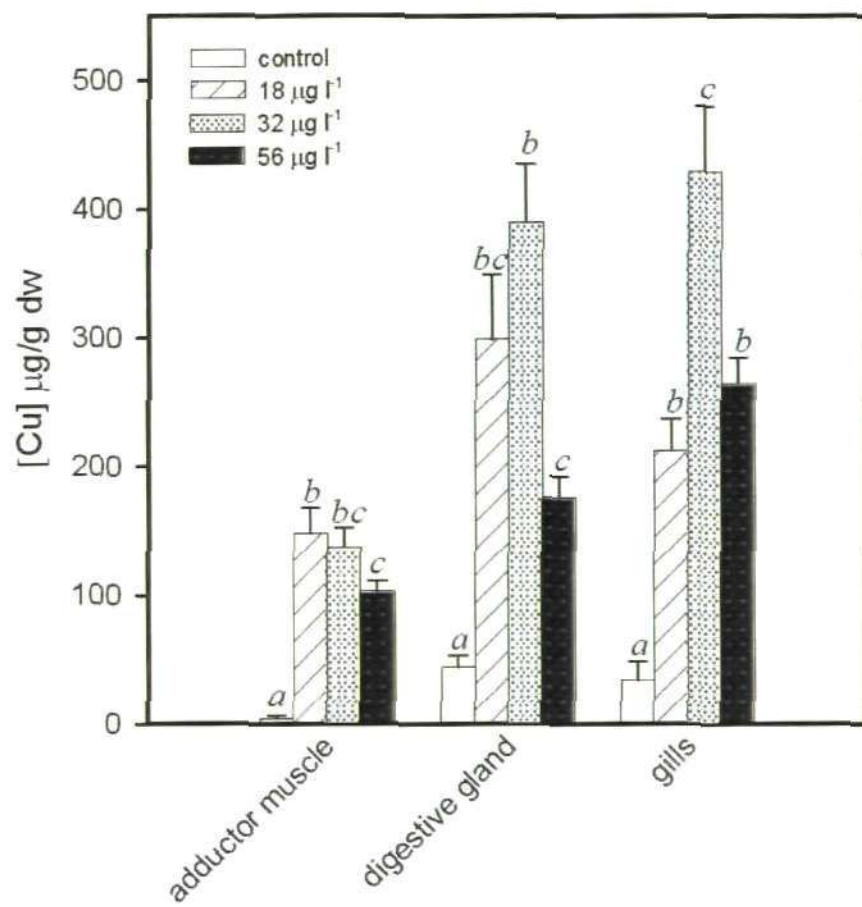


Fig. 5.6 Copper concentrations in adductor muscle, digestive gland and gills. Data are means \pm S.E.M., $n = 4$ mussel per treatment after 5 days of exposure. Different letters denote significant differences between data sets.

5.3.7 Correlation between genotoxicity and higher level biological responses

There was a significant relationship between Cu accumulation in gills and DNA damage (% tail DNA) in haemocytes ($R = 0.55$, $P = 0.02$; **Fig. 5.7B**). However, this was not the case for Cu accumulation in digestive gland and adductor muscle ($R = 0.34$, $P = 0.19$; $R = 0.27$, $P = 0.29$; respectively). In addition, there was a significant relationship between % tail DNA in haemocytes and total glutathione content in adductor muscle ($R = 0.79$, $P = 0.02$; **Fig. 5.7A**), and a significant negative correlation between % tail DNA in haemocytes and CR ($R = -0.56$, $P = 0.04$; **Fig. 5.7C**).

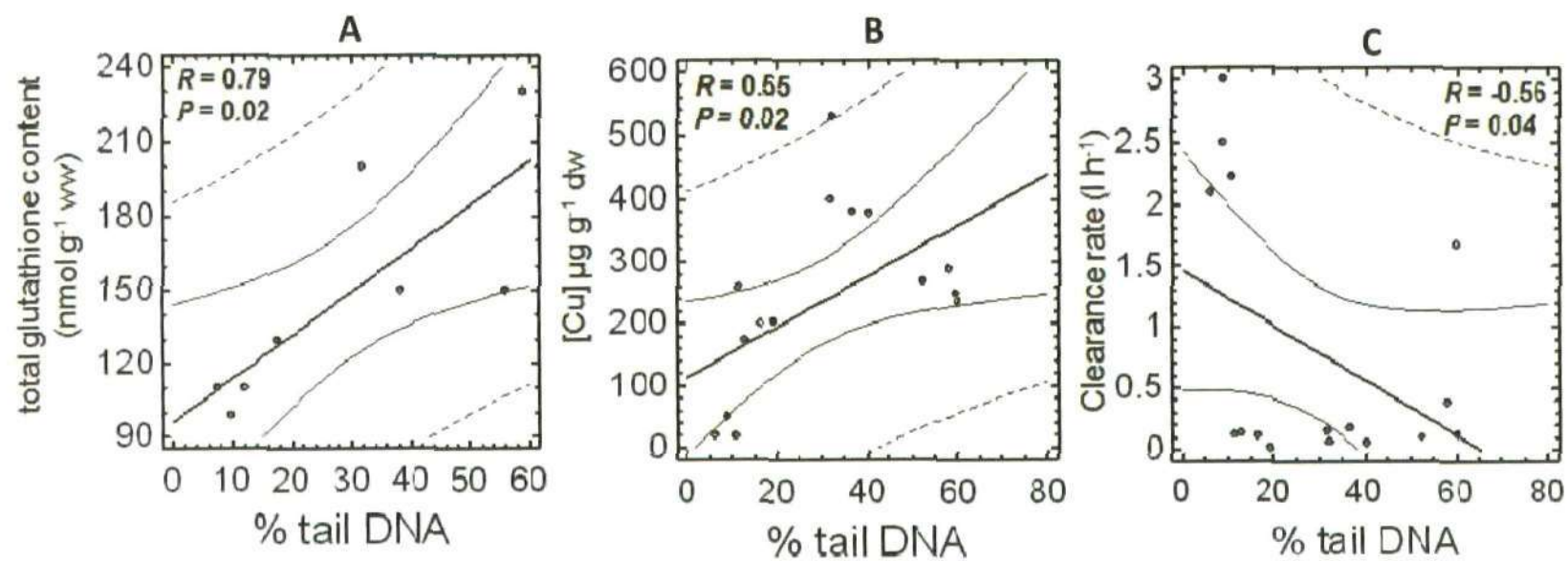


Fig. 5.7 Linear regression analysis illustrating correlations for genotoxic effects with (A) total glutathione level, (B) Cu accumulation in gills and (C) clearance rate in *Mytilus edulis* following 5 d exposure to Cu. The solid line is a linear regression and the dashed lines represent 95% confidence limits.

5.4 Discussion

In parallel with mammalian genotoxicological studies, the importance of MTC or MTD has been emphasized in aquatic ecotoxicological studies (Hutchinson et al. 2009). This is particularly so when determining the genotoxic effects of environmental contaminants. Whilst there have been several studies pertaining to evaluation of individual biological responses following exposure to environmental contaminants including metals in aquatic invertebrates such as mussels, to our knowledge there have not been many studies where an integrated approach has been adopted to concurrently evaluate DNA damage and effects at higher levels of biological organisation. In particular with physiological effects which could influence the ecotoxicological endpoints such as growth and reproductive success of the organisms (Jha 2008). In this study, we made an attempt to demonstrate that induction of DNA damage could precipitate or could have knock-on effects at higher level of biological organisation. The correlations between DNA damage and other biological responses however suggest that there might be a relation of such effects from lower to higher levels of biological organisation, however expression of different biological responses might not always be related (Canty et al. 2009). Several factors, including level of exposure, properties of contaminant and target cell or tissues could influence these manifestations.

It is widely accepted that bivalve molluscs can accumulate large amounts of Cu in their tissues (Lee et al. 2009b). While there are numerous reports that describe Cu accumulation in invertebrates (Mersch et al. 1993; Shi and Wang 2004b), to our knowledge, this is the first study that links the genotoxic effects of

Cu with other parameters at different levels of biological organisation (viz total glutathione at the biochemical level, accumulation and histological analysis at the tissue level, and finally, clearance rate at whole organism level). The results obtained demonstrate the responsiveness of the selected end points in *Mytilus edulis* to the toxic effects of Cu.

It is known that Cu plays a catalytic role in the initiation of free radical reactions under aerobic conditions. In this study, the oxidative status of exposed organisms was assessed using levels of total glutathione, an oxyradical scavenger, which can remove ROS to maintain cellular homeostasis. Thus, the significant increases in the total glutathione content reported in the present study could be explained as a immediate detoxification response by the organism to minimize the harmful effects of ROS in advance of induction of metallothioneins (Regoli et al. 2005). We have reported similar elevations of adductor muscle glutathione content in other studies using *Mytilus edulis* (5 days exposure to $40 \mu\text{g l}^{-1}$ Cu, (Al-Subiai et al. 2009); 3 days exposure to $56 \mu\text{g l}^{-1}$ (Trevisan et al. 2011). Overall, these data contrast with the observations of Canesi et al., (1999), who found an initial decrease (after 1 day) in total glutathione in the gills and digestive gland of mussels (*M. galloprovincialis*) exposed to $0.6 \mu\text{M}$ ($38 \mu\text{g l}^{-1}$) Cu, followed by a partial recovery by days 4 and 7 of exposure. They suggested that under exposure conditions an increase in γ -glutamyl-cysteine synthetase (GCS, the rate-limiting enzyme in glutathione biosynthesis) (Canesi and Viarengo 1997) seen in the digestive gland after 7 days would tend to restore glutathione levels.

In the present study, a significant correlation was found between the biochemical (glutathione content) and genotoxicity (% tail DNA) parameters

(Fig. 5.7A). This is not surprising since it would be expected that failure of the antioxidant defences to remove the additional ROS induced by Cu exposure, could lead to oxidative damage to macromolecules including DNA. Several studies have shown enhanced levels of DNA damage in aquatic organisms exposed to high concentrations of heavy metals in water (Barbosa et al. 2010; Emmanouil et al. 2007). In the present study a concentration-dependent increase in DNA strand breaks induced by Cu was observed (Fig. 5.2). This is clear evidence of genotoxic effects of Cu in mussels exposed under in vivo conditions, in agreement with that of Trevisan et al. (2011) who reported 70% increase in DNA damage using Comet assay after 3 days of exposure to $56 \mu\text{g l}^{-1}$ Cu in *Mytilus edulis*. Genotoxicity can possibly be interpreted in relation to the tissue-specific bioaccumulation patterns and animal physiology (Richardson et al. 2008).

Our findings indicate significant differences in the accumulation in mussel tissues, with the highest concentration in the gills. The relatively high accumulation in the gills and digestive gland supports previous findings and suggests their central role in Cu intake (Viarengo et al. 1981). In the present study, in general, accumulation of copper increased with increasing concentration of copper mainly in gills and digestive gland and to a lesser extent in the adductor muscle. These findings were in agreement with an earlier laboratory study which reported greater accumulation in gills and digestive gland after exposure for 3 weeks to $60 \mu\text{g l}^{-1}$ Cu (Regoli and Principato 1995). The highest Cu accumulation in the gills was expected since the gills are the first tissue barrier. However, at $56 \mu\text{g l}^{-1}$ exposure, Cu accumulation decreased relative to that seen with exposure to $32 \mu\text{g l}^{-1}$ Cu. It is unclear why this should be, but similar results have been obtained previously by Sanders et al., (1994)

who found a relationship between reduced accumulation at high Cu exposure with clearance rate (CR) reduction. However, CR here was affected to much the same extent by all three Cu concentrations, although the rate was tested at the end of the exposure, leaving the possibility that CR was affected earlier by $56 \mu\text{g l}^{-1}$ compared to $32 \mu\text{g l}^{-1}$ Cu. Another possibility is that at $56 \mu\text{g l}^{-1}$ some preferential distribution of Cu to other parts of the body such as the valves, byssus threads and mucous secretions could have occurred. Byssus threads are an important excretory route where preferential accumulation of Cu has been found previously in the zebra mussel *Dreissena polymorpha* (Gundacker, 1999), and the distribution of transuranic nuclides in marine mussels has been shown to be influenced by mucous secretions (McDonald et al. 1993). A third possibility is that by the end of the experiment tissue damage caused by exposure to $56 \mu\text{g l}^{-1}$ Cu had led to a partial release of Cu that had earlier been accumulated in tissues. In line with our observations, Sanders et al. (1994) reported a similar accumulation pattern in gills of *Mytilus edulis*, in which exposure to $32 \mu\text{g l}^{-1}$ Cu for 7 days led to the accumulation of more Cu than exposure to $100 \mu\text{g l}^{-1}$ Cu (about 89 and $44 \mu\text{g g}^{-1}$ dw, respectively). In the present study, the recorded Cu concentration in gills was approximately 5 times higher ($429.2 \pm 50.5 \mu\text{g g}^{-1}$ dw, at $32 \mu\text{g l}^{-1}$) which was consistent with the observations of Sanders et al. (1994) since in our study exposure was renewed every day over the 5 day exposure period.

Accumulation of Cu in mussel tissues provides an important link to the adverse effects on histological and physiological parameters. Higher concentrations of Cu within a particular tissue lead to enhanced ROS production and DNA strand breaks. Interestingly, the genotoxic response determined in the haemocytes showed good correlation with Cu accumulation in the gills (Fig. 5.7B), which

could be a reason for the morphological alteration in mussels' organs observed in our study. Sunila (1986) reported that the histological changes in the gills of mussels exposed to $100 \mu\text{g l}^{-1}$ Cu for just 1 day continue to be present a year after exposure. Histological changes are usually associated with general behavioural responses to stress. Filtration of water-borne food particles from water is the primary function of the cilia (Silverman et al. 1996). The de-ciliation (erosion) seen in the histopathology could explain the rapid reduction in the mussel clearance rates seen after Cu exposure. Clearance rate reductions in mussels have been reported in many studies after Cu exposure. For example, Shi and Wang (2004a) showed that clearance rate was significantly inhibited in mussels pre-exposed to 4 and $30 \mu\text{g l}^{-1}$ Cu for 7 days of exposure. In contrast, clearance rates measured in *P. perna* by Anandraj et al.(2002) after 8 days of exposure to $50 \mu\text{g l}^{-1}$ Cu were not significantly different from control values. The *apparent lack of reduction in CR in their study could be attributed to several factors including individual variability in metabolic activity between organisms, or possibly differences in methodology, since individual mussels in their study were allowed to filter algal particles for 30 min in comparison with 20 min in our present study. Previous work in our laboratory using reference genotoxins (methyl methane sulfonate, MMS, and cyclophosphamide, CP) (Canty et al. 2009) has demonstrated strong correlation between induction of DNA strand breaks and the clearance rate which is in line with our current study using Cu (Fig. 5.7C).*

5.5 Conclusions

In conclusion, short-term exposure to environmentally realistic levels of Cu induces a range of responses at different levels of biological organisation in the marine mussels, *M. edulis*. The DNA damage induced by Cu showed some correlations with biochemical and physiological measures. Although a direct correlation between DNA damage (quantitative data) and histopathological responses (qualitative data) was not possible, most of the histopathological responses appeared to be indicator of oxidative stress. Since there is an increasing need to link induction of DNA damage with other ecotoxicologically relevant parameters, even if the expression of different responses might not always be linked-up, our study goes some way towards identifying the levels of biological organisation which could be used as sensitive indicators in an stressed ecosystem.

Chapter 6

Interactive toxic effects of C₆₀ fullerenes and fluoranthene in adult marine mussels, *Mytilus edulis*

Results from this chapter have been presented at the 40th EEMS annual meeting, Oslo, Norway, Sep 2010 (poster presentation) and the Marine Institute Conference 2010, Plymouth, UK, Dec 2010. the results also have been presented at the University of Plymouth, Plymouth, UK (oral presentation) Nov 2010.

Hypothesis: C₆₀ fullerenes enhances the toxic impact of a model PAHs, fluoranthene.

Abstract

While there is growing concern over the potential detrimental impact of engineered nanoparticles (ENPs) on the natural environment, little is known about their interactions with other contaminants. In three short exposures (3 days) mussels, *Mytilus sp.* were exposed to C₆₀ fullerenes (0.1-1.0 mg l⁻¹) and fluoranthene (32- 100 µg l⁻¹), a model polycyclic aromatic hydrocarbon (PAH), either alone or in combination. The first two experiments were conducted by exposing the organisms to differing levels of C₆₀ fullerenes and fluoranthene alone, in order to determine the effects on total glutathione, genotoxicity (DNA strand breaks using Comet assay in haemocytes), histopathological changes in different organs (adductor muscle, digestive gland and gills) and physiological effects (feeding or clearance rate). Subsequently, in the third experiment, a combined exposure of C₆₀ fullerenes plus fluoranthene (0.1 mg l⁻¹ and 32 µg l⁻¹, respectively) was carried out to evaluate all the endpoints mentioned above in addition to DNA adduct analysis by ³²P post-labelling. The levels of fluoranthene and C₆₀ fullerenes were determined using GC-MS and HPLC, respectively, in both water and tissue samples. Both fluoranthene and C₆₀ fullerenes on their own caused concentration-dependent increases in DNA strand breaks, but no DNA adducts were observed. The combined exposure to C₆₀ fullerenes and fluoranthene caused an enhanced increase in DNA strand breaks with a concomitant 2-fold increase in the total glutathione content. In addition, significant accumulations of C₆₀ fullerenes were observed in all organs, with highest levels in digestive gland (24.90 ± 4.91 µg C₆₀ fullerenes g⁻¹ ww). Interestingly, clear signs of abnormalities in adductor muscle, digestive gland and gills were also observed through histopathological examination. Clearance rates also indicated significant differences compared to control with exposure to

C_{60} fullerenes, and C_{60} fullerenes/fluoranthene combined treatments ($P = 0.0002$, $P = 0.017$, respectively), but not with fluoranthene exposure on its own. This study demonstrated that at the selected concentration, both C_{60} and fluoranthene evoke toxic responses and genetic damage. The combined exposure produced enhanced damage at approximately at an- "additive" rather than synergistic level, which appears to be as a result of oxidative stress.

6.1 Introduction

Since their discovery in 21st century, manufactured or engineered nanoparticles (ENPs; size ≤ 100 nm) have captured the attention of scientific organisations, government and industry worldwide. There has been much debate on the future implications of nanotechnology. ENPs have been widely used as crucial components for many emerging electronics, biomedicine, cosmetics and pharmaceuticals material (Singh et al. 2009). Given the widespread applications and their impending use in industry, both environment and humans will be increasingly exposed to ENPs in the near future; thus, early evaluations of their potential toxicological and health impacts are valuable. (Moore et al. 2007). While ENPs are being increasingly produced every year from industry, these materials may make their way into aquatic environment and still very little has been done to predict their impact in the ecosystem. Since, ENPs have a very large surface area to volume ratio, this unique feature can result in: (a) high affinity for organic and metallic pollutants (b) direct generation of reactive oxygen species (ROS) and (c) ability to penetrate cells. The recent report by European Agency for Safety and health at Work (EASW) 2009, suggested that ENPs pose the strongest emerging risk to human health. They recommended that *in vivo* toxicological investigations are necessarily needed in for nanomaterials to obtain more reliable data base to meet European standard regulations.

C₆₀ (Buckminsterfullerene or fullerenes) was chosen for the current study, as it is an elementary component in many of the modern manufactured products. In common with other ENPs, the potential health risk of C₆₀ fullerenes has not been properly evaluated. Previous *in vivo* studies have evaluated the oxidative

stress effects in embryonic zebrafish induced by C₆₀. Usenko et al. (2008) suggested that C₆₀ can act as pro-oxidant and enhance toxic response by interacting with macromolecule such as DNA, protein and lipid.

Fluoranthene is one of the most common pyrogenic PAHs contaminants in human food and environmental samples. Its concentration has been found in sediment to range from tens to hundreds $\mu\text{g g}^{-1}$ dry weight sediment (Gao et al. 1998). Due to the fact that fluoranthene can be metabolised by aquatic organisms and consequently may exert both acute toxic and genotoxic effects (Palmqvist et al., 2006), U.S. Environmental Protection Agency (EPA) has classified fluoranthene as one of the 16 priority PAHs.

In the environment, organisms are generally exposed to a cocktail of different pollutants (rarely occur alone). These include combination of organics, trace metals and ENPs (Boxall et al. 2007; Echols et al. 2009) and could interact in different ways (i.e. additively, synergistically, or antagonistically) to induce adverse biological response at different levels of biological organisation. In addition to direct interaction with biomolecules, these agents could also induce oxidative stress via generation of reactive oxygen species (ROS) (Guldi and Prato 2000). Following ROS induction, a series of remarkable biological responses is triggered by attacking DNA, proteins and lipid membranes. Yang et al. (2010) reported in their preliminary studies on the effect of suspended C₆₀ on the photo-induced toxicity of fluoranthene. Their assay showed fluoranthene may be transported from the surface of the cage-like structure of C₆₀ particles and then cross the membrane. Thus, they suggested that interaction between C₆₀ fullerenes and fluoranthene decreases both the uptake rate and increases the elimination rate of fluoranthene.

To investigate the potential oxidative stress and mechanisms of toxicity, an integrated approach is needed at different levels of biological organisation. The determination of cellular and subcellular response, as well as specific function and structure of organs and physiology to provide more holistic assessment of the overall biological significance of such environmental variations is required. The interactive effects of C₆₀ plus fluoranthene were determined at several levels of biological organisation. At the biochemical level, DNA strand breaks in haemocyte, DNA adduct in different tissues and total glutathione content in adductor muscle were determined. While, at the tissue and organ levels, C₆₀ accumulation and histopathology in adductor muscle, gills and digestive gland were evaluated. Finally, at the whole organism level, clearance rate was assessed. To the best of our knowledge, very little has been done with respect to investigate the ecotoxicological effects of contaminant exposure to PAHs and ENPs at different level of organisations.

The research carried out within this is targeting strongly two interacting main areas. The first main aim of the current study is to characterize C₆₀ fullerenes nanoparticles (i.e. the structure and properties). The second main aim is to study the role of C₆₀ in adsorption to other potential contaminants in the environment and to understand the influence such particles can have on our environment.

6.2 Materials & Methods

6.2.1 Chemicals

All chemicals and reagents were of the highest analytical reagent grade obtained from Sigma-Aldrich (Pool, UK.) unless stated otherwise.

6.2.2 Solution preparation

A primary stock solution (5.0 mg ml^{-1}) of fluoranthene was prepared in acetone. Individual test solutions were prepared by adding the appropriate volume of the primary stock to the dilution acetone. The fluoranthene concentration in the dilution water was measured using GC-Mass on a Varian SpectrAA 600. Fullerenes, C_{60} , with purity 99.5%; lot number 11401DB (according to the manufacturer's information) was obtained from Sigma-Aldridge and Elicarb SW. Nanomaterial was dissolved in filtered seawater to avoid the interactions with residual organic solvent. The stock solution of 0.1 and $1.0 \text{ mg l}^{-1} \text{C}_{60}$ fullerenes was ultrasonicated (35 kHz frequency, Fisherbrand FB 11010) for 1 h to ensure uniform dispersion and size distribution.

6.2.3 Animals collection and maintenance

Mussels (*Mytilus edulis*) of similar shell length (51-58 mm) were collected at low tide (April 2008) from Trebarwith (Cornwall, UK), a relatively clean site. After collection, animals were transported immediately in cool box to the laboratory and were kept under controlled condition, as described in section 2.1.

6.2.4 Exposure condition

The experiments were divided into 3 short-term (3 day) exposures to assess the toxicity of C₆₀ either alone or in combination with fluoranthene. The first two experiments were conducted by differing levels of exposure to fluoranthene and C₆₀ concentrations, to evaluate potential dose response relationships for toxicological responses.

6.2.4.1 Fluoranthene exposure

Initially, this experiment was designed (Fig. 6.1) to validate the sensitivity of genotoxicity test, Comet assay, by using fluoranthene as a reference genotoxic agent. Exposure concentrations range for fluoranthene was chosen based on published results to determine lysosomal membrane damage in this species (Lowe et al., 1995). The other concentration range was however slightly modified to fit the semi-logarithmic scale which is widely used in ecotoxicological studies. In 2 L glass beaker (3 animal beaker⁻¹), individuals were exposed with (32, 56, 100 µg l⁻¹) fluoranthene. Exposure of *Mytilus edulis* to fluoranthene was carried out following 3 days exposure, with removal of mussels at the end of exposure period for estimation of the DNA damage, histopathology and feeding rate. Exposure to solvent controls was also carried out; in these acetone was (0.05 g ml⁻¹) added in place of fluoranthene. The seawater was changed daily and re-dosed with appropriate dose of fluoranthene. Animals were not fed during the experiment. All treatments were set up in triplicate.

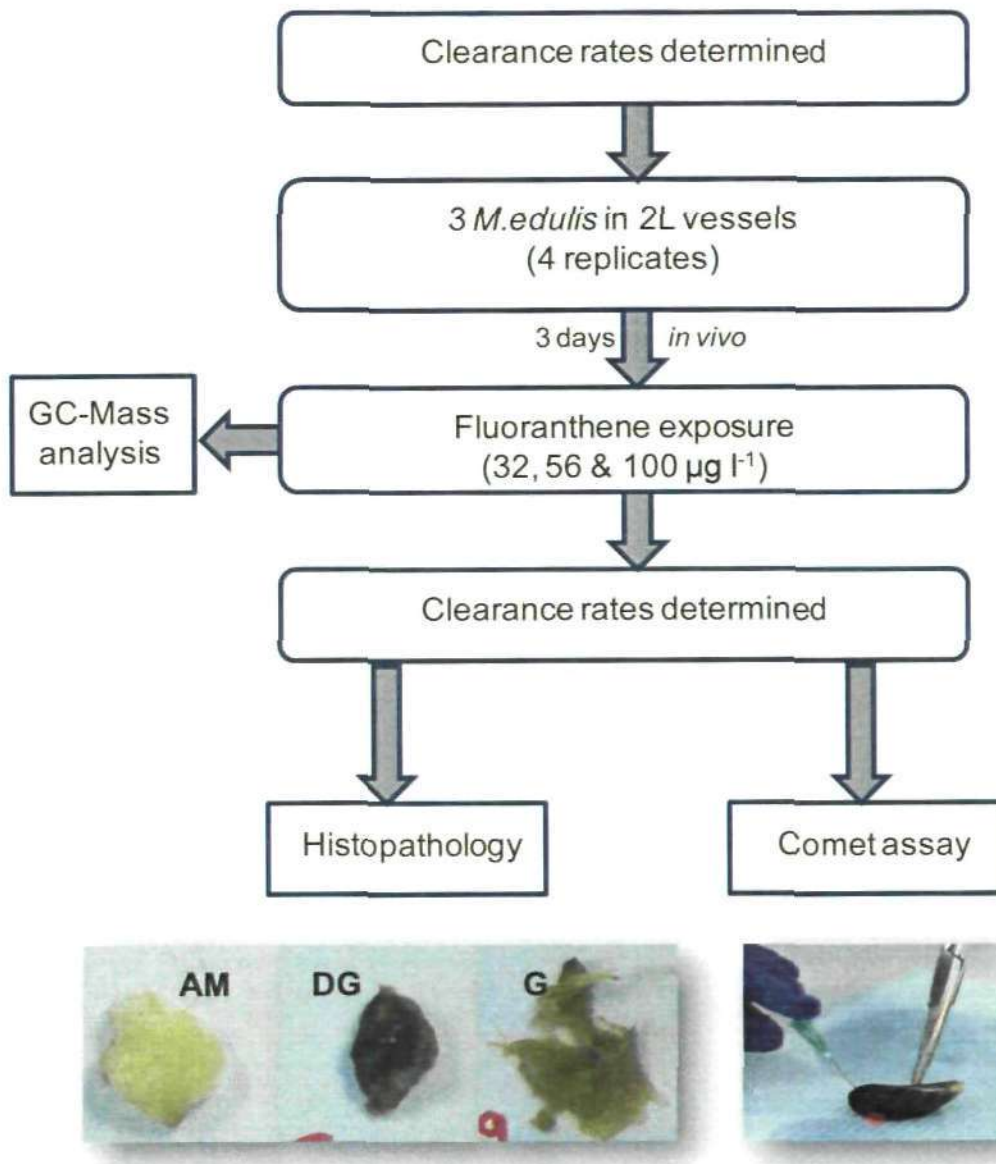


Fig. 6.1 Fluoranthene exposure experimental design. AM = adductor muscle; DG = digestive gland; G = gills.

6.2.4.2 *C₆₀ exposure*

In 10 L glass tanks (10 animal tank⁻¹), mussels were exposed with (0.1 and 1.0 mg l⁻¹) C₆₀, as illustrated in **Fig. 6.2** for 3 days. At the end of exposure period, three animals from each tank were taken and the tissues (i.e. adductor muscle, digestive gland and gills) were dissected and prepared for biochemical, histopathological, behavioural and chemical determination. In parallel, exposure with 32 µg l⁻¹ fluoranthene was also carried out as positive control. The seawater was changed daily and re-dosed with appropriate concentration of C₆₀. Animals were not fed during the experiment. All exposures groups were in triplicate.

6.2.4.3 *Combined exposures of C₆₀ fullerenes and fluoranthene*

Hundred and twenty mussels (*Mytilus edulis*) were divided between twelve 10 L glass tanks (10 animals per tank) of sea water. In three tanks per exposure, individuals were exposed to 0.1 mg l⁻¹ C₆₀ fullerenes, 32 µg l⁻¹ fluoranthene and mixture of C₆₀ fullerenes plus fluoranthene at the same concentrations. In this experiment (as shown in **Fig. 6.3**), two exposure periods were considered: three days exposure and three days post exposure, with removal of mussels at the end of each period for analysis of DNA damage, total glutathione contents, histopathology, C₆₀ fullerenes accumulation and clearance rate. The seawater was changed daily and re-dosed with appropriate dose of C₆₀ fullerenes and fluoranthene. Animals were not fed during the experiment. Three mussels were randomly collected from each tank. Immediately, for each mussel, haemolymph and tissue (i.e. adductor muscle, gills, and digestive gland) samples were collected, and were transferred carefully into an eppendorf tube and placed on ice for analysis.

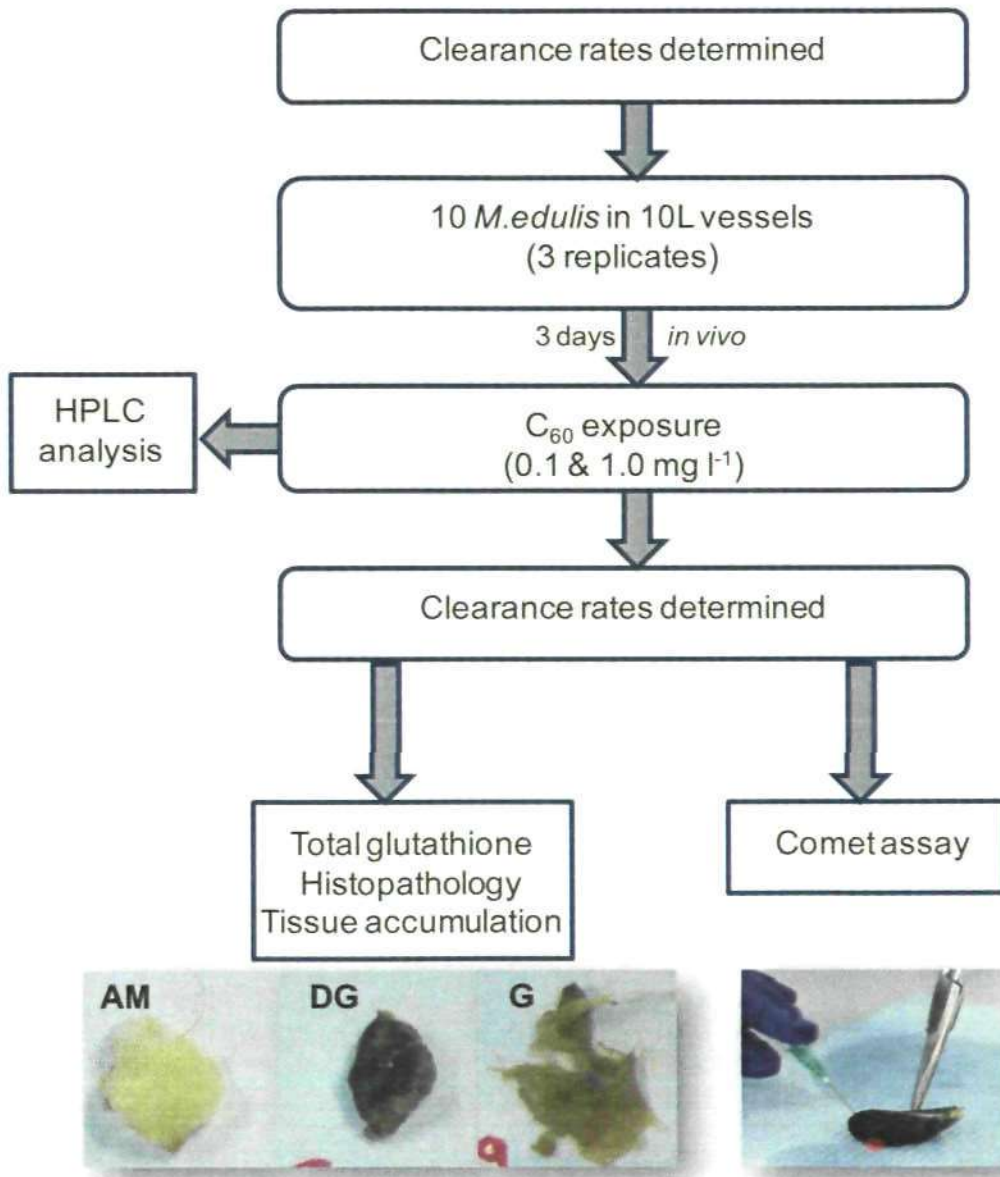


Fig. 6.2 C_{60} fullerene exposure experimental design. AM = adductor muscle; DG = digestive gland; G = gills.

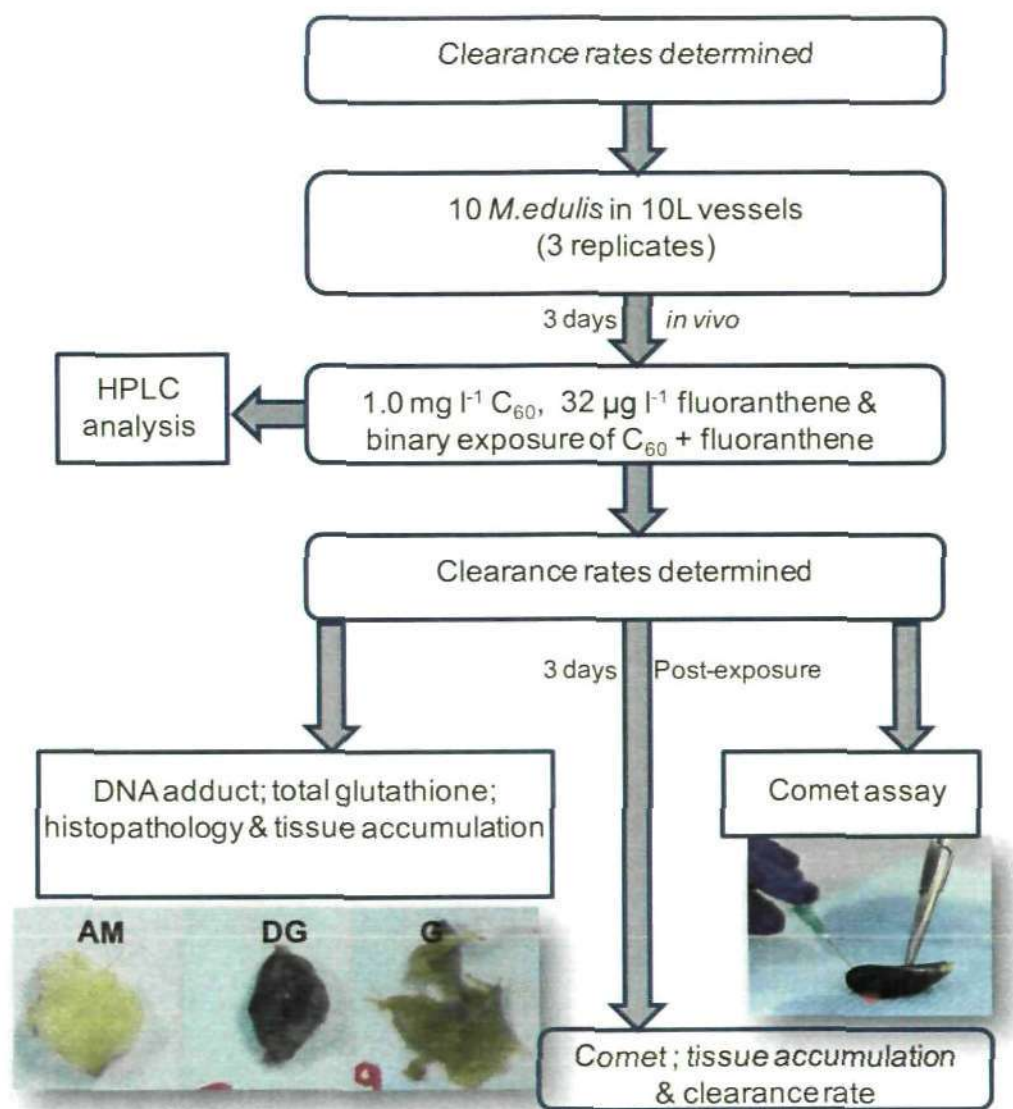


Fig. 6.3 Experimental design for C_{60} , fluoranthene & binary exposure of C_{60} + fluoranthene. AM = adductor muscle; DG = digestive gland; G = gills.

6.2.4.4 Collection of haemolymph samples and preparation of adductor muscle extract

From each individual, approx. 0.2 ml of haemolymph was extracted from the posterior adductor muscle into 0.2 ml physiological saline, as described in section 2.3.1. haemolymph samples were held on ice to minimise cellular stress. The posterior adductor muscles from two mussels (approximately 0.2 g wet weight) were dissected out and were homogenized in 1:3 ratio (w/v), as described in section 2.3.2, for total glutathione analysis.

6.2.5 Determination of DNA strand breaks using the Comet assay

Haemocytes viability was checked by using Eosin Y assay, as described in section 2.4.1 and the DNA damage in the haemocytes of mussels was determined using the alkaline Comet assay, as described in section 2.4. The level of DNA damage in 100 cells per sample was measured by Komet 5.0 image-analysis system (Kinetic Imaging, Liverpool, UK) using epifluorescence microscope (Leica, DMR). Data for percentage tail DNA were presented as a measure of single-strand DNA breaks/alkali labile sites.

6.2.6 DNA adduct analysis

6.2.6.1 DNA extraction

DNA samples were extracted as described in Jaeschke et al., (2011) using a standard manual chloroform/isoamyl alcohol technique using nucleic acid purification grade materials. Small piece of tissue (1-3 mm³) was briefly homogenised into eppendorf with 100 µl cetyltrimethylammonium bromide (CTAB) buffer. One microliter of proteinase K (20 µg ml⁻¹) was then added and incubated at 65°C for 60 min. The digest was then extracted with 100 µl of chloroform:isolamyl alcohol (24 :1) and mixed for 2 min. To obtain clear

aqueous phase, DNA samples were centrifuged for 10 min at 10,500 g_{av} and the supernatant (clear layer) was placed in new clean eppendorf tube. Upon precipitation, the DNA was washed twice with 200 μ l of 70% ethanol and centrifuged for 20 min at 10,500 g_{av} . After centrifugation, DNA pellet was allowed to dry in air and dissolved in 100 μ l of distilled water. DNA concentration and purity was determined spectrophotometrically, using a NanoDropTM1000 spectrophotometer (USA) Spectrophotometrical analysis of the $A_{230} : A_{260}$ and $A_{260} : A_{280}$ ratios indicated that the samples were essentially free from RNA contamination and protein, respectively (**Fig. 6.4**).

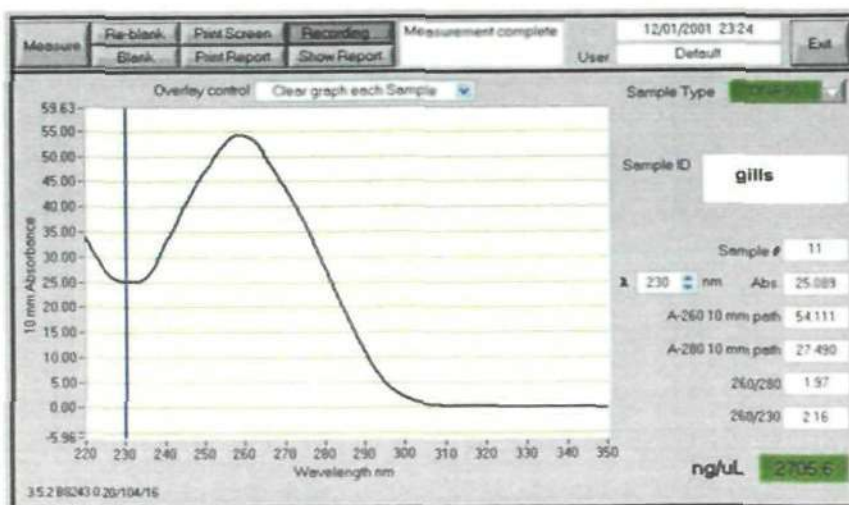
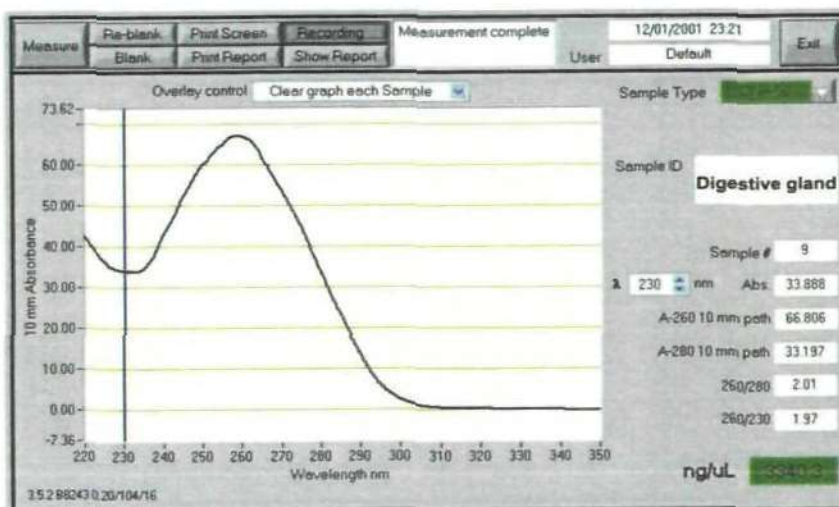
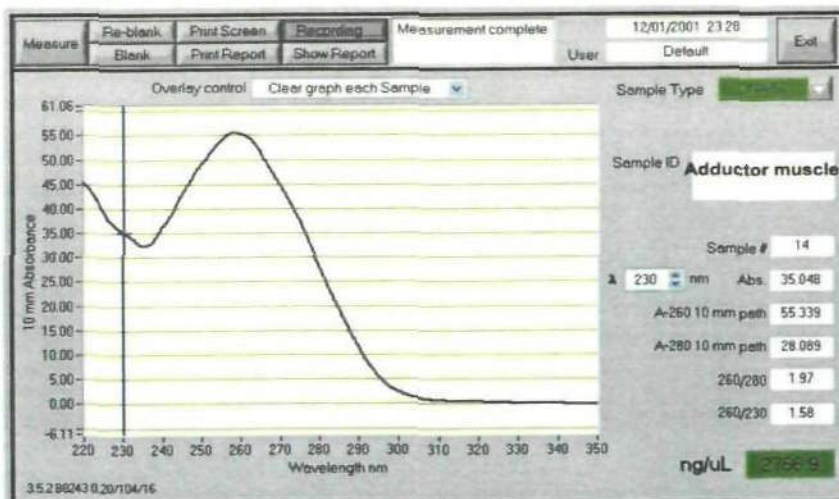


Fig. 6.4 DNA purity and concentrations data from different tissues of *Mytilus edulis*. Highlighted number is DNA concentration in 2 μ l of the sample.

6.2.6.2 DNA ³²P-post labelling

DNA adducts analysis for each DNA sample were carried out at Institute of Cancer Research (ICR) (Surrey; UK) by Dr. V. Arlt using the ³²P-postlabelling method as described previously by Arlt (2008); Phillips and Arlt (2007). Briefly, DNA samples (4 µg) were digested with micrococcal nuclease (120 mU, Sigma, UK) and calf spleen phosphodiesterase (40 mU, Calbiochem, UK) in digestion buffer (16.6 mM sodium succinate, 8.3 mM CaCl₂, pH 6.0) overnight at 37°C in a total volume of 4.8 µl. For nuclease P1 enrichment, digests were incubated with 1.2 µg nuclease P1 (Sigma, UK) in 4.8 µl of buffer containing 125 mM sodium acetate, pH 5.0, 0.4 mM zinc chloride for 60 min at 37°C. The reaction was terminated by the addition of 1.9 µl tris base (0.5 M). DNA digests were then ³²P-labelled with carrier-free [γ -³²P]ATP (50 µCi, appr. 6000 Ci mmol⁻¹, Hartmann Analytik, Germany) in a mixture of 4 µl consisting of 80 mM bicine pH 9.0, 40 µM magnesium chloride, 40 mM dithiotreitol, 4 mM spermidine and 6 U T4 polynucleotide kinase (USB, UK) for 30 min at 37°C. Resolution of ³²P-labelled adducts was carried out by chromatography on polyethyleneimine-cellulose (PEI-cellulose) thin-layer chromatography (TLC) sheets (10x20 cm, Macherey-Nagel, Düren, Germany) using the following solvents: D1, 1.0 M sodium phosphate, pH 6.0; D3, 4 M lithium-formate, 7 M urea, pH 3.5; D4, 0.8 M lithium chloride, 0.5 M Tris, 8.5 M urea, pH 8.0. TLC sheets were scanned using a Packard Instant Imager (Dowers Grove, IL, USA) and DNA adduct levels (RAL, relative adduct labelling) were calculated from the adduct cpm, the specific activity of [γ -³²P]ATP and the amount of DNA (pmol of DNA-P) used. Results were expressed as DNA adducts 10⁸ nucleotides⁻¹. An external BPDE-

DNA standard (Phillips and Castegnaro 1999) was employed for identification of adducts in experimental samples.

6.2.7 Determination of total glutathione level in adductor muscle extract

The total glutathione (i.e. reduced, GSH, and oxidised, GSSG) content of adductor muscle extract was determined essentially according to section 2.5. The rate of absorbance decrease at 412 nm was measured by microplate reader (Optimax, Molecular Devices, Sunnyvale, CA) over 5 min using 96 well plates. The assay temperature in each case was 22 °C.

6.2.8 Histological preparation for adductor muscle, digestive gland and gills

Tissues collected from exposed animals (i.e. adductor muscle, digestive gland and gills) were examined by normal histological methods as described in section 2.6 in details. Fixation of the samples was in 10% buffered formal saline, and then the specimens were processed in ascending grades of alcohol. Tissue samples were impregnated in paraffin and cut with microtome at 5-7 µm thickness.

6.2.9 Clearance rate

Clearance or feeding rates of individual mussel were determined as described elsewhere in section 2.7. Water samples were analysed on Backham™ Coulter Particle Size and Count Analyser (Z2), with a 100 µm aperture fitted and set to count particles between 4.0-10.0 µm in diameter.

6.2.10 Chemical analysis of fluoranthene and C₆₀ using analytical techniques

6.2.10.1 GC-analysis of fluoranthene in water samples

Water samples were placed into glass vial with dichloromethane (DCM) and stored at dark -20 °C. One microlitre of sample extract was injected in Agilent Technologies 6890 N Network GC system interfaced with an Agilent 5973 series mass selective detector. For separation, an HP-5MS (crosslinked 5% phenyl methyl siloxane) capillary column (30 m) was used with a film thickness of 0.25 µm and internal diameter 0.25 mm. Helium (He) was used as a carrier gas (maintained at a constant flow rate of 1 ml min⁻¹). Column temperature was programmed for 40 °C for 1 min, 40– 300 °C for 15 min and was held at 300 °C for 5 min. Samples were screened for fluoranthene using selected ion monitoring, in which the target ions was 202 and qualifying ions was 188 for Phen d₁₀. Prior to sample analysis, the system was calibrated using standard mixture (Grob mixture). In addition, solvent blank was run in between samples analysis for quality assurance purposes (Fig. 6.5).

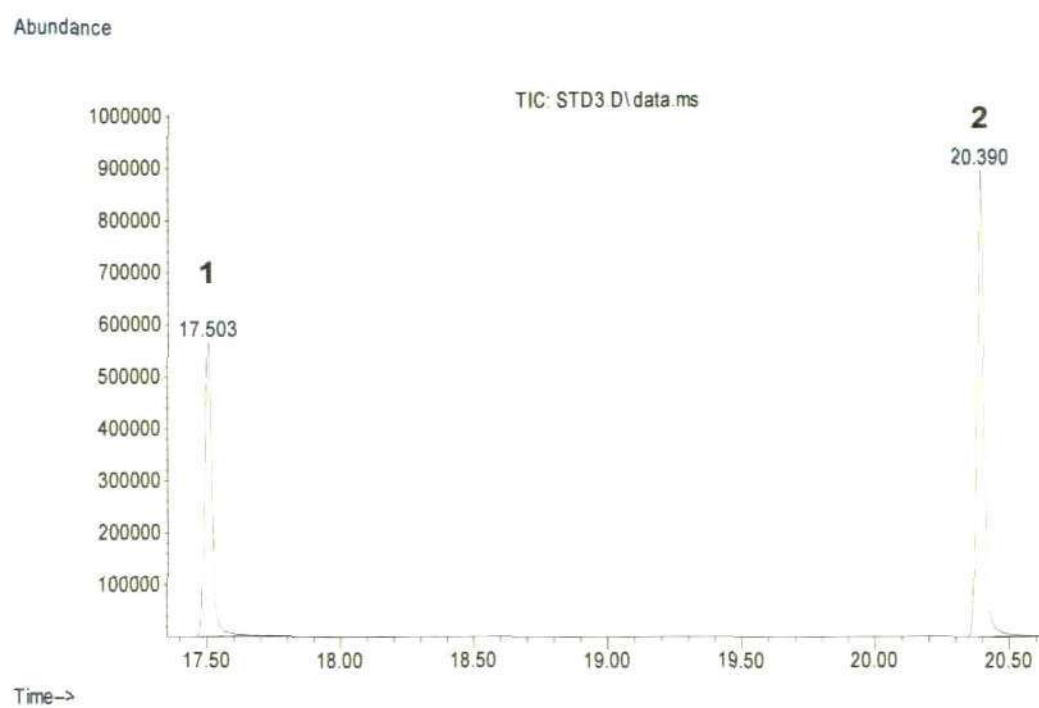


Fig. 6.5 Total ion current GC-MS chromatograms of standard compounds (1 = Phen d_{10} ; 2 = fluoranthene).

6.2.10.2 HPLC-analysis of C_{60} in tissue samples

HPLC method was developed for C_{60} analysis using Hypersil (5 μ) Elite C18 (250 X 4.6 mm I.D.) column, as described elsewhere in section 2.8. In case of mixed samples (C_{60} + F) Plgel 5 μ m 50Å (manufactured by Agilent Technologies; USA) column was used. The mobile phase was composed of pure toluene. For both columns used, a standard curve was generated for C_{60} concentrations (dissolved in toluene) ranging from 0.125 and 2.0 mg l⁻¹ (Fig. 6.6). Concentration of test samples was determined by comparison to the standard curve.

6.2.11 Statistical analyses

Statistical analyses were performed using statistical package Stat graphics plus version 5.1 (Statistical Graphics Corp). All results are presented as mean \pm S.E. Significant differences between groups were studied using one way ANOVA analysis of variance or Kruskal-Wallis test, followed by multiple range tests to differentiate between the groups of data, and only $P < 0.05$ was accepted as significant.

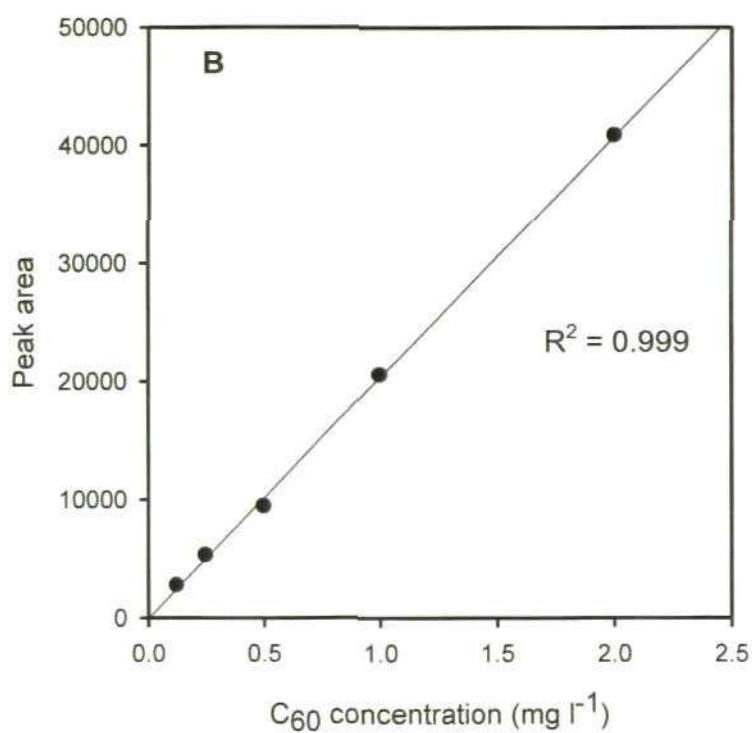
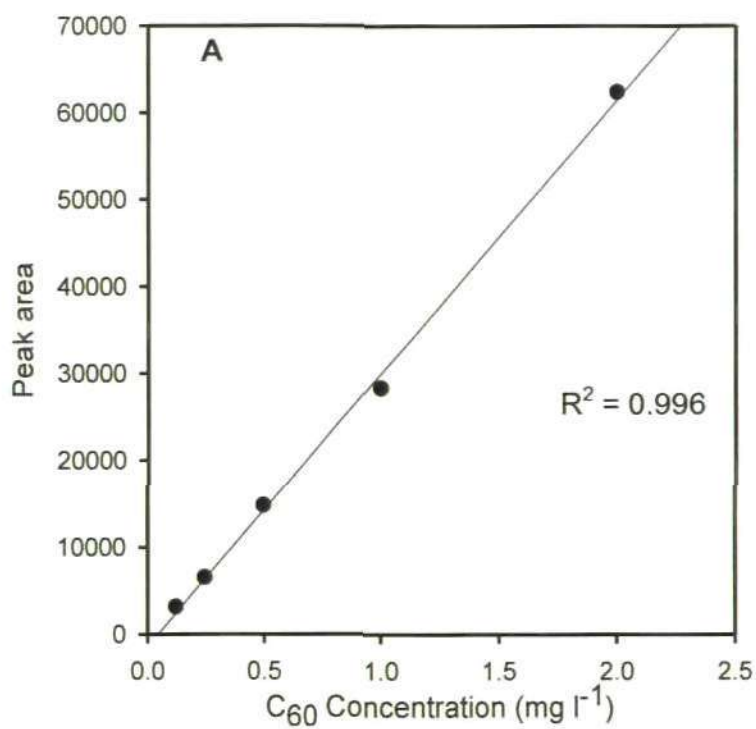


Fig. 6.6 A standard curve for C₆₀ (dissolved in toluene) using different concentrations dissolved in toluene ranging from 0.125 and 2 mg l⁻¹ using (A) Elite C18 and (B) Plgel 5µm 50Å.

6.3 Results

Initially our experiments were designed to establish concentration-response relationships. In three separate experimental exposures, mussels were exposed to different levels of exposure: fluoranthene, C_{60} and binary mixture (i.e. C_{60} + fluoranthene). A validation experiment was conducted to optimise the exposure condition for fluoranthene, as a reference exposure. To demonstrate knowledge of the interactive effects of C_{60} with model PAHs, another two experiments were conducted to obtain a broader picture. In the first exposure, a preliminary experiment was conducted by using two different concentrations of C_{60} (0.1 and 1.0 mg l⁻¹) to determine the effective C_{60} concentration. Selection of these concentrations was based on earlier study to determine NRR (Moore et al. 2009). Then, based on the results coming out from the previous two separate experiments with fluoranthene and C_{60} , third experiment was carried out using binary exposure of C_{60} plus fluoranthene in order to investigate the potential interactive effects between the two contaminants. The effects of exposure in mussel haemolymph and tissues were determined at different levels of organisation: genotoxicological, biochemical, histopathological and behavioural assays to measure potential adverse effects of each exposure.

6.3.1 Characterisation of C_{60} nanoparticle

To characterise C_{60} stock sample, buckyballs were dissolved in Milli-Q water. The distribution, size and shape of the particles were obtained by transmission electron microscopy (TEM) analysis. Observing the C_{60} stock sample under the transmission electron microscope (TEM), we found them to be mostly as hexagonal shape. From a total of 129 nanoparticles adsorbed on 1 grid, we determined that approximately 125 particles had diameters or lengths

across their longest dimensions of less than 100 nm, and over 45% out of these particles had diameters less than 40 nm as presented in **Fig. 6.7**. Nanoparticle suspensions were applied to Cu coated grids and allowed to stand for 5 minutes for nanoparticle attachment. Particle size was measured with ImageJ software (ImageJ, U. S. National Institutes of Health, Bethesda, Maryland, USA, <http://rsb.info.nih.gov/ij/>).

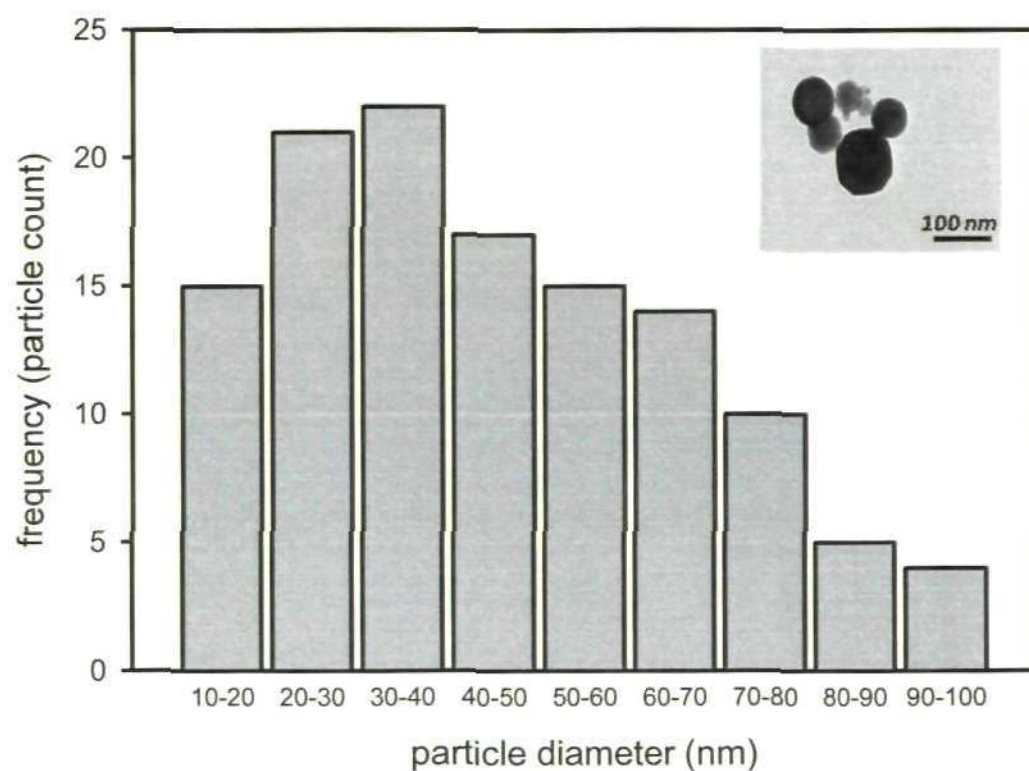


Fig. 6.7 Representative of TEM image of C₆₀ (inset) and histogram of C₆₀ particles diameter determined by TEM.

6.3.2 Determination of DNA damage

No significant loss of cell viability for haemocytes was observed (cell viability > 90% in all samples after Eosin Y staining) following exposure to either in fluoranthene, C₆₀ or C₆₀ + fluoranthene (C₆₀ + F) experiment. Since the Comet data were not normally distributed, the non-parametric Kruskal-Wallis test was applied to demonstrate significant difference between groups.

The Comet results showed that there was a concentration response effect between fluoranthene concentration and %tail DNA (**Fig. 6.8A**). Also, in the second experiment a significant difference was found between the control and C₆₀ exposures ($P = 0.0036$) with higher DNA damage in 1.0 mg l⁻¹ C₆₀-exposed animals (**Fig. 6.8B**). Multiple range test (LSD) showed significant difference between all exposures. An equivalent DNA damage response was also observed with +ve control (fluoranthene, 32 µg l⁻¹) indicating the robustness of the Comet assay.

6.3.2.1 Combined exposures of C₆₀ and fluoranthene

Mussels showed a significant elevation in DNA damage in exposed animals in comparison with control. The results of Comet assay for single and joint effects of C₆₀ + F showed that combined exposure, led to a highest DNA damage among single exposure (**Fig. 6.8C**). After 3 days of post exposure, there was a significant decrease in DNA damage under all conditions, but the decrease was faster in the presence of fluoranthene. Comet data were analysed using 2-way ANOVA test and a significant interaction was found between exposure type and time of measurement ($P = 0.0001$).

Overall these results suggest that in all three exposures (F, C₆₀ and C₆₀ + F), there is evidence that C₆₀-induced DNA damage recovered to the normal level after the end of the exposure, and C₆₀ interaction with PAHs contribute in enhanced genotoxic effect in the haemocytes.

6.3.2.2 Determination of DNA adduct

The main radioactive spot (adduct) was detected in reference DNA (+ve control) exposed *in vitro* to B[a]P (**Fig. 6.9**). In the same zone, no adducts were evident by testing adductor muscle, digestive gland and gills DNA of mussels exposed to single exposure of C₆₀, fluorathene or binary exposure of both.

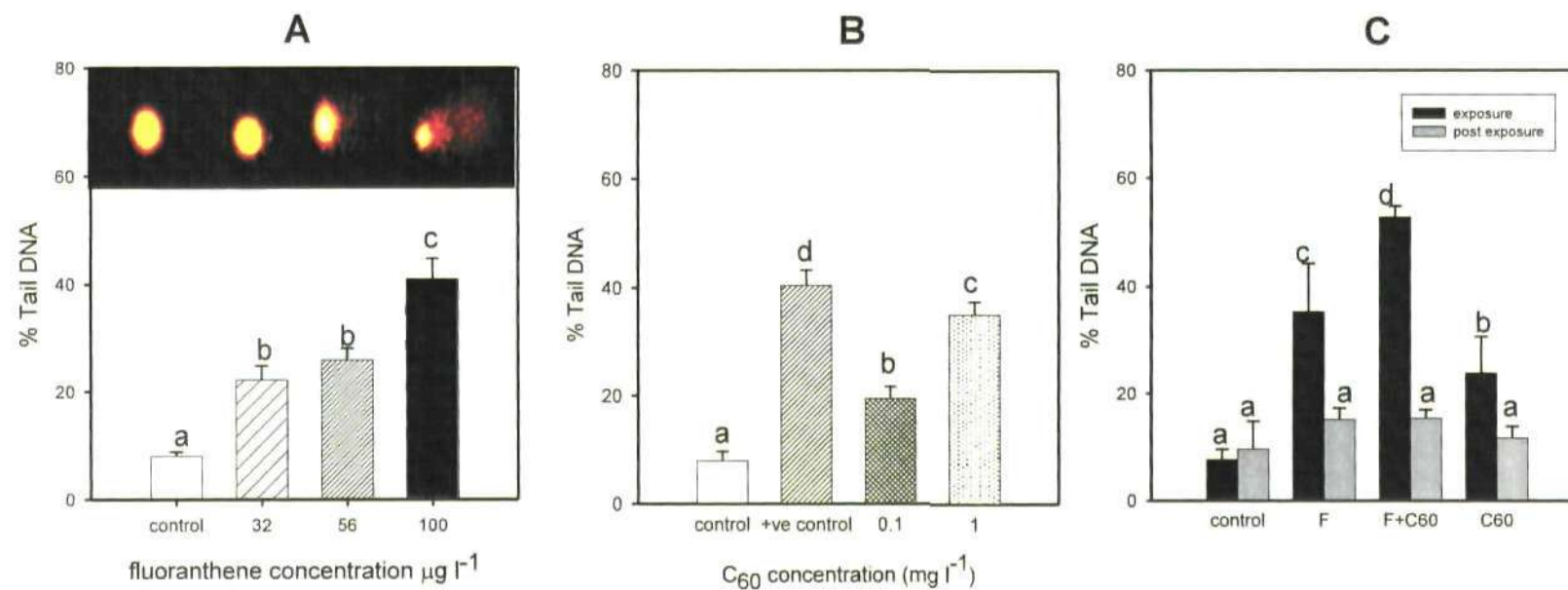


Fig. 6.8 Induction of DNA strand breaks, represented as %Tail DNA in *Mytilus edulis* haemocytes following 3 days *in vivo* exposure to: (A) fluoranthene (32, 56 and $100 \mu\text{g l}^{-1}$); (B) C_{60} (0.1 and 1.0 mg l^{-1}); and (C) C_{60} + fluoranthene (0.1 mg l^{-1} C_{60} and $32 \mu\text{g l}^{-1}$ fluoranthene). The values are mean \pm S.E. Bars with the same letters are not significantly different according to the multiple range test (LSD).

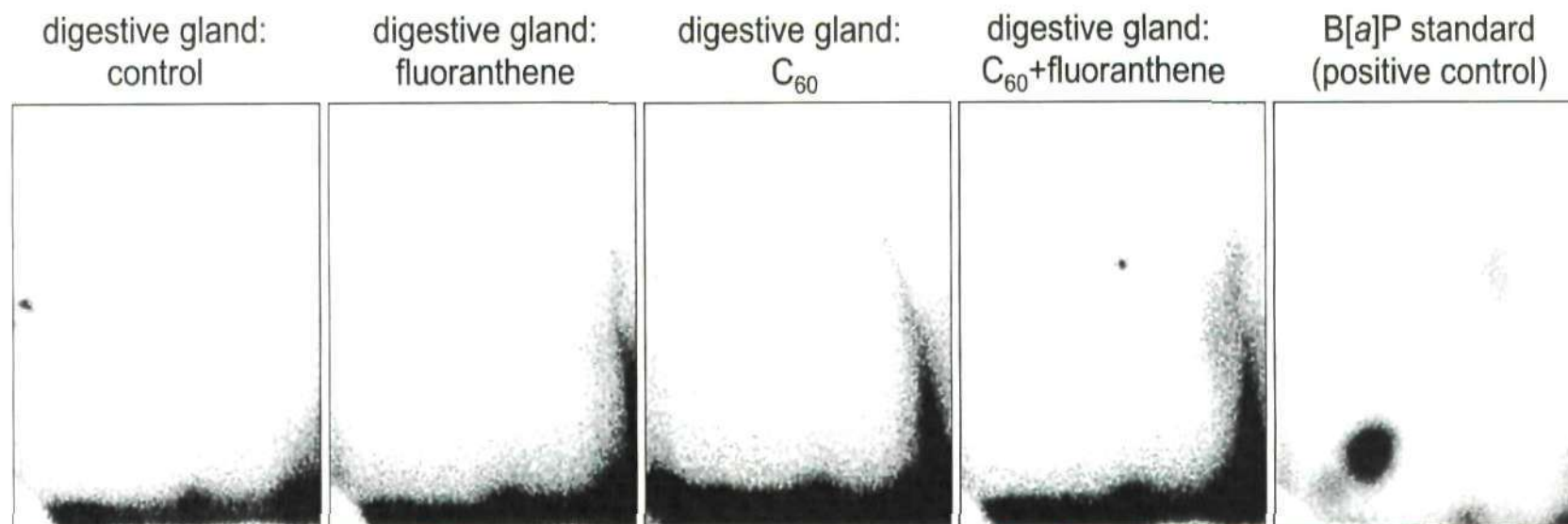


Fig. 6.9 ³²P-post labelling analysis of DNA from cells exposed to C₆₀, fluoranthene and C₆₀ + fluoranthene. DNA adduct profiles measured in digestive gland. Same results were obtained with gills and adductor muscle.

6.3.3 Determination of total Glutathione level in adductor muscle

Both C_{60} exposures (0.1 and 1.0 mg l⁻¹) did cause a slight increase in the total glutathione content, but did not significantly affect glutathione content in adductor muscle in comparison to control, as indicated in **Fig 6.10A**. On the other hand, a significant increase ($P < 0.05$, ANOVA) in total glutathione levels was reported in $C_{60} + F$ exposed animals. About 2-fold increase in total glutathione contents was seen in the adductor muscle after exposure to C_{60} and fluoranthene mixture in comparison to other groups. Multiple range test (LSD) showed significant differences at the 95% confidence levels, between the $C_{60} + F$ and fluoranthene exposure alone (**Fig. 6.10B**). It is worth mentioning that total glutathione levels in control samples from $C_{60} + F$ experiment were lower than the control from C_{60} experiment, but this effect could be attributed to seasonal variation.

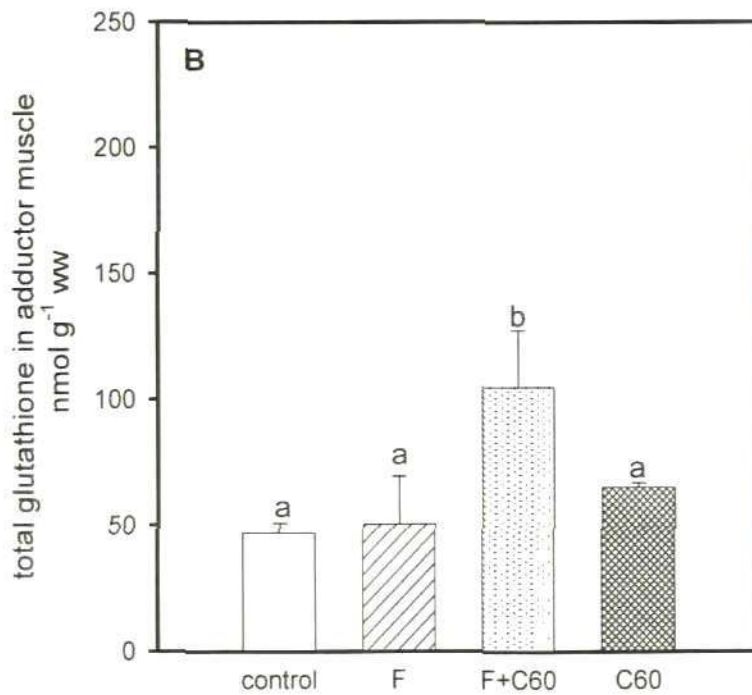
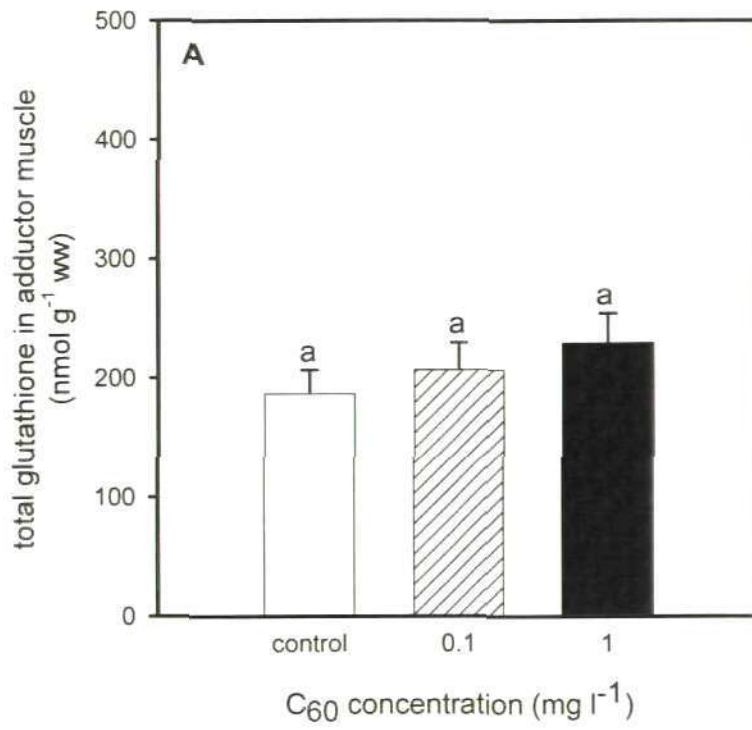


Fig. 6.10 Total glutathione levels in the adductor muscle extract following 3 days *in vivo* exposure to: (A) C₆₀; and (B) mixture of C₆₀ + fluoranthene (0.1 mg l⁻¹ C₆₀ and 32 µg l⁻¹ fluoranthene). The values are mean ± S.E. Bars with the same letters are not significantly different according to the multiple range test (LSD).

6.3.4 Histological studies

Histological observations indicated that there were no pathological signs in control specimens such as: haemocyte infiltration, necrosis or other injuries. Different tissues however showed varying degrees of abnormalities after exposure as summarised below.

6.3.4.1 Posterior adductor muscle

Adductor muscle specimens from 'C₆₀ exposure' did not show any histological abnormalities with the 0.1 mg l⁻¹ C₆₀, but high C₆₀ concentration did cause atrophy in myocyte cells and decrease extracellular spaces between muscle bundles in 3 out of 9 examined animals (**Fig. 6.11B**). Similar effects to 1.0 mg l⁻¹ C₆₀ were also observed with the adductor muscle exposed to binary exposure of C₆₀ + fluoranthene with more adverse effect in which 6 animals showed abnormalities with 2 animals showing hypertrophy (swelling) and loss of muscle bundle s organisation (**Fig. 6.11C**), and another 4 with muscle atrophy and decrease in extracellular spaces between muscle bundles.

6.3.4.2 Gills

Histological examination of the gills at the end of 'C₆₀' experiment showed that 0.1 mg l⁻¹ C₆₀ caused 22% abnormalities. Two mussels at the low C₆₀ concentration had evidence of hypoplasia in frontal and lateral cilia. Progressively more abnormalities were seen with high C₆₀ exposure (1.0 mg l⁻¹), in which 4 animals out of 9 observed specimens showed hypoplastic effect in the frontal and lateral cilia (**Fig. 6.11 H**). Whereas, gills examined after 'C₆₀ + F' exposure showed areas with cilia erosion and filaments necrosis in 3 of the observed specimens (**Fig. 6.11I**).

6.3.4.3 Digestive gland

The histological observations in digestive gland specimens from 'C₆₀ exposure' showed that the both C₆₀ concentration caused alteration in the digestive tubules (**Fig. 6.11E**). Low C₆₀ exposure caused loss of definition of the digestive tubules probably caused by necrosis in 3 out of 9 specimens, whereas 6 specimens exhibited necrosis in the digestive tubules. The effects of C₆₀ (low concentration) was enhanced even more when fluoranthene interacted with it in 'C₆₀ + F' experiment. The histological changes was characterised by necrosis in digestive cells within the digestive tubules. These changes were observed in all animals examined as atrophy of digestive tubule epithelium in which the epithelium cells shrank and exhibited thin tubules, only basement membrane remained and cellular debris was often observed within the lumen of digestive tubules (**Fig. 6.11F**). Stomach obstruction by haemocyte infiltration was also found in some of the examined sections.

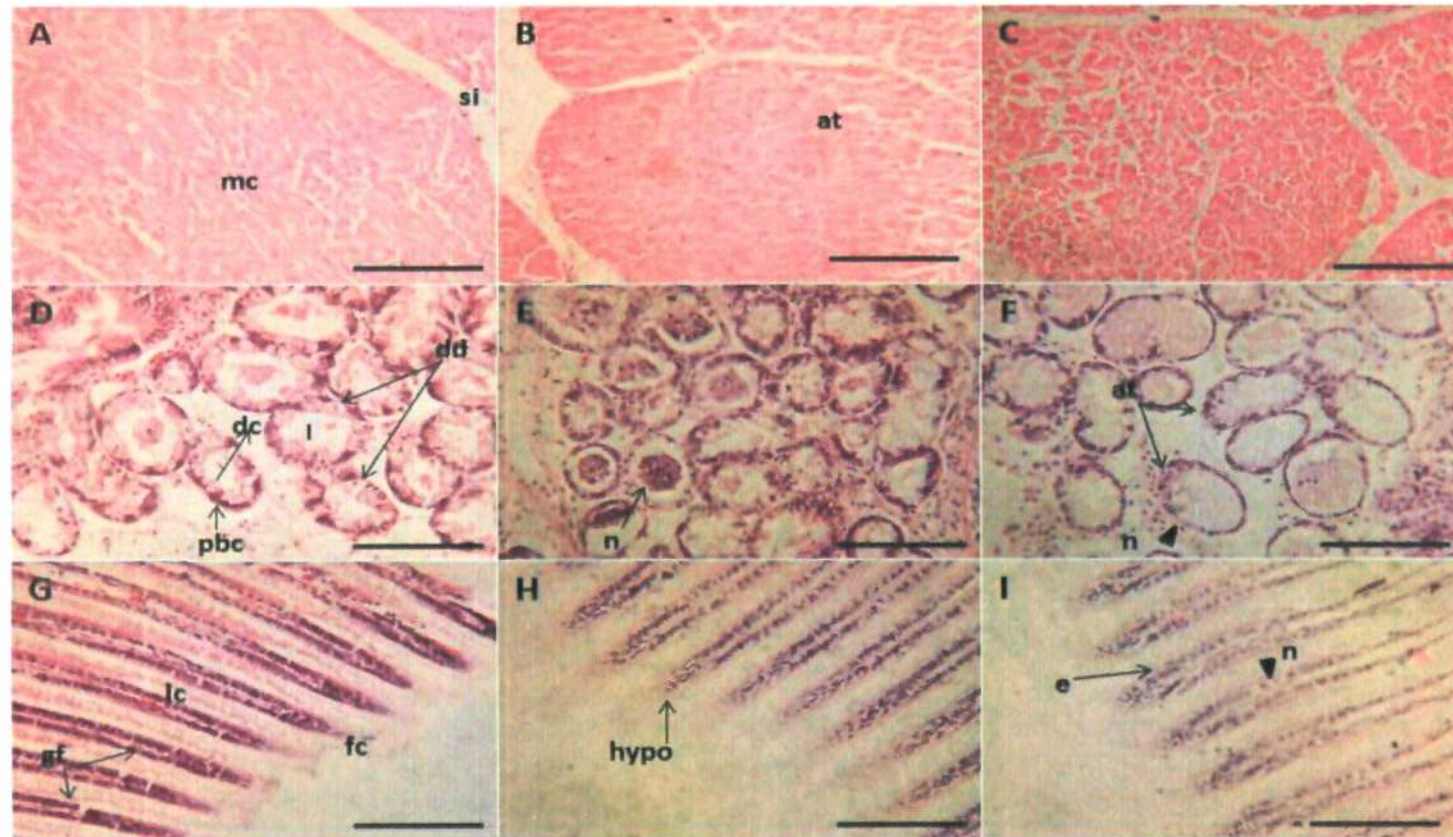


Fig. 6.11 Light micrographs of sections through adductor muscle, gills & digestive gland of *M. edulis* showing histological structure of control and treated mussels stained with H & E at 5-8 μm thickness. (A, D & G) control; (B, E & H) exposed to C_{60} , (C, F & I) exposed to C_{60} + fluoranthene. mc = myocyte cell; si = sinus; dc = digestive cell; pbc = pyramidal basophilic secretory cell; dd = digestive diverticula; gf = gill filaments; fc = frontal cilia; lc = lateral cilia; ge = gill epithelium; dt = digestive tubules; at = atrophy; n = necrosis; hypo = hypoplasia; e = erosion. Scale bar: 100 μm .

6.3.5 C_{60} accumulation

In order to understand the pattern of C_{60} accumulation in mussel tissues, adductor muscle, digestive gland and gills were analyzed for C_{60} content after 3 days of exposure using HPLC analysis (**Plate 6.1**).

6.3.5.1 C_{60} exposure

The subcellular distribution of C_{60} in the organs of the mussel from ' C_{60} ' exposure has been compared in **Fig. 6.12A**. The ranking of organs according to the increasing C_{60} concentration was identical in both concentrations: adductor muscle < gills < digestive gland. No significant difference was found in the adductor muscle in comparison to the control. The gills displayed a significant increase in C_{60} concentration in animals exposed to $0.1 \text{ mg l}^{-1} C_{60}$, but no significant difference was observed with the higher exposure ($P = 0.15$, ANOVA). In contrast, significant differences in C_{60} levels were found with 0.1 and 1.0 mg l^{-1} exposure for digestive gland ($P = 0.04$ and $P = 0.03$, ANOVA; respectively), with the highest C_{60} concentrations measured in the 1.0 mg l^{-1} exposed animals ($24.90 \pm 4.91 \mu\text{g } C_{60} \text{ g}^{-1} \text{ ww}$).

6.3.5.2 Combined exposures of C_{60} and fluoranthene

Results of C_{60} accumulation are summarised in **Fig. 6.12B, C & D**. The distribution of C_{60} in tissues showed very different profiles following the type of exposure. Significant increases in C_{60} accumulation in all organs occurred immediately after 3 days of exposure. In post C_{60} exposure samples; there was a significant decrease in C_{60} content in all organs ($P < 0.05$) except adductor muscle. Based on the observed concentrations of accumulated C_{60} , the digestive gland also appeared to be an important target tissue.

We also observed that C_{60} accumulated more in animals exposed to C_{60} alone than those exposed to the binary exposure. To distinguish more precisely the contributions attributable to type of exposure versus time of measurement, used two-way ANOVA was used on the entire raw data set. In adductor muscle, there was no significant interaction between type of exposure and time of measurement ($P = 0.401$), so this was omitted from the model (**Fig. 6.12B**). Significant interaction was however found between exposure type and time of measurement in digestive gland and gills ($P = 0.007$, $P = 0.0005$; respectively). The main effects of 'type of exposure' were always highly significant in adductor muscle, digestive gland and gills ($P = 0.0007$, $P = 0.0005$, $P = 0.0001$, respectively).

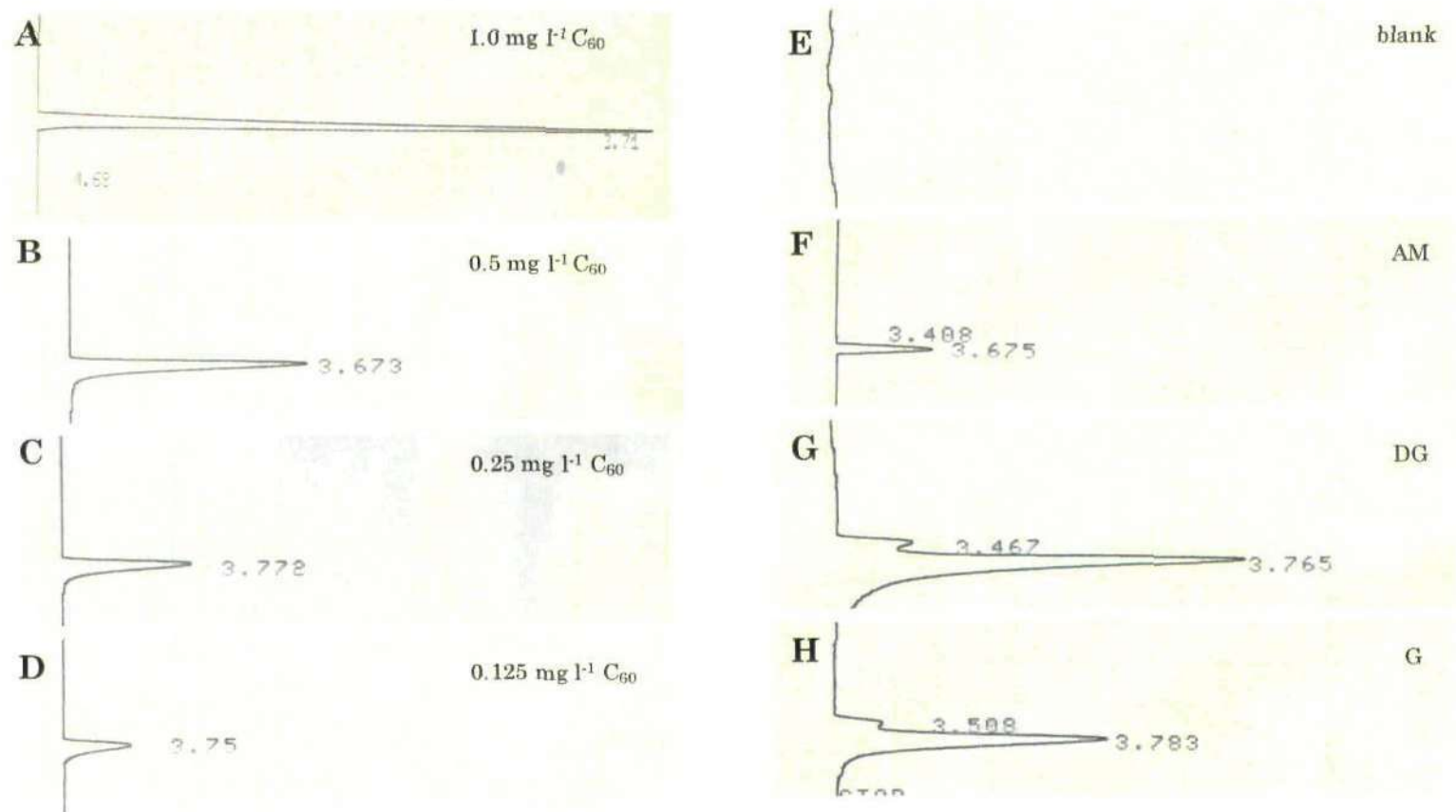


Plate 6. 1 HPLC chromatogram results.(A-D): C_{60} standard; (F-H): C_{60} exposed mussels. (E): blank (toluene); AM= adductor muscle; DG = digestive gland; G = gill.

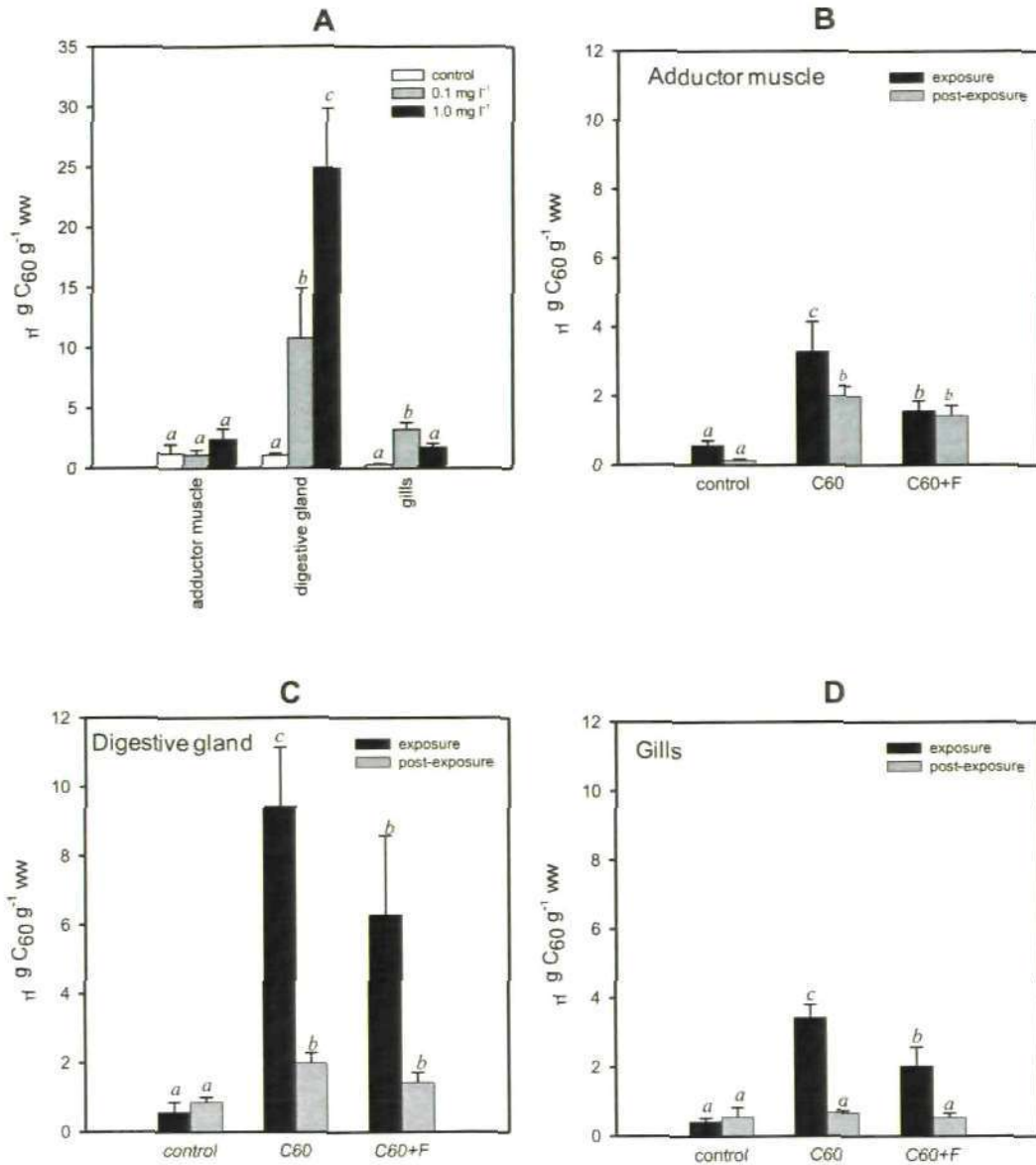


Fig. 6. 12 C₆₀ concentrations in *Mytilus edulis* tissues. (A) accumulation of C₆₀ in adductor muscle, digestive gland and gills after exposure to 0.1 & 1.0 mg l⁻¹. (B, C & D) accumulation of C₆₀ after exposure to mixture of C₆₀ + fluoranthene (adductor muscle, digestive gland and gills, respectively). Data are mean ± S.E., n = 3 mussel per treatment after 3 days of exposure. Bars with the same letters are not significantly different according to the multiple range test (LSD).

6.3.6 Clearance rate (CR)

The CR data measured in mussels exposed to 0.1 and 1.0 mg l⁻¹ C₆₀ were presented in **Fig. 6.13A** and showed that mussels exposed to the high concentration 1.0 mg l⁻¹ C₆₀ were significantly affected ($P < 0.05$, ANOVA). Surprisingly, in 'C₆₀ + F' experiment a significant difference in CR was detected in the 0.1 mg l⁻¹ exposed animals ($P = 0.0002$, t test) in comparison with control. Moreover, mussels exposed to the binary exposure of C₆₀ plus fluoranthene showed a significant decrease in CR ($P = 0.017$, t test; **Fig. 6.13B**). It is worth mentioning that clearance rate in control animals from 'C₆₀ + F' experiment was lower than 'C₆₀' experiment. Apparently, when mussels were kept, filtration activity started to decrease despite the stable laboratory conditions (12/12 h light/dark regime, constant temperature and water quality). After 3 days of post-exposure, CRs of C₆₀ and C₆₀ + fluoranthene increased significantly, indicating that the feeding activity of the mussels had recovered. To check if there is any interaction between effect of exposure and time of measurement on CR, 2-way ANOVA was applied. There was however no significant interaction between the two factors ($P = 0.34$).

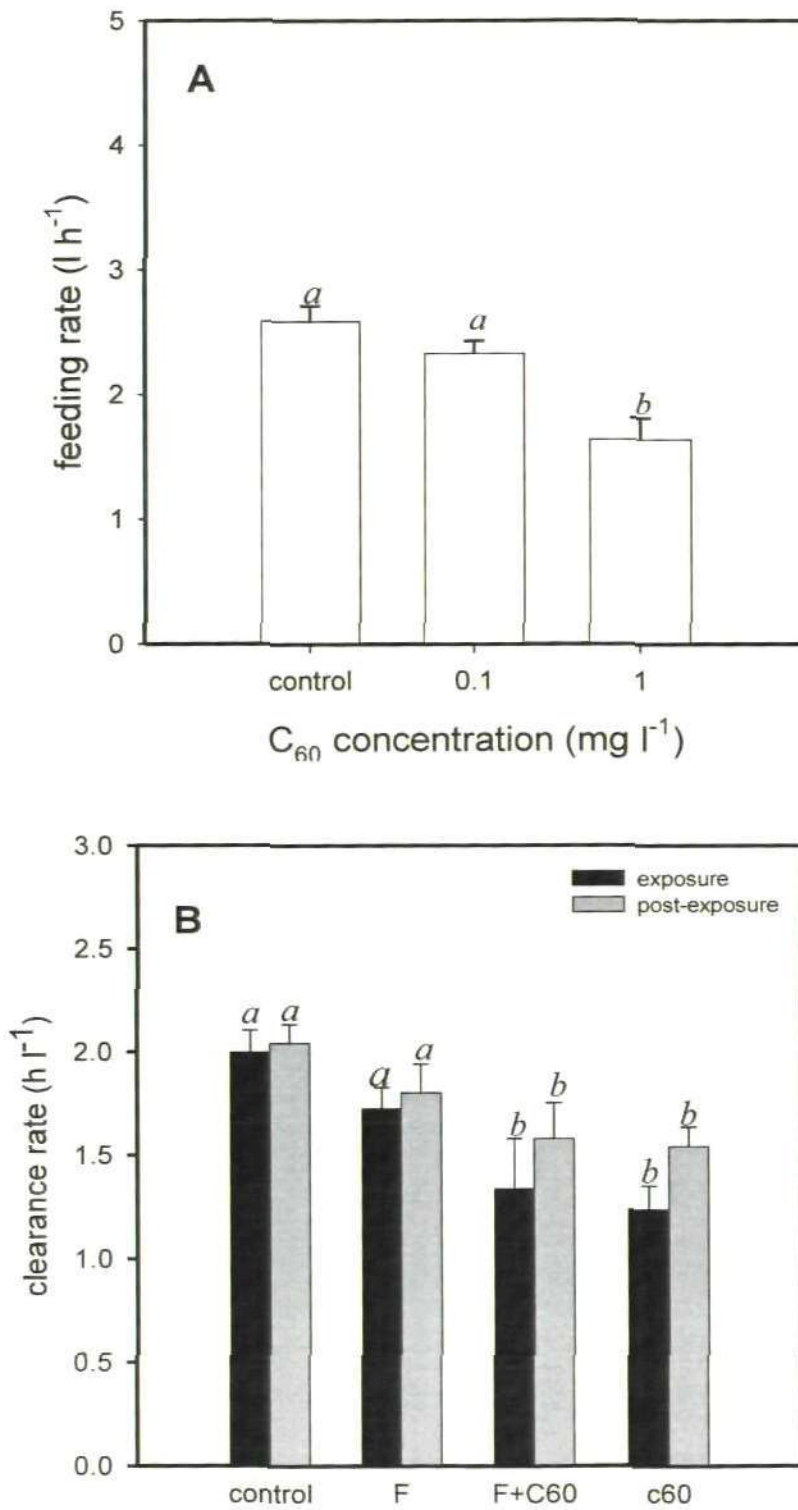


Fig. 6.13 Clearance rate (represent as $l\ h^{-1}$) in *Mytilus edulis* following 3 days *in vivo* exposure to: (A) C_{60} (0.1 & 1.0 $mg\ l^{-1}$), and (B) mixture of C_{60} + fluoranthene (0.1 $mg\ l^{-1}$ C_{60} and 32 $\mu g\ l^{-1}$ fluoranthene). The values are mean \pm S.E. Bars with the same letters are not significantly different according to the multiple range test (LSD).

6.4 Discussion

In the aquatic ecosystem, mussels are exposed not only to a single class of contaminants but to various classes of compounds, concurrently or sequentially. Thus, the *in vivo* assessment of the interactions between C_{60} nanoparticle and organic contaminants, such as fluoranthene, represent an area of research that has not yet been fully covered. It is well known that C_{60} derivatives generate ROS and exert some toxicity (Guldi and Prato 2000) and a number of studies have demonstrated the toxicity of fullerenes (C_{60}) to aquatic organisms such as *D. magna*, *Micropterus salmoides*, *Pimphales promelas*, exposed to low concentrations (Oberdörster et al. 2006; Usenko et al. 2008; Zhu et al. 2006). Besides the toxic effect of ENPs mentioned earlier, many studies have shown that PAHs such as fluoranthene have the ability to produce ROS species resulting in oxidative damage (Coles et al. 1994; Lotufo 1998; Lowe et al. 1995; Palmqvist et al. 2006). However, only one recent preliminary study using fresh water flea (*D. magna*) reported the effect of ENPs-PAHs complex on marine organisms (Baun et al. 2008). Given ubiquitous presence of PAHs in the environment, the interaction between ENPs and PAHs therefore represent an interesting area of research that has not yet been adequately addressed to any extent.

Not only interactive effect has seldom been attempted, also linking the responses at different levels of biological organisation has not been investigated. In the present study, different responses of mussel to single and combined stress of C_{60} and fluoranthene at genotoxic, biochemical and physiological levels were observed. The results indicated that C_{60} and

fluoranthene cause oxidative damages to *Mytilus edulis*, possibly by generating reactive-oxygen stress.

The first effects of contaminants including ENPs initially occur at the cellular or subcellular level and can be good indicators of oxidative stress to organism (Singh et al. 2009). In our study, results from the Comet assay indicated that C₆₀ nanoparticles are in fact genotoxic in their own right, without fluoranthene addition, as both concentrations tested produced a significant increase in the % tail DNA. Under the condition of binary exposure of C₆₀ plus fluoranthene, we found that fluoranthene could significantly increase C₆₀-induced DNA damage in *M. edulis* in comparison with the control animals. There are several conflicting reports on the genotoxicity of fullerene C₆₀ in the literature. Review of literature carried out by Landsiedel et al., (2009) suggested that out of 26 studies on the genotoxicity of nanomaterial, 20 were positive and only 6 were negative. Our Comet assay results compare favourably with recent studies on mammalian lymphocytes which have investigated the genotoxic potential of C₆₀ nanoparticles (Dhawan et al. 2006). They investigated the genotoxicity of colloidal C₆₀ prepared by ethanol to water solvent exchange (EthOH/nC₆₀ suspensions) and extended mixing in water (aqu/nC₆₀ suspensions). They found that aqu/nC₆₀ suspensions caused higher genotoxic response than ethanol suspension. However, there seems to be some evidence to the contrary. Jacobsen and colleagues (Jacobsen et al. 2008) found that fullerenes did not induce significant increases in DNA strand breakages as detected by the Comet assay.

Moreover, highly reactive metabolites can lead to covalent binding with DNA forming DNA adduct. The presence of DNA adducts following dietary exposure

(50 mg kg⁻¹ d w) to benzo[a]pyrene have previously been reported in mussels (Akcha et al. 2000). Another study also showed tissue specific differences in DNA adduct formation in *M. galloprovincialis* collected from PAH-contaminated sites (Pisoni et al. 2004). However, in the present investigation, 3 days *in vivo* exposure to 32 µg l⁻¹ fluoranthene did not show any adduct pattern in any of the tested organs. Contrary to this, Wessel (2010) demonstrated the formation of two adducts following *in vitro* exposure of *Solea solea* microsomes to 100 µM of fluoranthene for 24 h. In mussels, there is a general lack of information on the potential formation of DNA adduct either by fluoranthene or C₆₀ fullerenes. The possible explanation of unexpected results of radio-labelled DNA obtained from exposed mussels is that either fluoranthene was not able to form an adduct or some adducts might have been repaired or removed already before DNA adduct analysis.

At the biochemical level, the binary exposure of C₆₀ plus fluoranthene has caused a significant increase in the levels of glutathione in the adductor muscle. In our previous study, it was found that adductor muscle was a useful organ to determine biomarker responses for oxidative damage. The elevation of glutathione content in adductor muscle has been reported in *Mytilus edulis* after 5 days acute exposure to Cu (40 µg l⁻¹) (Al-Subiai et al. 2009). A possible explanation for this induction is that under exposure conditions mussels tend to activate γ-glutamyl-cysteine synthetase (GCS) to restore glutathione levels. If the activation of GCS maintained for several days this could lead to increase GSH levels, as was suggested by Yan et al.(1997). Peña-Llopis et al., (2002) found that the higher the muscular GSH or GSH/GSSG ratio is, the longer mussels are expected to live under fenitrothion exposure. Different results on

glutathione content have been obtained for organisms exposed to different time and types of chemical compounds. The variability in these investigations may be due to a number of factors including the C₆₀ treatment regime (exposure time and nanomaterial preparation), the cell type or organism used, the DNA repair capabilities, as well as, the metabolic/antioxidant capacity and nutritional status of the organism.

After the cellular changes, a sequence of histopathological, tissue accumulation and behavioural alterations was observed in exposed animals to study interactive effect of C₆₀ and fluoranthene at all levels. The effects of C₆₀ fullerenes, were investigated in tissues that are responsible for health of the organism (adductor muscle), metabolism (liver) and absorption (gills), in the blue mussel, *Mytilus edulis*. Adductor muscle in C₆₀ + fluoranthene exposed animals, exhibited a clear adverse atrophy in myocyte cells which loosening of muscle bundle structure and therefore decrease in extra-cellular spaces of connective tissue. De Oliveira Ribeiro et al., (2008) also found similar effect in exposed muscles of adult male zebrafish, *Danio rerio* to methylmercury. There was a decrease of the space between fibre bundles and a disorganization of myofibrils. Unfortunately, no literatures were found on the effect of any exposure on the histological structure of the adductor muscle in mussels. In addition, gills and digestive gland tissues showed marked degenerative changes. In gills of C₆₀ plus fluoranthene exposed mussel, cilia erosion and filament necrosis was observed. Similar kinds of toxicity effects were noticed earlier in *Mytilus edulis* exposed to other toxicants including heavy metals (Sunila 1988). It is well known that gills are critical organs for respiratory and osmoregulatory functions in mussel. Therefore, injuries in gill tissues may affect

the oxygen consumption and weaken the physiological function of the gills. The apparent reductions in clearance rate observed in the current study are the normal result for erosion happening in the cilia which lead to the failure in physiological processes in the whole organism (Gregory et al. 2002). Moreover, C₆₀ fullerenes exposure caused reduction in digestive tubule thickness (tubule atrophy) as a result of losing of digestive cell and basophilic secretory cells within the lumen of digestive tubules. The effects of the C₆₀ was enhanced when fluoranthene was added, with the more severe changes observed in digestive tubules. Digestive gland of the exposed mussels showed necrosis (diffuse nuclei and no clear distinction in some epithelial cells), adverse atrophy of digestive tubule and stomach obstruction epithelium. Weinstein (1997) has found that oysters *Crassostrea virginica* exposed to 100 µg l⁻¹ fluoranthene in the laboratory for 21 day also exhibited a reduction in their mean digestive epithelial thickness. Digestive gland tissue of mussel is the main site for metabolism and detoxification contaminants (Livingstone 1996). Histological changes in the digestive tubules have been used to assess the effects of environmental contaminant (Auffret 1988; Bignell et al. 2008; Lowe and Pipe 1987).

We further investigated C₆₀ accumulation in exposed mussels to link it with other parameters. Chemical analyses showed predominant accumulation of C₆₀ in digestive gland with modest accumulation in gill and adductor muscle exposed to C₆₀ alone. In contrast, lower accumulation of C₆₀ was found in tissues from animals co-exposed to C₆₀/fluoranthene. The accumulation of C₆₀ was influenced by co-exposure to fluoranthene. Animals exposed to single C₆₀ exposure accumulated more C₆₀ than binary exposed mussels. Limited

information available in the literature shows differential pattern of tissue-specific accumulation of contaminant and/or when used in combination. For example, whilst co-exposure of phenanthrene in C₆₀ suspensions showed higher bioaccumulation of phenanthrene (no C₆₀ was measured) (Baun et al. 2008), in another recent study, gold nanoparticle (GNP) showed enhanced accumulation when used singly, but no GNP was detectable in tissue when used in combination with menadione (Tedesco et al. 2010). They referred that as a result of menadione toxicity which may have affected accumulation of GNP during feeding.

6.5 Conclusions

We have shown for the first time that C₆₀ nanoparticles alone and in the presence of fluoranthene are potentially genotoxic to haemocytes cells, along with elevation in glutathione levels which occurred after exposure to combined exposure of C₆₀ and fluoranthene. This effect becomes more pronounced in the other levels of biological organisation. Longer exposure times are now required to explore the potential effects of these C₆₀ fullerenes further. This study underlines the advantages of using *Mytilus edulis* as a model organism for future investigations on the environmental effects of engineered nanomaterials.

Chapter 7

Investigation of the toxic effect of aged C_{60} in different life stages of *Mytilus edulis*

The results from this chapter have been presented at the 21st SETAC Europe annual meeting, Milan, Italy, May 2011 (poster presentation). Some of the results have also been published in *Environmental Science and Technology* (Kadar et al., 2011).

Hypothesis: *C₆₀ fullerenes suspension in seawater exposed to sunlight are more toxic to marine mussel, *Mytilus edulis*.*

Abstract

While several recent reports have described the toxicity of *C₆₀* fullerene nanoparticles, few studies have reported the toxicity resulting from photo oxidation of *C₆₀* fullerene nanoparticles. To address this knowledge gap, fresh (*FC₆₀*) and aged (*AC₆₀*) *C₆₀* fullerenes nanoparticles were subjected to characterization by advanced analytical techniques such as DLS, AFM, TEM and XRD which cumulatively indicate changes in surface charge and particle size distribution of the *C₆₀* fullerenes occurring after aging process in the presence of sunlight. Following this characterization, somatic and germ cells from marine mussels, *Mytilus edulis* were exposed under *in vitro* and *in vivo* conditions to *FC₆₀* and *AC₆₀* fullerene nanoparticles. Genotoxic effects in sperm (germ) and haemocyte (somatic) cells were assessed directly after exposure by the single cell gel electrophoresis or the Comet assay. In addition, fertilisation success and embryo-larval developments were monitored after 1 and 48 h, respectively. Whilst *FC₆₀* was capable of inducing DNA damage in its own right, Comet assay results indicated statistically significant increase in DNA damage in *AC₆₀* exposed sperm ($P = 0.015$, ANOVA) and haemocytes ($P = 0.0001$). The implications of sperm DNA damage were reflected on the early life stages assay, in which fertilisation success and the percentage of normal *D*-shell larvae were greatly significantly affected by *AC₆₀* exposure than *FC₆₀* exposure ($P < 0.05$, LSD), whereas adult stage showed induction of glutathione levels in adductor muscle. Significant accumulations of *FC₆₀* and *AC₆₀* fullerenes, as determined by HPLC were observed in all organs, with highest levels in digestive gland ($P = 0.012$). Interestingly, clear signs of abnormalities in

adductor muscle, digestive gland and gills were also observed through histopathological examination. In general, the results showed for the first time, genotoxic and developmental impact of the photochemical transformed C_{60} in the early life stages in marine invertebrates. Further research is required to identify the C_{60} degraded products and to understand the mechanism by which AC_{60} induces biological responses including oxidative stress and affect ecologically relevant aquatic organisms at different life stages.

7.1 Introduction

While most of pollutants in the aquatic environment (such as polynuclear aromatic hydrocarbons (PAHs), polychlorobiphenyls (PCBs) and metals) are known to enhance genotoxicity in the living organisms (Livingstone 2001), there is currently very limited information available about genotoxicity of the newly developed substances (such as manufactured or engineered nanoparticles, ENPs). The rapid production of ENPs in the recent years raised lots of safety concern questions regarding the possible impact on human and environmental health (Moore 2006; Royal Society 2004).

ENPs have different properties from their mother bulk and molecular analogues, due to the fact that they have a very small size and large surface area to volume ratio. These unique features could facilitate their accumulation in living organisms and also increase their reactivity in the environment. Among the manufactured nanoparticles, C₆₀ fullerenes are considered to be one of the model ENPs by United States Environmental Protection Agency (USEPA) to develop strategy for environmental protection (USEPA 2010). C₆₀ fullerenes, a Nobel Prize winning molecule in 1996 had been discovered by Kroto et al., (1985). It is composed of a polygonal structure made up with 60 carbon atoms and poorly soluble in water ($< 10^{-9}$ mg l⁻¹) (Heyman 1996). Because of its outstanding properties (magnetic, thermal and electrical) fullerenes have been extensively used in a variety of areas, starting from electronics and energy to medicine and cosmetics (Ema et al. 2010).

Due to the unique properties of C₆₀ and their widespread applications, evaluation of the ecotoxicological effects of these nanoparticles on living organisms is necessary. In the literature, there are some contradictory studies

about C₆₀ toxicity (Landsiedel et al. 2009). C₆₀ fullerenes has been shown to cause toxicity in human. Recent evidence has showed that C₆₀ is cytotoxic to dermal fibroblasts, liver carcinoma cells (HepG2), and neuronal astrocytes at doses $\geq 50 \mu\text{g l}^{-1}$ after 2 days exposure (Sayes et al. 2004). Up-regulation of many genes involved in inflammatory response, such as the *Cxcl2*, *Cxcl6*, *Orm1*, and *Spp1* genes have also been reported in rat lung exposed by intratracheal instillation with 1.0 mg C₆₀ particles (Fujita et al. 2010). However, conversely others have described C₆₀ as a free radical scavenger (Mori et al. 2006; Sun and Xu 2006).

The environmental contamination by C₆₀ fullerenes is expected, but to date very little is known about their fate and biological effects in the environment. In this context, photochemical degradation process is one of the possible fate for C₆₀ nanoparticles in the environment. While several recent reports have described their toxicity, none have reported the potential toxicity resulting from photochemical transformation of C₆₀ fullerene nanoparticles in aquatic vertebrates or invertebrates.

Generally, early and adult life stages of marine invertebrates are mostly used for ecotoxicological studies (see review by His et al., (1999)). Early life stages however appear to be the more sensitive than adult stage following exposure to pollutants (Dixon et al. 2002; Jha 2004). In this context, there is paucity of information in the literature related to potential impact of pollutants or contaminants on the germ cells of aquatic organisms. Despite, extremely compacted and condensed nature of sperm chromatin (DNA with nuclear protein), compared to oocytes, sperm are potentially more vulnerable to damage induced by environmental agents which often produce reactive oxygen

species (ROS). This is because sperm has limited capacity for DNA repair mechanisms and antioxidant defence and secondly, spermatozooids are rich in polyunsaturated fatty acids which make them more susceptible to lipid peroxidation and therefore loss of the diffusion barrier and the integrity of the DNA (Jha 2008). Thus, it is very necessary to protect sperm DNA from genotoxic damage as it can be passed on to future generations and the induced damage could also impact development and survival of the early life stages. In addition, induced genotoxicity during early life stages may have consequence impacts that functionally manifest themselves in the adult organisms.

Given that there is no information available on the reproductive and developmental toxicity of C_{60} fullerenes, here we aimed to study (1) the genotoxic effects following paternal exposure of mussels, *M. edulis* to fresh C_{60} (FC_{60}) and aged C_{60} (AC_{60}) and the reproductive consequences at early life stages (2) the efficiency of adult to compensate with the potential toxic effects of FC_{60} and AC_{60} to better understand the adverse effects of degraded C_{60} .

7.2 Materials and Methods

7.2.1 C_{60} preparation

Uncoated 99.5% pure fullerenes; lot number 11401DB (according to the manufacturer's information) was obtained from Sigma-Aldrich (UK). The stock suspension of 1 mg l^{-1} C_{60} in sea water (**Plate 7.1**) was ultrasonicated (35 kHz frequency, Fisherbrand FB 11010) for 2 h, and then exposed to the natural sunlight for 30 days at room temperature (sonication was carried out every day for 2 h) to obtain brown colour deposit 'aged C_{60} ' (AC_{60}). A fresh C_{60} (FC_{60}) suspension was prepared prior to start day of the experiment.

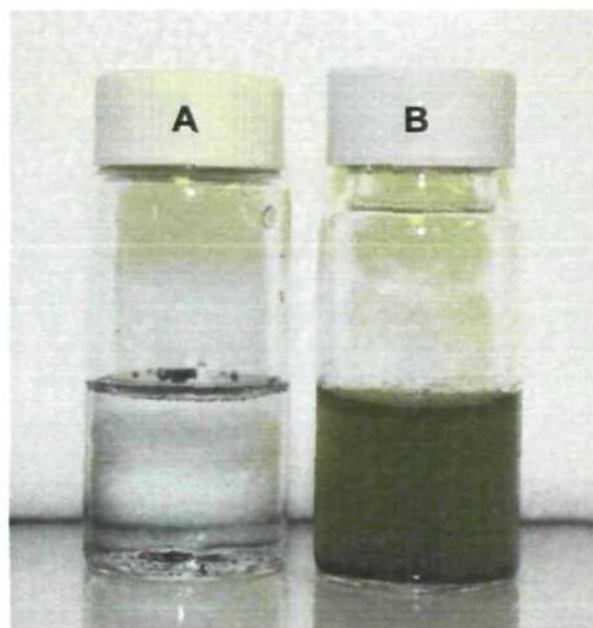


Plate 7.1 C_{60} fullerene solutions in seawater at concentration of 1.0 mg l^{-1} ; (A) fresh C_{60} ' FC_{60} ', (B) Aged C_{60} ' AC_{60} ' stored at room temperature exposed to natural sunlight light for 30 days.

7.2.2 *Mussels collection and experimental design*

Adult mussels of (shell length: 51-58 mm) were collected at low tide (June 2010, within natural breeding season) from Trebarwith Strand, Cornwall, UK (grid reference: SW972 905), a relatively clean site. After collection they were immediately transported to the laboratory and placed in highly aerated seawater as described in section. 2.1. Toxicity of photochemically degraded C_{60} versus freshly prepared C_{60} was assessed into two separate experiments. The first experiment was conducted by *in vitro* exposure to 1.0 mg l^{-1} FC_{60} and AC_{60} , to evaluate genotoxicity in male germ cells and consequently the reproductive developmental consequences in *Mytilus* larvae. In the second experiment, *in vivo* exposures were carried out on adult mussels to assess the toxicity of each C_{60} form (i.e. fresh and aged) at different levels of biological organisation (i.e. biochemical, tissue and individual levels).

7.2.3 *In vitro exposure*

7.2.3.1 *Induction of spawning and gametes collection*

Mussel embryos are known to be highly sensitive to changes in sea water, therefore all sea water parameters were checked before inducing spawning. The regular seawater parameters were found within the acceptable range (dissolved oxygen $7.4 - 8.0 \text{ mg l}^{-1}$; pH 8.25 ± 0.25 ; salinity $34 \pm 0.5\%$, temperature $15 \pm 2^\circ\text{C}$). To induce spawning, twenty mussels were injected with 1 ml of 0.50 M KCl into their posterior adductor muscle and placed in four 5 litre tank containing fresh filtered ($0.22 \mu\text{m}$) sea water (FSW), followed by addition of food supply (*Isochrysis galbana*) and combined with heat shock from 11°C to

16°C (ASTM 1997). They were then replaced individually after 30 min into the beakers which had the contents replenished with new seawater held at 15 °C. The sexes of the individuals were easily distinguished; males produced a milky stream of white sperm (illustrated in **Plate 7.2A**) and females produced a mass of orange-pink eggs (illustrated in **Plate 7.2B**).

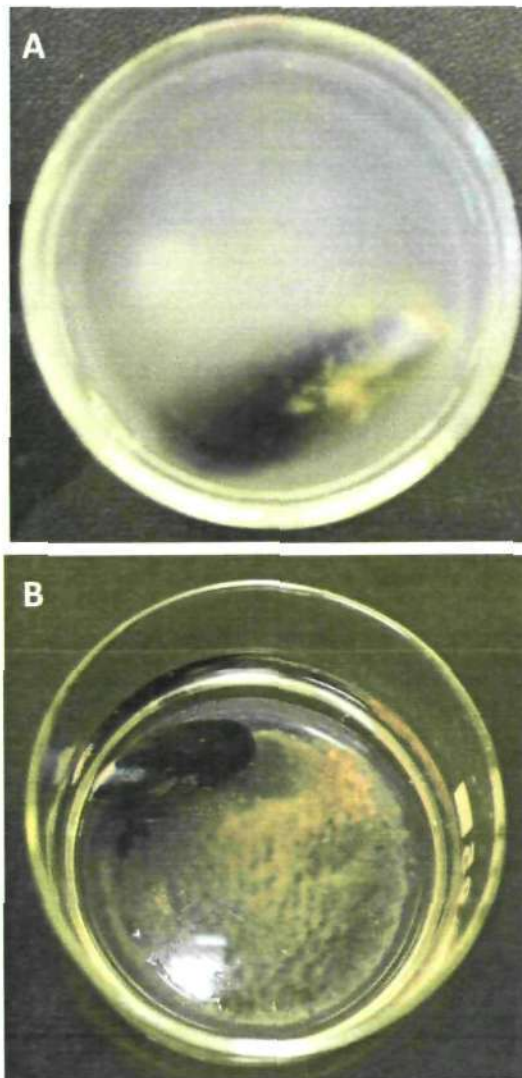


Plate 7.2 Photomicrographs showing the mussels releasing the gametes, (A) male with released sperms (B) female with released eggs.

7.2.3.2 Gamete collection and checking

All gametes were sieved to remove large debris by passing eggs and sperm through pre-rinsed sterile 200 μm nylon sieve in FSW. Eggs were collected and held (during the 2 h sperm exposure) in oxygen saturated 0.2 μm filtered seawater (FSW) at 15 °C, and sperm were passed through a 40 μm sieve. Gametes were counted and checked for general health status, as indicated by a rounded and spherical shape for mature egg under microscope and sperm were checked for viability after exposure by analytical flow cytometry (AFC) (described later in section 7.2.3.5). Eggs and sperm suspensions were made up to the required concentration (100 eggs ml^{-1} and 250×10^3 sperm ml^{-1}) by sieving the eggs through 30 μm mesh and diluted the sperm in FSW.

7.2.3.3 Experimental design and embryo development assay

In six-well Cellwells™ plate, 4 ml of sperm at concentration of 250×10^3 sperm ml^{-1} were exposed in two sets of experiment under static condition. Three replicates were performed for each exposure condition. In the first set, copper sulphate (CuSO_4 ; 99% purity) was used as an environmentally relevant genotoxin agent for validation purposes of the embryo-larval developmental and survival studies. Previous work (Kadar et al. 2011) also used this chemical for validation of the embryo-larval stages of the marine mussel *Mytilus galloprovincialis*. Sperm were exposed for 2 h to three concentrations of CuSO_4 at 0.1, 0.5 and 1.0 $\mu\text{g l}^{-1}$. In the second set, sperms were exposed to 1 mg l^{-1} of FC_{60} and AC_{60} (Fig. 7.1); along with procedural positive control (1.0 $\mu\text{g l}^{-1}$ CuSO_4) and negative control (i.e. 10 μm filtered sea water). After 2 h of

exposure prior to fertilization, sperm were analysed for cell viability (AFC) and DNA damage.

7.2.3.4 *In vitro fertilisation*

Following induction of spawning, fertilisation was conducted using previously developed method (Kadar et al. 2011). Briefly, the oocytes were concentrated to reach the required concentration of 100 eggs ml⁻¹ and mixed with pooled sperm (250 x10³) at a ratio of 1:10³. The density was adjusted to approximately 100 embryo well⁻¹. Constant temperature of 15 ± 1°C and salinity (35 ± 0.52 ‰) were maintained during embryo development. Following fertilisation, dividing cells were counted after 2 h of fertilisation on live specimen and fertilisation success was calculated based on the following formula

$$\frac{\text{number of fertilised oocytes}}{\text{number of fertilised + unfertilised oocytes}}$$

Only samples (control) where the fertilization success exceeded 80% were used for the experiment. Embryos were allowed to grow for 48 hour following which they were fixed (10% formalin) in each well and assessed for number of normal and abnormal developments when the distinguishable D-shell stage was reached. Embryos with no clear D-shell (i.e. delay in reaching the trochophore stage, protruding mantle or concave shells) were considered abnormal.

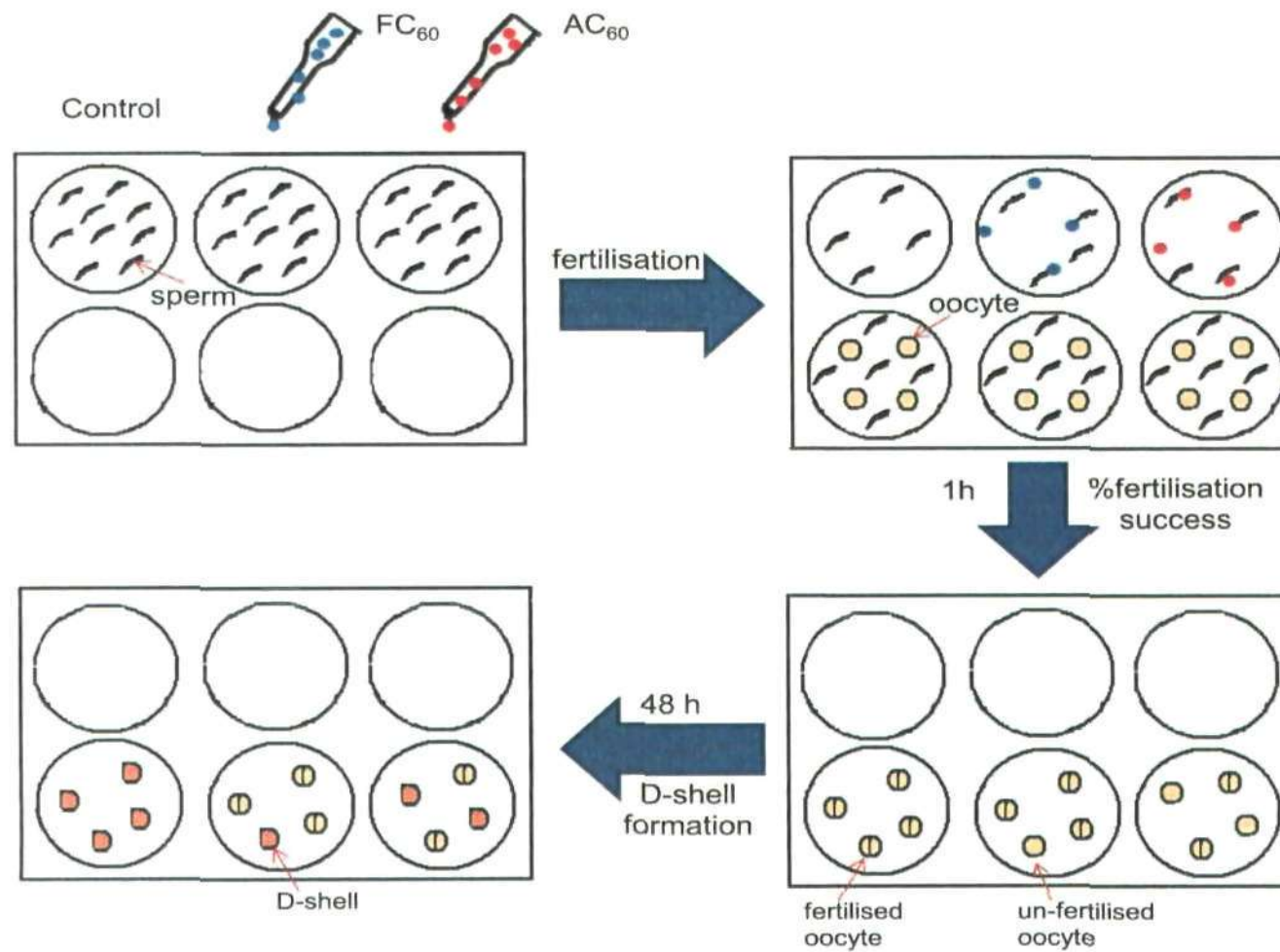


Fig. 7.1 Experimental design for in vitro sperm exposure and embryo development assay.

7.2.3.5 Sperm viability assay using analytical flow cytometry (AFC)

SYTOX Green nucleic acid fluorescent stain (Cat # S7020, Invitrogen;UK) was used to assess sperm viability. This stain is composed of cyanine dye which has the ability to stain cells with compromised plasma membranes with brightly green fluorescence. Sperm viability was estimated after exposure to FC₆₀ and AC₆₀ using analytical flow cytometry (AFC) as described by Kadar (2011). Briefly, 0.5 ml of freshly diluted sperm (25-fold) was stained with 10 µl of 0.1 mM SYTOX Green, and placed in the dark for 10 min prior to AFC measurements. Samples were analyzed with a FACSort flow cytometry (Becton Dickinson, Oxford, UK) equipped with an air-cooled argon ion laser providing blue light at 488 nm. Beside counting the cells, the flow cytometer also measured green fluorescence from stained cells (530 nm ±15 nm), forward and side scatter (light scattered in the same plane and at ninety degrees to the plane of the laser respectively). Data acquisition was triggered on side scatter. The flow rate of the flow cytometry was calibrated daily using Beckman Coulter Flowset fluorospheres of known concentration. Detection of light scatter and fluorescence were made using CellQuest software (Becton Dickinson, Oxford, UK) with log amplification on a four decade scale with 1024 channel resolution. Data were exported and stored in listmode format and analysed using WinMDI software version 2.8 (Joseph Trotter). A bivariate scatter plot of forward scatter against side scatter was used to discriminate sperm from debris and aggregates. A region was drawn around the sperm population and then a second bivariate plot of side scatter against Sytox Green fluorescence of just the sperm from the region in the previous plot was created to discriminate and count dead and live sperm (**Fig. 7.2**).

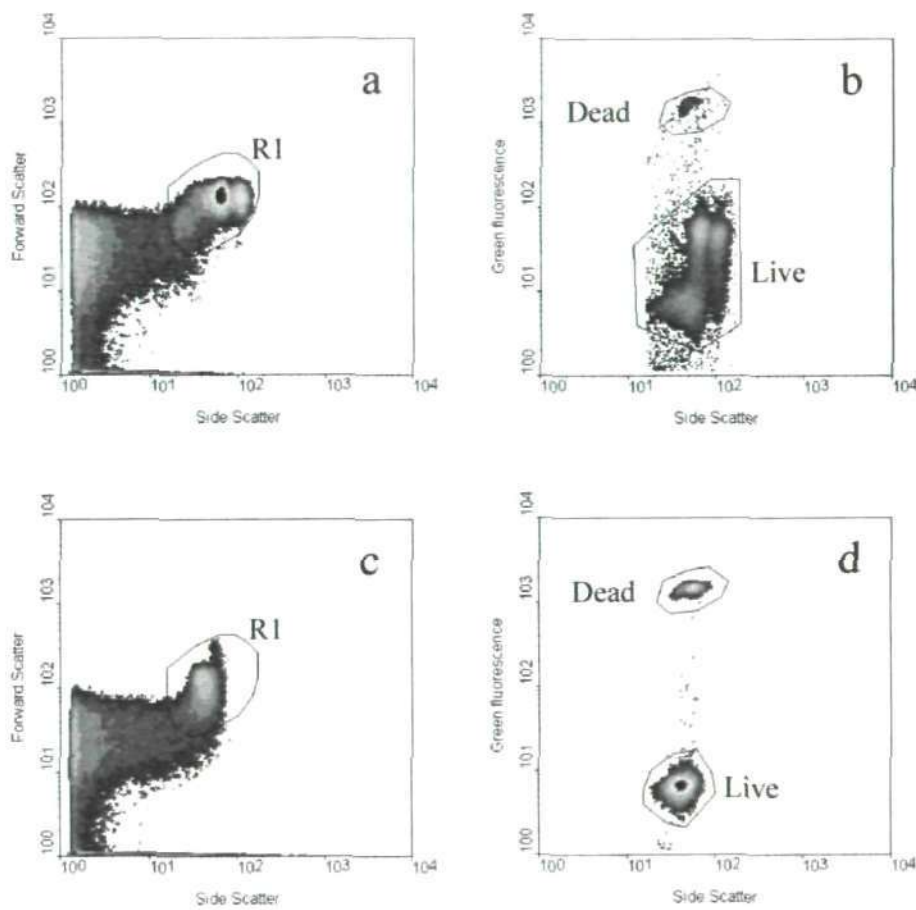


Fig. 7.2 Flow cytometry of control *Mytilus* spermatozoa stained with Sytox Green. Density plots for control samples of side versus forward light scatter; (a and b) side scatter versus green fluorescence in control samples (i.e. unexposed sperm); (c and d) sperm exposed to CuSO₄ (1.0 μg l⁻¹). An approximate region (R1) was placed around sperm identified from their light scattering properties (a and c) and then the data within R1 were re-analysed to observe the side scatter and Sytox Green fluorescence properties of the samples (b and d), and to discriminate between live and dead sperm.

7.2.3.6 Determination of DNA strand breaks using the Comet assay in sperm cells

Applying haemocyte Comet assay (section 2.5) condition to sperm cells is not possible due to the unique structure of sperm cells. We have started from standard procedure of the Comet assay on human sperm (Queens University, Belfast). The procedure is very similar to haemocyte Comet assay, except that (1) human sperm lysis solution did not required addition of the *N*-lauroyl-sarcosine and dimethyl sulphoxide (DMSO); and (2) human sperm required additional step to separate the protamines and decondense the DNA. We have applied this extra step to *Mytilus edulis* sperm cells, and we found that decondensation step caused high DNA damage maybe because of the differences in protein composition since *Mytilus edulis* sperm has histones instead of protamines in human (which provide tighter wrapping of the sperm DNA). Based on this finding we decided to exclude the decondensation step from the procedure, but we kept the same lysis solution (human sperm) which composed of 5.2 M NaCl, 0.1 M EDTA, 0.001 M Tris base, and 1% Triton X-100 (added fresh just before use), adjusted to pH 10 with 10 M NaOH. The unwinding and electrophoresis steps were modified to find the optimal condition for the assay by investigating the effects of different unwinding and electrophoresis times (i.e. 20, 30 and 40). The Comet assay has been also standardised following 10 min *in vitro* H₂O₂ exposure of *Mytilus edulis* sperm as procedural positive control (Fig. 7.3).

Briefly, 10 µl of sperm suspension at concentration of approximately 6×10^4 cells ml⁻¹ was gently mixed with LMP agarose and dropped onto pre-coated slides with HMP agarose. Slides were then submerged for 1 h in lysis solution, followed by 20 min denaturation in freshly prepared electrophoresis buffer and

electrophoresis process was carried out for 20 min at 25 V and 300 mA. Slides were neutralization and then stained with ethidium bromide (EtBr) to observe under epifluorescence microscopy. One hundred comets per slide were quantified by Komet 5.0 image analysis software.

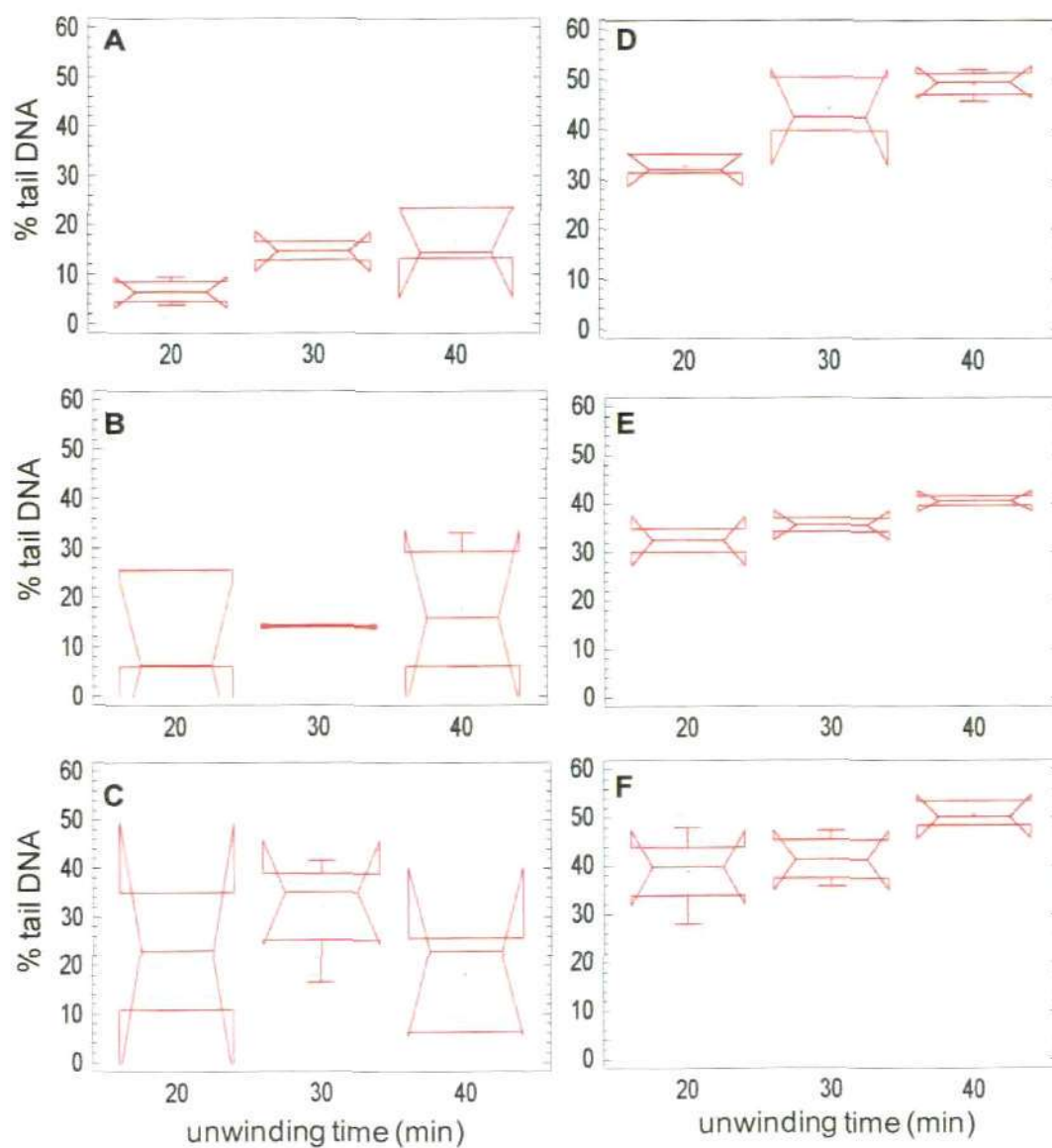


Fig. 7.3 The effect of unwinding time (A-C) negative control; (D-F) positive control- 50 μM H_2O_2 (A & D) 20 min electrophoresis (B & E) 30 min electrophoresis (C & F) 40 min electrophoresis; $n = 3$.

7.2.4 *In vivo* exposure

Mussels were divided between twenty 5L tanks (5 animals per tank) comprising 4 treatments: (a) fresh seawater (FSW) (b) aged seawater (ASW) (c) 1.0 mg l⁻¹ fresh C₆₀ (FC₆₀) and (d) 1.0 mg l⁻¹ aged C₆₀ (AC₆₀). In this experiment (**Plate 7.3** shows different tanks holding mussels for the experiment), two exposure periods were considered: (a) three days exposure and (b) three days post-exposure, with removal of mussels at the end of each period for analysis of (a) DNA damage (b) total glutathione contents, (c) histopathology (d) C₆₀ accumulation and (e) clearance rate. The seawater was changed daily and re-dosed with appropriate concentrations of FC₆₀ and AC₆₀. Animals were not fed during the experiment. After the exposure period, two mussels were randomly collected from each tank, immediately from each mussel, haemolymph and tissue (i.e. adductor muscle, gills, and digestive gland) samples were collected and were transferred carefully into an eppendorf tube and placed on ice for further analysis.

7.2.4.1 *Collection of haemolymph samples and preparation of adductor muscle extract*

From each individual approx. 0.20 ml of haemolymph was extracted from the posterior adductor muscle into 0.20 ml physiological saline, as described in section 2.3.1. Haemolymph samples were held on ice to minimise cellular stress. The posterior adductor muscles from two mussels (approximately 0.20 g wet weight) were dissected out and were homogenized in 1:3 ratio (w/v), as described in section 2.3.2, for total glutathione analysis.

7.2.4.2 Determination of DNA strand breaks using the Comet assay in haemocytes

Haemocytes viability was checked by using Eosin Y assay, as described in section 2.5.1 and the DNA damage in the haemocytes of mussels was determined using the alkaline Comet assay, as described in section 2.5. The level of DNA damage in 100 cells per sample was measured by Komet 5.0 image-analysis system (Kinetic Imaging, Liverpool, UK) using epifluorescence microscope (Leica, DMR). Data for percentage tail DNA were presented as a measure of single-strand DNA breaks/alkali labile sites.

7.2.4.3 Determination of total glutathione level in adductor muscle extract

The total glutathione (i.e. reduced, GSH, and oxidised, GSSG) content of adductor muscle extract was determined essentially according to section 2.4. The rate of absorbance decrease at 412 nm was measured by microplate reader (Optimax, Molecular Devices, Sunnyvale, CA) over 5 min using 96 well plates. The assay temperature in each case was 22 °C.



Plate 7.3 Experimental setup for a short-term (3 d) exposure of *Mytilus edulis* to FSW, ASW, FC₆₀ and AC₆₀ in individual 5 L aerated tanks.

7.2.4.5 Histological preparation for adductor muscle, digestive gland and gills

Tissues collected from exposed animals (i.e. adductor muscle, digestive gland and gills) were examined by normal histological methods as described in section 2.6 in details. Fixation of the samples was carried out in 10% buffered formal saline, and then the specimens were processed in ascending grades of alcohol. Tissue samples were impregnated in paraffin and cut with microtome at 5-7 μm thickness.

7.2.4.6 Clearance rate

Clearance or feeding rates of individual mussel were determined as described in section 2.7. Water samples were analysed on Backham TM Coulter Particle Size and Count Analyser (Z2), with a 100 μm aperture fitted and set to count particles between 4.0-10.0 μm in diameter.

7.2.5 HPLC-analysis of C_{60} in tissue samples

HPLC method was developed for C_{60} analysis using Hypersil (5 μ) Elite C18 (250 X 4.6 mm I.D.) column, as described in section 2.7. The mobile phase was composed of pure toluene. For both columns used, a standard curve was generated for C_{60} concentrations (dissolved in toluene) ranging from 0.125 and 2.0 mg l^{-1} . Concentration of test samples was determined by comparison with the standard curve.

7.2.6 C₆₀ characterisation

7.2.6.1 Dynamic Light Scattering (DLS) and zeta potential

The mean particle size was determined using Dynamic light scattering (DLS) technique as described by Baalousha et al., (2008). Measurements were conducted for measuring the random motion of the particles suspended within a liquid (the larger the particle, the slower motion will be). Measurements were carried out at 90° scattering angle at constant temperature (15 ± 2 °C). The zeta average diameter and polydispersity index (PDI) were automatically provided by Malvern Zetasizer, (ZEN3600, Malvern instruments Ltd, Worcestershire, UK; **Plate 7.4**) using cumulant analysis. All DLS measurements were performed in low volume disposable cuvettes and the zeta average of three measurements. Zeta potential measurements for each sample were also obtained, but from the average of 5 measurements to give more information about size distribution and charge of the nanoparticles.

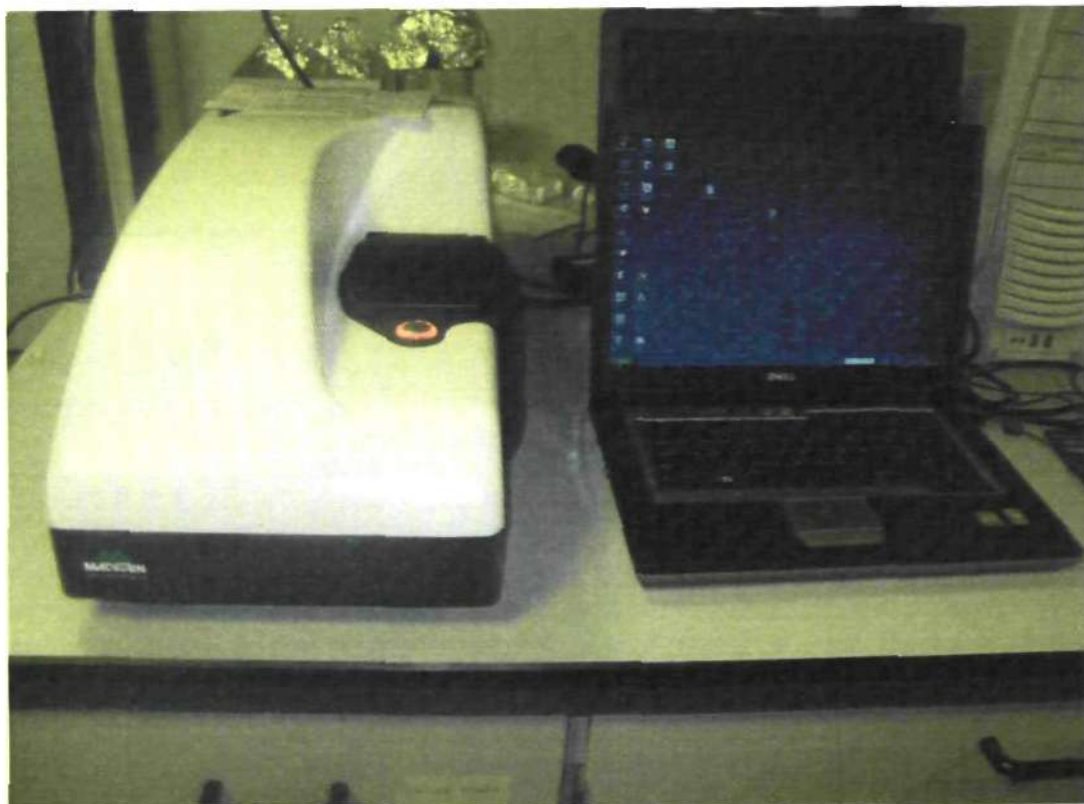


Plate 7.4 Malvern Zetasizer (model ZEN3600) used for DLS analysis.

7.2.6.2 *Transmission electron microscopy (TEM) and energy-dispersive X-ray spectrometry (EDX)*

Transmission electron microscopy (TEM) was used to determine the relative size of the particles from fresh and aged C₆₀ fullerenes suspensions. The procedure has been described in details elsewhere (Kadar et al. 2010). Briefly, C₆₀ fullerenes suspensions were prepared at concentration of 10 mg ml⁻¹ to achieve optimal surface coverage. Ten microlitre of suspension was dropped on coated copper grid (Agar scientific, Essex, UK) and allowed to dry completely for 30 min. Then, grid was rinsed three times in pure water and left to dry overnight (**Plate 7.5**). C₆₀ fullerenes particles were also investigated by energy-dispersive X-ray spectrometry (EDX) (Phillips Technai F20, **Plate 7.6**) to quantify elemental composition for single particles.

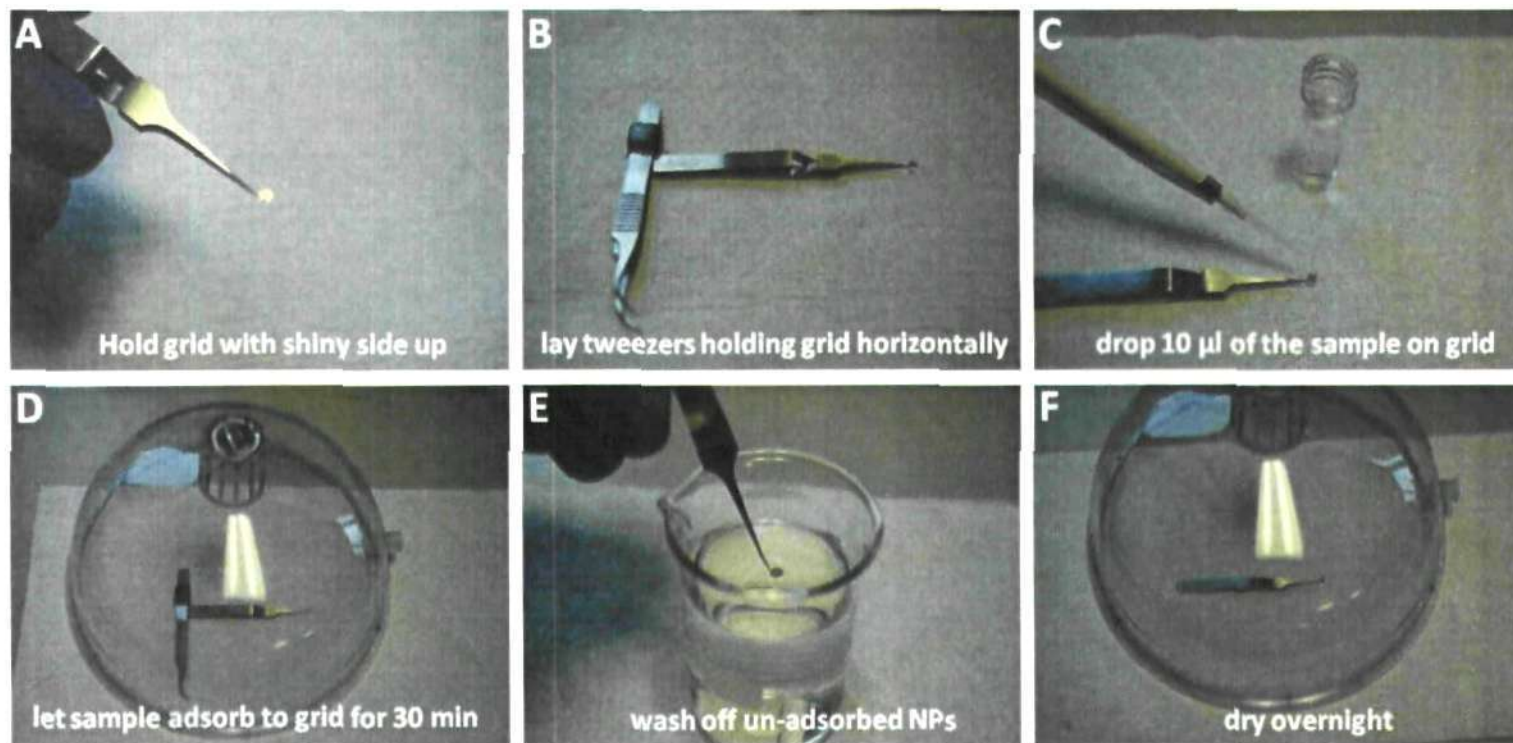


Plate 7.5 TEM drop deposition procedure steps.



Plate 7.6 Phillips Technai F20 used for TEM analysis.

7.2.6.3 Atomic force microscopy (AFM)

Atomic force microscopy (AFM) technique was applied to determine the size, shape and aggregation of C_{60} . AFM samples were prepared by using the drop deposition method on mica sheet (**Plate 7.7**) according to Lead et al., (2005). AFM images were obtained using a system of XE-100 microscope (Park Systems Corp., South Korea) inside a hermetically sealed enclosure (to minimise the vibration noise), **Plate 7.8**. All AFM images were obtained using 'non-contact' mode using aluminium coated silicon probes of nominal spring constant = 42 N m^{-1} and nominal resonant frequency = 330 kHz (Budgetsensors, Germany). In this mode of operation, the cantilever is vibrated with very small amplitude at a fixed frequency near the intrinsic resonance of the cantilever. As the tip of the cantilever approaches mica sheet, the London-van der Waals attractive force between the cantilever and the C_{60} fullerenes particles surface acts upon the cantilever vibration. Cantilevers were replaced after some amount of usage to ensure minimal tip damage. Samples were analysed at room temperature and relative humidities ($\sim 40\%$). For every sample studied, more than 100 particles were counted on three different randomly selected sites on every mica sheet and the average size for each sample was measured.

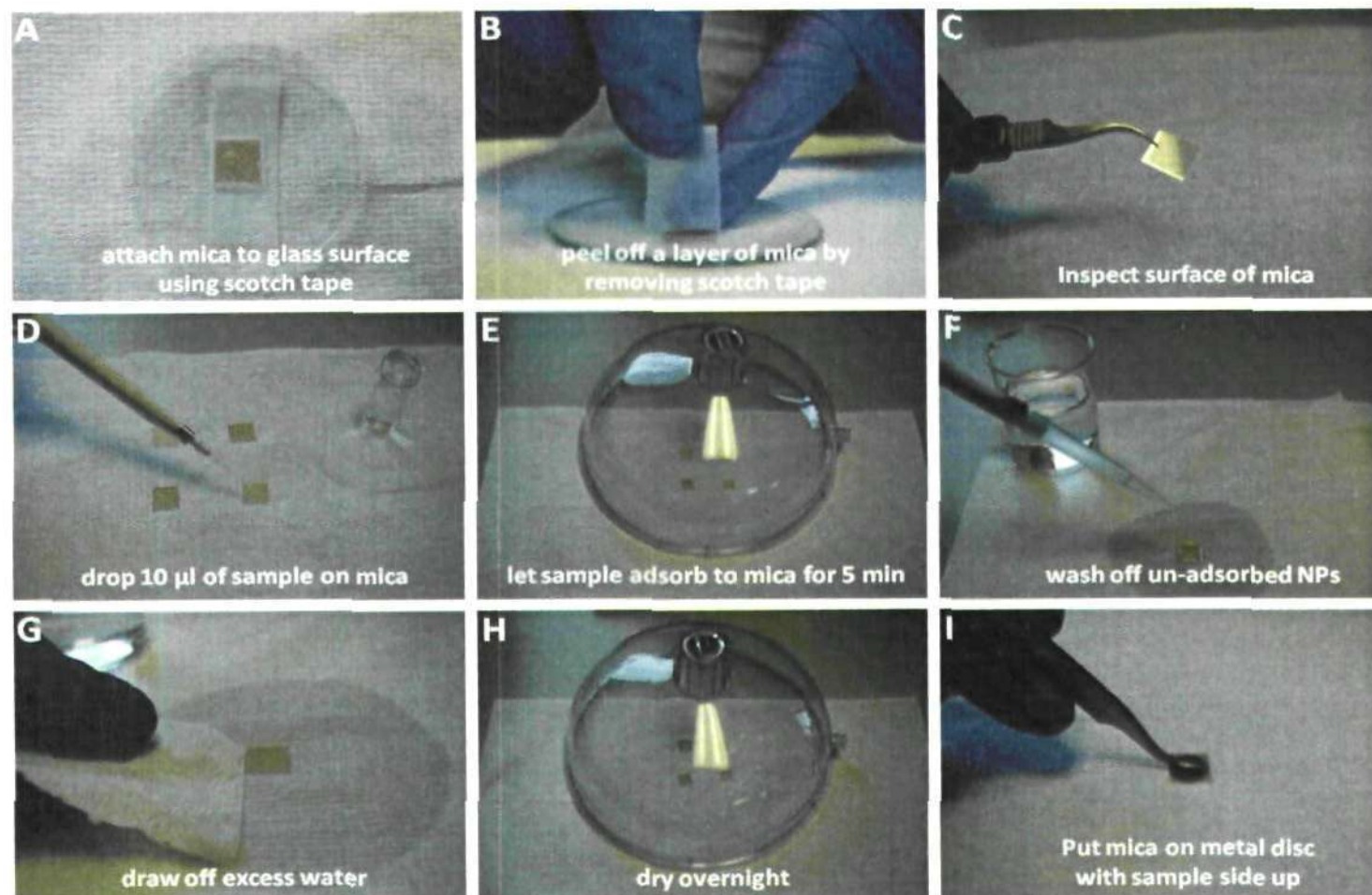


Plate 7.7 AFM drop deposition procedure steps.



Plate 7.8 XE-100 microscope used for AFM analysis

7.2.6.4 X-ray diffraction (XRD)

X-ray diffraction (XRD) was performed on C_{60} powder to identify crystal structure and crystallite size as described Kadar et al., (2010) using Bruker AX D8 (Karlsruhe, Germany) Autosampler; **Plate 7.9**. EVA software program was used for the analysis of reflections of the XRD pattern. The C_{60} fullerenes crystallite sizes were calculated using the Scherrer equation.



Plate 7.9 Bruker AX D8 used for XRD analysis.

7.2.8 *Statistical analyses*

Statistical analyses of the obtained results were performed using Statgraphics plus v5.1 (Statistical Graphics Corp). All results are presented as mean \pm S.E. Bartlett's test was applied for variance check. Significant differences between groups were determined using either one-way ANOVA for parametric data or Kurskal-Wallis test for non-parametric data, followed by multiple range tests (Fisher's LSD) at $P < 0.05$ levels.

7.3 Results

7.3.1 C_{60} characterisation

DLS analysis confirmed the formation of large aggregates in seawater as indicated with large Z-average diameters for C_{60} fullerenes particles. In addition, high polydispersity indexes were also observed which suggest that both large and smaller aggregate sizes are present (**Fig. 7.4**). In the case of FC_{60} , the Z-average was lower than AC_{60} particles, as indicated in **Table 7.1**. For XRD analysis, crystallite size can be determined normally by comparing the width of the peaks with XRD-spectra of a sample with very large crystallites. Al_2O_3 crystallites were used to determine the instrumental broadening. The widths of C_{60} , fullerenes peaks were not different from the Al_2O_3 sample (**Fig. 7.5**). This indicates that the C_{60} crystallite size is very large, and cannot be determined by XRD. This was surprising, since crystallite size is supposed to be smaller than or equal to the size of the nanoparticles. The only explanation is that the samples contain some crystals which are very large which give very strong signal for XRD, and therefore dominate over the smaller crystallites as suggested by Dr. Bjorn Stolpe (personal communication, University of Birmingham).

EDX analysis of fresh and aged C_{60} -fullerene suspension on the TEM grid revealed negligible contamination in which most of the particles contain carbon (C) element. There is some oxygen (O) and copper (Cu) elements; the later element mainly comes from the TEM-grids (**Fig 7.6**). A few of the spectra show low count rates for other elements such as silicon (Si), magnesium (Mg), sodium (Na), iron (Fe) and chloride (Cl), these were from a particle that looked very different from fullerenes, probably a contaminant. TEM micrographs of air

dried particles in both C_{60} form agree very well with the AFM images confirming distinct aggregation pattern: large compact aggregates for FC_{60} and loose aggregates varying in sizes in AC_{60} . FC_{60} and AC_{60} particles determined by AFM showed lower diameter values compared with DLS (Table 7.1 and Fig. 7.7), with approximate size of 121.88 and 18.80, respectively. It is worth mentioning that large aggregates have been washed off after 5 min deposition on the mica, therefore they are unlikely to adhere into mica sheet.

Table 7.1 Results showing characterisation measurements of fresh (F_{60}) and aged C_{60} (AC_{60}) using different techniques. Values are mean \pm S.E; n=3.

Particles characterisation	Method	Fresh C_{60}	Aged C_{60}
Z-average diameter (nm)	DLS	675.37 ± 19.06	911.8 ± 98.68
Polydispersity	DLS	0.57 ± 0.018	0.667 ± 0.06
Zeta potential	Zeta-sizer	-12.73 ± 1.18	-8.832 ± 0.90
Mean particle size (nm)	AFM	121.9 ± 6.13	18.80 ± 1.29

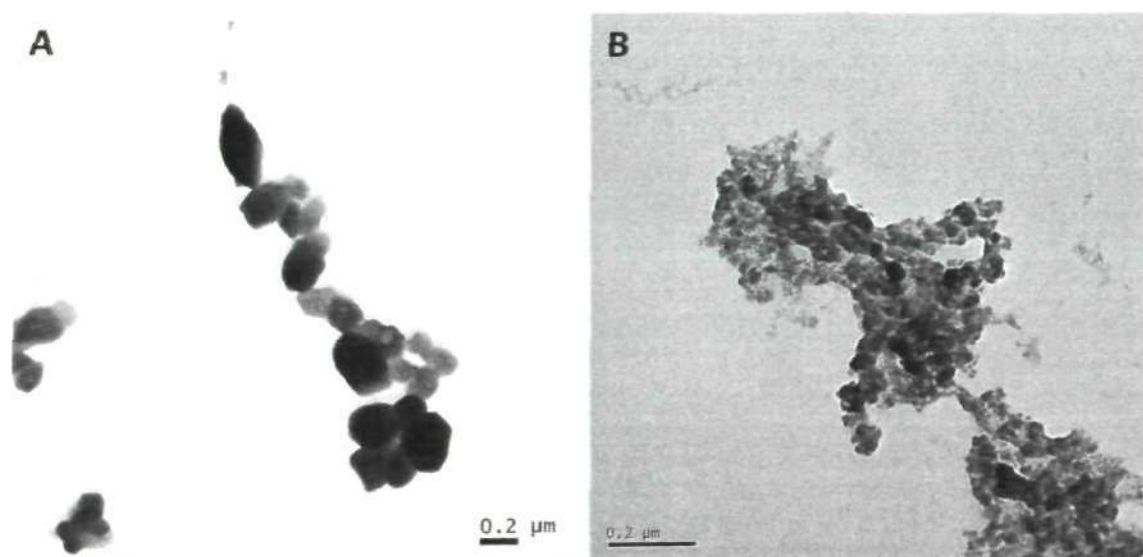


Fig. 7.4 Transmission electron microscopy (TEM) micrograph showing (A) large aggregates of FC_{60} particles and (B) aggregates with smaller size particles of AC_{60} .

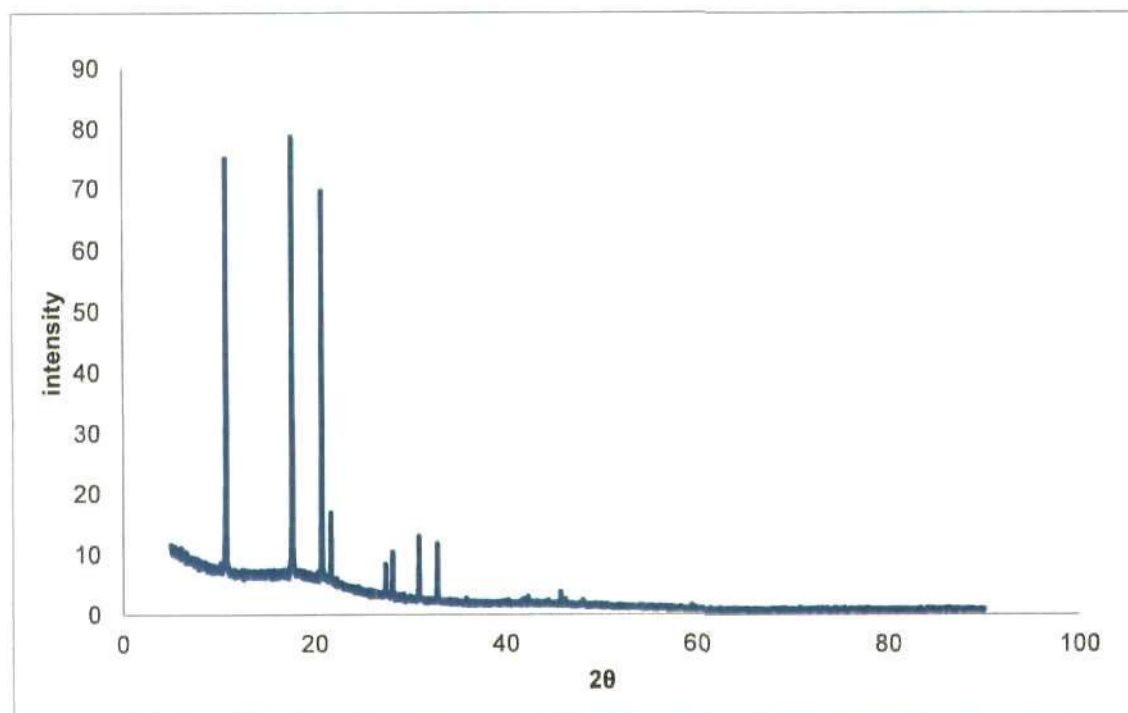


Fig. 7.5 X-Ray diffraction pattern (diffractogram) of C_{60} crystallites powder.

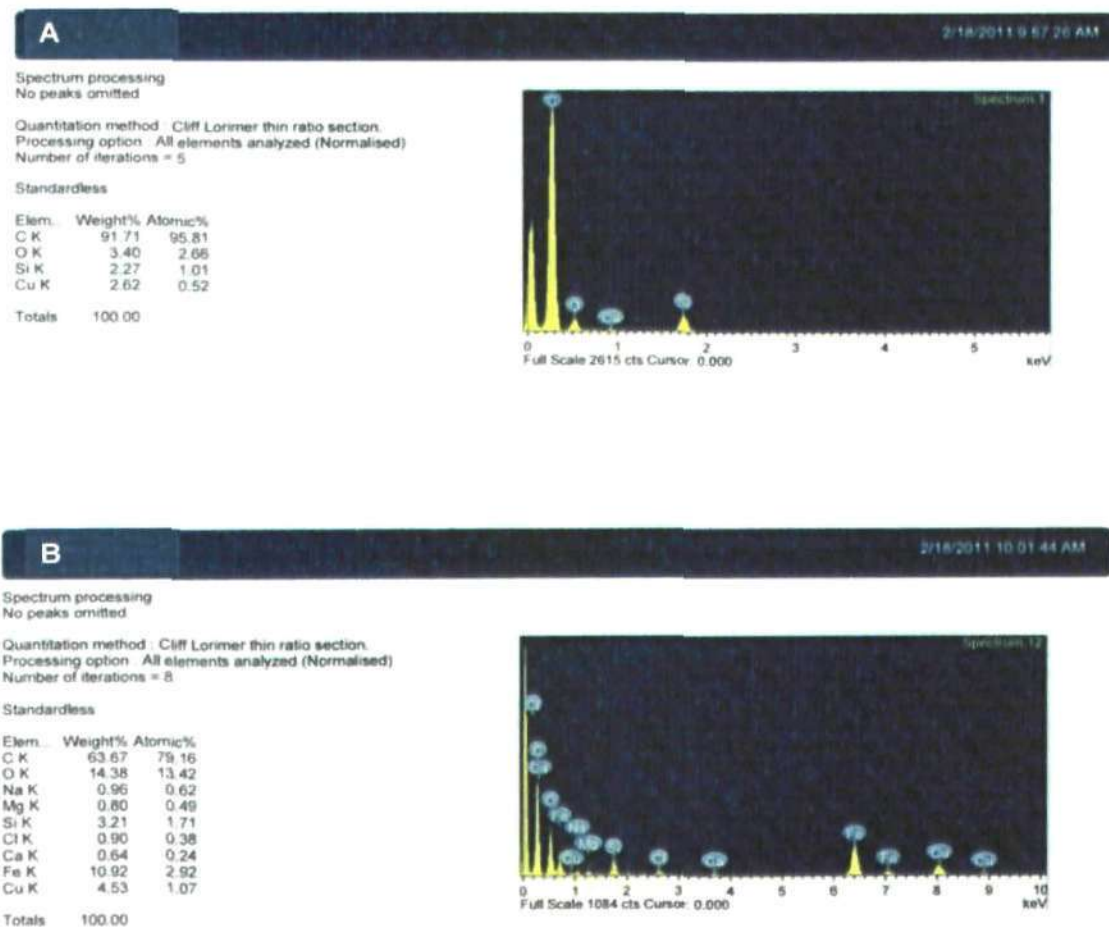


Fig. 7.6 EDX analysis of (A) fresh and (B) aged C_{60} -fullerene suspensions on the TEM grid.

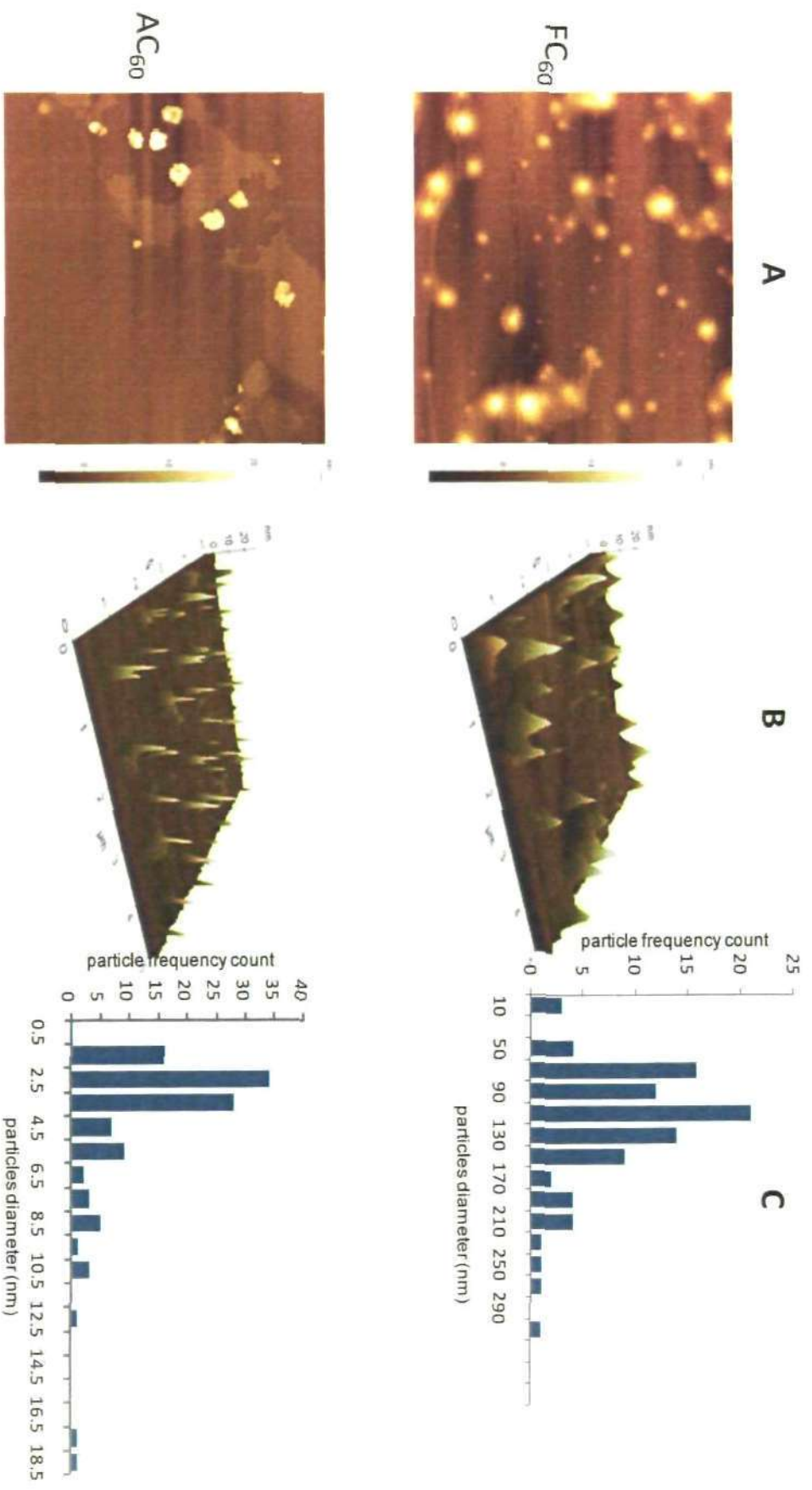


Fig. 7.7 Characterisation of FC_{60} versus AC_{60} particles using AFM: (A) partially representative AFM image; (B) 3-D AFM image; (C) particle size-distribution.

7.3.2 *In vitro* exposure

7.3.2.1 *Determination of sperm viability by AFC*

A validation experiment was conducted using different concentrations of CuSO_4 in order to optimise the analytical flow cytometry (AFC) to measure sperm viability. The results of the AFC indicated that there is a very strong dose-response effect for copper treatments. The values of % dead sperm and live to dead (sperm) ratio obtained after exposure to range of CuSO_4 exposures were correlated with the Cu concentration. According to the values of R^2 and the slope of the curves, both % dead sperm ($R^2 = 0.982$) and live to dead ratio ($R^2 = 0.902$) showed an excellent linear dose-response relationship with Cu exposure (**Fig. 7.8**). Based on this result we considered % dead sperm as an indicator for sperm viability. Measurement of sperm viability with AFC showed normal level of damage (~10% dead sperm) in the freshly collected sperm prior to exposure as illustrated in **Fig 7.9**. The percentages of dead sperm were significantly increased ($P < 0.05$, one-way ANOVA) following 2 h exposure to different concentration of CuSO_4 ($0.1\text{-}1.0 \mu\text{g l}^{-1}$) reaching 5-fold increase in the highest concentration. On the other hand, FC_{60} and AC_{60} did not show any significant increase in sperm mortality after 2 h exposure (**Fig. 7.9B**).

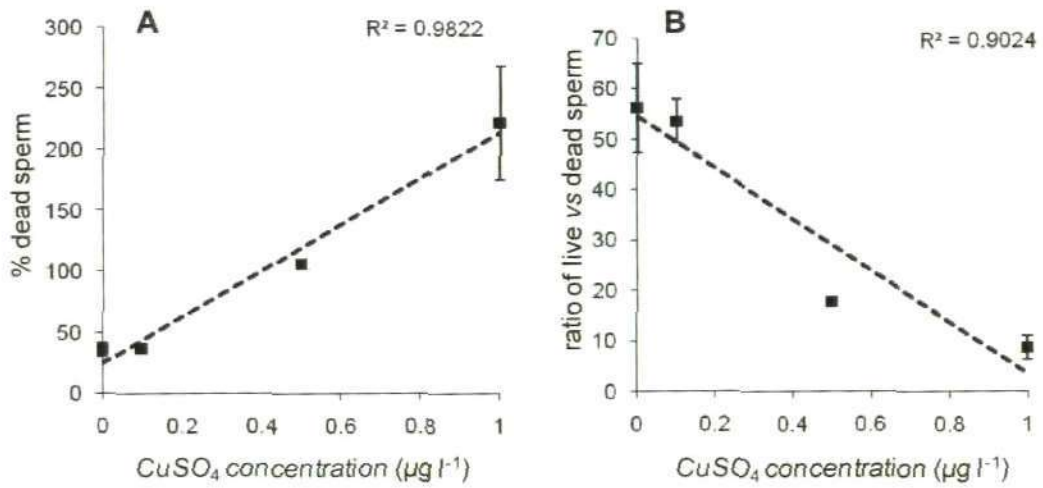


Fig. 7.8 Flow cytometric analysis of sperms viability following 2 h exposure to range of CuSO_4 concentrations ($0.1\text{-}1.0 \mu\text{g l}^{-1}$). (A) %dead sperm; (B) ratio of live to dead sperm.

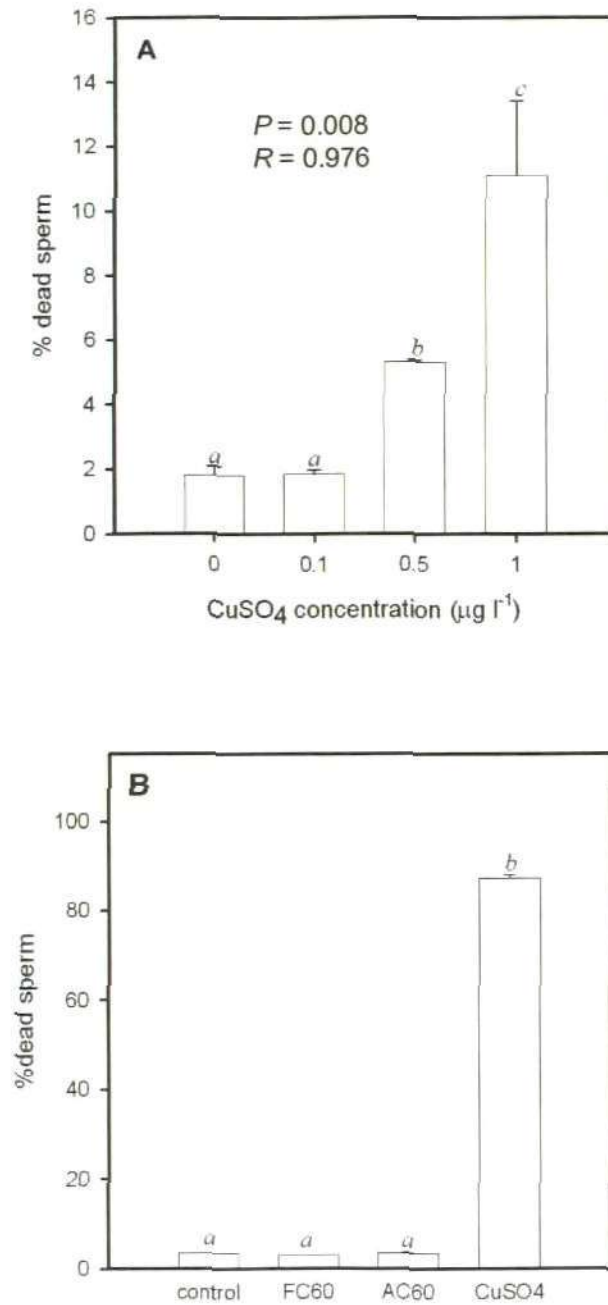


Fig. 7.9 The effect of *in vitro* exposure of different agents on sperm viability as determined by analytical flow cytometry (AFC). (A) Sperm exposed to different concentration (0.1, 0.5 and 1.0 µg l⁻¹) of CuSO₄; (B) sperm exposed to 1.0 mg l⁻¹ FC₆₀ and AC₆₀. Vertical bars represent mean ± S.E percentage of dead cell counts from the total counts per second using AFC. Bars with the same letters are not significantly different according to the multiple range test (LSD).

7.3.2.2 Sperm DNA damage assessment

Comet assay procedure on the sperm was validated using Cu (reference genotoxic agent) to validate the reproducibility and sensitivity of the assay. Regression analysis reveals significant linear dose-response relationship between CuSO_4 exposure and percentage DNA in the Comet tail (**Plate 7.10**) (linear relationship $P = 0.008$, $R^2 = 0.976$) of spermatozoa exposed *in vitro* to different levels of CuSO_4 , as illustrated in **Fig. 7.10A**. *In vitro* exposure to two form of C_{60} , fullerenes at 1.0 mg l^{-1} showed an increase in %tail DNA in the sperms. FC_{60} caused an increase in the %tail DNA, however this increase was not significant (**Fig. 7.10B**). AC_{60} resulted in significantly increased DNA strand breaks following 2 h exposure ($P = 0.015$, one-way ANOVA). Interestingly, procedural positive control ($1.0 \mu\text{g l}^{-1} \text{CuSO}_4$) resulted in 50% tail DNA, which was consistent with previously established dose-response relationship.

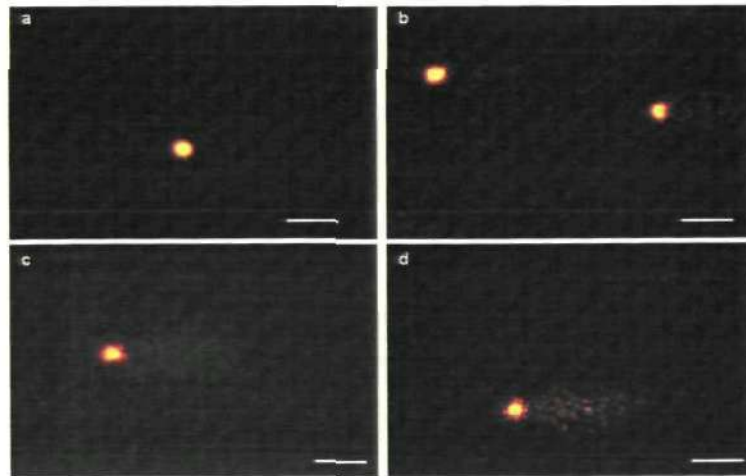


Plate 7.10 Typical Comets for: (a) control sperm in natural seawater showing nuclei with no DNA migrating into the tail; (b-d) sperm exposed to 0.1 , 0.5 and $1.0 \mu\text{g l}^{-1} \text{CuSO}_4$, respectively, showing a head with DNA fragments migrating into the tail region as a result of strand break.

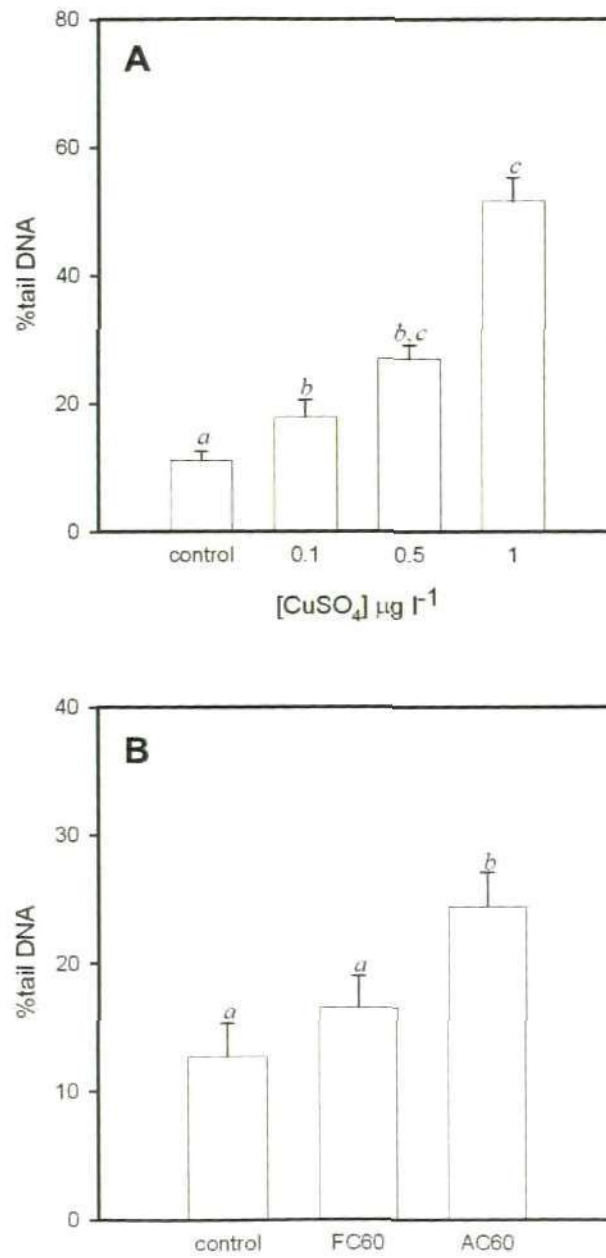


Fig. 7.10 DNA single strand breaks in sperm cells after 2 h exposure to (A) different concentrations of CuSO₄ and (B) 1.0 mg l⁻¹ FC₆₀ and AC₆₀ fullerenes. Vertical bars represent mean ± S.E. Bars with the same letters are not significantly different according to the multiple range test (LSD).

7.3.2.3 Determination of fertilization success

Fertilisation success was significantly affected by DNA damage in sperm induced through post exposure to FC_{60} and AC_{60} ($P < 0.001$, one-way ANOVA,). Only approximately 79% and 71% of cells were dividing following fertilization performed with sperm exposed to 1.0 mg l^{-1} of FC_{60} and AC_{60} , respectively (Fig. 7.11). Exposure to 1.0 mg l^{-1} AC_{60} and FC_{60} significantly reduced the fertilising ability of sperm by 15.8% and 6.5%; respectively. Procedural +ve control ($CuSO_4 \cdot 5H_2O$) caused a reduction in fertilisation by 89.5%. Furthermore, multiple range test (LSD) indicated that sperm fertilising capabilities were significantly impaired more by exposure to AC_{60} than FC_{60} .

7.3.2.4 Embryo development assessment

When the larvae aged 48 h, morphological development was analysed. By this period, embryos developed in control condition in filtered sea water (negative control) exhibited $94.7 \pm 0.4\%$ normal 'D-shell' larvae at the temperature (Fig. 7.12) (ASTM 1997). The percentage of normal D-shell larvae significantly decreased following exposure to FC_{60} and AC_{60} ($P = 0.023$, Kruskal-Wallis) (Fig. 7.13). Similar proportions of normal D-shell were observed in both FC_{60} and AC_{60} and did not appear to be dependent on the form of C_{60} (i.e. fresh or aged). The morphological abnormalities were characterized by delayed in trochophore stage, concave, malformed or damaged shell and protruding mantle as per the standard guidelines (ASTM 1997) (Fig. 7.12D&E).

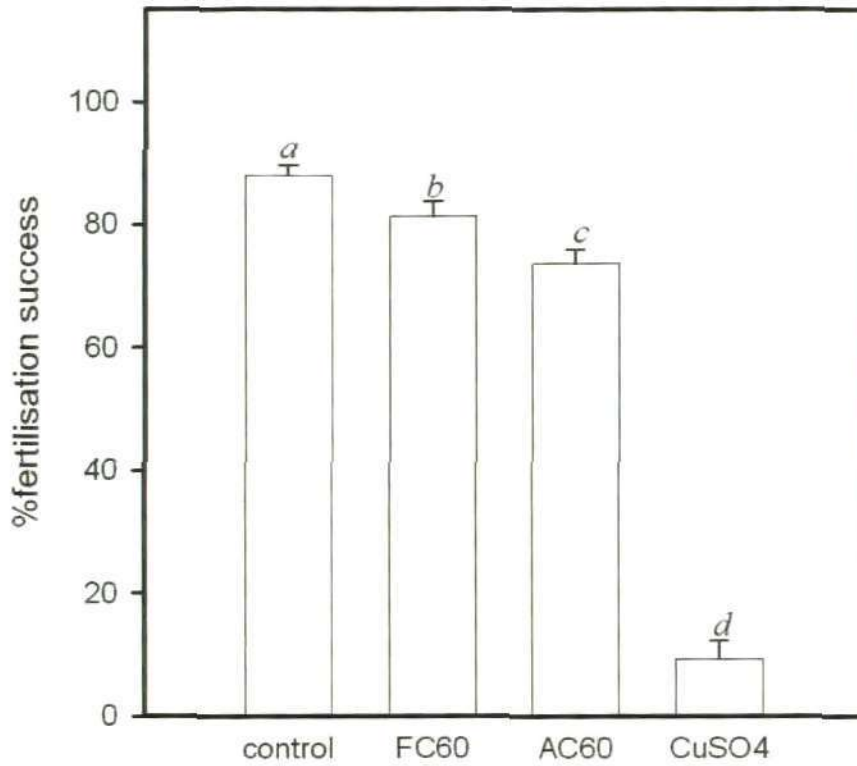


Fig. 7.11 The effect of FC_{60} and AC_{60} on fertilisation capability of sperm. Vertical bars represent mean \pm S.E percentage of dividing cells within 2 h from *in vitro* fertilisation of eggs by pre-exposed (2 h) sperm. Bars with the same letters are not significantly different according to the multiple range test (LSD).

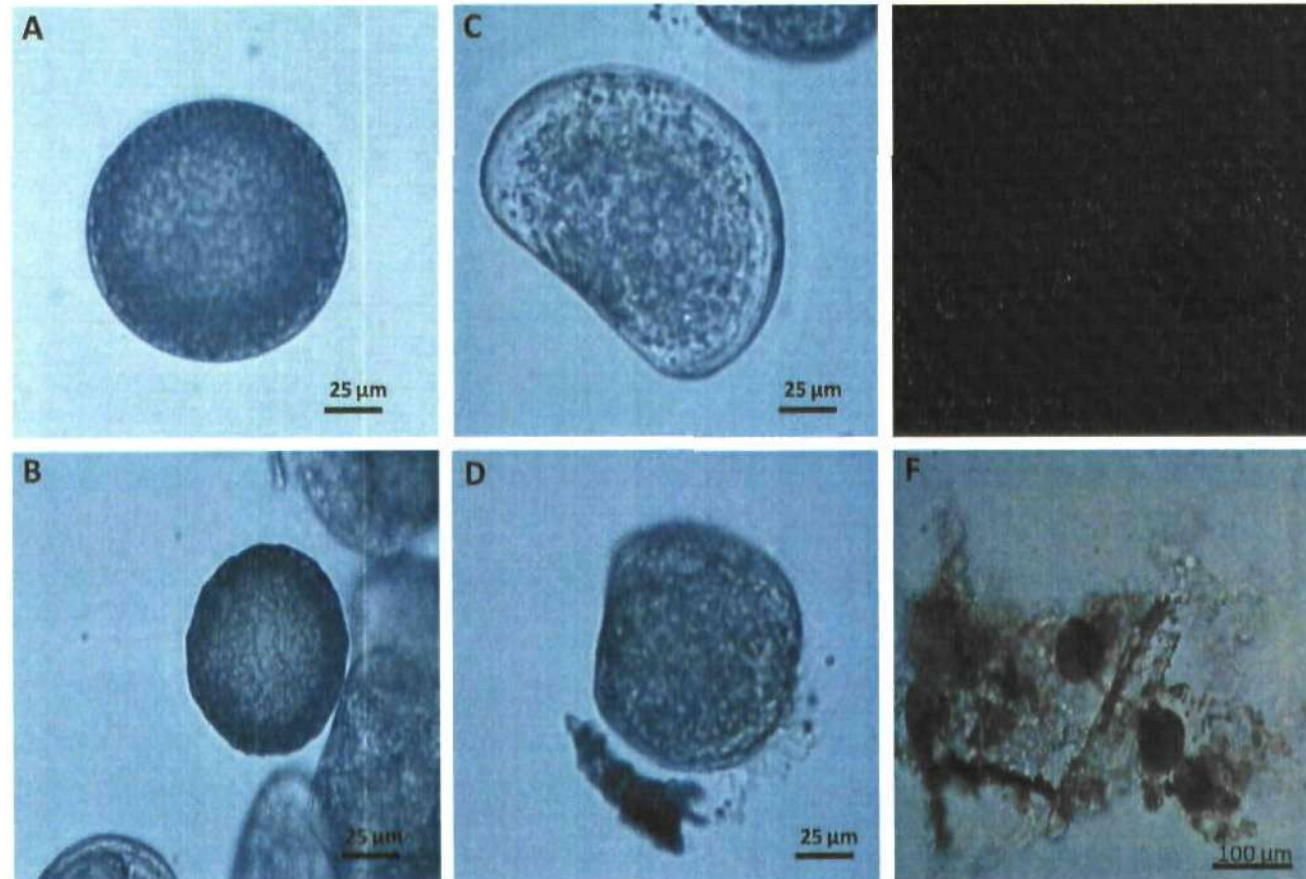


Fig. 7.12 Light-microscopy photographs of the typical early developmental stages of *Mytilus edulis* at 48 h (at 15 °C). (A) normal egg; (B) abnormal egg; (C) normal 'D-shell' stage; (D) delayed trochophore; (E) abnormal D-shell with protruding mantle; (F) cell debris and decaying materials.

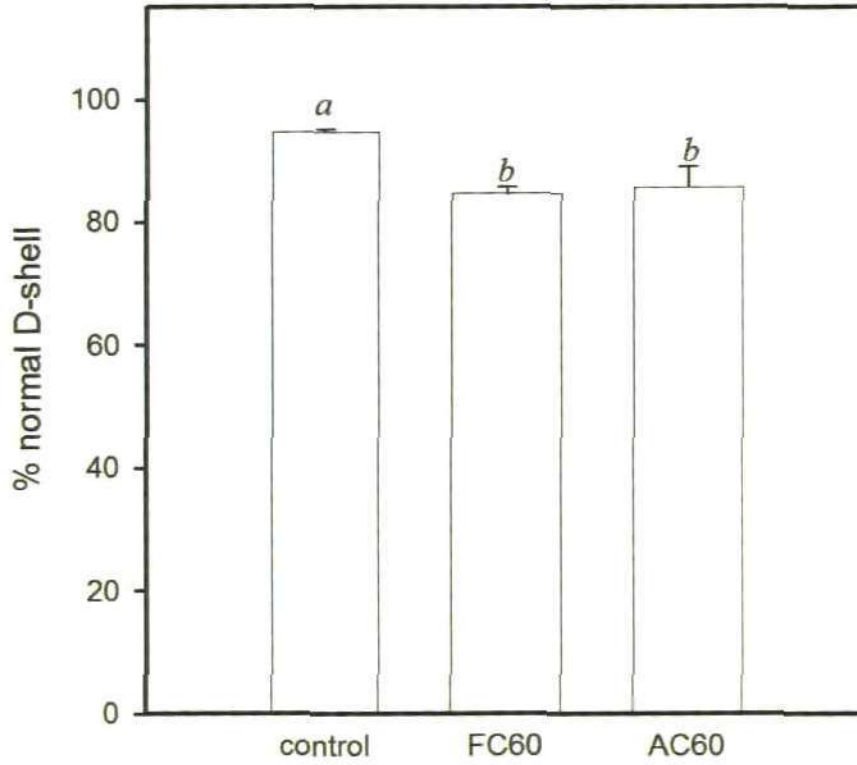


Fig. 7.13 The effect of FC_{60} and AC_{60} fullerenes on embryo development. Vertical bars represent mean \pm S.E percentage of normal D-shell stage larvae after 48 h from *in vitro* fertilisation of eggs by pre-exposed sperm. Bars with the same letters are not significantly different according to the multiple range test (LSD).

7.3.3 *In vivo* exposure

7.3.3.1 *Determination of DNA damage*

No significant loss of cell viability for haemocytes was observed (cell viability > 90% in all samples after Eosin Y staining) following exposure to either FC₆₀ or AC₆₀. Since the Comet data were not normally distributed, the non-parametric Kruskal-Wallis test was applied to demonstrate significant difference between groups.

The Comet results showed significant increase in DNA damage in exposed mussels in comparison with control ($P = 0.0001$, Kruskal-Wallis; **Fig. 7.14**). The percentage of DNA damage in haemocytes was significantly higher in AC₆₀ than FC₆₀ (Multiple range test; LSD). After 3 days of post-exposure, there was a significant decrease in DNA damage under all conditions, however % tail DNA in AC₆₀ exposed animals was significantly higher than control ($P = 0.04$, Kruskal-Wallis). 2-way ANOVA indicated a significant interaction between exposure type and time of measurement ($P = 0.0001$).

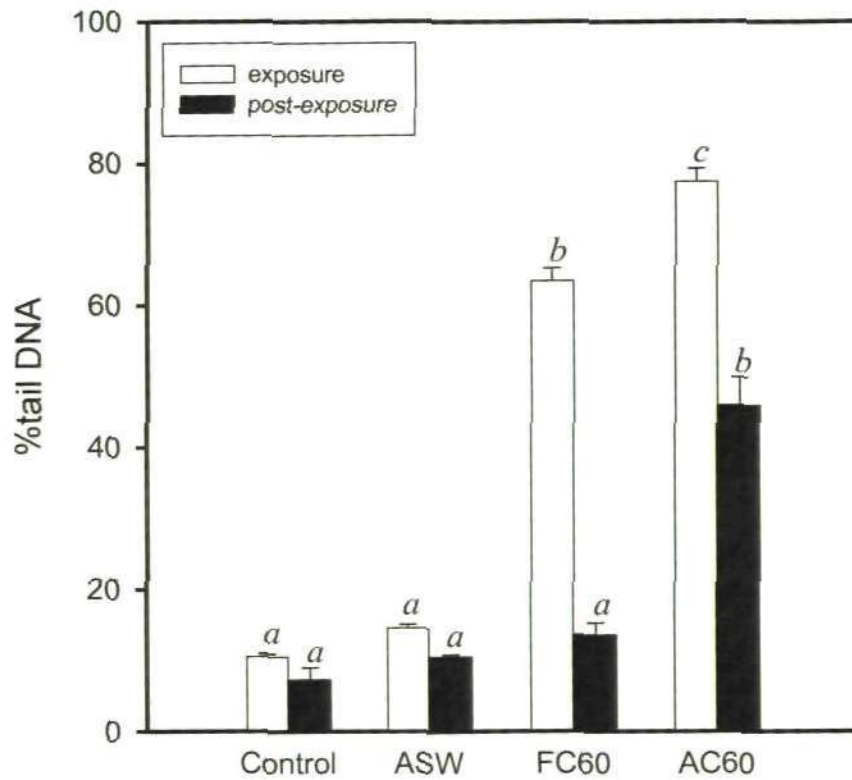


Fig. 7.14 DNA single strand breaks as determined by the comet assay in haemocytes of mussels after 3 days exposure and post-exposure to aged seawater (ASW), C_{60} in fresh seawater (FC_{60}) and aged seawater (AC_{60}). Vertical bars represent mean \pm S.E. percentage of tail DNA. Bars with the same letters are not significantly different according to the multiple range test (LSD).

7.3.3.2 *Determination of total glutathione level in adductor muscle*

Neither ASW nor FC₆₀ exposure significantly altered total glutathione levels. A significant increase in total glutathione (~ 2-fold) was however observed in *Mytilus edulis* subjected to 1.0 mg l⁻¹ AC₆₀ exposure ($P = 0.008$, ANOVA) in comparison to control, as indicated in **Fig 7.15**. Following the post-exposure, glutathione levels in individuals from AC₆₀ group had returned to control levels, a significant decrease was observed after 3 days of post-exposure period. A significant change in glutathione content was observed as a result of an interaction between treatment and exposure time ($P = 0.001$, 2-way ANOVA).

7.3.3.3 *Histological studies*

All the mussels exposed to control and aged seawater (ASW) did not show any histopathological signs such as: haemocyte infiltration, necrosis or other injuries. However, different tissues showed varying degrees of abnormalities after exposure to FC₆₀ and AC₆₀ as summarised below.

7.3.3.3.1 *Posterior adductor muscle*

Histological analysis of adductor muscle from FC₆₀ and AC₆₀ treatments showed atrophy in myocyte cells (cells were swallowed) (**Fig. 7.16B**). The atrophy effect in the adductor muscle was more adverse in AC₆₀-exposed animals in which degeneration and increase in the space around myocyte cells was observed (**Fig. 7.16C**).

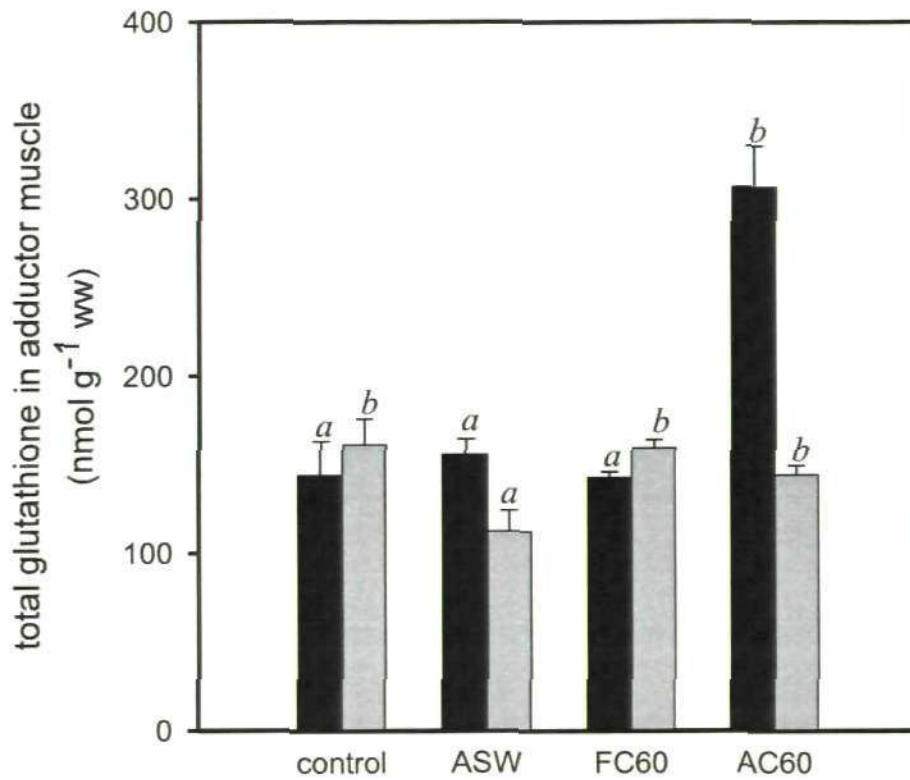


Fig. 7.15 Total glutathione levels in the adductor muscle extract following 3 days *in vivo* exposure and post-exposure in the clean seawater to ASW, FC₆₀ and AC₆₀ (1.0 mg l⁻¹). The values are mean \pm S.E. Bars with the same letters are not significantly different according to the multiple range test (LSD).

7.3.3.3.2 Gills

Neither FC₆₀ nor AC₆₀ exposure showed adverse abnormalities in gill structure. Only one mussel at each C₆₀ exposure had evidence of hypoplasia in frontal cilia (loss of frontal cilia), as shown in **Fig. 7.16I**

7.3.3.3.3 Digestive gland

Both the exposure conditions with C₆₀ (i.e. fresh and aged) caused alteration in the digestive tubules (**Fig. 7.16E**). The histological changes was characterised by necrosis in digestive cells within the digestive tubules, cellular debris was often observed within the lumen of digestive tubules (**Fig. 7.16F**).

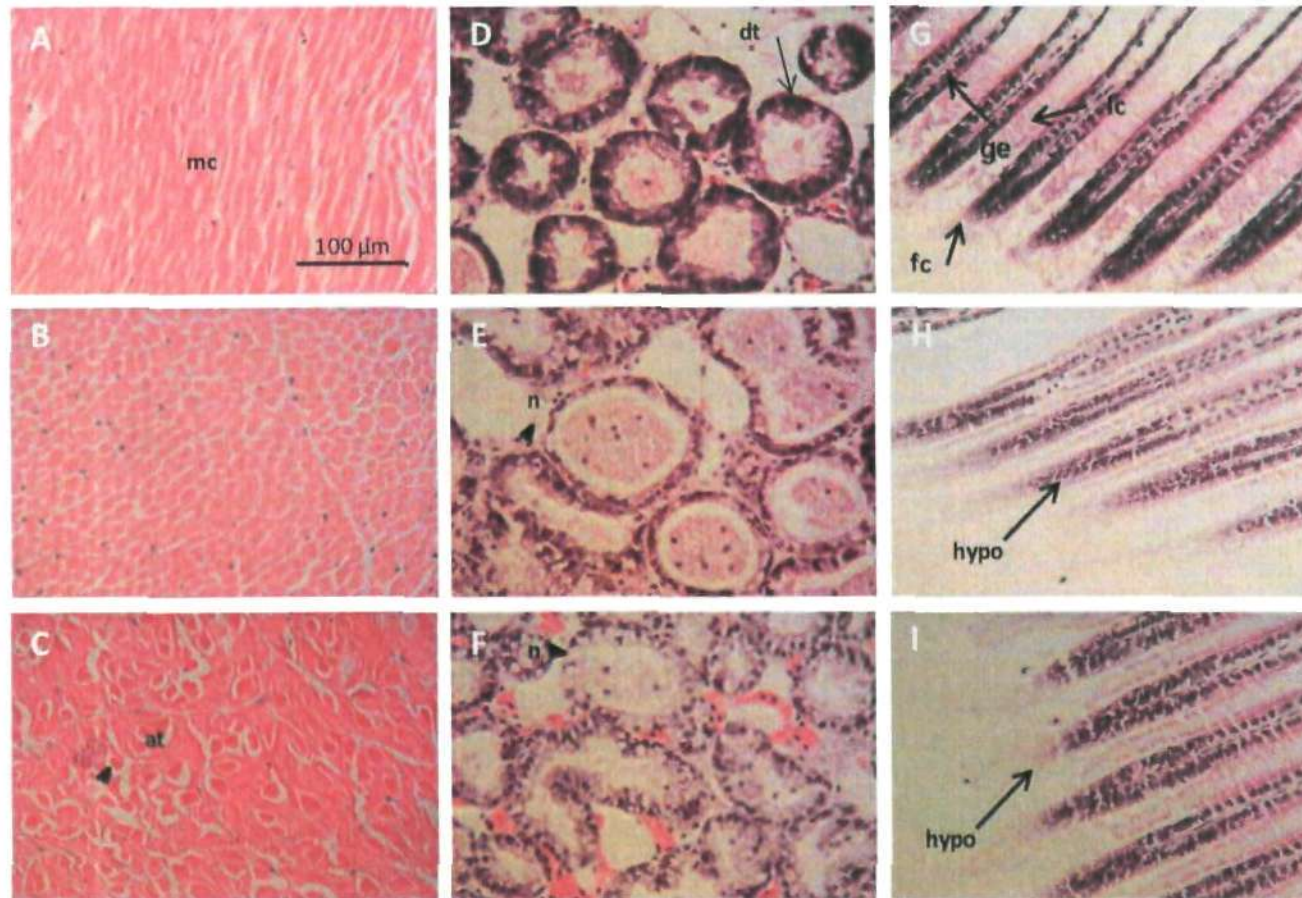


Fig. 7.16 Light micrographs of sections through adductor muscle, digestive gland & gills showing histological structure of control and treated mussels stained with H & E at 5-8 μm thickness. (A, D & G) control; (B, E & H) exposed to FC_{60} , (C, F & I) exposed to AC_{60} . mc = myocyte; dt = digestive tubules; fc = frontal cilia; lc = lateral cilia; ge = gill epithelium; at = atrophy; n = necrosis; hypo = hypoplasia. Scale bar: 100 μm .

7.3.3.4 C_{60} accumulation

Following 3 days exposure to FC_{60} and AC_{60} , C_{60} was accumulated in the digestive gland to a much greater extent than in the gills and adductor muscle (**Fig. 7.17**). The trend of accumulation was in line with our previous finding (section 6.3.5). Based on the observed concentrations of accumulated C_{60} , the digestive gland also appeared to be an important target tissue. One typical C_{60} peak (as compared with standard) was reported at retention time (RT) 3.5 min (**Plate 7.11**) in all FC_{60} and AC_{60} samples. Nevertheless, another peak was observed at RT 3.2 min in AC_{60} samples which could be the degradable products of either C_{60} or some other metabolites (**Plate 7.12 G-I**). Since C_{60} degradable products are not defined yet, we measured the typical peak for C_{60} at 3.5 min. Both adductor muscle and digestive gland displayed a significant increase in C_{60} concentration in animals exposed to $1.0 \text{ mg l}^{-1} FC_{60}$ in comparison to the control ($P = 0.025$, ANOVA; $P = 0.012$, Kurskal-Wallis; respectively). Moreover, a significant increase in C_{60} accumulation was also recorded in gills, but it was with both forms of C_{60} ($P = 0.001$, ANOVA).

In post C_{60} exposure samples, there was a significant decrease in C_{60} concentration in all organs ($P < 0.05$) except adductor muscle. To distinguish more precisely the contributions attributable to type of exposure versus time of measurement, two-way ANOVA was used on the entire raw data set. In adductor muscle, there was a significant interaction between type of exposure and time of measurement in adductor muscle, digestive gland and gills ($P = 0.018$, $P = 0.023$, $P = 0.0005$; respectively).

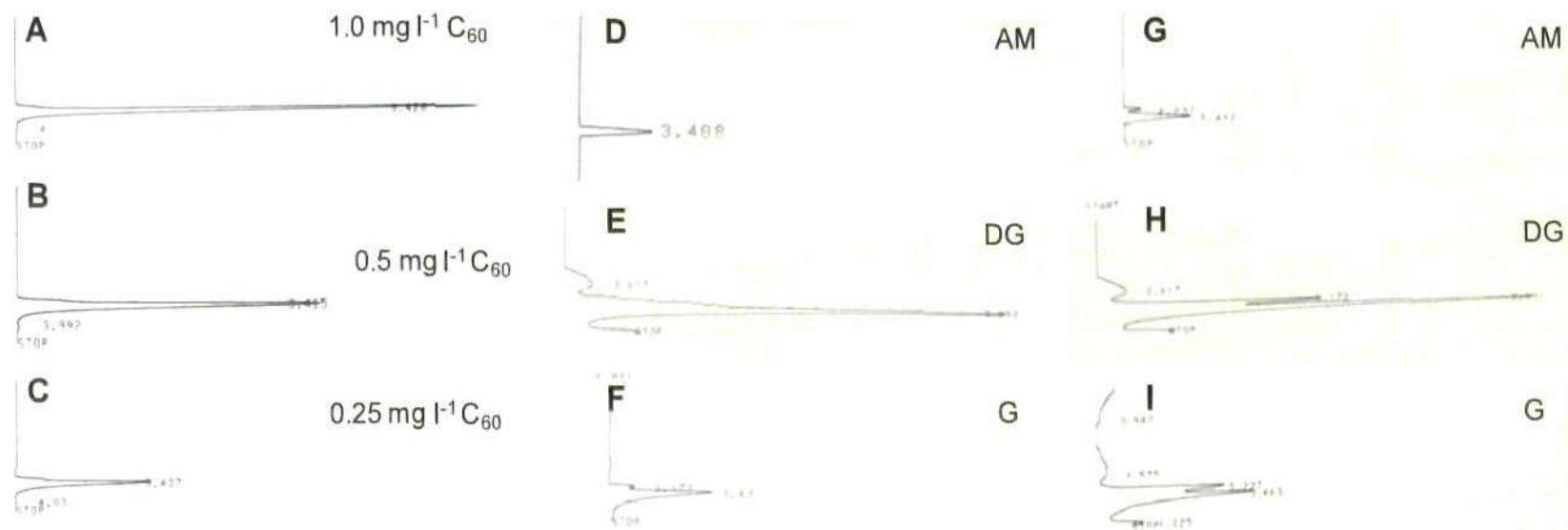


Plate 7.11 HPLC chromatogram results. (A-C): C_{60} standard; (D-F): FC_{60} exposed mussels. (G-I): AC_{60} exposed mussels; AM= adductor muscle; DG = digestive gland; G = gill.

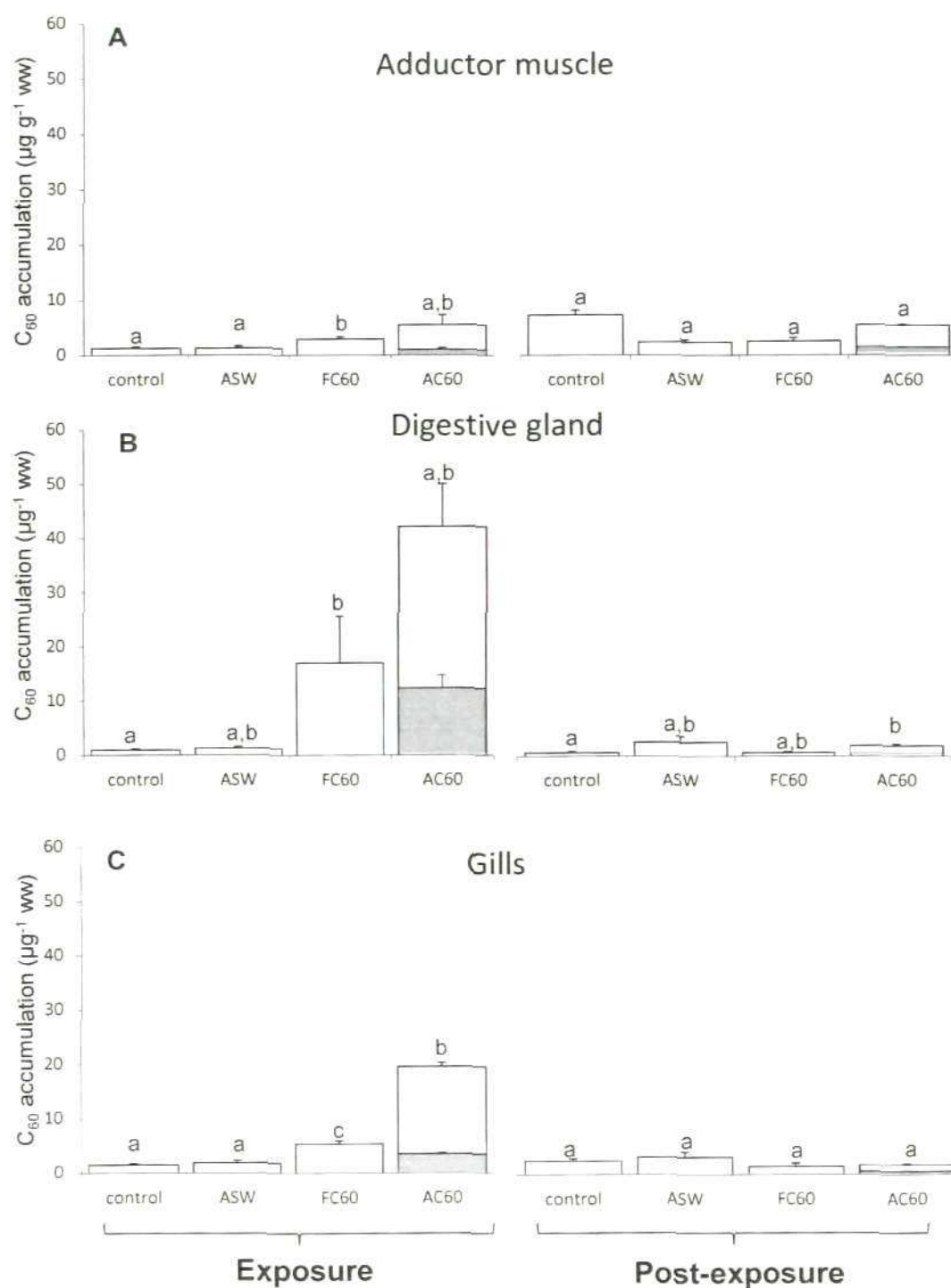


Fig. 7.17 C_{60} fullerenes accumulation pattern in *Mytilus edulis* tissues as analysed by (HPLC) (A) adductor muscle, (B) digestive gland and (C) gills after exposure to aged seawater (ASW), C_{60} fullerenes in fresh seawater (FC_{60}) and aged seawater (AC_{60}). Data are mean \pm S.E., $n = 5$. Bars with the same letters are not significantly different ($P < 0.05$) according to the multiple range test (LSD). White colour represent chromatogram peak at 3.5 min; grey colour represent chromatogram peak at 3.2 min.

7.3.3.5 Clearance rate (CR)

Interestingly, CR measurements indicated that mussels exposed to AC₆₀ evoked significant increase in CR in comparison to control ($P = 0.047$, ANOVA). Clearance efficiencies did not differ significantly between control and either ASW or FC₆₀ exposed mussels (**Fig. 7.18**). No significant differences were found in the clearance rate after 3 days of post-exposure period, except in control mussels where CR to 3.3 l h^{-1} . To check if there is any interaction between effect of exposure and time of measurement on CR, 2-way ANOVA was applied. There was however no significant interaction between the two factors ($P = 0.34$).

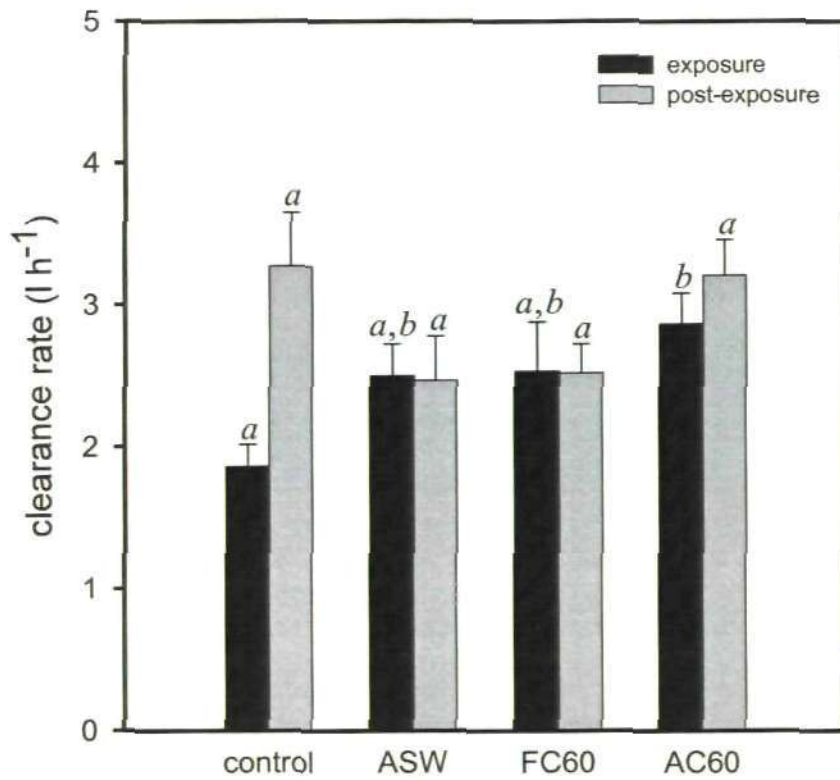


Fig. 7.18 Clearance rate in *Mytilus edulis* following 3 days *in vivo* exposure and post-exposure to ASW, FC₆₀ and AC₆₀. The values are mean \pm S.E. Bars with the same letters are not significantly different ($P < 0.05$) according to the multiple range test (LSD).

7.4 Discussion

During the last few years, there has been an exponential increase to evaluate toxicological properties of the manufactured or engineered nanoparticles (ENPs) and their potential impact on human and environment health (Handy et al. 2008; Hasselöv et al. 2008). A large body of information have been generated on one of the most important and environmentally relevant nanoparticles, C₆₀ fullerenes which are released either from industry or domestic wastewater in bulk quantities (USEPA 2010). Many studies have reported the toxicity of C₆₀ fullerenes in aqueous suspensions to aquatic organisms (Oberdörster et al. 2006; Zhu et al. 2006). Nevertheless, in the environment C₆₀ fullerenes may undergo degradation and transformation reactions. This includes photoreactive transformation following exposure to sunlight due to its strong light absorption capacity. There is evidence that the photoexcited C₆₀ fullerenes facilitates transfer of absorbed energy to triplet oxygen ³O₂ (³Σ_g) and produce highly reactive oxygen species (ROS), singlet oxygen ¹O₂ (¹Δ_g), which may cause oxidative damage to lipid, protein and DNA in exposed organisms (Lee et al. 2009a).

Characterization of ENPs, such as size, shape, surface area and aggregation, should be given due attention especially when evaluating the potential toxicity of the ENPs. The large C₆₀ fullerenes aggregation may occur once they are introduced into aquatic environment, including seawater. Using transmission electron microscopy (TEM) studies, we have demonstrated that the sizes of AC₆₀ particles were much smaller than those of the fresh C₆₀ fullerenes and the zeta potential of FC₆₀ fullerenes was more negative than AC₆₀ fullerenes.

7.4.1 Studies with *in vitro* exposure of sperms

The majority of marine invertebrate release millions of sperm and eggs freely into water where external fertilisation takes place. Hence, the gametes are directly exposed to pollutants present in the water. In the current work, the consequence of exposure of C₆₀ fullerenes in paternal germ cells (i.e. sperm) was studied using single cell electrophoresis or the Comet assay. A clear increase in DNA strand breaks as determined by %tail DNA reported in the present study indicates the interest of using this technique as a convenient tool to assess DNA damage in sperm cells of invertebrate species. Many studies confirm the sensitivity of this technique to assess the genotoxic effect of chemical induced DNA damage in germ cells (Kadar et al. 2011; Lewis et al. 2009). Our results have clearly demonstrated the genotoxic effect of C₆₀ fullerenes on mussel sperm cells. DNA strand breaks increased by approximately 2-fold after AC₆₀ fullerene exposure as compared to control, showing significant genotoxicity of the degraded C₆₀ fullerenes. Ecotoxicological studies have obtained similar results in other aquatic species exposed to genotoxin agent. Zhu et al. (2006) have shown that *in vitro* exposure of spermatozoa from mature common carp, *Cyprinus carpio* to 25 µM duroquinone for 2 h resulted in significant damage to the sperm DNA. Lewis and Galloway (2009) reported significant elevation in DNA strand breaks of *Arenicola marina* spermatozoa after 1 h of *in vitro* exposure to 18 mg l⁻¹ methyl methanesulfonate (MMS). Lacaze et al. (2010) developed and optimised the comet assay in the fresh water invertebrate, *Gammarus fossarum* using different cell types (i.e. haemocytes, oocytes and spermatozoa). Their results suggested a clear dose or concentration dependent increase for the induction of DNA strand breaks,

demonstrating the effectiveness and usefulness of the assay. Transferring of genetic damage to new generation is a main concern for scientists and regulators in the human health area (Aitken et al. 2004), but it has also ecotoxicological implications on living organisms (Jha 2004).

Several mechanisms have been suggested to explain the genotoxic effects of engineered nanoparticles (Landsiedel et al. 2009; Singh et al. 2009). One of the suggested mechanisms of ENPs-induced genotoxic effects is through generation of reactive oxygen species (ROS). The exact mechanism of oxidative stress induced by C₆₀ fullerenes is however still largely unknown, but given that C₆₀ nanoparticles have small size and lipophilic nature, it is possible that C₆₀ fullerenes can penetrate through cell membrane and trigger intracellular toxicity by formation of ROS, leading to oxidative damage (i.e. lipid peroxidation and DNA damage).(Singh et al. 2009). It is also possible that ENPs could bind to biomolecules inside the cell, including perhaps with DNA, inflicting a cascade of effects (Xu et al. 2009).

The implications of sperm DNA damage were reflected on the early life development stages. Studies have shown that, in general, early life stages of organisms tend to be the most sensitive to pollutants (His et al. 1999). Fertilisation success was significantly reduced after *in vitro* exposure of sperms to both FC₆₀ and AC₆₀ fullerenes. This result is in contrast to that reported by Devaux et al., (2011) who showed that genetically damaged fish sperm are still able to fertilise eggs. Several factors including age of the donors contribute to the quality of sperms (Singh et al. 2003) and subsequently their fertilisation capabilities (Fernández et al. 2009). A possible explanation for our result is that

C₆₀ fullerenes exposure compromised plasma membrane of the sperm cell. Sperm quality and properties (i.e. composition of sperm head and tail) are very important to make contact with spawned egg. As viability of sperms have been implicated in oocytes penetration (Grunewald et al. 2007), we investigated the plasma membrane integrity. Flow cytometry technique has been commonly used in a variety of mammalian species to assess live and dead sperm but rarely employed in ecotoxicological studies. Sperm membrane integrity as measured by SYSTOX Green fluorescence staining was not affected in sperm exposed either to FC₆₀ or AC₆₀ fullerenes (**Fig. 7.2**). Thus, the reduction in fertilisation success observed in our study does not appear to be related with the membrane integrity. It is possible that due to electrostatic charges C₆₀ co-aggregate with the sperm. This may decrease fluorescence intensity leading to underestimation of the dead cells.

Interestingly, embryos demonstrated a significant increase in abnormal development approximately at the same level with both the C₆₀ treatments (i.e. AC₆₀ and FC₆₀). Although the percentage abnormal larvae in both exposures for sperms were approximately at the same level, AC₆₀ exposure showed more severe developmental defects such as protruding mantle. Fitzpatrick et al. (2008) also reported an increase in developmental abnormalities of *Mytilus trossulus* larvae developed from gametes exposed to copper. Additionally, this effect was also observed in early developmental stages of the *Mytilus edulis* in which zero-valent iron nanoparticles (nZVI) exposed sperm produced larvae with delayed development and abnormal trochophore larvae (Kadar et al. 2011).

7.4.2 Studies with *in vivo* exposure of adult mussels

Although there is no universal marker for oxidative stress, alterations in the antioxidant defence systems or DNA damage could be the best indicators of oxidative stress *in vivo* (Halliwell and Gutteridge 2007). There are many evidences in the literatures showing that ENPs increase ROS production and can cause oxidative damage in biomolecules such as DNA, proteins, and lipids (Nowack and Bucheli 2007; Scown et al. 2010). Furthermore, we have documented oxidative stress as indicated by elevation of DNA damage and glutathione levels from the previous experiment. In the current chapter, effect of photochemical transformation of C₆₀ was studied across different levels of biological organisation (i.e. biochemical, molecular, cellular and physiological) on adult mussels.

Induction of DNA damage in haemocytes following exposure to C₆₀ fullerenes was comparable to our previous observations in mussels (chapter 6). The level %tail DNA in AC₆₀-exposed animals increased to a greater degree in comparison to all treatments (ASW and C₆₀). It clearly appears from the *in vitro* and *in vivo* exposures that AC₆₀ is more genotoxic compared to FC₆₀ fullerenes. Analysis of the % tail DNA (section 7.3.3.1) demonstrated 14% increase in single strand breaks in AC₆₀-exposed mussel in comparison to mussels exposed to FC₆₀. A possible explanation for the observed disparity in effective toxicity may be due to changed C₆₀ properties after exposure to sunlight, leading to differential genotoxic effects. Taylor et al., (1991) found that C₆₀ fullerenes degrade under sunlight and the degradable products contain open cages C₆₀ with aldehydes and /or ketones. Although no direct study has been reported on genotoxicity of photochemical transformation of C₆₀, a recent study

on algae suggests a sound proof for the toxicity of AC₆₀ (Gelca et al. 2010). Overall, whilst previous work on mammalian systems have demonstrated genotoxic effects on human lymphocytes (Dhawan et al. 2006) and mouse primary fibroblasts (Xu et al. 2009), there are only few studies on the genotoxic effects of C₆₀ fullerenes on aquatic organisms. In the present study, whilst we have evaluated generic DNA damage using the comet assay, it would have been more appropriate to use modified comet assay which uses bacterial enzymes which specifically target oxidised purine and pyrimidine bases. This approach has been adopted to evaluate titanium dioxide induced oxidative DNA damage in fish cells under in vitro conditions (Reeves et al. 2008; Vevers and Jha 2008) as well as fish exposed to chronic hyperoxic and hypoxic conditions (Mustafa et al., 2011).

Elevation of glutathione level is however seen as an indication of oxidative stress and results from Chapter 5 suggested this was a predisposing factor in adverse effects of oxidative damage (Al-Subiai et al. In press). Given that glutathione is an important scavenger of ROS, and necessary for the operation of a number of enzymes (e.g. GPx, GR and GST) (Perendija et al. 2007), it is likely that this increase in glutathione content is an up regulation of antioxidant defences as a result of the increased ROS production by AC₆₀. The elevation in adductor muscle glutathione in the current study corresponded with induction of DNA damage in haemocytes, providing further evidence that glutathione respond defensively to the increased level of oxyradicals or in another word oxidative stress, as proposed by Regoli and Principato (1995). A similar increase in total glutathione level has been reported in adult zebra fish, *Danio rerio*, exposed to 30, 60 and 120 mg l⁻¹ silver nanoparticle (AgNP) (Choi et al.

2010). However, Oberdorster (Oberdorster 2004) has demonstrated that C₆₀ fullerenes can cause a significant elevation of lipid peroxidation and marginal glutathione depletion in largemouth bass, *Micropterus salmoides*, a pattern that was not observed in this study. It was suggested that the loss of glutathione may inhibit cellular anti-oxidant defences and therefore the accumulation of ROS will be expected.

Considering the fact that contaminant accumulation is an important process as it is usually a precursor to toxicity (Luoma and Rainbow 2008), it is essential to consider this process when evaluating potential toxicity of ENPs. We therefore investigated the accumulation of C₆₀ fullerenes in adductor muscle, digestive gland and gills after potential photochemical transformation reaction. Whilst there was no proof available to support the assumption that 3.2 min peak observed in HPLC chromatogram (**Plate 7.11**) is a degradable products of C₆₀, we concluded to exclude it from our calculations. Animals exposed to FC₆₀ incorporated these nanoparticles in their tissues, i.e. adductor muscle, digestive gland and gills leading to a 1.5, 13 and 4-fold increase compared to control levels; respectively. Interestingly, there was lower accumulation of AC₆₀ in the tissues, in which no increases in C₆₀ concentration were reported in adductor muscle; 9-fold increase in digestive gland and 2-fold increase was observed in gills (**Fig. 7.17**). The obtained results pertaining to accumulation of C₆₀ fullerenes suggests that the digestive gland could be the main target for toxic effects of C₆₀ fullerenes, this probably being due to the fact that C₆₀ fullerenes particles are present in sea water mainly as big and small agglomerates (**Table 7.1, Fig. 7.4**) which are taken up by the feeding and digestive system. Unfortunately, there are no data available in the literature regarding the

accumulation of C₆₀ fullerenes in living organisms to compare with other systems and the possible products that result from C₆₀ degradation in biological systems.

Organisms from the present study showed histological changes in all the tissues studied (i.e. adductor muscle, digestive gland and gills), associated with FC₆₀ and AC₆₀ exposures. However, AC₆₀ treatment had more severe injuries in comparison to FC₆₀ group. Similar inflammation effect in adductor muscle (i.e. atrophy and necrosis) was reported in blue mussel *Mytilus edulis* exposed to 50 µg l⁻¹ mercury (Hg) (Sheir et al. 2010). Moreover, exposure to both forms of C₆₀ fullerenes induced injuries in digestive tubule as a result of losing of digestive cell and basophilic secretory cells within the lumen of digestive tubules. The effect of the C₆₀ fullerenes was enhanced when photochemical transformation process occurred, with more severe changes observed in digestive tubules. Digestive gland of the AC₆₀-exposed mussels showed necrosis (diffuse nuclei and no clear distinction in some epithelial cells), adverse atrophy of digestive tubule and stomach obstruction epithelium. Histological changes in the digestive tubules have been used to assess the effects of environmental contaminant (Auffret 1988; Lowe and Pipe 1987). In gills similar hypoplastic response was observed with FC₆₀ and AC₆₀. The gills exhibited loss of frontal cilia, but this level of injury did not appear to affect the physiological function (i.e. clearance rate) in either FC₆₀ or AC₆₀ exposed groups. The relatively low clearance rate observed in control mussel (**Fig. 7.18**) may have been linked to post-spawning events. Bayne and Widdows (1978) also observed that mussels in pre-spawning period increase clearance rate followed by decrease in post-spawning period.

7.5 Conclusions

In summary, acute *in vitro* exposure to sperms and *in vivo* exposure of adult *Mytilus edulis* to AC₆₀ fullerene impaired development in the early life stages and enhanced toxicological injury in adult stage of the blue mussel. This study brings forward evidence for the instability of photochemical transformed C₆₀ fullerenes under environmentally relevant condition and toxicity of AC₆₀ at different life stages of *Mytilus edulis*. Additional toxicological assessments involving isolation, identification and characterization of the breakdown products of aged C₆₀ fullerenes are needed to develop a better and more conclusive understanding of the toxic mechanism by which AC₆₀ causes toxicological stress and affects aquatic organisms at different levels of biological organisation.

Chapter 8

General Discussion

8.1 Discussion

This thesis focused on evaluating the ecotoxicological effects of ENPs, C₆₀ fullerenes either alone or in combination with a representative poly cyclic aromatic hydrocarbons (PAHs) on the marine mussel, *Mytilus edulis*. Currently, assessing the toxicity, behaviour and fate of ENPs has become a worldwide issue. The assays used in this study were chosen to reflect responses at different levels of biological organisation (i.e. biochemical, morphological and behavioural levels) to assess potential toxicity of C₆₀ fullerenes. The parameters used in the experimental chapters (chapter 5-7) focused on specific end points. The analysis of these end points or responses indicated their efficiency as a tool for monitoring the relative health status of mussels after exposure to emerging contaminant, i.e. ENPs. The Comet assay determined the genotoxic effects of C₆₀ fullerenes on adult and early life stages of *Mytilus edulis*; either alone or in combination with PAHs or sunlight (chapter 6 and 7). Also, determination of total glutathione in adductor muscle (chapter 3) complemented the results for Comet assay in all the relevant experimental chapters (chapter 5-7), in which elevation of glutathione levels were always seen following effective exposure. We were aiming to optimise the biotransformation enzyme P-450 as molecular tool and good progress (chapter 4) was made in standardising P-450 in mussels but unfortunately we could not apply P-450 measurement effectively due to technical limitations. Morphological observations such as inflammation and necrosis were very helpful in explaining how cells and tissues respond to a metallic contaminant (i.e. Cu) and C₆₀ fullerenes accumulation (chapter 5-7). It also helped in the interpretation of behavioural assay (i.e. clearance rate) and

Cu/C₆₀ accumulation where animals failed to compensate with toxic exposures, i.e. Cu (chapter 5).

8.1.1 Environmental pollution-current and future prospect

The debate over how pollution emissions will affect the future of the marine and coastal environment is hard to ignore with increasing number of chemicals produced and discharged into the environment every year. Meanwhile, the long hold-up time between occurrence of pollution and regulatory testing to ascertain acceptable levels of contaminants may result in unpredictable consequences for the environment. In the last decade legislation and regulation advocated by many organisations such as OSPAR (OSPAR 2004) and European Union's Water Framework Directive (WFD-2000/60/EC) for environmental risk assessments have been developed in response to concern over potential impact of increasing levels of pollutants on ecosystem health. In particular, the WFD of EU emphasises the detection of those contaminants which could be potentially carcinogenic, mutagenic and could induce reproductive toxicity (Borja et al. 2004). These endpoints have been given some emphasis in the present study. Environmental policy development is however highly complicated often involving uncertainties due to difficulties in developing an adequate ecological risk assessment and classification in ecosystem (EU 2003). For example, policies are not consistent for chemicals such as pharmaceuticals in which testing is always compulsory and conducted to the highest standard of *experimental testing before reaching the market*. In contrast, manufacturers do not have to assess the environment or human health impact of other products or chemicals (i.e. personal care or domestic products) before releasing them into the market. For any precautionary purposes it is easier and economic to

protect the environment than clean up or repair the resultant harmful effects. There is an increasing need to test the potential detrimental effects of emerging chemical such as ENPs using environmentally realistic early bio-indicators in the model organisms before releasing them to the market for societal benefit.

8.1.2 Environmental risk assessment (ERA)

Environmental risk assessment (ERA) provides a systematic procedure for predicting potential risks and consequence of exposure to various hazards to human or ecosystem health. At present, ERA is a widely established process on which many decisions of environmental management are based on. ERA consists of three main steps based on environmental protection agency (EPA), USA: risk identification, risk assessment (dose-response) and exposure assessment. The integration of the earlier steps results in the risk characterisation by estimating the numbers of measures indicating environmental damage (**Fig. 8.1**). Our experimental results mentioned in chapters 5 and 6 contribute towards the first and second stages in the ERA procedure through detection of the genotoxic effects of exposure (i.e. Cu in chapter 5 and fluoranthene/C₆₀ fullerenes in chapter 6) on *Mytilus edulis*. Toxicity bioassays have been recognised as promising tools for ERAs on standardized test species such as earthworm *Caenorhabditis* or water flea *Daphnia*, however the results from this type of assay might or might not be relevant to the organism's exposure at environmental concentrations since there are a relatively narrow range of doses used in these assays.

Another very useful approach that could elucidate cause-effect and dose-effect relationships of the contaminant is biomarkers of exposure. Over the years,

measurements of biomarker responses have been carried out for biological monitoring to assess the effect of the exposure to contaminants. These biomarkers could provide the critical link between chemical exposure and health impairment and have been proved to be a valuable tool in ERA. Despite such encouraging premises, ERA research on biomarkers is facing overwhelming problems, as they have to be appropriate (answer important public health questions or concerns) and undergo of proper optimisation and validation (as discussed in detail later, section 8.1.3). With growing developments in the post-genomic era with genomic data available for a large number of sentinel or model species, we are able to know more about how the organisms respond with the changes at molecular and genetic levels (Jha, 2004). These functional responses at the levels of gene expression will enhance our understanding of how organisms perceive changes, adapt to the environment and inflict pathophysiological and environmental changes. Indeed, environmental toxicogenomics will play an increasingly important role in environmental sustainability (Leroy et al. 2010; Snape et al. 2004). In this process computer modelling will also play a vital role. (Moore et al. 2004).

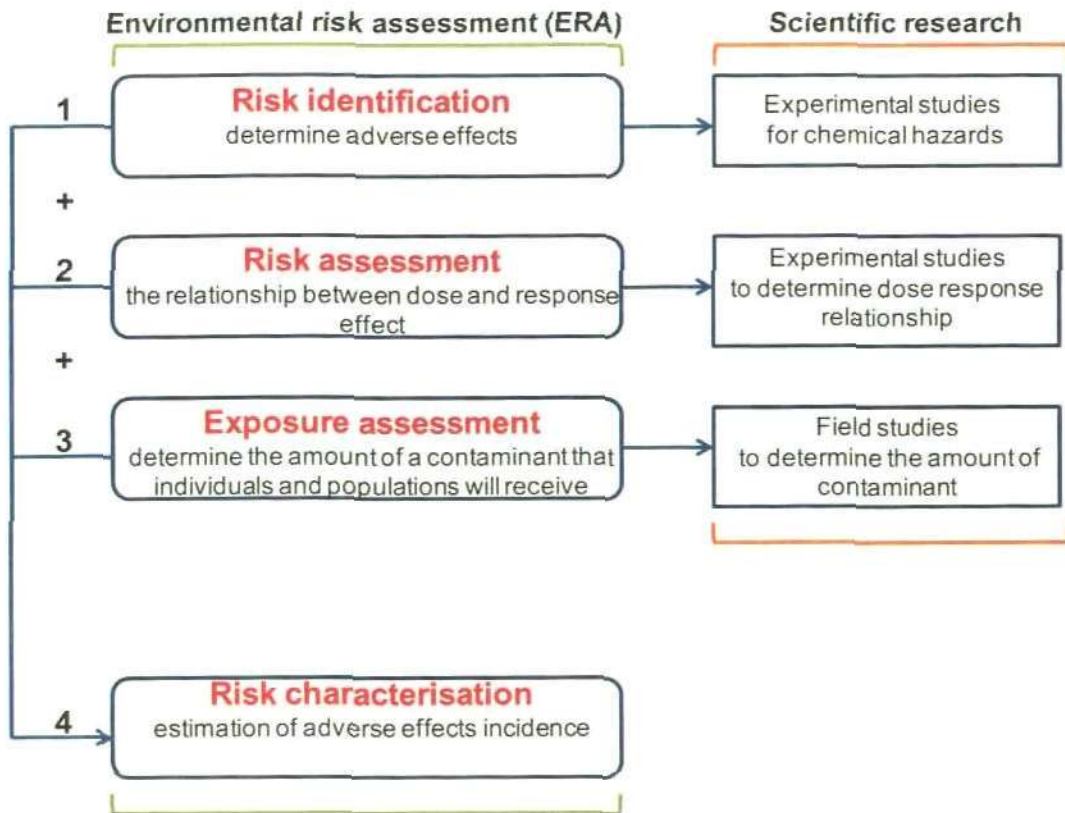


Fig. 8.1 The generalised diagram showing key steps in environmental risk assessment process for chemical substances (modified from IPCS (2001)).

8.1.3 Validation and robustness of the biomarkers

The critical driving force due to acceptance of biomarkers in ERA will depend on its validity and robustness. Validity of biomarkers has been widely discussed (Moore et al. 2004). Validity is a complex laboratory characterisation that describes the best approximation of the truth which should reflect what it purports to indicate in a biological system. To the laboratory scientists, the sensitivity of the assay to identify a dose-response effect, and the ability of the response to be specific for a specific effect are indications of robustness of the biomarker (Moore et al. 2004). But, the scientist needs to know what other external factors that might influence an assay in the field and the reliability of the assay.

The factors that could affect the validity and feasibility of biomarkers could be classified into two groups: internal and external factors. Examples of internal factors that could affect the validity and feasibility of biomarker studies are: confounding factors that could influence marker (physical, chemical and biological factors), lack of dose-response curves between exposure level and marker concentration and individual variability (age, sex and various behavioural factors) in relation to the estimation and specificity to pollutant. In addition, external factors such as sampling time (seasonal variation), number of samples (for accuracy procedures), degree of destructiveness of the sampling procedure, methods of the sample storage, and standardization of the procedure. Only when optimisation at the laboratory has been established, biomarker is ready for use in the full range of environmental research (Huet 2000).

8.1.4 Model organisms for biomarker responses

"Model organisms are those that useful data sets have been already gathered to describe basic biological processes. And they are more amenable to asking certain questions due to their simplicity of structure and features" (Bolker 1995). Ecotoxicological research has relied heavily on model organisms for decades, but other types of research also use these organisms (e.g. biomedical research). Generally, most model organisms share a set of common features that make them amenable to study in the laboratory: (1) short life cycles to enable researchers to monitor the patterns of growth, development and reproductive capacity over many generations; (2) generally small, easy, and inexpensive to maintain under the laboratory conditions, and (3) wide, nearly international, distribution in the ecosystem.

Further than these common features, some model organisms have one or several unique properties that make them ideal for a particular line of research. For instance, zebrafish *Danio rerio*, whose genome has been sequenced now, has a nearly transparent body which provides easy access to visualise the internal anatomy throughout its developmental life. Availability of genomic sequences for some of the aquatic species allows elucidation of mechanistic pathways and response of genes in relation to exposure to different contaminants. Use of these reared organisms has however limited applications in field studies. Under field conditions, apart from mussels, different groups of organisms, at different trophic levels and habitat have been used. They each have different advantages and disadvantages. For example, shore crab, *Carcinus maenas* exhibits characteristic and measurable physiological and behavioural end points during inter-individual competition for resources. Despite

being widely used, blue mussels, *Mytilus edulis* being filter feeders with an open circulatory system, are considered to have relatively low metabolic transformation rates. In addition, mussels are intertidal organisms and might not be exposed to sediment bound contaminants which is the ultimate sink for all the contaminants disposed in the marine environment. It is important that prior to application of biomarker responses in the field condition, they should be properly validated under the laboratory condition, as carried out in the present study. It is also important that these biological responses are optimised and validated in a range of organisms as it is commonly seen that at contaminated sites all the representative organisms are not available (Jha 2004). Our study on marine mussels therefore needs to extend to other environmentally and ecologically relevant organisms such as *Caenorhabditis elegans*.

Given the emphasis on minimising the use of animals (especially vertebrates) in toxicological and ecotoxicological research, for ethical, economic and legal reasons it is important to use *in vitro* studies especially for mechanistic studies. In this context, whilst many cell lines of fish origin are available (e.g. Papis et al., 2011), attempts to grow cells of invertebrate origin have not been very successful (Dixon et al. 2002). This is an area which needs attention especially when mechanism and mode of action of emerging and new chemicals are to be established (ECETOC 2009).

It is important to consider that properties of cells / tissues or organs influence the expression of biomarker responses (Jha 2008). As described in this study, different organs show differential or tissue specific accumulation of contaminants. The inherent properties of the organs need to be linked with specific pathophysiological conditions in the organisms.

8.1.5 Application of integrated approach

The correlation between the biomarker response and the exposure may vary depending on the deposition steps in the organism which comprises rate of absorption, distribution, metabolism, excretion and repair of DNA (Jha et al. 2000). These processes could be influenced by genetic makeup of the individuals in a population. In human health arena, polymorphisms in several genes (e.g. genes involved in metabolism of chemicals, DNA repairs etc.) have been associated with susceptibility to environmental agents and pathophysiological (e.g. development of cancer) conditions. Given that a large number of genes (e.g. oncogenes and anti-oncogenes, DNA repair genes) have been evolutionary conserved (Rotchell et al. 2001), it is likely that the wild organisms would exhibit similar responses as observed in humans. In this context, it is well established that in common with humans, aquatic organisms (e.g. fish and bivalve molluscs) exhibit similar malignancies (Jha, 2004). Given that fundamental mechanisms of many diseases (e.g. cancer) are the same across different groups of organisms, toxicological studies in the aquatic organism, as carried out in the present study could well serve as sentinel and surrogate to human health (Jha, 2004, 2008).

In line with human health arena, the biomarker responses could be divided into (a) biomarker of exposure (b) biomarker of effect and (c) biomarker of susceptibility (Timbrell 1998). Thus a good relationship between exposure and the biomarker responses may not always be observed as the underlying mechanisms could be influenced by various factors. It is therefore important to apply an integrated and holistic approach to establish exposure-response relationship across many levels of biological organisation and in a range of

ecologically relevant species, i.e. multiple biomarkers and multiple species approach (Canty et al. 2009; Regoli et al. 2004).

Pollutants first act by altering their chemistry, structural or functional properties influencing essential or vital cellular functioning. As such, in order to better predict and understand the effects of pollutants on organisms, populations and communities, it is important to establish the effects at lower levels of biological organisation (Owen et al. 2008). Our understanding of these sensitive biochemical, physiological, histological / morphological and behavioural endpoints (biomarkers) (**Fig. 8.2**) can indicate exposure- effect relationships following exposure to pollutants (Depledge and Fossi 1994). While, biomarker responses occurring at lower level take place over much shorter timescales compared to higher levels (i.e. populations and communities), which are considered to be more relevant from ecotoxicological point of view (**Fig. 8.2**). Significant relationships between biomarkers at the lower levels of biological organisation (biochemical) and the individual level (e.g. physiological and behavioural markers) have been demonstrated in the blue mussel *Mytilus edulis* following exposure to the Cu as a model metallic toxicant (chapter 5). We reported significant correlations between increased DNA damage and reduced feeding rate in *M. edulis*. Also in line with our previous findings in chapter 6 and 7, as mentioned earlier, recent studies have highlighted the value of using a suite of biomarkers to allow rapid assessment of exposure and effects to contaminants (Brown et al. 2004; Federici et al. 2007; Kalpaxis et al. 2004).

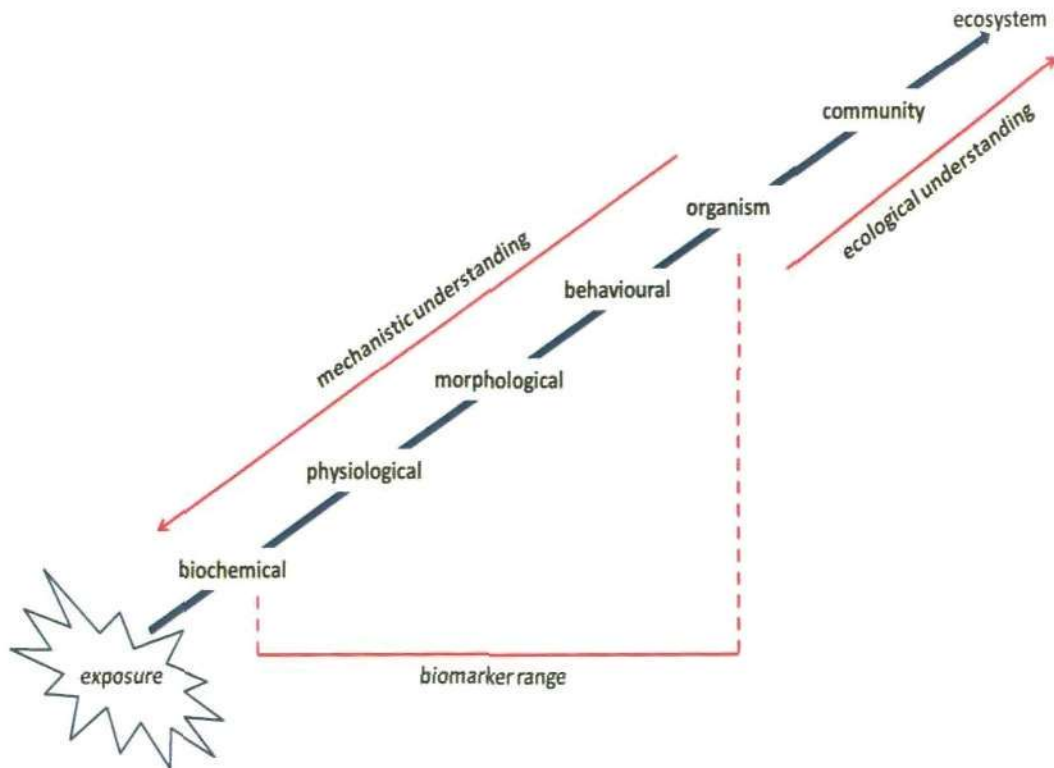


Fig. 8.2 Diagram showing different levels of biological organisation at which potential toxic exposure could affect natural ecosystem.

Overall, the recent advances using multiple biomarker responses following exposure to a range of existing and emerging contaminants supported by our traditional reliance on analytical (chemical) techniques. This collaboration between the two branches of science (biology and chemistry) will ensure that we protect vulnerable environment which has finite capacity to cope with increasing amount and diverse mode of pollutants action, while maintaining the *global economic and industrial growth*. *The present study goes some way towards achieving this goal.*

References

References

- Adams JD, Lauterburg BH, Mitchell JR. 1983. Plasma glutathione and glutathione disulfide in the rat: regulation and response to oxidative stress. *Journal of Pharmacology and Experimental Therapeutics* 227:749-754.
- Aitken RJ, Koopman P, Lewis SEM. 2004. Male germs of concern. *Nature* 432:2-6.
- Akcha F, Izuel C, Venier P, Budzinski H, Burgeot T, Narbonne JF. 2000. Enzymatic biomarker measurement and study of DNA adduct formation in benzo[a]pyrene-contaminated mussels, *Mytilus galloprovincialis*. *Aquatic Toxicology* 49:269-287.
- Al-Subiai SN. 2006. Effects of PAHs on biotransformation enzymes, oxidative stress and DNA-damage in the mussel (*Mytilus edulis*). MRes thesis.
- Al-Subiai SN, Jha AN, Moody AJ. 2009. Contamination of bivalve haemolymph samples by adductor muscle components: implications for biomarker studies. *Ecotoxicology* 18:334-342.
- Al-Subiai SN, Moody AJ, Mustafa SA, Jha AN. In press. A multiple biomarker approach to investigate the effects of copper on the marine bivalve mollusc, *Mytilus edulis*. *Ecotoxicology and Environmental Safety*.
- Anandraj A, Marshall DJ, Gregory MA, McClurg TP. 2002. Metal accumulation, filtration and O₂ uptake rates in the mussel *Perna perna* (Mollusca: Bivalvia) exposed to Hg²⁺, Cu²⁺ and Zn²⁺. *Comparative Biochemistry and Physiology Part C: Toxicology and Pharmacology* 132:355-363.
- Ariese F, Ernst WHO, Sijm DTHM. 2001. *Natural and synthetic organic compounds in the environment-a symposium report*. *Environmental Toxicology and Pharmacology* 10:65-80.
- Arlt VM, Stiborova M, Henderson CJ, Thiemann M, Frei E, Aimova D, Singh R, Gamboa da Costa G, Schmitz OJ, Farmer PB and others. 2008. Metabolic activation of benzo[a]pyrene in vitro by hepatic cytochrome P450 contrasts with detoxification in vivo: experiments with hepatic cytochrome P450 reductase null mice. *Carcinogenesis* 29:656-665.
- ASTM. 1997. *Standard guide for conducting bioconcentration tests with fishes and saltwater bivalve molluscs E-1022-94*. Philadelphia, P.A.: American Society for Testing of Materials.
- Auffret M. 1988. Histopathological changes related to chemical contamination in *Mytilus edulis* from field and experimental conditions. *Marine Ecology Progress Series* 46:101-107.
- Baalousha M, Manciuola A, Cumberland S, Kendall K, Lead J. 2008. Aggregation and surface properties of iron oxide nanoparticles: Influence of pH and natural organic matter. *Environmental Toxicology and Chemistry* 27:1875-1882.
- Barata C, Lekumberri I, Vila-Escalé M, Prat N, Porte C. 2005. Trace metal concentration, antioxidant enzyme activities and susceptibility to oxidative stress in the tricoptera larvae *Hydropsyche exocellata* from the Llobregat river basin (NE Spain). *Aquatic Toxicology* 74:3-19.
- Barbosa JS, Cabral TM, Ferreira DN, Agnez-Lima LF, Batistuzzo de Medeiros SR. 2010. Genotoxicity assessment in aquatic environment impacted by the presence of heavy metals. *Ecotoxicology and Environmental Safety* 73:320-325.

- Barouki R, Morel Y. 2001. Repression of cytochrome P450 1A1 gene expression by oxidative stress: mechanisms and biological implications. *Biochemical Pharmacology* 61:511-516.
- Baun A, Sørensen SN, Rasmussen RF, Hartmann NB, Koch CB. 2008. Toxicity and bioaccumulation of xenobiotic organic compounds in the presence of aqueous suspensions of aggregates of nano-C60. *Aquatic Toxicology* 86:379-387.
- Bayne BL, Widdows J. 1978. The physiological ecology of two populations of *Mytilus edulis* L. *Oecologia* 37:137-162.
- Becker TW, Krieger G, Witte I. 1996. DNA single and double strand breaks induced by aliphatic and aromatic aldehydes in combination with copper (ii). *Free Radical Research* 24:325-332.
- Beg MU, Saeed T, Al-Muzaini S, Beg KR, Al-Bahloul M. 2003. Distribution of petroleum hydrocarbon in sediment from coastal area receiving industrial effluents in Kuwait. *Ecotoxicology and Environmental Safety* 54:47-55.
- Benedetti M, Martuccio G, Fattorini D, Canapa A, Barucca M, Nigro M, Regoli F. 2007. Oxidative and modulatory effects of trace metals on metabolism of polycyclic aromatic hydrocarbons in the Antarctic fish *Trematomus bernacchii*. *Aquatic Toxicology* 85:167-175.
- Bickham JW, Sandhu S, Hebert PDN, Chikhi L, Athwal R. 2000. Effects of chemical contaminants on genetic diversity in natural populations: implications for biomonitoring and ecotoxicology. *Mutation Research/Reviews in Mutation Research* 463:33-51.
- Bignell JP, Dodge MJ, Feist SW, Lyons B, Martin PD, Taylor NGH, Stone D, Travalent L, Stentiford GD. 2008. Mussel histopathology: effects of season, disease and species. 2:1-15.
- Biney C, Amuzu AT, Calamari D, Kaba N, Mbome IL, Naeve H, Ochumba PBO, Osibanjo O, Radegonde V, Saad MAH. 1994. Review of heavy metals in the African aquatic environment. *Ecotoxicology and Environmental Safety* 28:134-159.
- Bolker JA. 1995. Model systems in developmental biology. *BioEssays* 17:451-455.
- Bolognesi C, Landini E, Roggieri P, Fabbri R, Viarengo A. 1999. Genotoxicity biomarkers in the assessment of heavy metal effects in mussels : Experimental studies. *Environmental and molecular mutagenesis* 33:287-292.
- Borja A, Valencia V, Franco J, Muxika I, Bald J, Belzunce MJ, Solaun O. 2004. The water framework directive: water alone, or in association with sediment and biota, in determining quality standards? *Marine Pollution Bulletin* 49:8-11.
- Boxall ABA, Tiede K, Chaudhry Q. 2007. Engineered nanomaterials in soils and water: how do they behave and could they pose a risk to human health? *Nanomedicine* 2:919-927.
- Bremner I. 1998. Manifestations of copper excess. *American Journal of Clinical Nutrition* 67:1069-1073.
- Brown M, Davies IM, Moffat CF, Redshaw J, Craft JA. 2004. Characterisation of choline esterases and their tissue and subcellular distribution in mussel (*Mytilus edulis*). *Marine Environmental Research* 57:155-169.
- Brown RJ, Galloway TS, Lowe D, Browne MA, Dissanayake A, Jones MB, Depledge MH. 2004. Differential sensitivity of three marine invertebrates

- to copper assessed using multiple biomarkers. *Aquatic Toxicology* 66: 267-278.
- Canesi L, Viarengo A. 1997. Age-related differences in glutathione metabolism in mussel tissues. *Comparative Biochemistry and Physiology Part B: Biochemistry and Molecular Biology* 116:217-221.
- Canesi L, Viarengo A, Leonzio C, Filippelli M, Gallo G. 1999. Heavy metals and glutathione metabolism in mussel tissues. *Aquatic Toxicology* 46:67-76.
- Canty MN, Hutchinson TH, Brown RJ, Jones MB, Jha AN. 2009. Linking genotoxic responses with cytotoxic and behavioural or physiological consequences: Differential sensitivity of echinoderms (*Asterias rubens*) and marine molluscs (*Mytilus edulis*). *Aquatic Toxicology* 94:68-76.
- Carballal MJ, Lo'pez MC, Azevedo C, Villalba A. 1997. Hemolymph cell types of the mussel *Mytilus galloprovincialis*. *Diseases of Aquatic Organisms* 29:127-135.
- Cavaliere EL, Rogan EG. 1995. Central role of radical cations in metabolic activation of polycyclic aromatic hydrocarbons. *Xenobiotica* 25:677-688.
- Cheung P-Y, Wang W, Schulz R. 2000. Glutathione protects against myocardial ischemia-reperfusion injury by detoxifying peroxynitrite. *Journal of Molecular and Cellular Cardiology* 32:1669-1678.
- Cheung VV, Depledge MH, Jha AN. 2006. An evaluation of the relative sensitivity of two marine bivalve mollusc species using the Comet assay. *Marine environmental research: pollutant responses in marine organisms PRIMO* 13 62:301-305.
- Choi JE, Kim S, Ahn JH, Youn P, Kang JS, Park K, Yi J, Ryu D-Y. 2010. Induction of oxidative stress and apoptosis by silver nanoparticles in the liver of adult zebrafish. *Aquatic Toxicology* 100:151-159.
- Coles JA, Farley SR, Pipe RK. 1994. Effects of fluoranthene on the immunocompetence of the common marine mussel, *Mytilus edulis*. *Aquatic Toxicology* 30:367-379.
- Collins AR, Cadet J, Möller L, Poulsen HE, Viña J. 2004. Are we sure we know how to measure 8-oxo-7,8-dihydroguanine in DNA from human cells? *Archives of Biochemistry and Biophysics* 423:57-65.
- Correia AD, Costa MH, Luis OJ, Livingstone DR. 2003. Age-related changes in antioxidant enzyme activities, fatty acid composition and lipid peroxidation in whole body *Gammarus locusta* (Crustacea: Amphipoda). *Journal of Experimental Marine Biology and Ecology* 289:83-101.
- Coughlan J. 1969. The estimation of filtering rate from clearance of suspensions. *Marine Biology* 2:356-358.
- Coughlan M, O'Carra P. 1996. The lysopine and octopine dehydrogenase activities of *Mytilus edulis* are catalysed by a single enzyme. *Biochemical Society Transactions* 24:S128.
- Dauberschmidt C, Diestrich DR, Schlatter C. 1997. Esterases in the zebra mussel *Dreissena polymorpha*: activities, inhibition, and binding to organophosphates. *Aquatic Toxicology* 37:295-305.
- de Oliveira Ribeiro CA, Nathalie M-D, Gonzalez P, Yannick D, Jean-Paul B, Boudou A, Massabuau JC. 2008. Effects of dietary methylmercury on zebrafish skeletal muscle fibres. *Environmental Toxicology and Pharmacology* 25:304-309.
- Dean RT, Gieseg S, Davies MJ. 1993. Reactive species and their accumulation on radical-damaged proteins. *Trends in Biochemical Sciences* 18:437-441.

- Degtyarenko KN, Kulikova TA. 2001. Evolution of bioinorganic motifs in P450-containing systems. *Trends in Biochemical Sciences* 29:139-147.
- Deneke SM, Fanburg BL. 1989. Regulation of cellular glutathione. *American Journal of Physiology* 257:163-173.
- Depledge MH, Fossi MC. 1994. The role of biomarkers in environmental assessment (2). Invertebrates. *Ecotoxicology* 3:161-172.
- Devaux A, Fiat L, Gillet C, Bony S. 2011. Reproduction impairment following paternal genotoxin exposure in brown trout (*Salmo trutta*) and Arctic charr (*Salvelinus alpinus*). *Aquatic Toxicology* 101:405-411.
- Dhawan A, Taurozzi JS, Pandey AK, Shan W, Miller SM, Hashsham SA, Tarabara VV. 2006. Stable colloidal dispersions of C₆₀ fullerenes in water: Evidence for genotoxicity. *Environmental Science and Technology* 40:7394-7401.
- Dixon DR, Pruski AM, Dixon LRJ, Jha AN. 2002. Marine invertebrate ecogenotoxicology: a methodological overview. *Mutagenesis* 17:495-507.
- Doyotte A, Cossu C, Jacquin M-C, Babut M, Vasseur P. 1997. Antioxidant enzymes, glutathione and lipid peroxidation as relevant biomarkers of experimental or field exposure in the gills and the digestive gland of the freshwater bivalve *Unio tumidus*. *Aquatic Toxicology* 39:93-110.
- EASW. 2009. Approaches to safe nanotechnology. Managing the health and safety concerns associated with engineered nanomaterials.
- ECETOC. 2009. *Guidance on identifying endocrine disrupting effects*. Brussels.
- Echols KR, Meadows JC, Orazio CE, Gene EL. 2009. Pollution of aquatic ecosystems II: hydrocarbons, synthetic organics, Radionuclides, heavy metals, acids, and thermal pollution. *Encyclopedia of Inland Waters*. Oxford: Academic Press. p 120-128.
- Ellman GL, Courtney KD, Andres V, Featherstone RM. 1961. A new and rapid colorimetric determination of acetylcholinesterase activity. *Biochemical Pharmacology* 7:88-95.
- Ema M, Kobayashi N, Naya M, Hanai S, Nakanishi J. 2010. Reproductive and developmental toxicity studies of manufactured nanomaterials. *Reproductive Toxicology* 30:343-352.
- Emmanouil C, Sheehan TMT, Chipman JK. 2007. Macromolecule oxidation and DNA repair in mussel (*Mytilus edulis* L.) gill following exposure to Cd and Cr(VI). *Aquatic Toxicology* 82:27-35.
- Esterbauer H, Schaur RJ, Zollner H. 1991. Chemistry and biochemistry of 4-hydroxynonenal, malonaldehyde and related aldehydes. *Free Radical Biology and Medicine* 11:81-128.
- EU. 2003. Common implementation strategy for the European water framework directive, guidance document 5, transitional and coastal waters, OPEC. <http://europa.eu.int>. Luxembourg.
- Federici G, Shaw BJ, Handy RD. 2007. Toxicity of titanium dioxide nanoparticles to rainbow trout (*Oncorhynchus mykiss*): Gill injury, oxidative stress, and other physiological effects. *Aquatic Toxicology* 84:415-430.
- Fent K, Bättscher R. 2000. Cytochrome P450A induction potencies of polycyclic aromatic hydrocarbons in a fish hepatoma cell line: demonstration of additive interactions and an induction equivalency concept. *Environmental Toxicology and Chemistry* 19:2047-2058.

- Fernández JL, de la Calle JFV, Tamayo M, Cajigal D, Agarwal A, Gosálvez J. 2009. Sperm DNA integrity and male infertility: current perspectives. *Archives of Medical Science* 5:55–62.
- Feron VJ, Groten JP. 2002. Toxicological evaluation of chemical mixtures. *Food and Chemical Toxicology* 40:825–839.
- Fitzpatrick JL, Nadella S, Bucking C, Balshine S, Wood CM. 2008. The relative sensitivity of sperm, eggs and embryos to copper in the blue mussel (*Mytilus trossulus*). *Comparative Biochemistry and Physiology Part C: Toxicology and Pharmacology* 147:441–449.
- Fujita K, Morimoto Y, Endoh S, Uchida K, Fukui H, Ogami A, Tanaka I, Horie M, Yoshida Y, Iwahashi H and others. 2010. Identification of potential biomarkers from gene expression profiles in rat lungs intratracheally instilled with C₆₀ fullerenes. *Toxicology* 274:34–41.
- Funabara D, Kanoh S, Siegman MJ, Butler TM, Hartshorne DJ, Watabe S. 2005. Twitchin as a regulator of catch contraction in molluscan smooth muscle. *Journal of Muscle Research and Cell Motility* 26:455–460.
- Ga'de G, Grieshaber MK. 1975. A rapid and specific enzymatic method for the estimation of L-arginine. *Analytical Biochemistry* 66:393–399.
- Ga'de G, Grieshaber MK. 1986. Pyruvate reductases catalyze the formation of lactate and opines in anaerobic invertebrates. *Comparative Biochemistry and Physiology Part B* 83:255–272.
- Gaetke LM, Chow CK. 2003. Copper toxicity, oxidative stress, and antioxidant nutrients. *Toxicology* 189:147–163.
- Galloway TS, Millward N, Browne MA, Depledge MH. 2002. Rapid assessment of organophosphorous/carbamate exposure in the bivalve mollusc *Mytilus edulis* using combined esterase activities as biomarkers. *Aquatic Toxicology* 61:169–180.
- Gao JP, Maguhn J, Spitzauer P, Kettrup A. 1998. Distribution of polycyclic aromatic hydrocarbons (PAHs) in porewater and sediment of a small aquatic ecosystem. *International Journal of Environmental Analytical Chemistry* 69:227–242.
- Gelca R, Surowiec K, Anderson TA, Cox SB. 2010. Photolytic breakdown of fullerene C₆₀ cages in an aqueous suspension. *Nanoscience and Nanotechnology* 10:1–5.
- GESAMP. 2007. International Maritime Organisation. Estimates of oil entering the marine environment from sea-based activities. In: Group of Experts on the Scientific Aspects of Marine Pollution (Ed.). International Maritime Organisation. London.
- Gilewicz M, Guillaume JR, Carles D, Leveau M, Bertrand JC. 1984. Effects of petroleum hydrocarbons on the cytochrome P450 content of the mollusc bivalve *Mytilus galloprovincialis*. *Marine Biology* 80:155–159.
- Giustarini D, Milzani A, Dalle-Donne I, Rossi R. 2008. Red blood cells as a physiological source of glutathione for extracellular fluids. *Blood Cells, Molecules and Diseases* 40:174–179.
- Gornall AC, Bardawill, C.J. and David, M.M. 1949. Determination of serum proteins by means of the Biuret reaction. *Journal of Biology and Chemistry*. 177:751–766.
- Gregory MA, Marshall DJ, George RC, Anandraj A, McClurg TP. 2002. Correlations between metal uptake in the soft tissue of *Perna perna* and gill filament pathology after exposure to mercury. *Marine Pollution Bulletin* 45:114–125.

- Grøsvik BE, Jonsson H, Rodríguez-Ortega MJ, Roepstorff P, Goksøyr A. 2006. CYP1A-immunopositive proteins in bivalves identified as cytoskeletal and major vault proteins. *Aquatic Toxicology* 79:334-340.
- Grunewald S, Said TM, Paasch U, Glander HJ, Agarwal A. 2007. Relationship between sperm apoptosis signalling and oocyte penetration capacity. *International Journal of Andrology* 31:325-330.
- Guldi DM, Prato M. 2000. Excited-state properties of C₆₀ fullerene derivatives. *Accounts of Chemical Research* 33:695-703.
- Gustafson LL, Stoskopf MK, Bogan AE, Showers W, Kwak TJ, Hanlon S, Levine JF. 2005. Evaluation of a nonlethal technique for hemolymph collection in *Elliptio complanata*, a freshwater bivalve (Mollusca: Unionidae). *Diseases of Aquatic Organisms* 65:159-165.
- Hagger JA, Atienzar FA, Jha AN. 2005. Genotoxic, cytotoxic, developmental and survival effects of tritiated water in the early life stages of the marine mollusc, *Mytilus edulis*. *Aquatic Toxicology* 74:205-217.
- Hall M, Grover PL. 1990. Polycyclic aromatic hydrocarbon: metabolism, activation and tumor initiation. Grover CaPL, editor. Berlin: Springer-Verlag.
- Halliwell B. 1999. Oxygen and nitrogen are pro-carcinogens. Damage to DNA by reactive oxygen, chlorine and nitrogen species: measurement, mechanism and the effects of nutrition. *Mutation Research/Genetic Toxicology and Environmental Mutagenesis* 443:37-52.
- Halliwell B, Gutteridge JMC. 2007. Free radicals in biology and medicine. New York: Oxford University Press, Oxford.
- Handy RD, Owen R, Valsami-Jones E. 2008. The ecotoxicology of nanoparticles and nanomaterials: current status, knowledge gaps, challenges, and future needs. *Ecotoxicology* 17:315-325.
- Handy RD, Runnalls T, Russell PM. 2002. Histopathologic biomarkers in three spined sticklebacks, *Gasterosteus aculeatus*, from several rivers in Southern England that meet the freshwater fisheries directive. *Ecotoxicology* 11:467-479.
- Hasselöv M, Readman JW, Ranville JF, Tiede K. 2008. Nanoparticle analysis and characterization methodologies in environmental risk assessment of engineered nanoparticles. *Ecotoxicology* 17:344-361.
- Heffernan LM, Winston GW. 1998. Spectral analysis and catalytic activities of the microsomal mixed-function oxidase system of the sea anemone (phylum: Cnidaria). *Comparative Biochemistry and Physiology Part C: Pharmacology, Toxicology and Endocrinology* 121:371-383.
- Heyman D. 1996. Solubility of C₆₀ in alcohols and alkanes. *Carbon* 34:627-631.
- His E, Beiras R, Seaman MNL. 1999. The assessment of marine pollution-bioassays with bivalve embryos and larvae. In: A.J. Southward PAT, Young CM, editors. *Advances in Marine Biology*: Academic Press. p 1-178.
- Hlavica P. 2006. Functional interaction of nitrogenous organic bases with cytochrome P450: A critical assessment and update of substrate features and predicted key active-site elements steering the access, binding, and orientation of amines. *Biochimica et Biophysica Acta (BBA) - Proteins and Proteomics* 1764:645-670.
- Hoeger B, van den Heuvel MR, Hitzfeld BC, Dietrich DR. 2004. Effects of treated sewage effluent on immune function in rainbow trout (*Oncorhynchus mykiss*). *Aquatic Toxicology* 70:345-355.

- Honkoop PJC, Bayne BL, Underwood AJ, Svensson S. 2003. Appropriate experimental design for transplanting mussels (*Mytilus* sp.) in analyses of environmental stress an example in Sydney Harbour (Australia). *Journal of Experimental Marine Biology and Ecology* 197:253–268.
- Huet MC. 2000. OECD Activity on Endocrine Disrupters Test Guidelines Development. *Ecotoxicology* 9:77–84.
- Hutchinson TH, Bögi C, Winter MJ, Owens JW. 2009. Benefits of the maximum tolerated dose (MTD) and maximum tolerated concentration (MTC) concept in aquatic toxicology. *Aquatic Toxicology* 91:197–202.
- Im SC, Waskell L. 2011. The interaction of microsomal cytochrome P450 2B4 with its redox partners, cytochrome P450 reductase and cytochrome b5. *Archives of Biochemistry and Biophysics* 507:144–153.
- Ioannides C. 2007. Bioactivation of chemicals by cytochromes P450. *Environmental Biotechnology* 3:1–9.
- IPCS. 2001. Biomarkers in risk assessment: Validity and validation. Geneva: WHO.
- Jacobsen NR, Pojana G, White P, Moller P, Cohn CA, Korsholm KS. 2008. Genotoxicity, cytotoxicity, and reactive oxygen species induced by single-walled carbon nanotubes and C(60) fullerenes in the FE1-Mutatrade mark Mouse lung epithelial cells. *Environmental and Molecular Mutagenesis* 49:476–487.
- Jaeschke BC, Millward GE, Moody AJ, Jha AN. 2011. Tissue-specific incorporation and genotoxicity of different forms of tritium in the marine mussel, *Mytilus edulis*. *Environmental Pollution* 159:274–280.
- Jha AN. 2004. Genotoxicological studies in aquatic organisms: an overview. *Mutation Research/Fundamental and Molecular Mechanisms of Mutagenesis* 552:1–17.
- Jha AN. 2008. Ecotoxicological applications and significance of the Comet assay. *Mutagenesis* 23:2207–2221.
- Jha AN, Cheung VV, Foulkes ME, Hill SJ, Depledge MH. 2000. Detection of genotoxins in the marine environment: adoption and evaluation of an integrated approach using the embryo-larval stages of the marine mussel, *Mytilus edulis*. *Mutation Research/Genetic Toxicology and Environmental Mutagenesis* 464:213–228.
- Jha AN, Dogra Y, Turner A, Millward GE. 2005. Impact of low doses of tritium on the marine mussel, *Mytilus edulis*: Genotoxic effects and tissue-specific bioconcentration. *Mutation Research/Genetic Toxicology and Environmental Mutagenesis* 586:47–57.
- Jonsson H, Schiedek D, Goksoyr A, Grosvik BE. 2006. Expression of cytoskeletal proteins, cross-reacting with anti-CYP1A, in *Mytilus* sp. exposed to organic contaminants. *Aquatic Toxicology* 78:42–48.
- Ju-Nam Y, Lead JR. 2008. Manufactured nanoparticles: An overview of their chemistry, interactions and potential environmental implications. *Science of the Total Environment* 400:396–414.
- Juhasz AL, Naidu R. 2000. Bioremediation of high molecular weight polycyclic aromatic hydrocarbons: a review of the microbial degradation of benzo[a]pyrene. *International Biodeterioration and Biodegradation* 45:57–88.
- Kadar E, Simmance F, Martin O, Voulvoulis N, Widdicombe S, Mitov S, Lead JR, Readman JW. 2010. The influence of engineered Fe₂O₃ nanoparticles and soluble (FeCl₃) iron on the developmental toxicity

- caused by CO₂-induced seawater acidification. *Environmental Pollution* 158:3490-3497.
- Kadar E, Tarran GA, Jha AN, Al-Subiai SN. 2011. Stabilization of engineered zero-valent nanoiron with Na-acrylic copolymer enhances spermiotoxicity. *Environmental Science and Technology* 45:3245–3251.
- Kalpaxis DL, Theos C, Xaplanteri MA, Dinos GP, Catsiki AV, Leotsinidis M. 2004. Biomonitoring of gulf of Patras, N.Peloponnesus, Greece. Application of a biomarker suite including evaluation of translation efficiency in *Mytilus galloprovincialis* cells. *Environmental Research* 94:211–220.
- Knap A, Dewailly E, Furgal C, Galvin J, Baden D, Bowen RE, Depledge M, Duguay L, Fleming LE, Ford T and others. 2002. Indicators of ocean health and human health: developing a research and monitoring framework. *Environmental Health Perspectives* 110:839–845.
- Kroto HW, Heath JR, O'Brien SC, Curl RF, Smalley RE. 1985. C₆₀: Buckminsterfullerene. *Nature* 318:162.
- Kumaravel TS, Jha AN. 2006. Reliable Comet assay measurements for detecting DNA damage induced by ionising radiation and chemicals. *Mutation Research/Genetic Toxicology and Environmental Mutagenesis* 605:7-16.
- Lacaze E, Geffard O, Bony S, Devaux A. 2010. Genotoxicity assessment in the amphipod *Gammarus fossarum* by use of the alkaline Comet assay. *Mutation Research/Genetic Toxicology and Environmental Mutagenesis* 700:32-38.
- Landsiedel R, Kapp MD, Schulz M, Wiench K, Oesch F. 2009. Genotoxicity investigations on nanomaterials: Methods, preparation and characterization of test material, potential artifacts and limitations—Many questions, some answers. *Mutation Research/Reviews in Mutation Research* 681:241-258.
- Lawrence RA, Burck FB. 1976. Glutathione peroxidase activity in selenium-deficient rat liver. *Biochemical and biophysical research communications* 71:952–958.
- Lead JR, Muirhead D, Gibson CT. 2005. Characterization of freshwater natural aquatic colloids by atomic force microscopy (AFM). *Environmental Science and Technology* 39:6930–6936.
- Lee J, Cho M, Fortner JD, Hughes JB, Kim J. 2009a. Transformation of aggregated C₆₀ in the aqueous phase by UV irradiation. *Environmental Science and Technology* 43:4878–4883.
- Lee JA, Marsden ID, Glover CN. 2009b. The influence of salinity on copper accumulation and its toxic effects in estuarine animals with differing osmoregulatory strategies. *Aquatic Toxicology* 99:65-72.
- Leroy D, Haubruge E, De Pauw E, Thomé JP, Francis F. 2010. Development of ecotoxicoproteomics on the freshwater amphipod *Gammarus pulex*: Identification of PCB biomarkers in glycolysis and glutamate pathways. *Ecotoxicology and Environmental Safety* 73:343-352.
- Lewis C, and Galloway T. 2009. Reproductive consequences of paternal Genotoxin exposure in marine invertebrates. *Environmental Science and Technology* 43:928-933.
- Liebster DC. 1993. The role of metabolism in the antioxidant function of vitamin E. *Critical Reviews in Toxicology* 23:147-169.

- Livingstone DR. 1988. Responses of microsomal NADPH-cytochrome c reductase activity and cytochrome P-450 in digestive glands of *Mytilus edulis* and *Littorina littorea* to environmental and experimental exposure to pollutants. *Marine Biology* 46:37-43
- Livingstone DR. 1991a. Origins and evolution of pathways of anaerobic metabolism in the animal kingdom. *American Zoologist* 31:522-534.
- Livingstone DR. 1991b. Persistent pollutants in marine ecosystems: Persistent pollutants in marine invertebrates C.H. Walker, D.R. Livingstone, editors. Oxford: Pergamon press. p 1-33.
- Livingstone DR. 1996. Cytochrome P-450 in pollution monitoring use of cytochrome P-450 1A (CYP1A) as a biomarker of organic pollution in aquatic and other organisms. Richardson M, editor. London, UK: Taylor and Francis. p 143-160.
- Livingstone DR. 2001. Contaminant-stimulated reactive oxygen species production and oxidative damage in aquatic organisms. *Marine Pollution Bulletin* 42:656-666.
- Livingstone DR, Chipman JK, Lowe DM, Minier C, Pipe RK. 2000. Development of biomarkers to detect the effects of organic pollution on aquatic invertebrates: recent molecular, genotoxic, cellular and immunological studies on the common mussel (*Mytilus edulis* L.). *International Journal of Environment and Pollution* 13:56-91.
- Livingstone DR, Garcia Martinez P, Michel X, Narbonne JF, O'Hara S, Ribera D, Winston GW. 1990. Oxyradical production as a pollution-mediated mechanism of toxicity in the common mussel, *Mytilus edulis* L., and other molluscs functional. *Ecology* 4:415-424.
- Livingstone DR, Kirchin MA, Wiseman A. 1989. Cytochrome P-450 and oxidative metabolism in molluscs. *Xenobiotica* 19:1041-1062.
- Livingstone DR, Pipe RK. 1992. The mussel *Mytilus*: ecology, physiology, genetics and culture. *Developments in aquaculture and fisheries science*. Gosling E, editor. Amsterdam: Elsevier. p 425-64.
- Lopez-Torres M, Perez-Campo R, Cadenas S, Rojas C, Barja GA. 1993. Comparative study of free radicals in vertebrate. Non-enzymatic antioxidants and oxidative stress. *Comparative Biochemistry and Physiology - Part B: Biochemistry and Molecular Biology* 105:757-763.
- Lotufo GR. 1998. Bioaccumulation of sediment-associated fluoranthene in benthic copepods: uptake, elimination and biotransformation. *Aquatic Toxicology* 44:1-15.
- Lowe DM, Pipe RK. 1987. Mortality and quantitative aspects of storage cell utilization in mussels *Mytilus edulis* following exposure to diesel oil hydrocarbons. *Marine Environmental Research* 22:243-251.
- Lowe DM, Soverchia C, Moore MN. 1995. Lysosomal membrane responses in the blood and digestive cells of mussels experimentally exposed to fluoranthene. *Aquatic Toxicology* 33:105-112.
- Luoma S, Rainbow P. 2008. Metal contamination in aquatic environments: science and lateral management. Cambridge: Cambridge University Press.
- Marnett LJ. 1999. Lipid peroxidation--DNA damage by malondialdehyde. *Mutation Research/Fundamental and Molecular Mechanisms of Mutagenesis* 424:83-95.
- McDonald P, Baxter MS, Fowler SW. 1993. Distribution of radionuclides in mussels, winkles and prawns. Part 2. Study of organisms under

- laboratory conditions using alpha-autoradiography. *Journal of Environmental Radioactivity* 18:203-228.
- Meister A, Aderson ME. 1983. Glutathione. *Annual Review of Biochemistry* 52:711-760.
- Mersch J, Morhain E, Mouvet C. 1993. Laboratory accumulation and depuration of copper and cadmium in the freshwater mussel *Dreissena polymorpha* and the aquatic moss *Rhynchostegium riparioides*. *Chemosphere* 27:1475-1485.
- Monari M, Matozzo V, Foschi J, Marin MG, Cattani O. 2005. Exposure to anoxia of the clam, *Chamelea gallina* II: Modulation of superoxide dismutase activity and expression in haemocytes. *Journal of Experimental Marine Biology and Ecology* 325:175-188.
- Moody AJ, Rich PR. 1990. The effect of pH on redox titrations of haem a in cyanide-liganded cytochrome-c oxidase: experimental and modelling studies. *Biochimica et Biophysica Acta (BBA) - Bioenergetics* 1015:205-215.
- Moore MN. 2006. Do nanoparticles present ecotoxicological risks for the health of the aquatic environment? *Environment International* 32:967-976.
- Moore MN, Depledge MH, Readman JW, Leonard DRP. 2004. An integrated biomarker-based strategy for ecotoxicological evaluation of risk in environmental management. *Mutation Research* 552:247-268.
- Moore MN, Readman JAJ, Readman JW, Lowe DM, Frickers PE, Beesley A. 2009. Lysosomal cytotoxicity of carbon nanoparticles in cells of the molluscan immune system: An *in vitro* study. *Nanotoxicology* 3:40-45
- Mori T, Takada H, Ito S, Matsubayashi K, Miwa N, Sawaguchi T. 2006. Preclinical studies on safety of fullerene upon acute oral administration and evaluation for no mutagenesis. *Toxicology* 225:48-54.
- Munoz P, Meseguer J, Esteban MA. 2006. Phenoloxidase activity in three commercial bivalve species. Changes due to natural infestation with *Perkinsus atlanticus*. *Fish and Shellfish Immunology* 20:12-19
- Mustafa SA, Al-Subiai SN, Davies SJ, Jha AN. In press. Hypoxia-induced oxidative DNA damage links with higher level biological effects including specific growth rate in common carp, *Cyprinus carpio* L. *Ecotoxicology* 20: 1455-1466.
- Nadella SR, Fitzpatrick JL, Franklin N, Bucking C, Smith DS, Wood CM. 2009. Toxicity of Cu, Zn, Ni and Cd to developing embryos of the blue mussel (*Mytilus trossolus*) and the protective effect of dissolved organic carbon. *Comparative Biochemistry and Physiology Part C* 149:340-348.
- Nebert DW, Nelson DR, Coon MJ, Estabrook RW, Feyereisen R, Fujii-Kuriyama Y, Gonzalez FJ, Guengerich FP, Gunsalus IC, Johnson EF and others. 1991. The P450 superfamily: update on new sequences, gene mapping, and recommended nomenclature. *DNA Cell Biology* 10:1-14.
- Neff JM. 1985. Polycyclic aromatic hydrocarbons. Washington, DC.: Hemisphere Publishing Corporation. p 416-454.
- Nicholson S. 2003. Cardiac and branchial physiology associated with copper accumulation and detoxication in the mytilid mussel *Perna viridis* (L.). *Journal of Experimental Marine Biology and Ecology* 295:157-171.
- Nor YN. 1987. Ecotoxicity of copper to aquatic biota: a review. *Environmental Research* 43:274-282.
- Nowack B, Bucheli TD. 2007. Occurrence, behavior and effects of nanoparticles in the environment. *Environmental Pollution* 150:5-22.

- Oberdorster E. 2004. Manufactured nanomaterials (Fullerenes, C₆₀) induce oxidative stress in the brain of juvenile largemouth bass. *Environmental Health Perspectives* 112:1058–1062.
- Oberdörster E, Zhu S, Blickley TM, McClellan-Green P, Haasch ML. 2006. Ecotoxicology of carbon-based engineered nanoparticles: Effects of fullerene (C₆₀) on aquatic organisms. *Carbon* 44:1112-1120.
- Ohmiya, Yoshihiro, Wu, Chun; 2010. Composition and a method for suppressing the luminescence intensity decline in a luciferin-luciferase reaction. United States.
- Osman AM, van den Heuvel H, van Noort PCM. 2007. Differential responses of biomarkers in tissues of a freshwater mussel, *Dreissena polymorpha*, to the exposure of sediment extracts with different levels of contamination. *Journal of Applied Toxicology* 27:51-59.
- OSPAR. 2004. OSPAR/ICES Workshop on the evaluation and update of background reference concentrations (B/RCs) and ecotoxicological assessment criteria (EACs) and how these assessment tools should be used in assessing contaminants in water, sediment and biota. Hazardous Substances Series.
- Östling O, Johanson KJ. 1984. Microelectrophoretic study of radiation-induced DNA damages in individual mammalian cells. *Biochemical and Biophysical Research Communications* 123:291-298.
- Owen R, Buxton L, Sarkis S, Toasperm M, Knap A, Depledge M. 2002. An evaluation of hemolymph cholinesterase activities in the tropical scallop, *Euvola (Pecten) ziczac*, for the rapid assessment of pesticide exposure. *Marine Pollution Bulletin* 44:1010–1017.
- Owen R, Galloway TS, Hagger JA, Jones MB, Depledge MH. 2008. Biomarkers and environmental risk assessment: Guiding principles from the human health field. *Marine Pollution Bulletin* 56: 613–619.
- Owens CWI, Belcher RV. 1965. A colorimetric micro-method for the determination of glutathione. *Biochemical Journal* 94:705–711.
- Palmqvist A, Rasmussen LJ, Forbes VE. 2006. Influence of biotransformation on trophic transfer of the PAH, fluoranthene. *Aquatic Toxicology* 80:309-319.
- Pampanin DM, Camus L, Gomiero A, Marangon I, Volpato E, Nasci C. 2005. Susceptibility to oxidative stress of mussels (*Mytilus galloprovincialis*) in the Venice Lagoon (Italy). *Marine Pollution Bulletin* 50:1548-1557.
- Pan LQ, Ren J, Liu J. 2006. Responses of antioxidant systems and LPO level to benzo(a)pyrene and benzo(k)fluoranthene in the haemolymph of the scallop *Chlamys ferrari*. *Environmental Pollution* 141:443–451.
- Papis E, Davies S, Jha A. 2011. Relative sensitivity of fish and mammalian cells to the antibiotic, trimethoprim: cytotoxic and genotoxic responses as determined by neutral red retention, Comet and micronucleus assays. *Ecotoxicology* 20:208-217.
- Parry HE, Pipe RK. 2004. Interactive effects of temperature and copper on immunocompetence and disease susceptibility in mussels (*Mytilus edulis*). *Aquatic Toxicology* 69:311-325.
- Peña-Llopis S, Ferrando MD, Peña JB. 2002. Impaired glutathione redox status is associated with decreased survival in two organophosphate-poisoned marine bivalves. *Chemosphere* 47:485-497.
- Penning TM, Burczynski ME, Hung CF, McCoull KD, Palackal NT, Tsuruda LS. 1999. Dihydrodiol dehydrogenase and polycyclic aromatic hydrocarbon

- activation: generation of reactive and redox active o-quinones. *Chemical Research in Toxicology* 12:1-18.
- Perendija BR, Borkovic SS, Kovacevici TB, Pavlovic SZ, Stojanovic BD, Paunovic MM, Cakic PD, Radojici RM, Pajovic SB, Saicc ZS. 2007. Glutathione dependent enzyme activities in the foot of three freshwater mussel species in the Sava river, Serbia. *Archives of Biological Sciences* 59:169-175.
- Peters LD, Nasci C, Livingstone DR. 1998. Variation in levels of cytochrome P4501A, 2B, 2E, 3A and 4A-immunopositive proteins in digestive gland of indigenous and transplanted mussel *Mytilus galloprovincialis* in Venice Lagoon, Italy. *Marine Environmental Research* 46:295-299.
- Peters LD, O'Hara SCM, Livingstone DR. 1996. Benzo[a]pyrene metabolism and xenobiotic-stimulated reactive oxygen species generation by subcellular fraction of larvae of turbot (*Scophthalmus maximus* L.). *Comparative Biochemistry and Physiology Part C: Pharmacology, Toxicology and Endocrinology* 114:221-227.
- Peters LD, Shaw BJ, Nott M, O'Hara SCM, Livingstone DR. 1999. Development of cytochrome P450 as a biomarker of organic pollution in *Mytilus* sp.: field studies in United Kingdom ('Sea Empress' oil spill) and the Mediterranean Sea *Biomarkers* 4:425 - 441.
- Phillips DH, Arlt VM. 2007. The ³²P-postlabeling assay for DNA adducts. *Nature protocols* 2.
- Phillips DH, Castegnaro M. 1999. Standardization and validation of DNA adduct postlabelling methods: report of interlaboratory trials and production of recommended protocols. *Mutagenesis* 14:301-15.
- Pipe RK, Farley SR, Coles JA. 1997. The separation and characterisation of haemocytes from the mussel *Mytilus edulis*. *Cell and Tissue Research* 289:537-545.
- Pisoni M, Cogotzi L, Frigeri A, Corsi I, Bonacci S, Iacocca A, Lancini L, Mastrototaro F, Focardi S, Svelto M. 2004. DNA adducts, benzo(a)pyrene monooxygenase activity, and lysosomal membrane stability in *Mytilus galloprovincialis* from different areas in Taranto coastal waters (Italy). *Environmental Research* 96:163-175.
- Rainbow PS. 2002. Trace metal concentrations in aquatic invertebrates: Why and so what? *Environmental Pollution* 120:497-507.
- Ramu K, Kajiwara N, Sudaryanto A, Isobe T, Takahashi S, Subramanian A, Ueno D, Zheng GJ, Lam PKS, Takada H and others. 2007. Asian mussel watch program: Contamination status of polybrominated diphenyl ethers and organochlorines in coastal waters of Asian countries. *Environmental Science and Technology* 41:4580-4586.
- Rand GM. 1995. *Fundamentals of aquatic toxicology: Effects, environment fate, and risk assessment* London, UK: Taylor and Francis.
- Reeves JF, Davies SJ, Dodd NJF, Jha AN. 2008. Hydroxyl radicals (OH) are associated with titanium dioxide (TiO₂) nanoparticle-induced cytotoxicity and oxidative DNA damage in fish cells. *Mutation Research/Fundamental and Molecular Mechanisms of Mutagenesis* 640:113-122.
- Regoli F, Frenzilli G, Bocchetti R, Annarumma F, Scarcelli V, Fattorini D, Nigro M. 2004. Time-course variations of oxyradical metabolism, DNA integrity and lysosomal stability in mussels, *Mytilus galloprovincialis*, during a field translocation experiment. *Aquatic Toxicology* 68:167-178.

- Regoli F, Gorbi S, Machella N, Tedesco S, Benedetti M, Bocchetti R, Notti A, Fattorini D, Piva F, Principato G. 2005. Pro-oxidant effects of extremely low frequency electromagnetic fields in the land snail *Helix aspersa*. *Free Radical Biology and Medicine* 39:1620-1628.
- Regoli F, Principato G. 1995. Glutathione, glutathione-dependent and antioxidant enzymes in mussel, *Mytilus galloprovincialis*, exposed to metals under field and laboratory conditions: implications for the use of biochemical biomarkers. *Aquatic Toxicology* 31:143-164.
- Richardson BJ, Mak E, De Luca-Abbott SB, Martin M, McClellan K, Lam PKS. 2008. Antioxidant responses to polycyclic aromatic hydrocarbons and organochlorine pesticides in green-lipped mussels (*Perna viridis*): Do mussels "integrate" biomarker responses? *Marine Pollution Bulletin* 57:503-514.
- Rickwood CJ, Galloway TS. 2004. Acetylcholinesterase inhibition as a biomarker of adverse effect a study of *Mytilus edulis* exposed to the priority pollutant chlorfenvinphos. *Aquatic Toxicology* 67:45-56.
- Rikans LE, Hornbrook KR. 1997. Lipid peroxidation, antioxidant protection and aging. *Biochimica et Biophysica Acta (BBA) - Molecular Basis of Disease* 1362:116-127.
- Rotchell JM, Lee JS, J.K. C, Ostrander GK. 2001. Structure, expression and activation of fish ras genes. *Aquatic Toxicology* 55:1-21.
- Royal Society. 2004. Nanoscience and nanotechnologies: Opportunities and uncertainties. London: The Royal Society.
- Sanders BM, Martin LS, Howe SR, Nelson WG, Hegre ES, Phelps DK. 1994. Tissue-specific differences in accumulation of stress proteins in *Mytilus edulis* exposed to a range of copper concentrations. *Toxicology and Applied Pharmacology* 125:206-213.
- Sayes CM, Fortner JD, Guo W, Lyon D, Boyd AM, Ausman KD, Tao YJ, Sitharaman B, Wilson LJ, Hughes JB and others. 2004. The differential cytotoxicity of water soluble fullerenes. *Nano Letters* 4:1881-1887.
- Schägger H. 2006. Tricine-SDS-PAGE. *Nature Protocols* 1:16-22.
- Schmidt CW. 2009. Nanotechnology-related environmental, health and safety research: Examining the national strategy. *Environmental Health Perspectives* 117:158-161.
- Schwarzenbach RP, Escher BI, Fenner K, Hofstetter TB, Johnson CA, von Gunten U, Wehrli B. 2006. The Challenge of Micropollutants in Aquatic Systems. *Science of the Total Environment* 313:1072-1077.
- Scown TM, van Aerle R, Tyler CR. 2010. Do engineered nanoparticles pose a significant threat to the aquatic environment? *Critical Reviews in Toxicology* 40:653-670.
- Shaw JP, Large AT, Donkin P, Evans SV, Staff FJ, Livingstone DR, Chipman JK, Peters LD. 2004. Seasonal variation in cytochrome P450 immunopositive protein levels, lipid peroxidation and genetic toxicity in digestive gland of the mussel *Mytilus edulis*. *Aquatic Toxicology* 67:325-336.
- Sheir SK, Handy RD, T.S. G. 2010. Tissue injury and cellular immune responses to mercuric chloride exposure in the common mussel *Mytilus edulis*: Modulation by lipopolysaccharide. *Ecotoxicology and Environmental Safety* 73:1338-1344.

- Shi D, Wang W-X. 2004a. Modification of trace metal accumulation in the green mussel *Perna viridis* by exposure to Ag, Cu, and Zn. *Environmental Pollution* 132:265-277.
- Shi D, Wang W-X. 2004b. Modification of trace metal accumulation in the green mussel *Perna viridis* by exposure to Ag, Cu, and Zn. *Environmental Pollution* 132:265-277.
- Silverman H, Lynn JW, Dietz TH. 1996. Particle capture by the gills of *Dreissena polymorpha*: Structure and function of latero-frontal cirri. *Biological Bulletin* 191:42-54.
- Simonet BM, Valcárcel M. 2009. Monitoring nanoparticles in the environment. *Analytical and Bioanalytical Chemistry* 393:17-21.
- Singh N, Manshian B, Jenkins GJS, Griffiths SM, Williams PM, Maffei TGG, Wright CJ, Doak SH. 2009. NanoGenotoxicology: The DNA damaging potential of engineered nanomaterials. *Biomaterials* 30:3891-3914.
- Singh NP, Danner DB, Tice RR, McCoy MT, Collins GD, Schneider EL. 1989. Abundant alkali-sensitive sites in DNA of human and mouse sperm. *Experimental Cell Research* 184:461-470.
- Singh NP, McCoy MT, Tice RR, Schneider EL. 1988. A simple technique for quantitation of low levels of DNA damage in individual cells. *Experimental Cell Research* 175:184-191.
- Singh NP, Muller CH, Berger RE. 2003. Effects of age on DNA double-strand breaks and apoptosis in human sperm. *Fertility and Sterility* 80:1420-1430.
- Sjolin AM, Livingstone DR. 1997. Redox cycling of aromatic hydrocarbon quinones catalysed by digestive gland microsomes of the common mussel (*Mytilus edulis* L.). *Aquatic Toxicology* 38:83-99.
- Sloan J, Dunin-Borkowski RE, Hutchison JL, Coleman KS, Clifford Williams V, Claridge JB, York APE, Xu C, Bailey SR, Brown G and others. 2000. The size distribution, imaging and obstructing properties of C₆₀ and higher fullerenes formed within arc-grown single walled carbon nanotubes. *Chemical Physics Letters* 316:191-198.
- Snape JR, Maund SJ, Pickford DB, Hutchinson TH. 2004. Ecotoxicogenomics: the challenge of integrating genomics into aquatic and terrestrial ecotoxicology. *Aquatic Toxicology* 67:143-154.
- Soegianto A, Charmantier-Daures M, Trilles JP, Charmantier G. 1999. Impact of copper on the structure of gills and epipodites of the shrimp *Penaeus japonicus* (Decapoda). *Journal of Crustacean Biology* 19:209-223.
- Solé M, Livingstone DR. 2005. Components of the cytochrome P450-dependent monooxygenase system and '[NADPH-independent benzo[a]pyrene hydroxylase' activity in a wide range of marine invertebrate species. *Comparative Biochemistry and Physiology Part C* 141:20-31.
- Solé M, Peters LD, Magnusson K, Sjölin A, Grammo A, Livingstone DR. 1998. Responses of the cytochrome P450-dependent monooxygenase and other protective enzyme systems in digestive gland of transplanted common mussel (*Mytilus edulis* L.) to organic contaminants in the Skagerrak and Kattegat (North Sea). *Biomarkers* 3:49-62.
- Sono M, Roach MP, Coulter ED, Dawson JH. 1996. Heme-containing oxygenases. *Chemical Reviews* 96:2841-2887.
- Stegeman JJ. 1985. Benzo[a]pyrene oxidation and microsomal enzyme activity in the mussel (*Mytilus edulis*) and other bivalve mollusc species from the Western North Atlantic. *Marine Biology* 89:21-30.

- Stephensen E, Svavarsson J, Sturve J, Ericson G, Adolfsson-Erici M, Forlin L. 2000. Biochemical indicators of pollution exposure in shorthorn sculpin (*Myoxocephalus scorpius*), caught in four harbours on the southwest coast of Iceland. *Aquatic Toxicology* 48:431-442.
- Sterner O. 1999. *Chemistry, Health and Environment Michigan*: Wiley-VCH. 93.
- Storey KB. 1996. Oxidative stress: Animal adaptations in nature Brazilian. *Journal of Medical and Biological Research* 29:1715-1733.
- Sun T, Xu Z. 2006. Radical scavenging activities of [alpha]-alanine C₆₀ adduct. *Bioorganic and Medicinal Chemistry Letters* 16:3731-3734.
- Sunila I. 1986. Chronic histopathological effects of short-term copper and cadmium exposure on the gill of the mussel, *M. edulis*. *Journal of Invertebrate Pathology* 47:125-142.
- Sunila I. 1988. Acute histological responses of the gill of the mussel, *Mytilus edulis*, to exposure by environmental pollutants. *Journal of Invertebrate Pathology* 52:137-141.
- Taylor R, Parsons JP, Avent AG, Rannard SP, Dennis TJ, Hare JP, Kroto HW, Walton DRM. 1991. Degradation of C₆₀ by light. *Nature* 351:277.
- Tedesco S, Doyle H, Blasco J, Redmond G, Sheehan D. 2010. Exposure of the blue mussel, *Mytilus edulis*, to gold nanoparticles and the pro-oxidant menadione. *Comparative Biochemistry and Physiology Part C: Toxicology and Pharmacology* 151:167-174
- Thompson J, Donkersloot JA. 1992. N-(carboxylalkyl)amino acids: occurrence, synthesis and functions. *Annual Review of Biochemistry* 61:517-554.
- Timbrell JA. 1998. Biomarkers in toxicology. *Toxicology* 129:1-12.
- Timbrell JA. 2000. *Principles of biochemical toxicology*. London, UK: Taylor and Francis.
- Tran D, Moody AJ, Fisher AS, Foulkes ME, Jha AN. 2007. Protective effects of selenium on mercury-induced DNA damage in mussel haemocytes. *Aquatic Toxicology* 84:11-18.
- Trevisan R, Mello DF, Fisher AS, Schuwerack P-M, Dafre AL, Moody AJ. 2011. Selenium in water enhances antioxidant defenses and protects against copper-induced DNA damage in the blue mussel *Mytilus edulis*. *Aquatic Toxicology* 101:64-71.
- Usenko CY, Harper SL, Tanguay RL. 2008. Fullerene C60 exposure elicits an oxidative stress response in embryonic zebrafish. *Toxicology and Applied Pharmacology* 229:44-55.
- USEPA. 2001. Method for assessing the chronic toxicity of marine and estuarine sediment-associated contaminants with the Amphipod *Leptocheirus plumulosus*. Office of science and technology, office of water, Washington, D.C.
- USEPA. 2010. New Nano-specific Regulations Forthcoming from U.S. EPA. USA.
- Valavanidis A, Vlahogianni T, Dassenakis M, Scoullas M. 2006. Molecular biomarkers of oxidative stress in aquatic organisms in relation to toxic environmental pollutants. *Ecotoxicology and Environmental Safety* 64:178-189.
- van Duren LA, Herman PMJ, Sandee AJJ, Heip CHR. 2006. Effects of mussel filtering activity on boundary layer structure. *Journal of Sea Research* 55:3-14.
- Verlecar XN, Jena KB, Chainy GBN. 2008. Seasonal variation of oxidative biomarkers in gills and digestive gland of green-lipped mussel *Perna*

- viridis* from Arabian Sea. Estuarine, Coastal and Shelf Science 76:745-752.
- Vevers WF, Jha AN. 2008. Genotoxic and cytotoxic potential of titanium dioxide (TiO₂) nanoparticles on fish cells in vitro. Ecotoxicology 17:410-420.
- Viarengo A, Zanicchi G, Moore MN, Orunesu M. 1981. Accumulation and detoxication of copper by the mussel *Mytilus galloprovincialis* Lam: A study of the subcellular distribution in the digestive gland cells. Aquatic Toxicology 1:147-157.
- Vlahogianni T, Dassenakis M, Scoullou MJ, Valavanidis A. 2007. Integrated use of biomarkers (superoxide dismutase, catalase and lipid peroxidation) in mussels *Mytilus galloprovincialis* for assessing heavy metals' pollution in coastal areas from the Saronikos Gulf of Greece. Marine Pollution Bulletin 54:1361-1371.
- Walker CH, Hopkin SP, Sibly RM, Peakall DB. 2001. Principles of ecotoxicology. Taylor and Francis Press: London.
- Weinstein JE. 1997. Fluoranthene-induced histological alterations in oysters, *Crassostrea virginica*: Seasonal field and laboratory studies. Marine Environmental Research 43:201-218.
- Wessel N. 2010. Genotoxic and enzymatic effects of fluoranthene in microsomes and freshly isolated hepatocytes from sole (*Solea solea*). PhD thesis 129-148.
- WHO. 1998. Environmental health criteria. In: Copper Geneva: WHO.
- Widdows J. 2001. Bivalve clearance rates: inaccurate measurements or inaccurate reviews and misrepresentation? Marine Ecology Progress Series 221:303-305.
- Widdows J, Donkin P, Brinsley MD, Evans SV, Salkeld PN, Franklin A, Law RJ, Waldock MJ. 1995. Scope for growth and contaminant levels in North Sea mussels *Mytilus edulis* Marine Ecology Progress Series 127:131-148.
- Wild SR, Jones KC. 1995. Polynuclear aromatic hydrocarbons in the United Kingdom environment: A preliminary source inventory and budget. Environmental Pollution 88:91-108.
- Wilson K, Walker J. 2005. Principles and techniques of biochemistry and molecular biology. Ohlenieck K, editor. New York, USA: Cambridge University Press. p 117-124.
- Wootton AN, Herring C, Spry JA, Wiseman A, Livingstone DR, Goldfarb PS. 1995. Evidence for the existence of cytochrome P450 gene families (CYP1A, 3A, 4A, 11A) and modulation of gene expression (CYP1A) in the mussel *Mytilus* sp. Marine Environmental Research 39:21-26.
- Xu A, Chai Y, Nohmi T, Hei TK. 2009. Genotoxic responses to titanium dioxide nanoparticles and fullerene in gpt delta transgenic MEF cells. Particle and Fibre Toxicology 6:1-13.
- Xue W, Warshawsky D. 2005. Metabolic activation of polycyclic and heterocyclic aromatic hydrocarbons and DNA damage: A review. Toxicology and Applied Pharmacology 206:73-93.
- Yan T, Teo LH, Sin YM. 1997. Effects of mercury and lead on tissue glutathione of the green mussel, *Perna viridis* L. Bulletin of Environmental Contamination and Toxicology 58:845-850.
- Yang XY, Edelmann RE, Oris JT. 2010. Suspended C₆₀ nanoparticles protect against short-term UV and fluoranthene photo-induced toxicity, but cause

- long-term cellular damage in *Daphnia magna*. *Aquatic Toxicology* 100:202-210.
- Yawetz A, Manelis R, Fishelson L. 1992. The effects of aroclor 1254 and petrochemical pollutants on cytochrome P450 from the digestive gland microsomes of four species of mediterranean molluscs. *Comparative Biochemistry and Physiology Part C* 103:607-614.
- Zhu S, Oberdörster E, Haasch ML. 2006. Toxicity of an engineered nanoparticle (fullerene, C₆₀) in two aquatic species, *Daphnia* and fathead minnow. *Marine Environmental Research* 62:5-9.
- Zorita I, Ortiz-Zarragoitia M, Soto M, Cajaraville MP. 2006. Biomarkers in mussels from a copper site gradient (Visnes, Norway): An integrated biochemical, histochemical and histological study. *Aquatic Toxicology* 78:109-116.

Appendix I

Published papers

Contamination of bivalve haemolymph samples by adductor muscle components: implications for biomarker studies

Sherain N. Al-Subiai · Awadhesh N. Jha ·
A. John Moody

Accepted: 27 November 2008 / Published online: 14 December 2008
© Springer Science+Business Media, LLC 2008

Abstract Haemolymph samples and haemocytes collected via the adductor muscles of bivalve molluscs are extensively used in ecotoxicological studies. Withdrawal of haemolymph from mussels, *Mytilus edulis*, via the posterior adductor muscle, may lead to contamination with the intracellular contents of adductor myocytes. Lysopine dehydrogenase (LyDH) activity, an adductor myocyte marker, was used to investigate the impact of this potential contamination on levels of total glutathione, glutathione peroxidase (GPx) and acetylcholinesterase (AChE) measured in cell-free haemolymph. The mean glutathione content of cell-free haemolymph from 28 mussels was $3.2 \pm 1.8 \mu\text{M}$ (mean \pm SD). There was a linear relationship (slope = $0.28 \pm 0.03 \text{ min}$; mean \pm SE; $P < 0.0001$, $n = 28$) with haemolymph LyDH levels suggesting that at least some of the glutathione measured in cell-free haemolymph had arisen from contamination. Haemolymph LyDH activity was significantly higher in samples extracted using larger diameter needles, and also in samples where there had been some difficulty in the extraction. Exposure of mussels to oxidative stress using $40 \mu\text{g l}^{-1} \text{ Cu}$ for 5 days resulted in a 1.7 fold increase in glutathione ($P = 0.033$), but no increase ($P = 0.810$) in LyDH activity in adductor muscle. This was reflected in a similar increase in the slope of a plot of cell-free haemolymph glutathione versus LyDH activity ($P = 0.011$), consistent with both of these having originated from the adductor muscle. Cell-free haemolymph GPx and AChE activities also correlated with LyDH activity (Spearman rank correlation coefficients of

0.531 ($P = 0.0068$) and 0.537 ($P = 0.0062$), respectively, $n = 27$) suggesting that these also arise from contamination of the haemolymph. For GPx there was a significant linear relationship ($P = 0.025$) with haemolymph LyDH levels consistent with both enzymes originating from the myocytes. However, there was hyperbolic relationship ($P = 0.0004$) between haemolymph AChE and LyDH activities. It appears that this is because the AChE originates from a different compartment to the LyDH, i.e. cholinergic neuromuscular junctions in the adductor muscle. We conclude that it would be prudent, when considering the possibility of using a biomarker in cell-free haemolymph from bivalve molluscs, to check whether contamination could be an issue.

Keywords Opine dehydrogenase · Haemolymph · *Mytilus edulis* · Glutathione · Glutathione peroxidase · Acetylcholinesterase · Biomarkers · Copper

Introduction

The haemolymph of bivalve molluscs, like mammalian blood, is an attractive tissue to use in assessing biomarker responses to environmental stressors, such as hypoxia (Monari et al. 2005), parasite infestation (Muñoz et al. 2006), radionuclides (Jha et al. 2005), metals (Tran et al. 2007) and organic pollutants (Galloway et al. 2002; Pan et al. 2006; Rickwood and Galloway 2004). Both haemocytes and cell-free haemolymph (plasma) have been used in such investigations, e.g. haemocytes, for the assessment of DNA damage using single cell gel electrophoresis or Comet assay (Dixon et al. 2002; Jha et al. 2005; Jha 2008) or cell-free haemolymph, for the assessment of acetylcholinesterase levels (Galloway et al. 2002). The advantages of haemocytes over

S. N. Al-Subiai · A. N. Jha · A. J. Moody (✉)
Ecotoxicology and Stress Biology Research Centre, School of
Biological Sciences, University of Plymouth, Drake Circus,
Plymouth PL4 8AA, UK
e-mail: jm.moody@plymouth.ac.uk

cells from other tissues, such as gill tissue, for genotoxicological studies have been discussed by Dixon et al. (2002). Haemolymph is simple to extract via either the posterior or anterior adductor muscles, and there is the possibility of non-destructive sequential sampling of haemolymph from the same individuals, at least for some species (Gustafson et al. 2005; Owen et al. 2002; Dixon et al. 2002), which may help to elucidate toxicokinetic mechanisms.

In rats oxidative stress induced by exposure to reactive oxygen species (ROS) (e.g. *t*-butyl hydroperoxide), or ROS generators (e.g. diquat) causes an increase in plasma glutathione levels through excretion of oxidised glutathione by the liver (Adams et al. 1983). In contrast, acetaminophen or diethyl maleate, which cause oxidative stress by depletion of hepatic glutathione, cause a decrease in plasma glutathione. In mammals, contamination of plasma with glutathione from the lysis of red blood cells is a potential problem (Giustarini et al. 2008). However, this source of contamination is much less of an issue in bivalve haemolymph, where there is no equivalent to red blood cells, and where the abundance of haemocytes is low (Carballal et al. 1997; Pipe et al. 1997). Hence, the possibility of using glutathione levels in the cell-free component of bivalve haemolymph as an indication of 'global' oxidative stress, in an analogous way to that used by Adams et al. (1983) in rats, is particularly appealing.

However, during preliminary work aimed at testing this idea we found that total glutathione levels in the cell-free haemolymph of the blue mussel, *Mytilus edulis*, were highly variable. This led us to investigate whether the cell-free haemolymph could be being contaminated with glutathione derived from the adductor muscle through which it was extracted. To address this issue we used an opine dehydrogenase activity (lysopine dehydrogenase) as an intracellular marker (Gäde and Grieshaber 1986). We also investigated whether glutathione peroxidase and acetylcholinesterase activities, which have previously been measured in cell-free haemolymph, as part of ecotoxicological studies, could also arise from contamination of the haemolymph from compartments within the adductor muscle. This clearly has implications with respect to the interpretation of these measurements.

Materials and methods

All reagents were obtained from Sigma-Aldrich (Poole, UK.) unless otherwise stated.

Animal collection and maintenance

Mussels (*Mytilus edulis*) of similar shell length (51–58 mm) were collected at low tide from Port Quin or

Trebarwith Strand (Cornwall, UK), relatively clean sites. After collection they were immediately transported to the laboratory in a cool box (less than 2 h) and placed in aerated tanks with filtered (<10 µm) seawater (three animals/2 l), where they were kept at 15°C, and fed daily with micro algae (*Isochrysis galbana*, Liquifry, Interpet, Dorking, UK). The water was changed each day. At least 14 days were allowed for the mussels to acclimatise before use in experiments. In no cases were spawning animals used in experiments.

Extraction of haemolymph: method 1

To access the posterior adductor muscle, the valves were prised slightly apart approximately midway towards the posterior from the byssus by using a fixed blade knife. During this process the mussel was held with the posterior upwards, and with the anterior resting on a bed of paper towel, so that as the valves were prised apart any seawater would drain and be absorbed by the paper. This ensured that there was no possibility of accidentally drawing up seawater from a reservoir trapped by the valves. Haemolymph was withdrawn from the posterior adductor muscle using a 1 ml syringe fitted with a 21 gauge needle except where otherwise stated. Samples were centrifuged at 60g_{av} in a microfuge for 2 min to remove the haemocytes (pellet); the cell-free haemolymph (supernatant) was then either placed on ice until use, for opine dehydrogenase and glutathione peroxidase measurements, or stored at -80°C, for acetylcholinesterase activity and total glutathione level measurements.

Extraction of haemolymph: method 2

An alternative method for extracting haemolymph was also used in which a small notch was made across both valves using a 1 mm wide file. The notch (<1 mm in length) was made adjacent to the location of the posterior adductor, but sufficiently far from it (1–2 mm) so that it was not damaged by the file. Haemolymph was then extracted using a 21 gauge needle as described above.

Preparation of adductor muscle extract

The posterior adductor muscles from mussels were dissected out and were homogenised using a modification of the method of Livingstone (1988) by grinding with acid-washed sand (0.05 g) in Eppendorf tubes with ice-cold extraction buffer (20 mM Tris-chloride, pH 7.6, containing 0.15 M KCl, 0.5 M sucrose, 1 mM EDTA and protease inhibitor cocktail [Sigma-P2714; reconstituted and used according to manufacturer's instructions], and freshly supplemented with 1 mM DTT). A ratio of 3:1 of

extraction buffer was used. In cases where total glutathione was to be measured in the extract, the DTT was omitted from the extraction buffer. The crude homogenate was centrifuged for 35 min ($10,500g_{20}$ at 4°C) after which the supernatant was separated and either used immediately or stored at -80°C until use.

Exposure of mussels to copper

Forty-eight mussels (*Mytilus edulis*) were divided between six 8 l tanks (eight mussels per tank) of sea water. Mussels in three of these tanks were exposed to $40 \mu\text{g l}^{-1}$ Cu, by adding $\text{CuSO}_4 \cdot 5\text{H}_2\text{O}$, the other three tanks were used as controls. The exposure to copper was maintained for 5 days during which time the water was replaced daily, with the fresh water being re-dosed with $\text{CuSO}_4 \cdot 5\text{H}_2\text{O}$. The water in the control tanks was also replaced daily. Before replacing the water the tanks were checked for mortalities and any dead animals were removed; there were four dead mussels in the Cu-containing tanks, and none in the control tanks. The mussels were not fed throughout the exposure period.

This concentration and duration of exposure were chosen on the basis of published data on the genotoxic (micronucleus and alkaline elution methods) effects of Cu on the closely related species *Mytilus galloprovincialis* (Bolognesi et al. 1999); we have also found that $40 \mu\text{g l}^{-1}$ Cu is genotoxic (Comet assay) in *M. edulis*, but with no mortality, whereas $100 \mu\text{g l}^{-1}$ Cu caused complete mortality (unpublished data).

At the end of the exposure, haemolymph was extracted from each mussel using method 1 described above, and the total glutathione and lysopine dehydrogenase activity in each sample measured (see below), except for two control mussels, where insufficient haemolymph was extracted. The posterior adductor muscle was then dissected from each mussel, and adductor muscle extracts were prepared as described above. For this, adductor muscles from 3 to 4 mussels were pooled together; this meant that two extracts were prepared per tank. Total glutathione and lysopine dehydrogenase activity were also measured in these extracts.

Measurement of biochemical parameters

All biochemical parameters were measured in triplicate in a microplate reader (Optimax, Molecular Devices, Sunnyvale, CA, USA) using 96 well plates. The assay temperature in each case was $20\text{--}22^{\circ}\text{C}$.

Measurement of total glutathione

The total glutathione (i.e. reduced, GSH, and oxidised, GSSG) content of cell-free haemolymph was determined

essentially according to the method of Adams et al. (1983) which is based on the method of Owens and Belcher (1965). It is important to note that although Owens and Belcher (1965) used an acid deproteination step when preparing their samples, this was shown by Adams et al. (1983) to be unnecessary. We followed their example (a) because there is no interference from protein thiols using this method (Owens and Belcher 1965), and (b) because there was no need to prevent oxidation of GSH, since total glutathione was being measured. Samples were treated with DTNB by mixing them at a 1:1 ratio with buffered DTNB (10 mM DTNB in 100 mM potassium phosphate, pH 7.5, containing 5 mM EDTA). One hundred millimolar potassium phosphate ($210 \mu\text{l}$), pH 7.5, containing 5 mM EDTA and glutathione reductase (0.6 U, Sigma G-3664 from *Saccharomyces cerevisiae*), and $40 \mu\text{l}$ of DTNB-treated samples were mixed. After equilibration for 1 min the reaction was started by the addition of $60 \mu\text{l}$ of 1 mM NADPH. The decrease in absorbance at 412 nm was measured over 5 min. A linear relationship between rate of decrease of A_{412} and glutathione concentration was found using a range of GSH standards up to $20 \mu\text{M}$. However, routinely the glutathione contents of six samples at a time were measured along with a $20 \mu\text{M}$ GSH standard and a $0 \mu\text{M}$ blank, all in triplicate, using three columns in a 96-well plate. By using an eight-channel pipettor to add the NADPH there was synchrony between the sample assays, and the standard and the blank in each column.

Measurement of opine dehydrogenase (ODH) activity

The activity of ODH was measured essentially as described in the Sigma-Aldrich protocol for octopine dehydrogenase (Gäde and Grieshaber 1975) except that the assay pH was 7.5 rather than 6.5 (to decrease the background rate of autooxidation of NADH) and the L-arginine was replaced with different amino acid substrates. The complete assay mixture contained 50 mM potassium HEPES buffer, pH 7.5, containing 169 μM NADH, 4.8 mM amino acid (neutralised) and 4.5 mM sodium pyruvate. The sample, either $50 \mu\text{l}$ of cell-free haemolymph or $50 \mu\text{l}$ of adductor muscle extract (diluted appropriately with extraction buffer), was added to $250 \mu\text{l}$ of assay mixture, and the rate of decrease of absorbance at 340 nm (oxidation of NADH) was measured for 30 min. It is important to use fresh samples for these measurements as we found that storage at -80°C for 1 week introduced a lag in oxidation of NADH, and even after maximal rates were achieved these were substantially lower (around 8%) than those seen with fresh samples (data not shown).

Measurement of glutathione peroxidase (GPx) activity

GPx activity, using H_2O_2 as a substrate, was assayed by following the rate of oxidation of NADPH at 340 nm in the

coupled reaction catalysed by glutathione reductase (Lawrence and Burck 1976), as described by Tran et al. (2007), with the exception that either cyanide or azide was included here. Just before assay, a mixture containing 50 mM potassium HEPES buffer, pH 7.5, 1 mM EDTA, 0.13 mM NADPH, either 0.1 mM sodium cyanide or sodium azide, 1.1 U/ml glutathione reductase and 1 mM GSH was prepared. 290 μ l of this mixture and 15 μ l of cell-free haemolymph were mixed and the reaction was started by addition of 5 μ l of 12.4 mM H_2O_2 . The absorbance decrease was monitored for 5 min.

Measurement of acetylcholinesterase (AChE) activity

The AChE activity was determined in cell-free haemolymph using a modification of the colorimetric method of Ellman et al. (1961) as described by Galloway et al. (2002). Cell-free haemolymph (15 μ l) was incubated for 5 min with 280 μ l of buffered DTNB (270 μ M in 50 mM potassium phosphate, pH 7.5). The AChE-catalysed reaction was then started by addition of the 6 μ l of 3 mM acetylthiocholine iodide (ATCI), and was monitored by measuring the rate of increase of the absorbance at 412 nm, over 5 min.

Determination of protein

The total protein in cell-free haemolymph was determined spectrophotometrically using a commercial kit (BioRad) with bovine serum albumin as the standard.

Statistical analyses

Statistical analyses were performed using Statgraphics plus version 5.1 (Statistical Graphics Corp) and SigmaPlot 10.0 (Systat Software Inc.). Statistical significance is defined as $P < 0.05$ throughout unless otherwise stated.

Results and discussion

Measurements of glutathione levels in cell-free haemolymph

Initial results for the total glutathione (GSH and GSSG) content in mussel haemolymph showed considerable inter-individual variation ($3.2 \pm 1.8 \mu$ M, mean \pm SD, $n = 28$). A possible explanation for this is that the haemolymph was becoming more or less contaminated with intracellular glutathione depending on the amount of damage caused to the adductor muscle during extraction of the haemolymph. To test this hypothesis we measured the activity of an opine dehydrogenase, as a marker of cell damage. Opine dehydrogenases (also known as pyruvate reductases) are

functionally analogous to lactate dehydrogenase, which is almost absent in *Mytilus edulis* (Gäde and Grieshaber 1986, Livingstone 1991, Thompson and Donkersloot 1992). Their role is clearly intracellular, where they catalyse the reductive condensation of pyruvate with an amino acid to generate an opine (an imino acid derivative) with the concomitant regeneration of cytosolic NAD^+ , thereby allowing glycolytic ATP generation to be maintained under hypoxic conditions.

Several opine dehydrogenase activities have been reported in *M. edulis*. For example, octopine, alanopine and strombine dehydrogenases (Gäde and Grieshaber 1986, Livingstone 1991, Thompson and Donkersloot 1992), where the amino acid substrates are L-arginine, L-alanine and glycine, respectively; and lysopine dehydrogenase (Coughlan and O'Carra 1996), where the amino acid substrate is L-lysine. An experiment was carried out to find out which of these amino acid substrates gave the highest activity in adductor muscle extracts from *M. edulis* (Fig. 1). The activity with the five amino acids tested was ranked as follows: L-lysine > L-arginine >> glycine > L-alanine. No activity was observed with L-histidine (Fig. 1). Coughlan and O'Carra (1996) found that a single enzyme in *M. edulis* was responsible for both lysopine (L-lysine) and octopine (L-arginine) dehydrogenase activities, and that both substrates gave similar maximal activities. We found higher

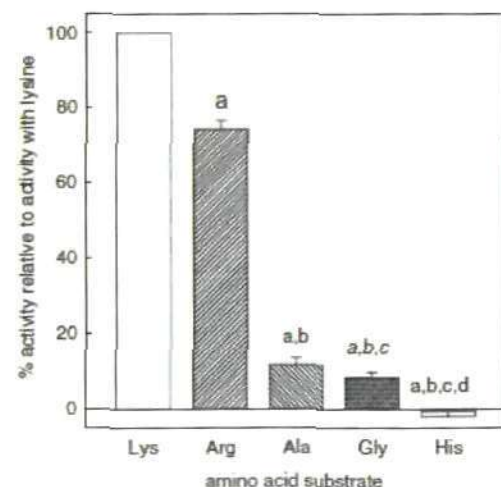


Fig. 1 Relative opine dehydrogenase activity in extracts from *Mytilus edulis* posterior adductor muscle. Activities are expressed as percentages relative to the activity with lysine as substrate (i.e. lysopine dehydrogenase activity) for the same extract. The data shown are means \pm SE, $n = 4$. In each case the activity in the absence of the amino acid substrate (1.5 ± 0.4 nmol NADH oxidised $\text{min}^{-1} \text{mg}^{-1}$ protein) was subtracted. Lysopine dehydrogenase activity was 27.2 ± 5.5 nmol NADH oxidised $\text{min}^{-1} \text{mg}^{-1}$ protein

activity with L-lysine than with L-arginine, this could be attributed to our using different assay conditions (pH and substrate concentrations) to those used by Coughlan and O'Carra (1996). It was decided to use L-lysine as the substrate, i.e. to measure NAD-dependent D-lysopine dehydrogenase (LyDH) activity as a marker to detect intracellular contamination of cell-free haemolymph by intracellular material from myocytes.

In the same haemolymph samples that we earlier measured glutathione levels in, we found a significant ($P < 0.0001$) linear relationship (slope = 0.28 ± 0.03 min; mean \pm SE) between glutathione levels and LyDH activity (Fig. 2). There are two explanations for this: either levels of glutathione and LyDH activity in cell-free haemolymph are co-regulated, or, more likely, some of the supposed haemolymph glutathione comes, along with LyDH activity, from an intracellular source. It seems reasonable to suppose that this co-release of glutathione and LyDH comes from damage caused to the adductor myocytes during the extraction. Extrapolation to zero LyDH activity gives a value for cell-free haemolymph glutathione (0.74 ± 0.29 μ M, mean \pm SE) which though low is significantly greater than zero ($P = 0.0169$) (Fig. 2). Note, however, that this was not always seen (see Fig. 3, for example).

It should be emphasised that we cannot be certain that LyDH activity is absent in mussel haemolymph in the absence of damage to the adductor muscle, although, as noted above, it is clearly an intracellular enzyme, and so would not be expected to be found in the cell-free

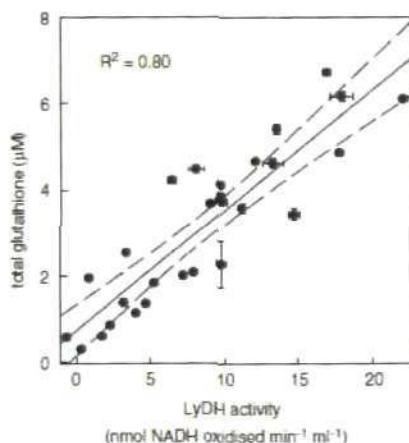


Fig. 2 Relationship between the glutathione content of cell-free haemolymph and lysopine dehydrogenase activity. The solid line is a linear regression, and the dashed lines represent 95% confidence limits. Each point represents an individual cell-free haemolymph sample; the error bars indicate the variability of the measurements (\pm SE, $n = 3$).

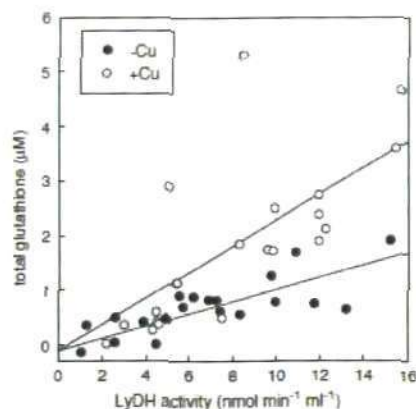


Fig. 3 Relationship between the glutathione content of cell-free haemolymph and lysopine dehydrogenase activity in mussels either exposed to $40 \mu\text{g l}^{-1}$ Cu (\circ) or not (\bullet). The lines show linear regressions derived from GLM analysis of the data where the model included the effects of LyDH ($P < 0.00005$) and the interaction between LyDH and Cu on total glutathione ($P = 0.0001$). The effect of Cu was omitted from the model because it was not significant (see text).

component of haemolymph. Nevertheless, we have often found cell-free haemolymph samples where LyDH activity is below the detection limit of the assay, consistent with it normally being absent from this compartment.

If we are correct that much of the LyDH activity and glutathione detected in the cell-free haemolymph arises from contamination by the contents of damaged adductor myocytes then LyDH activity and glutathione levels should be much higher in adductor muscle. This was investigated by extracting haemolymph from six mussels, after which the posterior adductor muscle was dissected out and extracts prepared (see "Materials and methods"). The total glutathione content and LyDH activities were then measured in both the cell-free haemolymph and the adductor muscle extracts. (N.B. the following experimental values are means \pm SE, $n = 6$.) The adductor muscle extracts contained $2,353 \pm 278$ $\text{nmol min}^{-1} \text{g}^{-1}$ LyDH activity and 131 ± 10 nmol g^{-1} glutathione. These are equivalent to intracellular concentrations in excess of $2,353$ $\text{nmol min}^{-1} \text{ml}^{-1}$ and 131 μM , respectively, both >100 fold higher than the concentrations, 13.8 ± 4.0 $\text{nmol min}^{-1} \text{ml}^{-1}$ and 1.20 ± 0.31 μM , respectively, found in cell-free haemolymph from the same mussels.

It seems likely that turbulence when extracting the haemolymph might increase the contamination by glutathione and LyDH from adductor myocytes, and that variation in the amount of turbulence might lead to variation in the level of contamination. A more significant

factor, however, might be the process of forcing the valves slightly apart in order to gain access to the posterior adductor muscle, given the catch phenomenon shown by mollusc adductor muscles (Funabara et al. 2005). In order to investigate these factors we carried out two experiments. In the first, haemolymph was extracted from mussels using different sized hypodermic needles and a record was made of whether or not there was any difficulty in extracting the haemolymph, e.g. a temporary vacuum in the syringe and/or air bubbles being drawn at the same time as the haemolymph. In the second experiment we tried an alternative method of gaining access to the adductor muscle, i.e. by using a file to make a small notch in the valves rather than forcing them apart (see "Materials and methods").

The haemolymph LyDH activity data from the first experiment was analysed using 2-way ANOVA. There was no significant interaction between needle size and difficulty of extraction ($P = 0.160$), so this was omitted from the model. LyDH activities in haemolymph extracted using 19 gauge (outer diameter, 1.07 mm), 21 gauge (outer diameter, 0.82 mm) and 27 gauge (outer diameter, 0.41 mm) needles were 17.9 ± 2.3 , 11.5 ± 2.3 and 11.0 ± 2.3 nmol $\text{min}^{-1} \text{ml}^{-1}$, respectively (mean \pm SE, $n = 8$ in each case). The effect of needle size on haemolymph LyDH was significant at the 90% confidence level ($P = 0.080$); multiple range tests (LSD) showed a significant differences at the 95 and 90% confidence levels, respectively, between the LyDH activities in haemolymph extracted using the largest (19 gauge) and smallest (27 gauge) needles, and the largest and middle-sized (21 gauge) needles. LyDH activity was higher (16.8 ± 1.9 nmol $\text{min}^{-1} \text{ml}^{-1}$, $n = 11$) in haemolymph extracted with difficulty (see above) compared to that in haemolymph where there was no difficulty in the extraction (10.1 ± 1.8 nmol $\text{min}^{-1} \text{ml}^{-1}$, $n = 13$). This effect was significant at the 95% confidence level ($P = 0.021$).

In the second experiment the LyDH activity obtained using the 'file' method was lower than in cell-free haemolymph obtained using the 'standard' method, on the same day (4.1 ± 0.7 nmol $\text{min}^{-1} \text{ml}^{-1}$, $n = 9$ versus 5.7 ± 0.9 nmol $\text{min}^{-1} \text{ml}^{-1}$, $n = 7$). However, the difference was not statistically significant ($P = 0.169$, Mann-Whitney U test). Overall these data suggest that increased needle size and turbulence during extraction contribute to contamination of the haemolymph with LyDH (and by implication with other adductor muscle components), whereas forcing the valves apart to the limited extent needed for the extraction does not.

The effect of copper exposure on glutathione levels detected in cell-free haemolymph

Despite the evidence for contamination of cell-free haemolymph with glutathione from adductor myocytes there

was still the possibility that this could be corrected for by also measuring LyDH activity, and hence that the effect of oxidative stress on haemolymph glutathione could be determined. Mussels were therefore exposed to copper, which is a well known cause of oxidative stress (e.g. Gaetke and Chow 2003). If oxidative stress were to lead to oxidation of glutathione and excretion of oxidised glutathione into the haemolymph then we might expect that the y -intercept in a plot of total glutathione against LyDH activity would be significantly elevated. To test this, mussels were exposed to $40 \mu\text{g l}^{-1}$ Cu for 5 days as described in "Materials and methods".

Figure 3 shows the relationship between total glutathione and LyDH activity in cell-free haemolymph from mussels exposed to $40 \mu\text{g l}^{-1}$ Cu compared to that from control mussels. This data was analysed using a general linear model, with glutathione as the dependent variable, presence or absence of Cu as a categorical variable, and LyDH activity as a continuous variable. In graphical terms this analysis shows (a) that there is a significant linear relationship between total glutathione and LyDH activity in the cell-free haemolymph, both from mussels that were exposed to Cu and those that were not ($P < 0.00005$); (b) that there is a significant effect of Cu exposure on the slope of the linear relationship between glutathione and LyDH activity ($P = 0.0111$); and (c) that there is no significant effect of Cu exposure on the value of the y -intercept ($P = 0.466$).

These data are inconsistent with the idea that 'global' oxidative stress in mussels might lead to excretion of glutathione into the haemolymph. In fact, in this case, in contrast to the data in Fig. 2, there is no evidence for a 'basal' level of glutathione in the haemolymph, since the y -intercept is not significantly different to zero. However, since Cu exposure affected the slope of the relationship between glutathione and LyDH activity, this suggests that Cu exposure has caused an increase in the levels of glutathione in the adductor muscle (which is, in turn, reflected in an increased level of contamination of the haemolymph samples by glutathione from the adductor myocytes). This was found to be the case: at $169 \pm 13 \mu\text{M}$ (mean \pm SE) the glutathione content of adductor muscle from mussels exposed to copper was significantly higher ($P = 0.033$, t test) than in control mussels, $101 \pm 17 \mu\text{M}$. In contrast, there was no difference in LyDH activity in adductor muscle from the two groups of mussels ($P = 0.810$, t test): $2.53 \pm 0.32 \mu\text{mol min}^{-1} \text{g}^{-1}$ for Cu exposed mussels, and $2.63 \pm 0.19 \mu\text{mol min}^{-1} \text{g}^{-1}$ for control mussels. In all cases here $n = 3$ since there were three tanks of mussels exposed to Cu and three tanks of control mussels. For each tank two extracts were prepared from pooled adductor muscles, and the mean glutathione contents and LyDH activities for each of these pairs of extracts were used in the statistical analysis.

Measurements of glutathione peroxidase and acetylcholinesterase in cell-free haemolymph

Given the apparent impact of intracellular contamination on cell-free haemolymph glutathione levels, the question arose as to whether damage caused during haemolymph extraction from the adductor muscle could influence the levels of other biochemical parameters commonly measured in mussel haemolymph. Hence, an experiment was undertaken to investigate two enzymes often used in ecotoxicological studies as biomarkers: glutathione peroxidase (GPx) and acetylcholinesterase (AChE). The activities of these enzymes together with LyDH activity and protein content were measured in 27 samples of cell-free haemolymph from *Mytilus edulis*.

Figure 4a, shows a plot of haemolymph GPx versus LyDH activities. There is a significant linear relationship between these activities ($P = 0.025$). This is further demonstrated in Fig. 4b where the GPx and LyDH data are plotted against the protein content. A similar, non-linear relationship is seen in both cases. A reasonable interpretation of these data is that GPx and LyDH come from the same compartment (presumed to be the cytosol of adductor myocytes) with the implication that much of the GPx activity measured in cell-free haemolymph was artefactual. However, in this case, because of the spread in the data, it is unclear whether there is a basal level of GPx in the cell-free haemolymph. Although extrapolation to zero LyDH activity gives a value of $5.90 \pm 4.21 \text{ nmol min}^{-1} \text{ ml}^{-1}$ ($\pm \text{SE}$), statistically this is not significantly greater than zero ($P = 0.174$).

Figure 5a shows a plot of cell-free haemolymph AChE activity against LyDH activity. Although there is clearly a relationship between the two activities, it seems in this case to be non-linear, with AChE activity levelling off at high LyDH activities. The possibility that this was simply caused by interference with the AChE assay was checked. Using a sample with a LyDH activity of $5.4 \text{ nmol min}^{-1} \text{ ml}^{-1}$ it was found that estimates of the AChE activity in the cell-free haemolymph were independent of the sample volume used in the assay (5–30 μl). It is, therefore, unlikely that there was a problem with the AChE assay. When AChE activity is plotted against protein content (Fig. 5b) a rather different relationship is seen compared to when GPx and LyDH activities are plotted against protein (Fig. 4b). In the case of GPx and LyDH there is 'lag', i.e. cell-free haemolymph samples containing $<0.22 \text{ mg ml}^{-1}$ protein that have virtually no GPx or LyDH activity. However, in the case of AChE, for these same samples, there is a significant linear relationship between AChE activity and protein ($P = 0.0136$).

Once again, the implication of these data is that AChE activity measured in cell-free haemolymph is largely

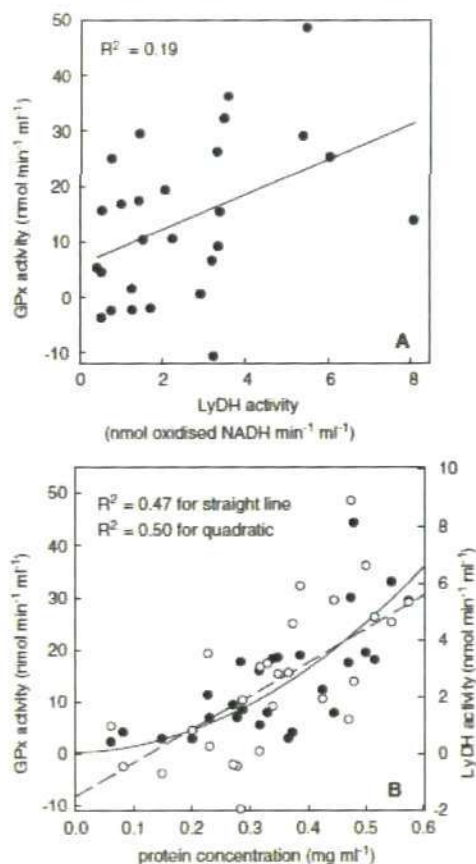


Fig. 4 a Relationship between the GPx activity and LyDH activity in cell-free haemolymph from *Mytilus edulis*; the solid line is a linear regression. The Pearson product moment and Spearman rank correlation coefficients for GPx versus LyDH are 0.536 ($P = 0.0040$) and 0.531 ($P = 0.0068$), respectively. b Relationships between GPx and LyDH activities and the protein content of cell-free haemolymph; the solid line is a mutual best fit linear regression, and the dashed line is a mutual best fit non-linear regression (quadratic). The Pearson product moment correlation coefficients for GPx versus protein and LyDH versus protein are 0.681 ($P = 0.0001$) and 0.711 ($P < 0.0001$), respectively. The Spearman rank correlation coefficients for GPx versus protein and LyDH versus protein are 0.743 ($P = 0.0002$) and 0.738 ($P = 0.0002$), respectively

artefactual. Furthermore, the difference in the behaviour of AChE activity compared to GPx activity may reflect its release into haemolymph from a different compartment, one that perhaps is more fragile than the myocyte cytosol. Mollusc adductor muscles are controlled by both cholinergic and serotonergic innervation (Funabara et al. 2005).

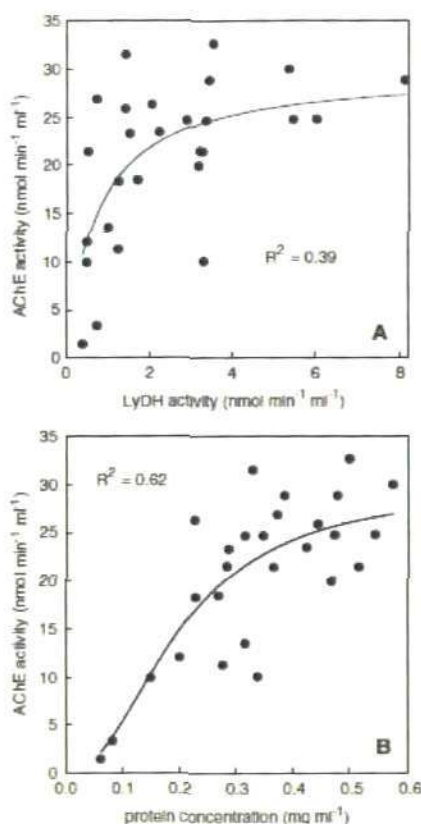


Fig. 5 a Relationship between AChE activity and LyDH activity in cell-free haemolymph from *Mytilus edulis*, the solid line is a non-linear regression (rectangular hyperbola, two parameter; $P = 0.0004$). The Pearson product moment and Spearman rank correlation coefficients for AChE versus LyDH are 0.509 ($P = 0.0068$) and 0.537 ($P = 0.0062$), respectively. b Relationship between AChE activity and the protein content of cell-free haemolymph, the solid line is a non-linear regression (logistic sigmoidal, three parameter). The Pearson product moment correlation coefficients for AChE versus protein and LyDH versus protein are 0.736 ($P < 0.0001$) and 0.711 ($P < 0.0001$), respectively

Given the role of AChE activity in cholinergic neuromuscular junctions, it seems reasonable to suppose that this is the compartment from which this activity is being released during extraction of the haemolymph. However, there is a lack of information relating to the morphology of neuromuscular junctions in *Mytilus edulis*, so it is not possible to judge whether the structure of cholinergic junctions is likely to be particularly fragile in this species. A neuromuscular origin for the AChE activity detected in mussel cell-free haemolymph may account for the variability seen in a previous study where an attempt was made to use

mussel haemolymph AChE activity as a biomarker of effect after organophosphorus exposure (Rickwood and Galloway 2004).

Conclusions

The evidence presented here suggests that cell-free haemolymph from *Mytilus edulis*, and, by extrapolation haemolymph from other bivalve species, may be significantly contaminated by adductor muscle components, e.g. intracellular contents of myocytes and contents of neuromuscular junctions. This could explain some apparent anomalies in the literature. For example, there have been doubts expressed (Brown et al. 2004) about the ecotoxicological relevance of measuring AChE activity in mussel haemolymph because of concerns that it does not originate from the nervous system, and therefore would be a "biomarker of exposure but not necessarily of effect". However, if, as suggested here, the AChE activity measured in haemolymph actually arises from neuromuscular junctions then it clearly is of relevance, although it would make more sense to measure this activity directly in adductor muscle extracts.

Despite the likelihood that haemolymph glutathione, and GPx and AChE activities arise from contamination, there are clearly other things in mussel haemolymph, where there are rationales for their presence, that are likely to be bone fide components of that compartment, e.g. phenoloxidase, which has an immune function (Muñoz et al. 2006). The implications of the work described here are two fold. First, when considering the possibility of using a biomarker in cell-free haemolymph, it may be prudent to check whether contamination could be an issue, e.g. by looking for a correlation with a myocyte marker such as opine dehydrogenase activity. Second, although the adductor muscle has sometimes been investigated, e.g. Dauberschmidt et al. (1997) looked at esterase activity in mussel posterior adductor muscle, as did Brown et al. (2004), it may be a more generally useful tissue in which to determine biomarker responses, e.g. in the glutathione/glutathione peroxidase system.

Acknowledgments We are grateful to Professor Francesco Regoli (Ancona, Italy) and Dr. David Livingstone (Plymouth, UK) for their comments during the preparation of an earlier draft of the manuscript. Sherin Al-Subai is financially supported by the Kuwait Institute for Scientific Research, State of Kuwait.

References

- Adams JD, Lauterburg BH, Mitchell JR (1983) Plasma glutathione and glutathione disulfide in the rat: regulation and response to oxidative stress. *J Pharmacol Exp Ther* 227:749-754

- Bolognesi C, Landini E, Roggeri P, Fabbrì R, Viarengo A (1999) Genotoxicity biomarkers in the assessment of heavy metal effects in mussels: experimental studies. *Environ Mol Mutagen* 33:287–292. doi:10.1002/(SICI)1098-2280(1999)33:4<287::AID-EM5>3.0.CO;2-G
- Brown M, Davies IM, Moffat CF, Redshaw J, Craft JA (2004) Characterisation of choline esterases and their tissue and subcellular distribution in mussel (*Mytilus edulis*). *Mar Environ Res* 57:155–169. doi:10.1016/S0141-1136(03)00067-9
- Carballal MJ, López MC, Azevedo C, Villalba A (1997) Hemolymph cell types of the mussel *Mytilus galloprovincialis*. *Dis Aquat Organ* 29:127–135. doi:10.3354/dao029127
- Coughlan M, O'Carra P (1996) The lysopine and octopine dehydrogenase activities of *Mytilus edulis* are catalysed by a single enzyme. *Biochem Soc Trans* 24:S128
- Dauberschmidt C, Diestrich DR, Schlatter C (1997) Esterases in the zebra mussel *Dreissena polymorpha*: activities, inhibition, and binding to organophosphates. *Aquat Toxicol* 37:295–305. doi:10.1016/S0166-445X(96)00831-4
- Dixon DR, Pruski AM, Dixon LRJ, Jha AN (2002) Marine invertebrate eco-genotoxicology: a methodological overview. *Mutagenesis* 17:495–507. doi:10.1093/mutage/17.6.495
- Ellman GL, Courtney KD, Andres V, Featherstone RM (1961) A new and rapid colorimetric determination of acetylcholinesterase activity. *Biochem Pharmacol* 7:88–95. doi:10.1016/0006-2952(61)90145-9
- Funahara D, Kanoh S, Sieghnan MJ, Butler TM, Hartshome DJ, Watabe S (2005) Twitchin as a regulator of catch contraction in molluscan smooth muscle. *J Muscle Res Cell Motil* 26:455–460. doi:10.1007/s10974-005-9029-2
- Gäde G, Grieshaber MK (1975) A rapid and specific enzymatic method for the estimation of L-arginine. *Anal Biochem* 66:393–399. doi:10.1016/0003-2697(75)90006-5
- Gäde G, Grieshaber MK (1986) Pyruvate reductases catalyze the formation of lactate and opiates in anaerobic invertebrates. *Comp Biochem Physiol B* 83:255–272. doi:10.1016/0305-0491(86)90364-0
- Gaetke LM, Chow CK (2003) Copper toxicity, oxidative stress, and antioxidant nutrients. *Toxicology* 189:147–163. doi:10.1016/S0304-483X(03)00159-8
- Galloway TS, Millward N, Browne MA, Depledge MH (2002) Rapid assessment of organophosphorous/carbamate exposure in the bivalve mollusc *Mytilus edulis* using combined esterase activities as biomarkers. *Aquat Toxicol* 61:169–180. doi:10.1016/S0166-445X(02)00051-6
- Giustarini D, Mäzani A, Dalle-Donne I, Rossi R (2008) Red blood cells as a physiological source of glutathione for extracellular fluids. *Blood Cells Mol Dis* 40:174–179. doi:10.1016/j.bcmd.2007.09.001
- Gustafson LL, Stoskopf MK, Bogan AE, Showers W, Kwak TJ, Hanlon S, Levine JF (2005) Evaluation of a nonlethal technique for hemolymph collection in *Elliptio complanata*, a freshwater bivalve (Mollusca: Unionidae). *Dis Aquat Organ* 65:159–165. doi:10.3354/dao065159
- Jha AN (2008) Ecotoxicological applications and significance of the Comet assay. *Mutagenesis* 23:207–221. doi:10.1093/mutage/gen014
- Jha AN, Dogra Y, Turner A, Millward GE (2005) Impact of low doses of tritium on the marine mussel, *Mytilus edulis*: genotoxic effects and tissue-specific bioconcentration. *Mutat Res* 586:47–57
- Lawrence RA, Burck FB (1976) Glutathione peroxidase activity in selenium-deficient rat liver. *Biochem Biophys Res Commun* 71:952–958. doi:10.1016/0006-291X(76)90747-6
- Livingstone DR (1988) Responses of microsomal NADPH-cytochrome c reductase activity and cytochrome P-450 in digestive glands of *Mytilus edulis* and *Littorina littorea* to environmental and experimental exposure to pollutants. *Mar Biol (Berl)* 46:37–43
- Livingstone DR (1991) Origins and evolution of pathways of anaerobic metabolism in the animal kingdom. *Am Zool* 31:522–534. doi:10.1093/icb/31.3.522
- Monari M, Matorzo V, Foschi J, Marin MG, Cattani O (2005) Exposure to anoxia of the clam, *Chamelea gallina* L.: Modulation of superoxide dismutase activity and expression in haemocytes. *Exp Mar Biol Ecol* 325:175–188. doi:10.1016/j.jembe.2005.05.001
- Muñoz P, Meseguer J, Esteban MA (2006) Phenoloxidase activity in three commercial bivalve species. Changes due to natural infestation with *Perkinsus atlanticus*. *Fish Shellfish Immunol* 20:12–19. doi:10.1016/j.fsi.2005.02.002
- Owen R, Buxton L, Sarkis S, Toasperm M, Knap A, Depledge M (2002) An evaluation of hemolymph cholinesterase activities in the tropical scallop, *Euvola (Pecten) ziczac*, for the rapid assessment of pesticide exposure. *Mar Pollut Bull* 44:1010–1017. doi:10.1016/S0025-326X(02)00139-X
- Owens CWL, Belcher RV (1965) A colorimetric micro-method for the determination of glutathione. *Biochem J* 94:705–711
- Pan LQ, Ren J, Liu J (2006) Responses of antioxidant systems and LPO level to benzo(a)pyrene and benzo(k)fluoranthene in the hemolymph of the scallop *Chlamys farreri*. *Environ Pollut* 141:443–451. doi:10.1016/j.envpol.2005.08.069
- Pipe RK, Farley SR, Coles JA (1997) The separation and characterisation of haemocytes from the mussel *Mytilus edulis*. *Cell Tissue Res* 289:537–545. doi:10.1007/s004410050899
- Rickwood CJ, Galloway TS (2004) Acetylcholinesterase inhibition as a biomarker of adverse effect: a study of *Mytilus edulis* exposed to the priority pollutant chlorfenvinphos. *Aquat Toxicol* 67:45–56. doi:10.1016/j.aquatox.2003.11.004
- Thompson J, Donkersloot JA (1992) N-(carboxylalkyl)amino acids: occurrence, synthesis and functions. *Annu Rev Biochem* 61:517–554
- Tran D, Moody AJ, Fisher AS, Foulkes ME, Jha AN (2007) Protective effects of selenium on mercury-induced DNA damage in mussel haemocytes. *Aquat Toxicol* 84:11–18. doi:10.1016/j.aquatox.2007.05.009

Seasonal Effect on Heat Shock Proteins in Fish from Kuwait Bay

Mirza Umair Beg · S. Al-Subiai · K. R. Beg ·
S. A. Butt · N. Al-Jandal · E. Al-Hasan ·
M. Al-Hussaini

Received: 4 February 2009 / Accepted: 6 November 2009 / Published online: 21 November 2009
© Springer Science+Business Media, LLC 2009

Abstract Heat shock proteins (HSP70) play a significant role in adaptation to temperature and have been proposed as an indicator of cellular stress. Since the water temperature in Kuwait's marine area varies from 13 to 35°C from winter to summer, HSP70 could be a valuable tool in aquaculture in Kuwait. HSP70 levels were quantified by Western blotting in liver, muscle and gill tissues of two varieties of native fish species captured during the winter and summer months from both inside and outside the highly stressed Kuwait Bay area. The HSP70 levels did not differ statistically between fish captured from the two sampling areas. The most common response in both species was higher median levels of HSP70 in winter months. This inverse relation between HSP70 levels in the fish and the water temperature may be due to either genetic adaptation in the fish to the hot climatic conditions of the region or other stressors, such as changes in pollutant levels in the surrounding water.

Keywords HSP70 · Gills · Liver · Muscle · Seabream · Tonguesole · Kuwait Bay

Kuwait Bay is considered to be a highly stressed area. It is one of Kuwait's most important areas, and has witnessed the rapid urban and industrial development since the

discovery of oil in the region. As a result, Kuwait Bay has received significant assaults on its natural environment; therefore, its environment has always been a cause of concern for regulatory authorities.

The average water temperature in the Kuwait marine area varies from 13 to 35°C during the year. Accordingly the concentration of dissolved oxygen, salinity and conductivity varies (EPA 1999). These climatic variations in the environment also cause stress on marine biota, causing them to undergo metabolic adjustments in order to perform normal physiological functions. Given the difference of around 20°C in the water temperature between the summer and winter seasons, it was considered important to study the levels of heat stress-inducible proteins in native fish species. Heat shock protein (HSP70) induction is a universal response of activated protein synthesis after exposure to various physical or chemical stimuli—especially heat stress (Werner et al. 2006). Heat shock proteins play a role in the repair of cellular damage and provide cells with protection from further damage, and thus have been proposed as indicators of cellular stress (Sanders 1993; Scofield et al. 1999; Varo et al. 2002). A correlation between exposure to environmental toxicants and stress protein synthesis has been established in several studies (Hassanein et al. 1999; Ait-Aissa et al. 2003; Padmini and Usha Rani 2008; Eder et al. 2009). The present study was conducted to determine seasonal effects on the expression of HSP70 in the liver, muscle and gill tissues of native fish species collected from the Kuwait marine area during the winter and summer months.

Materials and Methods

Two different types of fish, the predatory sea bream (locally known as shaem) (*Acanthopagrus latus*), and the

M. U. Beg (✉) · S. Al-Subiai · K. R. Beg ·
S. A. Butt · N. Al-Jandal · E. Al-Hasan
Environmental Sciences Department, Kuwait Institute for
Scientific Research, P.O. Box 24885, Safat 13109, Kuwait
e-mail: mbeg@ksr.edu.kw

M. Al-Hussaini
Mariculture and Fisheries Department, Kuwait Institute for
Scientific Research, P.O. Box 24885, Safat 13109, Kuwait

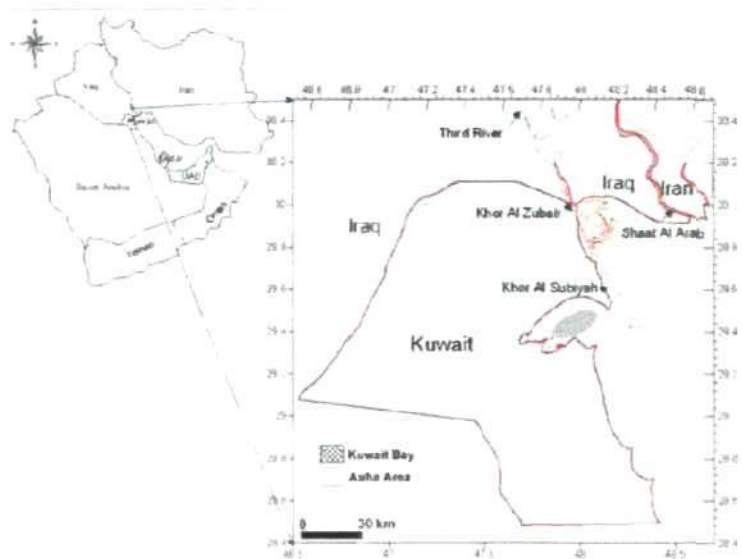
demersal tonguesole (locally known as lissan) (*Lesan al-hour*) were chosen for this study. Sample fish were collected from inside the Kuwait Bay area and from outside the Bay from the southwestern Auha area. The Kuwait Bay area is influenced by local municipal and industrial discharges with resuspension of sediment deposited pollutants, whereas, the Auha area is located outside Kuwait Bay near the southern tip of Failaka Island, where it is surrounded by depositions from the plume of Iraq's Third River (Fig. 1). Fish were collected by trawling (i.e., using a fish trawl net) in the winter months of December (18.2°C), January (13.6°C) and March (16.5°C) and in the summer months of June (30.4°C), August (34.2°C) and September (31.5°C). Approximately 15 fish of each variety from each of the two locations in each season were placed in liquid nitrogen immediately after capture for storage. In the laboratory, the fish samples were stored at -80°C before analysis. The determination of heat shock protein HSP70 was based on the original method of Varo et al. (2002) with some alteration required for better separation and transfer of the HSP70 protein for the samples.

The proteins were extracted from the liver, muscle and gill tissues of fish by mechanical homogenization of the tissue in extraction buffer containing 20 mM HEPES, 500 mM NaCl, and 12.5 mM KCl, freshly complemented with 1 mM dithiothreitol (DTT), 1 mM phenylmethylsulfonyl fluoride (PMSF), 0.1 g/ml trypsin inhibitor, and Igepal (1%), in a relation of 1:6 w/v. The homogenates were centrifuged for 90 min (39,500×g at 4°C), and the

supernatants containing the proteins were separated and stored in 100- μ l aliquots at -80°C until analysis.

Total protein was determined in the tissue homogenates using the Lowry method (Lowry et al. 1951) with bovine serum albumin as the standard. An aliquot of each sample was diluted to 5 mg/ml total protein with a buffer containing 50 mM Tris-HCl (pH 6.8), 100 mM DTT, 2% sodium dodecyl sulfate (SDS), 10% glycerol, and 0.1% bromophenol blue. Samples were then denatured by boiling for 5 min and allowed to cool before being used for protein detection. Proteins were separated by one-dimensional SDS-polyacrylamide gel electrophoresis (PAGE) on 12% polyacrylamide gel. Each 10-well plate was loaded (20 μ l) with a pre-stained molecular weight marker (i.e., a low range, pre-stained, SDS-PAGE standard), a commercial HSP70 standard, and an equal amount of protein from each sample. Gels were run on the electrophoresis system for 2–2.5 h at 60 V (constant) using a power supply. For transfer to a 0.45- μ m nitrocellulose membrane, a sandwich was made and kept in a trans-blot electrophoresis transfer system with the required buffer, and run overnight at 25 V at 4°C. After transfer, the membrane was carefully removed and quickly kept in blocking solution (i.e., 5% nonfat powdered milk in Tris-buffered saline, 100 mM Tris, 1.5 M NaCl [pH 8]) for 1 h with shaking. After blocking, membranes were probed for 3 h at 25°C, with a mouse monoclonal anti-HSP70 primary antibody (with dilution at 1:500) in 3% nonfat powdered milk in Tween 20 in TBS (T-TBS). Membranes were then washed three times with

Fig. 1 Sampling stations in Kuwait Bay and the Auha area



T-TBS and one time with TBS for 10 min each, and incubated for 2 h at 25°C with an anti-mouse IgG secondary antibody conjugated with peroxidase diluted at 1:200 in 3% nonfat powdered milk in T-TBS. Blots were washed again with T-TBS three times and once in TBS for 10 min each. The required number of 3,3'-diaminobenzidine tetra hydrochloride (DAB) (Sigma, D4418) and urea hydrogen peroxidase tablets were taken out of the freezer and allowed to reach room temperature. Then, 15 ml of distilled water was added to the tablets and the solution was vortexed until the tablets had dissolved. The solution was used within 1 h. The membrane was then put in the solution, and bound peroxidase was revealed after incubation for 5–10 min in the dark.

HSP70 was quantified using a Total Lab Ultra Lum V2.00 (Nonlinear Dynamics Ltd., UK) image analysis system that consists of an Ultracam digital gel imaging system equipped with a UV-Vis Transilluminator and a high-resolution digital camera with a hood fitted with a white light. The Ultracam package also included a software package for the identification of electrophoretic gels. The HSP70 concentrations in the tissue samples were determined by analyzing a digital image of the immunoblot against the intensity of a blot of a known concentration of HSP standard procured from Sigma Chemicals. To validate the detection accuracy, standard HSP70 was applied at six concentrations (i.e., 1.3, 2.6, 3.9, 5.2, 6.5, and 7.8 μg) for electrophoresis and immunoblotting. Images of the immunoblots were captured and analyzed using the intensity of the blot for each concentration as the standard, allowing the concentrations of the other applied bands to be calculated. The calculated values were within an accuracy level of $\pm 15\%$ compared to the applied concentrations, except the lowest applied concentration, which was detected as being around 30% higher than the actual applied concentration. The HSP70 concentrations reported for the liver, muscle and gill tissues were not corrected since appropriate standards were run along with tissue samples.

Results and Discussion

The present analysis revealed wide variations in the HSP70 levels in samples of two fish species captured from two sampling locations in Kuwait's marine areas during the summer and winter months. The data were subjected to the Kruskal–Wallis test, and between the two sampling areas, i.e., Kuwait Bay and Auha, the difference in the HSP70 levels in the fish tissues were statistically insignificant. Therefore, the data for the same types of tissue from fish from both sampling areas were combined and are presented in box plots to determine both the central tendency as

median values and the spread of values in the summer and winter months.

For sea bream, the box plots demonstrated higher median values in the winter months in all of the tissues examined. However, the difference in HSP70 levels between winter and summer months was statistically significant in liver and muscle tissues ($p < 0.05$) whereas the difference in gill tissues was statistically insignificant (Fig. 2).

For tonguesole, the median HSP70 values in the winter were also always higher than in the summer, but the difference was not statistically significant for any of the tissues analyzed. As with seabream, in tonguesole the spread of the HSP70 levels of liver and gill tissues was also higher in the winter samples, as is evident by the box length (Fig. 3).

In this study, large variations in the range of HSP70 levels were observed in both fish species; however, the median values for the summer and winter were 4.4 and 10.3 $\mu\text{g}/\text{mg}$ proteins in the liver, 4.0 and 9.9 $\mu\text{g}/\text{mg}$ proteins in the muscle and 7.3 and 11.6 $\mu\text{g}/\text{mg}$ proteins in the gill tissues of sea bream. In tonguesole, the median values for summer and winter were 5.4 and 8.0 $\mu\text{g}/\text{mg}$ proteins in liver, 6.6 and 10.3 $\mu\text{g}/\text{mg}$ proteins in muscle, and 5.9 and 8.2 $\mu\text{g}/\text{mg}$ protein in gill tissues respectively. The values obtained in this study were close to the reported HSP70 concentration in the gill tissue of the Pacific halibut (*Hippoglossus stenolepis*) which was averaged 4.6 $\mu\text{g}/\text{mg}$ proteins with levels ranging from 2.2 to 14.5 $\mu\text{g}/\text{mg}$ proteins (Scofield et al. 1999).

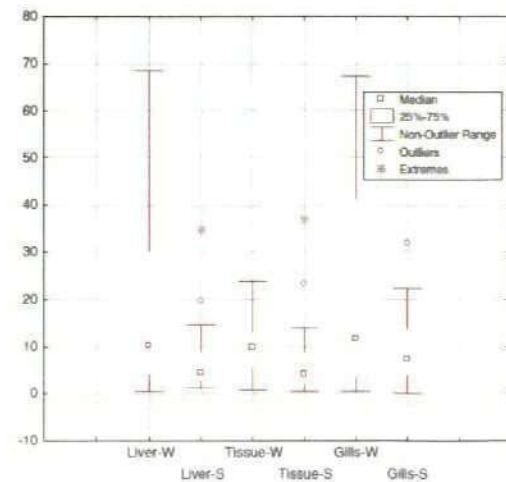


Fig. 2 Box plots of HSP70 levels ($\mu\text{g}/\text{mg}$ protein) in liver, muscle and gill of sea bream collected during the winter and summer seasons

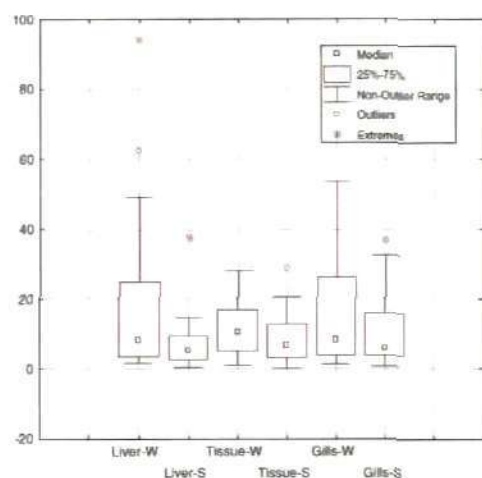


Fig. 3 Box plots of HSP70 levels ($\mu\text{g}/\text{mg}$ protein) in liver, muscle and gill of tongue sole collected during the winter and summer seasons

The most common finding in the current study was higher HSP70 levels in winter months, which was contrary to expectations and needs further explanation. Stress biomarkers represent a response to sublethal exposure to stressors that is quantifiable but very difficult to interpret, especially in field situations. In fact, the stress response entails the rapid synthesis of proteins, referred to as stress proteins, which are heat inducible, and for this reason, were initially referred to as heat shock proteins (Sanders 1993). Subsequent studies revealed that HSP 70 consists of an array of stress proteins with similar molecular sizes, some of which are heat inducible and others of which are constitutively expressed. Dunlap and Matsumura (1997) observed significant increase in HSP70 levels in fathead minnows upon experimental exposure to low temperatures. In addition, HSP70 is markedly induced under various other stresses including UV irradiation, and treatment with heavy metals and other pollutants.

The inverse relation between the HSP levels in fish and water temperature obtained in the current study may be due to genetic adaptation of the fish to the hot climatic conditions of this region. Fish adapted to long period of high water temperatures possibly exhibited sensitivity to the relatively low water temperatures occurring in the short winter months. It has been reported that the tide-pool sculpin, which is exposed to wider fluctuations in water temperature in upper tide pools, has higher constitutive liver HSP70 levels that were only slightly influenced by changes in water temperature, whereas, the fluffy sculpin, which prefers lower tide pools with smaller fluctuations in

water temperature, showed greater changes in liver HSP70 levels in response to thermal stress at lower temperatures (Iwama et al. 2003). Seasonal differences in the HSP70 levels detected in centipedes collected from the same area but at different time of the year led Pyza et al. (1997) to hypothesize that their HSP70 levels might be significant for adaptation to a periodically changing environment; however, it was not known whether seasonal changes in the HSP70 level appeared as the result of direct exposure to cold or heat, or were regulated by an endogenous clock in the circannual rhythm. Seasonal changes were also found in stream fish, with high levels of HSP70 being measured in the spring and low levels in the fall (Hoffmann and Somero 1995).

The wide variation in the HSP threshold-induction temperature among different marine species, and the wide variation in constitutive HSP levels among and within species may reflect not only recent thermal exposure but also a thermal history of the species during its evolution, and the occurrence of other stressors in the individual's habitat that are capable of activating the heat shock (stress) response (Dietz and Somero 1993; Hamer et al. 2004). Increased synthesis of the HSP70 group of proteins has been shown to be induced by a wide variety of stressors and a correlation between toxic exposure and stress protein synthesis has been established in several studies. Therefore, the higher HSP synthesis in the winter months in the current study might also have been a function of other stressors such as changes in pollutant and dissolved oxygen levels, and the conductivity and the salinity of the surrounding water. Werner (2004) showed that the ability to raise cellular HSP70 levels in response to heat shock was significantly impaired in bivalves collected from a low-salinity field site. In the current study, salinity was found to be slightly lower in the summer than in the winter months, possibly because increased evaporation at high temperature may cause an increased influx of low-salinity water through the Strait of Hormuz to the northern region of the Gulf resulting in decreased salinity in the summer months. The salinity changes are reported to interfere with HSP synthesis, as observed by Werner (2004) with bivalves.

HSP70 is also known to be induced by a number of other stimuli such as the trace elements cadmium, copper, and zinc (Urani et al. 2001), BaP, PCBs, PCP, HCH (Kohler et al. 1999), and PAHs (Cruz-Rodriguez and Chu 2002). Higher levels of PAHs have been observed in seabream collected during the winter months than in summer months (Beg et al. 2009), which may have some bearing on the higher HSP70 level found in the current study in the winter. In some fish small or undetectable levels of PAHs have been observed, whereas in others very high levels have been detected, which is analogous with the variation observed in the HSP70 levels. Further studies are required

to investigate a correlation between HSP expression and exposure to individual toxic substances or thermal stress under local environmental conditions. However, the current study provided a range of HSP70 levels in a demersal and a predatory fish collected from Kuwait's marine area which is influenced by mixed pollution and variable thermal stress in the winter and summer seasons.

Acknowledgments The authors are grateful to the Director Generals of the Kuwait Foundation for the Advancement of Sciences (KFAS) and the Kuwait Institute for Scientific Research (KISR) for their interest and financial support to this study.

References

- Ait-Aissa S, Pandard P, Magaud H, Arrigo AP, Thybaud E, Porcher JM (2003) Evaluation of an in vitro hsp70 induction test for toxicity assessment of complex mixtures: comparison with chemical analyses and ecotoxicity tests. *Ecotoxicol Environ Saf* 54:92–104
- Beg MU, Gevaio B, Al-Jandal N, Beg KR, Butt SA, Ali LN, Al-Hussaini M (2009) Polycyclic aromatic hydrocarbons in three varieties of fish from Kuwait Bay. *Polycycl Aromat Compd* 29:75–89
- Cruz Rodriguez LA, Chu FLE (2002) Heat-shock protein HSP70 response in the eastern oyster *Crassostrea virginica*, exposed to PAHs sorbed to suspended artificial clay particles and to suspended field contaminated sediments. *Aquat Toxicol* 60:157–168
- Dietz TJ, Somero GN (1993) Species- and tissue-specific synthesis patterns for heat-shock proteins HSP70 and HSP90 in several marine teleost fishes. *Physiol Zool* 66:863–880
- Dunlap DY, Matsumura F (1997) Development of broad spectrum antibodies to heat shock protein 70s as biomarkers for detection of multiple stress by pollutants and environmental factors. *Ecotoxicol Environ Saf* 37:238–244
- Eder KJ, Leutenegger CM, Kohler HR, Werner I (2009) Effect of neurotoxic insecticides on heat shock proteins and cytokine transcription in Chinook salmon (*Oncorhynchus tshawytscha*). *Ecotoxicol Environ Saf* 72:182–190
- EPA (1999) Annual report. Environmental Protection Agency, State of Kuwait
- Hamer B, Hamer DP, Muller WEG, Bartel R (2004) Stress-70 proteins in marine mussel *Mytilus galloprovincialis* as biomarker of environmental pollution: a field study. *Environ Int* 30:873–882
- Hassanein HM, Banhaway MA, Soliman FM, Abdel-Rehim SA, Muller WE, Schroder HC (1999) Induction of hsp70 by the herbicide oxyfluorfen (Goal) in the Egyptian Nile fish, *Oreochromis niloticus*. *Arch Environ Contam Toxicol* 37:78–84
- Hoffmann GE, Somero GN (1995) Evidence for protein damage at environmental temperatures seasonal changes in levels of ubiquitin conjugates and HSP70 in the intertidal mussel *Mytilus trossulus*. *J Exp Biol* 198:1509–1518
- Iwama GK, Afonso LOB, Todgham A, Ackerman P, Nakano K (2003) Are hsp70 suitable for indicating stressed states in fish? *J Exp Biol* 207:15–19
- Kohler HR, Knodler C, Zanger M (1999) Divergent kinetics of hsp70 induction in Isopoda *Oniscus asellus* in response to four environmental relevant organic chemicals (B(a)P, PCB52, γ -HCH, PCP): suitability and limits of a biomarker. *Arch Environ Contam Toxicol* 36:179–185
- Lowry OH, Rosebrough NJ, Farr AL, Randall RJ (1951) Protein measurement with folin phenol reagent. *J Biol Chem* 193:265–275
- Padmini E, Usha Rani M (2008) Impact of seasonal variation on HSP70 expression quantified in stressed fish hepatocytes. *Comp Biochem Physiol B* 151:278–285
- Pyza E, Mak P, Kramarz P, Laskowski R (1997) Heat shock proteins (HSP70) as biomarkers in ecotoxicological studies. *Ecotoxicol Environ Saf* 38:244–251
- Sanders BM (1993) Stress proteins in aquatic organisms: an environmental perspective. *Crit Rev Toxicol* 23:49–75
- Scofield E, Bowyer RT, Duffy LK (1999) Baseline levels of Hsp70, a stress protein and biomarker, in halibut from the Cook Inlet region of Alaska. *Sci Total Environ* 226:85–88
- Urani C, Melchiorretto P, Morazzoni F, Canevali C, Camatini M (2001) Copper and zinc uptake and hsp70 expression in HepG2 cells. *Toxicol In Vitro* 15:497–502
- Varo I, Serrano R, Pitarch E, Amat F, Lopez FJ, Navarro JC (2002) Bioaccumulation of chlorpyrifos through an experimental food chain: study of protein HSP70 as biomarker of sublethal stress in fish. *Arch Environ Contam Toxicol* 42:229–235
- Werner I (2004) The influence of salinity on the heat-shock protein response of *Bivalvia Potamocorbula amurensis*. *Mar Environ Res* 58:803–807
- Werner I, Viani MR, Rosenblum ES, Gantner AS, Tjeerdema RS, Johnson ML (2006) Cellular responses to temperature stress in steelhead trout (*Oncorhynchus mykiss*) parr with different rearing histories. *Fish Physiol Biochem* 32:261–273

Stabilization of Engineered Zero-Valent Nanoiron with Na-Acrylic Copolymer Enhances Spermioxicity[†]

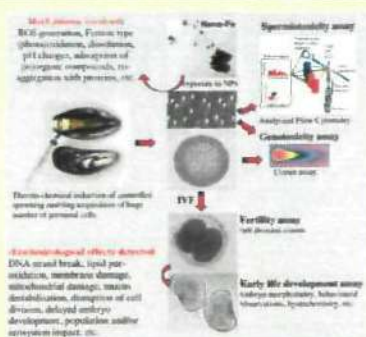
Eniko Kadar,^{1,*} Glenn A. Tarran,¹ Awadhesh N. Jha,² and Sherain N. Al-Subiai²

¹Plymouth Marine Laboratory, Prospect Place, The Hoe, Plymouth PL1 3DH, United Kingdom

²School of Biomedical and Biological Sciences, University of Plymouth, Drake Circus, Plymouth PL4 8AA, United Kingdom [†]Part of the Nanoscale Metal-Organic Matter Interaction Special Issue

S Supporting Information

ABSTRACT: Studies were carried out to assess the effects of stabilized (i.e., coated with organic polyacrylic stabilizer) and nonstabilized forms of zero-valent nanoiron (nZVI) on the development of *Mytilus galloprovincialis* embryos following 2 h exposure of the sperm prior to *in vitro* fertilization. Both forms of nZVI caused serious disruption of development, consisting of 30% mortality among spermatozoa with subsequent 20% decline in fertilization success, and delay in development, i.e., over 50% of the larvae were suspended in the trochophore stage. Significant DNA damage was also detected in sperm exposed to the highest exposure concentrations (10 mg L⁻¹). Distinct dose response to the two different types of nZVI observed are linked to aggregation behavior that is controlled by the surface stabilizers. This work reports on conventional biomarkers (for membrane integrity, genotoxicity, and developmental toxicity) applied for the rapid assessment of toxicity of nZVI, which are able to detect surface property-related effects to meet the requirements of risk assessments for nanotechnology. The study highlights the potential ecotoxicological impact of an environmentally relevant engineered nanoparticle. Implications of the NOM-nZVI interactions regarding soil and groundwater remediation and wastewater treatment are discussed.



INTRODUCTION

Zero-valent iron nanoparticles (nZVI) are widely used for the treatment of groundwater and soil decontamination.¹ The greater surface area to mass ratio that results when the particle size is reduced to the nanoscale is one of the reasons why the reactivity is greatly enhanced, which may be both desirable and undesirable at the same time. Performance trials in the United States and Europe have indicated that the technique is extremely effective at removing pollutants, while avoiding the build up of hazardous byproduct.¹ Although the potential benefits are significant, the evidence base regarding any potential risks to the environment is quite poor, especially regarding those with modifications to improve mobility (e.g., bimetallic, emulsified, or carbon-supported). With such improved mobility and very large quantities of nZVI being produced, the nanoremediation industry may disturb terrestrial and aquatic habitats.

Structural and chemical properties such as size, shape, surface chemistry, and composition of nanoparticles have previously been shown to affect their behavior in the environment.^{2–5} Little is known about Fe nanoparticle uptake pathways and fate in aquatic organisms,⁶ and there is no information on how zero-valent iron is handled in cells. A number of studies infer that exposure to

nanoiron (both oxides and zero-valent iron) cause generation of free radicals.^{7–11} These reactive oxygen species (ROS) cause inflammation of epithelial tissue and alteration of antioxidant enzymatic activity. Moreover, recent investigations comparing nZVI and iron oxide nanoparticles conclude that nZVI produces most ROS, and thus, it is most toxic.¹⁰ In contrast, other experiments showed no toxicity response to nanoiron in mice¹² or in bovine sperm cells.¹³ Such contradictory results may originate from specific particle characteristics that greatly influence toxicity of nanoparticles.

Early stages of marine invertebrates are suggested to be most sensitive to contaminants, with potentially widespread implications for population size, community structure, and biodiversity.^{14,15} The majority of marine invertebrates reproduce by direct release of their gametes into the environment, whereby sperm is exposed

Special Issue: Nanoscale Metal-Organic Matter Interaction

Received: September 1, 2010

Accepted: January 18, 2011

Revised: December 20, 2010

66 to contaminants with detrimental ecotoxicological consequences
67 that can be transmitted to future generations.¹⁰ The susceptibility of
68 sperm to environmentally induced DNA damage has human health
69 implications¹⁷ causing concern for scientists and regulators.

70 The present study aimed to test the hypothesis that organically
71 stabilized nanometals are more toxic compared to the nonstabi-
72 lized analogue by exposing the male germinal cells of marine
73 mussels to nZVI with distinctive surface properties for 2 h prior
74 to in vitro fertilization. Paternal genotoxicity was examined by
75 sperm viability, DNA-integrity, and in vitro fertilization assays as
76 indicative of sperm cell membrane integrity, genotoxicity, and/or
77 developmental toxicity. These conventional biomarkers were
78 employed in this study to test their suitability for the rapid assess-
79 ment of harmful effects of nZVIs, along with surface property-
80 related distinctive effects. A three-way crossed experimental design
81 was used to assess sperm viability, fertility, and DNA integrity
82 and the subsequent assessment of the percentage of normally
83 developing larvae at a well-distinguished growth-stage, the D-shell,
84 in response to pre-exposure of the sperm to three concentrations
85 of the two distinct nZVIs versus non-nano FeCl₃. Prior to eval-
86 uation, the assays were validated against a reference toxicant,
87 CuSO₄.¹⁸

88 ■ MATERIALS AND METHODS

89 **Preparation of Nanoparticle Suspension.** Aqueous disper-
90 sions of two different types of nZVIs with an average of 50 nm
91 diameter (kindly provided by Nanoiron Ltd., Czech Republic)
92 were used. NANOFEER 25S is the form with a special patented
93 surface modification, which is based on a combination of a
94 biodegradable organic- (Na acrylic copolymer) and inorganic-
95 stabilizer that provides a very low degree of agglomeration.
96 Conversely, NANOFEER 25 contains no additives and is inorgani-
97 cally stabilized solely by the Fe-water interactions, which re-
98 sults in a higher degree of agglomeration and faster sedimenta-
99 tion. The stock suspensions of 100 mg L⁻¹ were made up in
100 0.2 μm filtered seawater, which were then sonicated for 2 h in a
101 Lucas Dawe Ultrasonics bath (model 6456-A1). An iron chloride
102 (FeCl₃) solution was used as the non-nano analogue form that
103 has the same number of Fe³⁺ as those estimated to be surface-
104 bound on nanoparticles, i.e., 1 g of nanoiron has approximately
105 5 × 10²⁰ surface-bound Fe⁰, equivalent to 0.23 g FeCl₃ with the
106 same number of Fe³⁺. Estimation of equimolar nano Fe⁰ and
107 non-nano Fe³⁺ was made using the average surface area of
108 25 m² g⁻¹ of the nanoparticles (Nanoiron Ltd., product descrip-
109 tion sheet) and the atomic radius of Fe. Calculations were
110 performed under the assumption that all particles are spherical,
111 as shown by TEM (Figure S1 of the Supporting Information).
112 Stock solutions of 23 mg L⁻¹ FeCl₃ (Sigma, CAS: 10025-77-1)
113 and 200 μg L⁻¹ CuSO₄ (Sigma, CAS: 7758-98-7) were prepared
114 and sonicated same as the nZVI stocks.

115 **Nanoparticle Aggregation Characterization.** NanoSight
116 (NanoSight Ltd., Wiltshire, U.K.) single nanoparticle visualiza-
117 tion and sizing system was used to detect aggregation behavior of
118 particles.¹⁴ This technique uses the speed of the Brownian move-
119 ment of nanoparticles due to the random movement of water
120 molecules surrounding them. A diffusion coefficient is calculated
121 by tracking the movement of each particle, and then through
122 application of the Stokes–Einstein equation, particle size and
123 hydrodynamic diameter is calculated using the tracking software
124 (Figure 1). The instrument was calibrated using three standard ma-
125 terials (NanoSight Ltd. Wiltshire, U.K.): gold (particle size 35 nm),

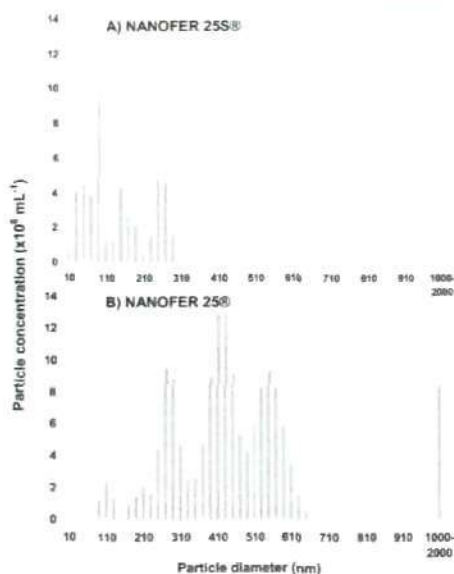


Figure 1. Particle size-distribution of (A) nZVI stabilized by an organic shell (i.e., acrylic copolymer stabilizer) and (B) nonstabilized nZVI after 2 h following sonication in seawater, e.g., corresponding to the experimental exposure media used for *Mytilus* sperm. The graphs are plots of particle size versus particle count mL⁻¹ and demonstrate the preponderance of particles with 86, 34, and 55 nm for NANOFEER 25S, while all particles formed by NANOFEER 25 have diameter over 100 nm.

126 polystyrene latex microspheres (particle size 46 nm), and poly-
127 styrene latex microsphere (particle size is 100 nm) diluted to
128 allow 100 tracks to be made in 20 s of analysis. Typically, this was
129 a 100-fold dilution of standard.

130 **Animal Maintenance and Gamete Collection.** Adult *Mytilus*
131 *galloprovincialis* were collected from Trebarwith Strand,
132 Cornwall, U.K. (50°8' N and 4°45' W) and were kept in aerated
133 seawater (temperature 15 ± 0.5 °C and salinity 35.1 ± 0.52 s.u.)
134 until induction of spawning (within 3 days after collection). Nat-
135 ural seawater was supplied from approximately 8 miles south of
136 Plymouth, U.K. (50° 15' N, 04° 13' W, water depth ~55 m).

137 Oocytes and spermatozooids were obtained by injection of 1
138 mL of 0.5 M KCl into the posterior adductor muscle followed by
139 provision of food supply (Phytofeast administered at approxi-
140 mately 1.25 × 10⁴ cells mL⁻¹) combined with heat shock from
141 15 to 25 °C. Gametes were inspected for general health, as indi-
142 cated by a spherical shape for eggs and viability for sperm, prior to
143 exposure and subsequent in vitro fertilization.

144 **Experimental Design.** Six-well cell well plates were used to
145 assess embryo development following the 2 h pre-exposure of the
146 male gametes to two different types of nZVIs and the equivalent
147 non-nano iron in static conditions, e.g., addition of the freshly
148 sonicated stock test solutions to the sperm suspension, to yield
149 the final concentration of 0.1, 1, and 10 mg L⁻¹, respectively.
150 Three replicates for each treatment were performed. After the 2 h

151 exposure of sperm, a 1 mL egg suspension was added, yielding
152 a ratio of approximately 1:10³, and then fertilization success
153 assessed, as described in detail below. The numbers of normal or
154 abnormal embryos were recorded at 48 h after fertilization, when
155 the distinguishable D-shell stage was reached (at 15 °C). Counts
156 and light-microscopy photographs of typical normal and abnormal
157 larvae were made on fixed specimens. An embryo was consid-
158 ered malformed if it had not reached D-shell by 48 h or when
159 some developmental defects were observed (i.e., concave, mal-
160 formed or damaged shell, or protruding mantle, as shown in
161 Figure S4 of the Supporting Information). All experiments were
162 conducted without addition of nutrients.

163 **Sperm Viability Assay Using Analytical Flow Cytometry**
164 (AFC). A fluorescent nucleic acid stain, SYTOX Green (Invitro-
165 gen), which does not penetrate living cells was used to assess
166 the integrity of sperm. This stain is an asymmetrical cyanine dye,
167 with three positive charges, that is excluded from live eukary-
168 otic and prokaryotic cells,¹⁹ which renders sperm with compro-
169 mised cell membranes brightly green fluorescent. The suspen-
170 sion obtained by pooling sperm from five mussels followed by a
171 25 times dilution was stained by adding 10 µL of 0.1 mM SYTOX
172 Green to 0.5 mL of sperm and incubated in the dark for 10 min
173 prior to AFC.

174 Flow cytometry was carried out with a Becton Dickinson
175 FACSort instrument (Oxford, U.K.) equipped with an air-cooled
176 argon ion laser providing blue light at 488 nm. Besides counting
177 the cells, the flow cytometer also measured green fluorescence
178 (530 nm ± 15 nm) and forward and side scatter. Data acquisition
179 was triggered on side scatter. The flow rate of the flow cytometer
180 was calibrated daily using Beckman Coulter flowset fluorospheres of
181 known concentration. Measurements of light scatter and fluor-
182 escence were made using CellQuest software (Becton Dickinson,
183 Oxford, U.K.), and data were analyzed using WinMDI software
184 version 2.8 (Joseph Trotter).

185 **Assessment of DNA Damage.** The Comet assay was used to
186 measure DNA strand breaks in sperm exposed to the distinct
187 nZVI types using the method previously described¹⁷ with some
188 modification. A total of 10 µL of sperm suspension (~6 × 10⁸ cells
189 mL⁻¹) was gently mixed with 0.75% low melting point agarose
190 (heated to 35 °C) and dropped onto slides previously coated
191 with 1% normal melting point agarose. The Comet assay was
192 performed using alkaline conditions at 4 °C. Briefly, 1 h lysis
193 using the mixture of 5.2 M NaCl, 0.1 M EDTA, 0.001 M Tris
194 base, and 1% Triton X-100, adjusted to pH 10 with 10 M NaOH.
195 This was followed by 20 min denaturation in freshly prepared
196 electrophoresis buffer (0.3 M NaOH and 1 mM EDTA) and then
197 by electrophoresis at 25 V and 300 mA for 10 min and by
198 neutralization. Slides were stained with 40 µL of ethidium bro-
199 mide (2 µg mL⁻¹ in Milli-Q water) and examined by epifluor-
200 escence microscopy (Leica, DMR) with excitation of 420–490
201 nm and emission of 520 nm. The blind scoring of the percentage
202 of DNA in the comet tail was performed on coded slides without
203 knowledge of the origin of samples. One hundred comets per
204 preparation (50 in each gel drop) were quantified by Comet 5.0
205 image analysis software (Kinetic Imaging, Liverpool, U.K.).

206 **In Vitro Fertilization.** In vitro cross-fertilization was per-
207 formed using oocytes pooled from five mussels and sperm
208 extracted from a separate group of five males. Fertilization
209 was performed using sterile laboratory equipment in salinity-
210 and temperature-adjusted, 0.2 µm-filtered (Anachem) seawater
211 (temperature 15 ± 0.5 °C and salinity 35.1 ± 0.52 s.u.). A
212 constant temperature of 15 ± 1 °C was maintained during

213 fertilization and throughout larval development. Fertilization
214 success was determined within 2 h following fertilization by light
215 microscopic observations and using the formula: (no. of fertilized
216 eggs)/(number of fertilized + unfertilized eggs) × 100. Fertiliza-
217 tion success was above 80% in all controls.

218 **Statistical Analysis.** Statistical analyses were performed using
219 Statgraphics plus v5.1 (Statistical Graphics Corp.). All results are
220 presented as means ± SE. Bartlett's test was applied for variance
221 check. Significant differences between groups were determined
222 using either one way ANOVA or the Kruskal–Wallis test,
223 followed by multiple range tests (Fisher's LSD) at *P* < 0.05 levels.

224 ■ RESULTS AND DISCUSSION

225 **Nanoparticle Aggregation.** The information regarding sur-
226 face properties of the two commercial nZVIs used in this study
227 were supplied by the producer (data is available <http://www.nanoiron.cz/en>): surface area of ≈ 25 m²g⁻¹ (NANOFER 25)
228 and average size of ≈ 50 nm, which was confirmed by the TEM
229 micrographs in Figure S1 of the Supporting Information. How-
230 ever, particle size-distribution rapidly changed in seawater, as
231 indicated by the NanoSight tracks (Figure 1). While the stabi-
232 lized nZVI (using Na-acrylic copolymer) remained as a mixture
233 of nanosized particles (as indicated by the preponderance of the
234 particles with diameters of 30, 50, and 80 nm, respectively in
235 panel (A) of Figure 1), the nonstabilized form aggregated into
236 larger particles (Figure 1B).

237 Similar rapid aggregation behavior was previously reported
238 for both the Fe oxide nanoparticles and the FeCl₃ salt¹⁷ and was
239 suggested to mitigate toxicity in mussels. However, in this study,
240 in spite of the rapid aggregation of nZVI into larger particles
241 under natural seawater pH and ionic strength conditions, the
242 aggregates and/or their byproduct can still cause cellular damage.
243 Surface passivation influences toxicity, most likely size-depend-
244 ently, e.g., nano-sized iron oxide particles are often reported to
245 be more toxic than the micrometer-sized analogues,²⁰ especially
246 when oxidative stress is considered. Mitochondrial and general
247 DNA damage do not seem to be influenced by particle size.²⁰

248 **Spermiotoxic Effect.** Approximately 10% of *Mytilus* sperm
249 was naturally compromised as indicated by control flow cyto-
250 metry readings made prior to exposure. This increased to about
251 12% in the unexposed controls maintained in the laboratory at
252 15 °C for 2 h (Figure 2). Mortality significantly increased fol-
253 lowing exposure to all concentrations of stabilized nZVI, reach-
254 ing 30% at the highest concentration (Figure 2). Curiously,
255 nonstabilized nZVI only increased sperm mortality at the lower
256 exposure concentration (0.1 mg L⁻¹), where aggregation is reduced.
257 Non-nano FeCl₃ and CuSO₄ did not have any statistically
258 significant effect on sperm viability following 2 h exposure.

259 Our evidence on spermiotoxicity of nZVI in *Mytilus* is con-
260 sistent with previous studies on the cytotoxic effects reported in
261 bacteria.^{9,21} Similarly, nanoscale iron oxides have been reported
262 to elicit low, but significant overall toxicity in vitro (both cyto-
263 toxicity and oxidative DNA damage).²⁰ Our rapid assessment of
264 sperm viability using AFC in conjunction with fluorescent dyes
265 showed that an increase in the fluorescent signal is a definite indi-
266 cation for loss of membrane intactness in response to acute
267 exposure to nZVI. However, the use of such dyes in the presence
268 of nanoparticles should be considered with caution as nanopar-
269 ticles may coaggregate with sperm, which may lead to under-
270 estimation of the fraction of dead cells. Nevertheless, our results
271 clearly showed a more than two-fold increase in fragmented
272

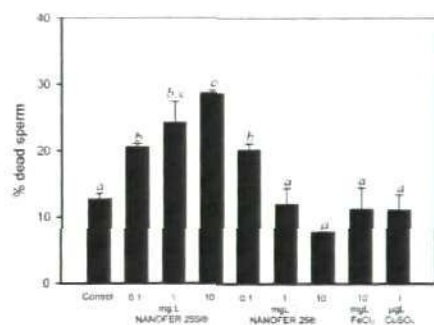


Figure 2. Effects of stabilized NANOFER 25S and nonstabilized NANOFER 25 on sperm viability. Vertical bars represent mean \pm SEM percentage of dead cell counts from the total counts per second, using flow cytometry. Statistical differences between controls and various treatments were tested by one-way analysis of variance. Bars with the same letters are not significantly different, according to the multiple range test (LSD), $P = 0.002$.

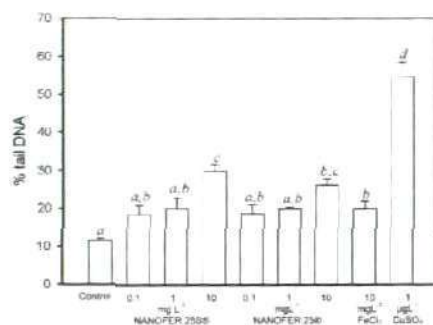


Figure 3. Effects of stabilized NANOFER 25S and nonstabilized NANOFER 25 on DNA integrity in *Mytilus* sperm. Vertical bars represent mean \pm SEM percentage of tail DNA following 2 h exposure of sperm to increasing concentrations of nZVI, both the stabilized and nonstabilized forms, non-nano Fe equimolar with the 10 mg L⁻¹ nZVI, and the effective dose of CuSO₄ (i.e., 1 μ g L⁻¹). Counts were made using the Comet software. Statistical differences between controls and various treatments were tested by one-way analysis of variance. Bars with the same letters are not significantly different according to the multiple range test (LSD), $P = 0.001$.

273 DNA following exposure to 10 mg L⁻¹ of the stabilized nZVI. In
 274 contrast, the nonstabilized form caused less DNA damage and
 275 did not increase with concentration, probably because of particle
 276 aggregation/sedimentation in the absence of the stabilizing
 277 agent. Other explanations are also possible, such as the contribu-
 278 tion of surface chemistry to surface protein associations/inter-
 279 actions.²² The effect of the capping agent itself can be ruled out
 280 because the Na-acrylic copolymer (known as BYK-381) is not
 281 considered to be hazardous, on the basis of its biodegradable
 282 nature and the ecotoxicological data available.²³ We believe that a
 283 distinct dose response observed for the two different types of
 284 nZVI in this study is most likely caused by differences in aggre-
 285 gation behavior: the product that is stabilized with sodium
 286 poly(acrylic acid) is more stable and also less reactive at low con-
 287 centrations, while the nonstabilized NANOFER 25 is very reactive
 288 at low doses but aggregates faster settling out from the water
 289 column. It is therefore crucial that in nanotoxicology studies,
 290 especially those that are relied on for risk assessment, considera-
 291 tion is given to aggregation behavior in addition to other param-
 292 eters.²⁴

293 **Sperm DNA Damage.** Stabilized nZVI increased DNA
 294 strand break following exposure of sperm for 2 h as indicated
 295 by the percentage of DNA fragments (Figure 3). The effect was
 296 concentration dependent and resulted in a 3-fold increase in tail
 297 DNA of sperm exposed to the highest concentrations as com-
 298 pared to that in the control. Exposure to the nonstabilized nZVI
 299 caused a small but significant increase in DNA damage at the
 300 lowest exposure dose, which did not increase with increasing
 301 concentration ($P = 0.003$).

302 The FeCl₃ exposure also increased DNA damage by only 5%
 303 compared to controls, which was statistically significant. Proced-
 304 ural positive controls were also performed (Figure S3 of the
 305 Supporting Information) by exposing sperm to the previously
 306 established effective dose of CuSO₄ (e.g., 1 μ g L⁻¹), which
 307 resulted in 50% tail DNA (Figure 3).

308 Marine invertebrates express similar types of chemically
 309 induced DNA damage as those reported in higher organisms,¹⁶
 310 which point toward putative wide-ranging implications of the

311 genotoxic effects of nZVIs. Moreover, spermotoxicity is reported
 312 in response to other metal oxide nanoparticles such as ZnO and
 313 TiO₂, extensively used in personal care products, which infers
 314 human health-related risks.²⁵

315 The Comet assay is a fast and convenient approach to assess
 316 the sensitivity of molluscan spermatozoa to nanoparticles. In line
 317 with our observations, several studies have indicated that when
 318 sperm collected from both humans and natural biota are
 319 exposed to both direct and indirect acting genotoxins under in
 320 vitro conditions, concentration- or dose-dependent DNA dam-
 321 age is observed.^{16,17} It is suggested that the Comet assay
 322 provides a valuable tool in nanotoxicology, whereby a measurable
 323 genotoxic effect can be detected even at threshold exposure levels
 324 of nZVI over a relatively short time (2 h), under realistic envi-
 325 ronmental conditions. This approach can identify not only the
 326 scale of toxicity of nZVIs but also the influence of surface
 327 modifiers recently being applied to improve their dispersion in
 328 the environment.¹

329 **Fertilization Success.** Exposure to both types of nZVI re-
 330 sulted in decreased sperm fecundity. Approximately 65% of cells
 331 were dividing following fertilization performed with sperm
 332 exposed to 10 mg L⁻¹ of stabilized nZVI and 70% when sperm
 333 was exposed to the nonstabilized form, but statistically significant
 334 surface property-related differences were not detected at high
 335 concentrations. However, at low exposure levels the nonstabi-
 336 lized nZVI was more toxic (Figure 4). The non-nano FeCl₃ salt
 337 did not affect significantly the fertilization success, while CuSO₄
 338 caused a reduction of dividing cells to below 50% of control levels
 339 (Figure 4).

340 The effects observed on sperm fecundity for both types of
 341 nZVI indicate a noncausal relationship between sperm mortality
 342 and fertilization capacity. This may imply that neither surface
 343 modification nor size played a major role in fertilization success.
 344 It is certainly possible that aggregation size played a role, but the
 345 effects may have been masked due to the high sperm to egg ratio

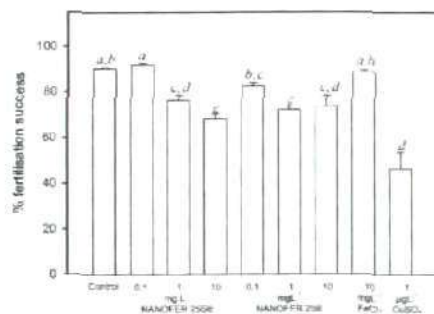


Figure 4. Effects of stabilized NANOFEr 25S and nonstabilized NANOFEr 25 on sperm fertility. Vertical bars represent mean \pm SEM percentage of dividing embryos after 1 h from the *in vitro* fertilization of eggs by pre-exposed sperm. Counts were performed on live specimens using a stereo microscope. Statistical differences between controls and various treatments were tested by one-way analysis of variance. Bars with the same letters are not significantly different according to the multiple range test (LSD), $P < 0.001$.

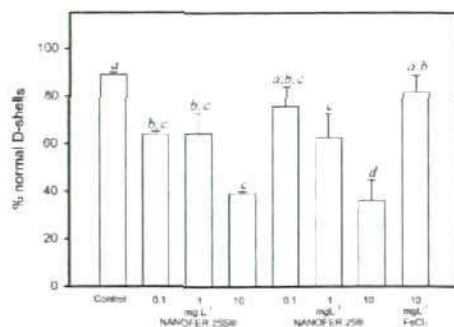


Figure 5. Effects of stabilized NANOFEr 25S and nonstabilized NANOFEr 25 on embryo development. Vertical bars represent mean \pm SEM percentage of normal D-shell stage larvae after 48 h from the *in vitro* fertilization of eggs by pre-exposed sperm. Counts were performed on fixed specimens using an inverted light microscope. Statistical differences between controls and various treatments were tested by one-way analysis of variance. Bars with the same letters are not significantly different according to the multiple range test (LSD), $P = 0.002$.

(e.g., $10^6:1$). Also, specific sperm damage caused by stabilized nZVI may not immediately affect fecundity, i.e., the ability to penetrate the egg and launch cellular division. Thus, assessment of fertilization success, in spite of enabling quick detection of biological impact, in itself may not be suitable to indicate specific surface property-related effects.

Embryo Development and Larger-Scale Implications. Exposure of sperm to nZVI resulted in a severe impairment of larva development as indicated by the decrease in normal D-shape larvae from an average 90% in control conditions to below 40% at the highest concentrations (i.e., 10 mg L^{-1}) for both types of nZVIs (Figure 5). However, at the lowest exposure concentration, the stabilized nZVI seemed slightly more toxic than the non-stabilized form. The non-nano soluble salt did not significantly affect embryo development ($P = 0.001$), while CuSO_4 caused a complete (100%) mortality of D-shell stage larvae (data not shown in Figure 5).

Malformations on embryos produced from sperm pre-exposed to nZVI ranged from delay in trochophore stage (equivalent to a 24 h development stage in controls at the same temperature), protruding mantle indicating distress, or eggs that failed to fertilize showing shrinkage and damaged membranes (Figure S4 of the Supporting Information). Dark deposits of aggregated nZVI were ubiquitous, but did not seem to affect embryo development.

Embryo toxicity has a direct impact on recruitment rate and subsequent diminishing population size with implications on community structure and biodiversity. Even if the "abnormal larvae" are suspended in the trochophore stage because of slower development and may eventually develop into normal adults, a prolonged residence of larvae in the plankton by itself could have indirect systemic effects on communities.^{14,26} The delay may be a nonspecific natural defense mechanism to survive temporary poor environmental conditions, as also reported in mussel embryos exposed to CO_2 -induced acidic water.¹⁴ Further longer-term investigations are needed to assess whether such delay caused by nZVI exposure allows resuming normal postlarval development. Also, additional research is needed to confirm whether similar

effects are observed in the presence of aged nZVI (oxidized) or with coexposure to NOM. Previous studies on nano- Fe_2O_3 failed to detect significant nanorelated toxic effects in mussel embryos¹⁴ despite evidence for distinct cellular uptake mechanisms when *in vitro* absorption through gill epithelium was investigated.⁸ With regard to bioaccumulation, it is intriguing to speculate on putatively higher trophic transference factors (TF) of metals when offered in nanofom. This could be a possible explanation to uniquely positive Fe-TFs reported in hydrothermal species²⁷ that live in metal-rich environments²⁸ where conditions facilitate Fe-rich nanoparticle formation.²⁹

The research described in this paper affords a multiplex approach to provide evidence for the environmental risks carried by nZVIs and contrasts assumptions on safety simply on the basis of the nontoxic nature of the macro scale analogue.³⁰ Because of the acute genotoxicity and subsequent developmental impairments in the common sentinel bivalve reported here, it is clear that uncontrolled and widespread application of nZVI products in nanoremediation could pose serious environmental risks. Estuaries that act as a sink for catchment-derived contaminants³¹ are vulnerable to discharges of engineered nanoparticles. It is stipulated that in natural estuarine waters, nZVI will be rapidly encapsulated by iron oxides and will aggregate into increasingly larger porous aggregates (refs 3, 6, and this study), possibly following a pathway determined by Fe corrosion chemistry.³² The situation, however, may be aggravated by the presence of photosensitizing compounds³³ and/or surface-sorbed contaminants carried by nanoscale colloids to large distances, depending on the composition of contaminants and hydrological conditions.³⁴

Humic substances, common constituents of natural organic matter (NOM) that are known to interact with various metal oxides, were reported to mitigate direct cellular toxicity to *Escherichia coli*,²¹ which may suggest low environmental impact. However, complexation of nZVI with NOMs may also have indirect interactive effects, which can generate reactive species and/or catalyze reactions. The interaction mechanisms are largely

unknown but may involve photo-Fenton production of $\sum \text{OH}$ catalyzed by Fe^{2+} and its complexes that are known to play a significant role in the photoreactions of the absorbent fraction (CDOM) of the NOM.³³ Such photochemical interactions, currently under investigation in our laboratory, are likely to have major influence on nZVI aggregation and toxicity of subsequent reaction-products, if and when it reaches the coastal environment. The potential ability of NOM to inhibit aggregation of nZVI is likely to be the key factor determining its transport and fate in the environment and can move the nanomaterials between redox zones and facilitate or inhibit contaminant transport. Indeed, simulation experiments³⁵ indicate the ability of NOM-complexed nanoscale colloids to travel unexpectedly large distances in the environment. The mobility of natural or synthetic nanoparticles in the environment will strongly depend on whether the nanoparticles remain completely dispersed, aggregate and settle, or form mobile nanoclusters. Therefore, experimental studies of nZVI transport in porous media and models of colloid-facilitated transport should consider the mobility of NOM complexed, water-dispersible colloidal fraction.

Our results indicate that conventional biomarkers of membrane integrity,¹⁹ genotoxicity,^{16,17,20} and developmental toxicity^{14,15} are suitable not only for the rapid assessment of harmful effects of nZVIs but also for the detection of distinctive surface property-related dose responses to meet the requirements of risk assessments of the commercially used nanoparticles.²⁴ The model organism *Mytilus* used here is appropriate for establishing a comparative database of developmental and reproductive effects of various nanoparticles. Similar ecotoxicological studies on emerging nZVIs and their various stages of aging are needed to support risk/benefit analysis prior to implementation of this potentially valuable use of nanotechnology.

■ ASSOCIATED CONTENT

Supporting Information. Nanoparticle characterization data regarding particle size, morphology, surface topology, and crystallography provided by the supplier are shown in Figure S1. Details on the sperm viability assay using flow cytometry and Sytox Green fluorescent staining are shown in Figure S2. Linear dose response to CuSO_4 was included together with representative DNA-comet images in Figure S3. Light microscopic photographs of the typical early development stages of *M. galloprovincialis* and various degrees of malformations associated with nZVI exposure are shown in Figure S4. This information is available free of charge via the Internet at <http://pubs.acs.org/>.

■ AUTHOR INFORMATION

Corresponding Author
*Phone: +44.1752.633450 (direct); fax: +44.1752.633101; e-mail: enik@pml.ac.uk; Web site: <http://www.pml.ac.uk>

■ ACKNOWLEDGMENT

This work contributes to the NERC funded program Oceans 2025 (Theme 3—Coastal and shelf processes) Sheran Al-Subai is financially supported by the Kuwait Institute for Scientific Research (KISR), State of Kuwait. A.N.J. acknowledges support from the European Regional Development Fund, INTERREG IVA (Grant 4059).

■ REFERENCES

- Mueller, N. C.; Nowack, B. Nano Zero Valent Iron: The Solution for Water and Soil Remediation? Report of the ObservatoryNANO, 2010. www.observatorynano.eu/project/catalogue/2EVFO.
- Auffan, M.; Rose, J.; Bottero, J. Y.; Lowry, G.; Jolivet, J. P.; Wiesner, M. R. Towards definition of inorganic nanoparticles from an environmental, health and safety perspective. *Nat. Nanotechnol.* 2009, 4, 634–641.
- Baloussa, M.; Manculescu, A.; Cumberland, S.; Kendall, K. M.; Lead, J. R. Aggregation and surface properties of iron oxide nanoparticles: Influence of pH and natural organic matter. *Environ. Toxicol. Chem.* 2008, 27, 1875–1882.
- Handy, R. D.; von der Kammer, F.; Lead, R. J.; Hasselov, M.; Owen, R.; Crane, M. The ecotoxicology and chemistry of manufactured nanoparticles. *Ecotoxicol.* 2008, 17, 287–314.
- Hasselov, M.; Readman, W. J.; Ranville, F. J.; Tiede, K. Nanoparticle analysis and characterization methodologies in environmental risk assessment of engineered nanoparticles. *Ecotoxicol.* 2008, 17, 344–361.
- Kadar, E.; Lowe, D.; Sole, M.; Fisher, A. S.; Jha, A. N.; Readman, J. W.; Hutchinson, T. The uptake and biological responses to nano-Fe versus soluble FeCl_3 in excised mussel gills. *Anal. Bioanal. Chem.* 2010, 396, 657–666.
- Keenan, C.; Goth Goldstein, R.; Lucas, D.; Sedlak, L. D. Oxidative stress induced by zero-valent iron nanoparticles and Fe (II) in human bronchial epithelial cells. *Environ. Sci. Technol.* 2009, 43, 4555–4560.
- Li, H.; Zhou, Q.; Wu, Y.; Fu, J.; Wang, T.; Jiang, G. Effects of waterborne nano-iron on medaka (*Oryzias latipes*): Antioxidant enzymatic activity, lipid peroxidation and histopathology. *Ecotoxicol. Environ. Safety* 2009, 72, 684–692.
- Auffan, M.; Achouak, W.; Rose, J.; Roncato, M. A.; Chaneac, C.; Waite, D. T.; Masson, A.; Woicik, J. C.; Wiesner, M. R.; Bottero, J. Y. Relation between the redox state of iron-based nanoparticles and their cytotoxicity toward *Escherichia coli*. *Environ. Sci. Technol.* 2008, 42, 6730–6735.
- Fernaes, S.; Land, T. Increased iron-induced oxidative stress and toxicity in scrapie-infected neuroblastoma cells. *Neurosci. Lett.* 2005, 382, 217–220.
- Zhou, Y. M.; Zhong, C. Y.; Kennedy, I. M.; Pinkerton, K. E. Pulmonary responses of acute exposure to ultrafine iron particles in healthy adult rats. *Environ. Toxicol.* 2003, 18, 227–235.
- Rohner, F.; Ernst, F. O.; Arnold, M.; Hölbe, M.; Buehinger, R.; Ehrensperger, F.; Prastina, S. E.; Langhans, W.; Hurrell, R. F.; Zimmermann, M. B. Synthesis, characterization, and bioavailability in rats of ferric phosphate nanoparticles. *J. Nutr.* 2007, 137, 614–619.
- Makhluf, D. B. S.; Qasem, R.; Rubenstein, S.; Gedanken, A.; Breitbart, H. Loading magnetic nanoparticles into sperm cells does not affect their functionality. *Langmuir* 2006, 22, 9480–9482.
- Kadar, E.; Simmanec, F.; Martin, O.; Voulvoulis, N.; Widdicombe, S.; Mitov, S.; Lead, J. R.; Readman, J. W. The influence of engineered Fe_3O_4 nanoparticles and soluble (FeCl_3) iron on the developmental toxicity caused by CO_2 -induced seawater acidification. *Environ. Pollut.* 2010, 158, 3490–3497.
- Kadar, E.; Dashfield, S.; Hutchinson, T. Developmental toxicity of benzotriazole in the protochordate *Gammarus intestinalis* (Chordata, Ascidacea). *Anal. Bioanal. Chem.* 2010, 396, 641–656.
- Lewis, C.; Galloway, T. Reproductive consequences of paternal genotoxic exposure in marine invertebrates. *Environ. Sci. Technol.* 2009, 43, 928–933.
- Zenzes, M. T.; Puy, L. A.; Bielecki, R.; Reed, T. E. Detection of benzo(a)pyrene diol epoxide-DNA adducts in sperm of men exposed to cigarette smoke. *Fertil. Steril.* 1999, 72, 330–335.
- Oliveira, M.; Serafim, A.; Bebianno, M. J.; Pacheco, M.; Santos, M. A. European eel (*Anguilla anguilla* L.) metallothionein, endocrine, metabolic and genotoxic responses to copper exposure. *Ecotoxicol. Environ. Safety* 2008, 70, 20–26.

F

dx.doi.org/10.1021/es102846g | Environ. Sci. Technol. XXXX, XXX, 000–000

- 543 (19) Roth, B. L.; Poot, M.; Yue, S. T.; Millard, P. J. Bacterial viability
544 and antibiotic susceptibility testing with SYTOX green nucleic acid stain.
545 *Appl. Environ. Microbiol.* 1997, 63, 2421-2431.
- 546 (20) Karlsson, H. L.; Gustafsson, J.; Cronholm, P.; Moller, L. Size-
547 dependent toxicity of metal oxide particles: A comparison between
548 nano- and micrometer size. *Toxicol. Lett.* 2009, 188, 112-118.
- 549 (21) Li, Z.; Greden, K.; Alvarez, P. J. J.; Gregory, K. B.; Lowry, G. V.
550 Adsorbed polymer and NOM limits adhesion and toxicity of nano scale
551 zero-valent iron to *E. coli*. *Environ. Sci. Technol.* 2010, 44, 3462-3467.
- 552 (22) Mahmoudia, M.; Simchia, A.; Milanic, A. S.; Stroeve, P. Cell
553 toxicity of superparamagnetic iron oxide nanoparticles. *J. Colloid Inter-
554 face Sci.* 2009, 336, 510-518.
- 555 (23) Heisler, E. Irritant Effects of BYK-LP G 6334 on Rabbit Skin.
556 Project 3-86-93; Pharmatox: Hannover, Germany, 1993.
- 557 (24) Alvarez, P. J.; Colvin, V.; Lead, J.; Stone, R. V. Research
558 Priorities to Advance Eco-responsible Nanotechnology. *ACS Nano*
559 2009, 3, 1616-1619.
- 560 (25) Gopalana, R. C.; Osmana, I. F.; Amanib, A.; Matash, M.;
561 Anderson, D. The effect of zinc oxide and titanium dioxide nanoparticles
562 in the Comet assay with UVA photoactivation of human sperm and
563 lymphocytes. *Nanotoxicol.* 2009, 3, 33-39.
- 564 (26) Widdicombe, S.; Spicer, J. I. Predicting the impact of ocean
565 acidification on benthic biodiversity: What can animal physiology tell us?
566 *J. Exp. Mar. Biol. Ecol.* 2008, 366, 187-197.
- 567 (27) Kadar, E.; Costa, V.; Segonzac, M. Trophic influences of metal
568 accumulation in natural pollution laboratories at deep-sea hydrothermal
569 vents of the Mid-Atlantic Ridge. *Sci. Total Environ.* 2007, 373, 464-472.
- 570 (28) Kadar, E.; Costa, V.; Santos, R. S.; Powell, J. J. Enrichment in
571 trace metals Al, Mn, Co, Cu, Mo, Cd, Fe, Zn, Pb, and Hg of macro-
572 invertebrate habitats at hydrothermal vents along the Mid-Atlantic
573 Ridge. *Hydrobiol.* 2005, 548, 191-205.
- 574 (29) Kennedy, C. B.; Scott, S. D.; Ferris, F. G. Hydrothermal phase
575 stabilisation of 2-line ferrihydrite by bacteria. *Chem. Geol.* 2004, 212,
576 269-277.
- 577 (30) Zhang, W. Nanoscale iron particles for environmental remedia-
578 tion: An overview. *J. Nanoparticle Res.* 2003, 5, 323-332.
- 579 (31) Morris, A. W.; Mantoura, R. F. C.; Bale, A. J.; Howland, R. J. M.
580 Very low salinity regions of estuaries: Important sites for chemical and
581 biological reactions. *Nature* 1978, 274, 678-680.
- 582 (32) Turner, D. R.; Hunter, K. A. *The Biogeochemistry of Iron in*
583 *Seawater*, Series on Analytical and Physical Chemistry of Environmental
584 Systems, Wiley Blackwell: London, 2001.
- 585 (33) White, E. M.; Vaughan, P. P.; Zepp, R. G. Role of the photo-
586 Fenton reaction in the production of hydroxyl radicals and photobleach-
587 ing of colored dissolved organic matter in a coastal river of the south
588 eastern United States. *Aquat. Sci.* 2003, 65, 402-414.
- 589 (34) Kersting, A. B.; Efund, D. W.; Finnegan, D. L.; Rokop, D. J.;
590 Smith, D. K.; Thompson, J. L. Migration of plutonium in ground water at
591 the Nevada Test Site. *Nature* 1999, 397, 56-59.
- 592 (35) Gilbert, B.; Lu, G.; Kim, C. S. Stable cluster formation in
593 aqueous suspensions of iron oxyhydroxide nanoparticles. *J. Colloid*
594 *Interface Sci.* 2007, 313, 152-159.

Hypoxia-induced oxidative DNA damage links with higher level biological effects including specific growth rate in common carp, *Cyprinus carpio* L.

Sanaa A. Mustafa · Sherain N. Al-Subiai ·
Simon J. Davies · Awadhesh N. Jha

Accepted: 7 May 2011 / Published online: 8 June 2011
© Springer Science+Business Media, LLC 2011

Abstract Both hypoxia and hyperoxia, albeit in different magnitude, are known stressors in the aquatic environment. Adopting an integrated approach, mirror carp (*Cyprinus carpio* L.), were exposed chronically (i.e. 30 days) to hypoxic ($1.8 \pm 1.1 \text{ mg O}_2 \text{ l}^{-1}$) and hyperoxic ($12.3 \pm 0.5 \text{ mg O}_2 \text{ l}^{-1}$) conditions and resultant biological responses or biomarkers were compared between these two treatments as well as with fish held under normoxic conditions ($7.1 \pm 1.04 \text{ mg O}_2 \text{ l}^{-1}$). The biomarkers determined included the activities of glutathione peroxidase (GPx), measurement of oxidative DNA damage (using modified Comet assay employing bacterial enzymes: Fpg and Endo-III), haematological parameters, histopathological and ultrastructural examination of liver and gills. Specific growth rate (SGR) of the fish, as an important ecotoxicological parameter was also determined over the exposure period. The study suggested that while the levels of hepatic GPx were unaffected, there was a significant difference in activity in the blood plasma under different exposure conditions: the hyperoxic group showed increased GPx activity by approximately 37% compared to normoxic group and the hypoxic group showed a decrease by approximately 38% than the normoxic group. Interestingly, oxidative DNA damage was significantly higher in both hypoxic and hyperoxic by approximately 25% compared to normoxic conditions, Fpg showing enhanced level of damage compared to the Endo-III treatment ($P < 0.001$). The haematological parameters showed enhanced values under hypoxic conditions. Transmission electron microscopic (TEM) studies revealed damage to

liver and gill tissues for both the treatments. Interestingly, SGR of fish was significantly lowered in hypoxic by approx. 30% compared to normoxic condition and this was found to be correlated with DNA damage ($R = -0.82$; $P = 0.02$). Taken together, these results indicate that prolonged exposure to both hypoxic and hyperoxic conditions induce oxidative stress responses at both DNA and tissue levels, and hypoxia can result in compensatory changes in haematological and growth parameters which could influence Darwinian fitness of the biota with wider ecological implications.

Keywords Hypoxia · Hyperoxia · Oxidative DNA damage · Histopathology · Ultrastructural changes · Specific growth rate · Carp fish

Introduction

Chronic exposures to both hyperoxia and hypoxia could be damaging to aquatic organisms leading to suboptimal growth and biomass production (Wedemeyer 1997). Although lack of dissolved oxygen (DO) or hypoxia ($\text{DO} < 2.8 \text{ mg l}^{-1}$) could be a natural phenomenon caused by daily fluctuations in oxygen concentrations (Nikinmaa 2002), chronic hypoxic conditions prevailing in so called 'dead zones' in different parts of the world, which is linked to anthropogenic activities, often leads to mass mortality of sensitive biota and could lead to overall reduction in biodiversity (Diaz and Rosenberg 2008). With respect to hypoxia-induced biological responses, most of the mechanistic studies have been carried out using mammalian cells under in vitro conditions (Wu 2002). Our understanding of molecular responses using in vitro models therefore requires further elucidation at whole organism level.

S. A. Mustafa · S. N. Al-Subiai · S. J. Davies · A. N. Jha (✉)
School of Biomedical & Biological Sciences, University of
Plymouth, Drake Circus, Plymouth PL4 8AA, UK
e-mail: a.jha@plymouth.ac.uk

Fish as a group is considered to be prime models to study oxygen dependent processes as they demonstrate acclimatory or adaptive responses with respect to their requirements (Lushchak and Bagnyukova 2006; Nikinmaa 2002; Sotamo et al. 2001). Most of the studies carried out using fish involving hypoxic or hyperoxic exposures have however used only short term exposures (Wu 2002). Where a chronic exposure has been performed, only selected biochemical or physiological responses have been studied, which do not provide a holistic picture of the potential impact at the individual level. In this context, the significance of oxidative stress associated with both environmental contaminants and also in aquaculture related activities have been the subject of scientific investigations (Livingstone 2003; Lushchak 2011). For example, effects of hypoxia ($0.40 \text{ mg O}_2 \text{ l}^{-1}$) for 2, 6 or 10 h and subsequent normoxic recovery has shown induced oxidative stress and a compensatory changes of a range of antioxidant enzymes in different tissues of goby, *Perccottus glenii* (Lushchak and Bagnyukova 2007). A 42 day exposure to common carp, *Cyprinus carpio* L. to $0.50 \text{ mg O}_2 \text{ l}^{-1}$ has shown to induce DNA damage (determined by TUNEL signal) in liver cells, especially during the first week of exposure. There was however no change in other cellular parameters (e.g. proliferation, number or size, caspase activity) including induction of DNA single strand breaks (Poon et al. 2007). Gene expression analyses in gonads of mature zebrafish (*Danio rerio*) maintained under normoxia ($3 \text{ mg O}_2 \text{ l}^{-1}$) and hypoxia ($1 \text{ mg O}_2 \text{ l}^{-1}$) following short (4 days) and long term (14 days) exposures showed differential expression of genes associated with initial adaptive response (e.g. metabolism of carbohydrate, proteins, nucleic acid) and a suite of genes belonging to different ontology categories related with lipid metabolism, steroid synthesis and immune response which could lead to reproductive impairment (Martinovic et al. 2009). Field and laboratory studies in different fish species have also demonstrated that hypoxic conditions could potentially lead to abnormal developments of reproductive systems (Thomas and Rahman 2010; Wu 2002).

A 5 h exposure of rainbow trout to varying degrees of oxygen saturation ($3.30\text{--}21.10 \text{ mg l}^{-1}$) showed enhanced degree of DNA single strand breaks (as determined by the alkaline unwinding technique) under hypoxic and hyperoxic conditions compared to normoxic conditions (i.e. $11 \text{ mg O}_2 \text{ l}^{-1}$). The highest rate of DNA breaks occurred when the fish were kept under hypoxic conditions (Liepelt et al. 1995). Apart from this study, where a single endpoint was studied, to our knowledge there have been no further investigations to compare the biological responses of these two contrasting environmental conditions concurrently. In particular, comparison of levels of oxidative DNA damage is lacking. Whilst exposure to both hyperoxia and hypoxia have been shown to cause DNA damage and apoptosis in

cells of diverse origin (Cacciuto et al. 1993; Gozal et al. 2005; Poon et al. 2007), evaluation of oxidative DNA damage and its potential knock-on effects at individual level has not been elucidated. This is particularly important given that oxidative stress (including oxidative DNA damage) has been implicated in a variety of pathophysiological conditions including impairment of reproductive success in humans and, could well correlate to ecotoxicological parameters affecting other species (Jha 2008). Furthermore, although both hypoxic and hyperoxic conditions are commonly observed in the aquatic environment (van Raaij et al. 1994; Nikinmaa 2002), to our knowledge, concurrent comparison of impact of hyperoxia and hypoxia at different levels of biological organisation, elucidating cause-effects coupling is lacking. This is particularly important for illuminating the mechanisms of biological responses, as considerable overlap or commonalities in molecular pathways could exist for these contrasting conditions (Lushchak and Bagnyukova 2006).

In the backdrop of above information, the overall aim of this study was to compare the biological or biomarker responses at different levels of organisation (i.e. DNA to individual) in a representative carp species, *Cyprinus carpio* L. following chronic exposure (i.e. 30 days) to both hypoxic and hyperoxic compared to normoxic condition. This species has been used for such studies by different workers (e.g., Lushchak et al. 2005; Poon et al. 2007). We also aimed to test the correlations between DNA damage with other biomarkers and specific growth rate (SGR) of the fish. A modified single cell gel electrophoresis or the Comet assay was employed as a robust assay to determine oxidative DNA damage (Azqueta et al. 2009). Levels of antioxidant enzyme, glutathione peroxidase (GPx activity) in plasma and liver samples and, haematological parameters were also determined along with histopathological and ultrastructural studies in specific tissues. Finally, measurement of feed conversion rate (FCR) and specific growth rate (SGR) and its potential correlation with DNA damage were also determined.

Materials and methods

Chemicals and reagents

All chemicals and reagents were purchased from Sigma-Aldrich Ltd. (Poole, Dorset, UK) and Fisher Scientific Ltd. (Loughborough, Leicestershire, UK) unless stated otherwise.

Fish and their maintenance

Cyprinus carpio L. weighing 30–40 g were obtained from Hampshire carp hatcheries (Bowlake fish farm, UK) and

were transported to the Aquarium, 36 fish were acclimated and grown to attain an average weight of 97.30–98.60 g within 2 months in re-circulating (600 l h^{-1}) aerated freshwater tanks. Water temperature was maintained at $23.0\text{--}23.5^\circ\text{C}$ with an electric immersion heater, pH was between 6.5 and 8.0 and adjusted with NaHCO_3 as necessary. Dissolved oxygen (DO) concentration was maintained at 7.40 mg l^{-1} using air stones. All the water quality parameters were monitored and recorded daily using an electric meter (Hach HQ4d). Water was renewed weekly and nitrogenous compound were monitored weekly using a Hach Lange DR 2800 and cuvettes for ammonia (Lange, LCK 304), nitrite (Lange, LCK 341) and nitrate (Lange, LCK 340) (Hach Lange Ltd., Salford, UK). The following levels of nitrogenous compounds were considered acceptable: ammonia (un-ionized) ($<0.10\text{ mg l}^{-1}$), nitrite ($<1.0\text{ mg l}^{-1}$), nitrate ($<50\text{ mg l}^{-1}$). Mechanical filtration media was washed twice a week to maintain high filtration efficiency and reduce biological loading on the filter system.

Experimental design

Following the acclimation period, 36 fish (weighing 97.30–98.60 g) were randomly distributed into six 80-l fiberglass tanks (duplicate tanks treatment $^{-1}$), normoxia (control group) at $7.10 \pm 1.04\text{ mg O}_2\text{ l}^{-1}$, hypoxic treatment group at $1.80 \pm 1.10\text{ mg O}_2\text{ l}^{-1}$ [achieved using pumping nitrogen gas (purity: 99.99%) at specific water flow through system $\approx 1\text{ l min}^{-1}$] and a hyperoxic treatment group at $12.30 \pm 0.50\text{ mg O}_2\text{ l}^{-1}$ [pumping O_2 (purity 99.95%)] for 30 days. The concentration of oxygen in the water was measured three times daily by using an oxygen electrode (Oxy Guard, Handy Polaris, DK). Water temperature was maintained at $23.0\text{--}23.5^\circ\text{C}$ and pH was maintained at 6.5–8.0. A 12 h light/12 h dark photoperiod was maintained through the exposure duration. The exposure start time began when the desired dissolved oxygen levels were achieved, which was within 2 days after the initiation of nitrogen and oxygen pumping. During the experimentation period the fish in each treatment group were fed commercial feed pellets (Ewos, Micro 20 p, Ewos Ltd., Westfield, Bathgate, West Lothian, UK) at 2% biomass per day provided in equal rations at 09:00, 13:00 and 17:00 h. Daily feed was corrected weekly following batch weighing after a 36 h starvation period. At the end of experimental period (i.e. 30 days), fish were euthanised by overdose with tricaine methane sulphonate MS222 (200 mg l^{-1} water for 10 min) (MS222, Pharmaq, Fordingbridge, UK) followed by destruction of the brain.

Measurement of glutathione peroxidase activity

Glutathione peroxidase (GPx) activity was measured in plasma and liver as described by Lushchak et al. (2005) with slight modifications. Liver samples were weighed and homogenized (1:9 w/v) using a Potter-Elvehjem glass homogenizer in 100 mM Tris-HCl (pH 7.5) containing 2.5 mM dipotassium EDTA, 0.01% Triton X-100 and 2.5 mM sodium azide. Homogenates were centrifuged (4°C for 20 min at $10,500\times g$) and the supernatant was transferred to a polypropylene microcentrifuge tube. Just prior to the GPx assay, a mixture containing 50 mM potassium HEPES buffer (pH 7.5), 1 mM dipotassium EDTA, 0.21 mM NADPH, 1 U ml^{-1} glutathione reductase (Sigma G-3664 from *Saccharomyces cerevisiae*) and 1 mM GSH was prepared; 270 μl of this mixture and 50 μl of sample were then mixed and the reaction was initiated by the addition of 5 μl of 12.4 mM H_2O_2 . The decrease in absorbance was monitored for 60 s in a microplate reader (Optimax, Molecular Devices, Sunnyvale, CA, USA) using 96 well plates. All measurements were carried out in triplicate at $20 \pm 2^\circ\text{C}$. Activity was expressed as $\text{nmol min}^{-1}\text{ ml}^{-1}$ in plasma and $\text{nmol min}^{-1}\text{ g}^{-1}\text{ ww}$ (wet weight) in liver.

Determination of oxidative DNA damage

A modified Comet assay was performed using the bacterial enzymes formamidopyrimidine DNA glycolase (Fpg) and Endonucleases III (Endo-III) to allow the assessment of oxidized purines and pyrimidines, as described by Reeves et al. (2008). Prior to performing, the assay using blood samples of fish was thoroughly optimized and validated under in vitro conditions using hydrogen peroxide as a reference agent as described by other workers (Belpaeme et al. 1998; Frenzilli et al. 2004). The results (not included) showed a concentration dependent increase for the induction of DNA strand breaks in line with our earlier in vitro studies (Reeves et al. 2008). Cell viability of the erythrocytes in the validation and in the present experiments were assessed through trypan blue exclusion dye, which were in the acceptable range for all treatments (data not shown). For the Comet assay, erythrocytes were pelleted in a microcentrifuge tubes and suspended in 180 μl of low melting point agarose (0.5% in PBS). 170 μl of the cell suspension were placed on the frosted ends of glass slides coated with agarose (1% in PBS), covered with a cover slip and placed on ice for 10 min, the cover slips then were removed and the slides immersed in a lysis solution (4°C for 1 h). Following cell lysis, the slides were washed three times with enzyme reaction buffer (4 mM HEPES, 0.01 mM KCl, 0.05 mM EDTA, and 0.02 mg ml^{-1} bovine

serum albumin, pH 8) and Fpg and Endo-III enzymes (1 unit of enzyme diluted in 50 μ l of buffer per gel) were added. After enzyme addition, cover slips were added and the slides were incubated in a humid chamber at 37 °C for 45 min. Following incubation, the slides were processed identically to those undergoing the standard protocol which included steps of unwinding (15 min), electrophoresis (25 V, 300 mA for 20 min) and neutralization (0.4 M Tris-HCl, pH 7.4; 5 min (Singh et al. 1988, Belpaeme et al. 1998; Frenzilli et al. 2004). Finally, to visualise comets, 40 μ l of 0.2% ethidium bromide stain was applied to each gel. Scoring was conducted using a fluorescence microscope (Leica DMR) using Comet 5.0 image analysis software (Kinetic Imaging, Ltd., Liverpool, UK). For comet scoring, 100 cells for each slide (50 cells per gel from each exposed individual fish) were compared to reference slides (buffer incubation with no enzymes). Tail DNA (%) was chosen as a measure of single strand DNA break/alkali labile sites (Kumaravel and Jha 2006).

Determination of haematological parameters

Fish were removed from their tank and placed into an aerated anaesthetic bath consisting of tricaine methane sulphate, (MS222 at a concentration of 100 mg l⁻¹ for 10 min). Samples (three fish tank⁻¹; $n = 6$) were taken ethically from the caudal vein using a 25 gauge needle and 1-ml syringe. All haematological parameters were determined according to standard methods (Handy and Depledge 1999). Haematocrit values were determined by the micro-haematocrit method and reported as percentage packed cell volume (% PCV). Leucocyte and erythrocyte (RBC) counts were determined by diluting whole blood in Dacie's solution (1/50 dilution) and enumerated subsequently in a haemocytometer. Haemoglobin concentration (Hb) was determined based on Drabkin's cyanide-ferricyanide solution. To prepare blood plasma samples for the analyses of GPx activity, the remaining blood was centrifuged at 10,500 \times g for 10 min, plasma samples were collected and stored at -80 °C until they were required for analysis.

Histopathological and transmission electron microscopic (TEM) studies

The prefixed tissue (i.e. liver and gill) samples were processed by a routine histological method (Camargo and Martinez 2007; Myers et al. 1998). Sections were cut at 5 μ m thickness and subsequently stained with counter stain (H&E). Images of gill and liver sections were obtained by light microscopy using an Olympus Vanox-T microscope and photographed using a digital camera (Olympus camera C-2020 Z) at total magnifications of \times 400. For TEM studies, samples were prepared as described by Au et al.

(1999). Liver and gill tissues were cut into 1 mm³ cubes and fixed in cold 2.5% glutaraldehyde in 0.1 M cacodylate buffer (pH 7.2). Tissue samples were fixed overnight at 4 °C followed by washings (in buffer, 1 l of buffer deionized water and then deionized water, 10 min each step) before post fixing in 1% aqueous osmium tetroxide for 2 h. Samples were rinsed thoroughly with sodium cacodylate buffer followed by dehydration through a graded ethanol series, then infiltrated gradually in Spur's resin for several days and finally the resin was polymerised in a small beam capsule. Ultrathin sections were stained in 2% uranyl acetate and lead citrate for 15 min for each stain to produce high contrast and to stain many cellular components to be examined under a transmission electron microscope (JEOL, TEM-1200 EX II) at 120 kV and imaged using soft Imaging system (Mega View 3). Quantitative assessment of ultrastructural damage to tissue morphology was determined by standard statistical methods (ANOVA).

Growth performances measurements

Growth performance and feed utilisation were assessed by weight gain, specific growth rate (SGR) and feed conversion ratio (FCR). Calculations were conducted according to Cech et al. (1984) using the following formulae: $SGR = 100(\ln FW - \ln IW)/T$, $FCR = FI/WG$. Where FW = final weight (g), IW = initial weight (g), T = duration of feeding (days), WG = wet weight gain (g), FI = feed intake (g).

Statistical analysis

Statistical analysis was performed using Statgraphics v5.1 software (StatSoft, USA). All data were presented as mean \pm standard error (S.E.) and analysed using one way analysis of variance (ANOVA) or Kruskal-Wallis test followed by multiple range tests. For the modified Comet assay, data presented as median \pm S.E. were analysed using multifactor analysis of variance (ANOVA) followed by Turkey's multiple comparison test. P values < 0.05 were considered significant. Any correlations between variables were determined using the Pearson's correlation coefficient.

Results

Determination of GPx activity

The liver GPx activity in hyperoxic reared fish was significantly decreased by about 32% in comparison with normoxic group ($P = 0.04$). Also, the GPx activity in hypoxia decreased by approximately 22%, but it was not

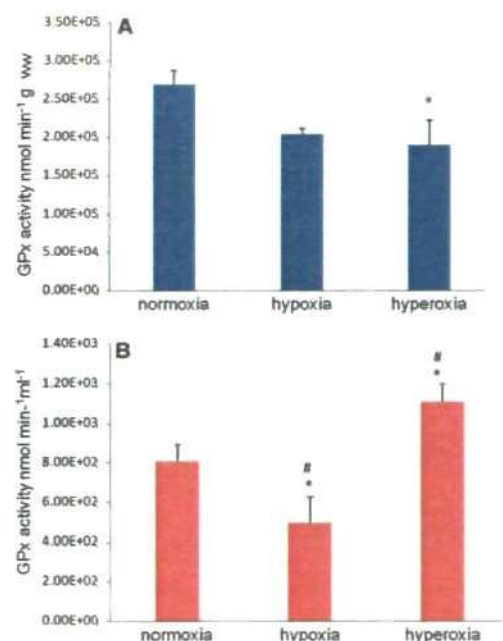


Fig. 1 Activity of GPx **a** in liver **b** in plasma, following 30 days of exposure to normoxia, hypoxia and hyperoxia. Values are mean \pm S.E. * Indicates significant differences from normoxic group; # indicates significant differences between the hypoxia and hyperoxia groups at $P < 0.05$; $n = 6$

significantly different from the normoxic group. Moreover, multiple range tests indicated that there was no significant difference between the hypoxic and hyperoxic group (Fig. 1a). Over all, the GPx activity in the liver tissue of mirror carp appeared to be unaffected by hypoxic condition for the exposure periods, (i.e. 30 days). In contrast to liver, a significant (i.e. 38%) decrease in GPx activity was observed in the blood plasma in hypoxic compared to normoxic group (Fig. 1b). On the other hand, the hyperoxic group showed significant (approx. 37%) increased GPx activity compared to normoxic group, indicating increased oxidative stress in this treatment group. Also, a highly significant difference was detected between hypoxic and the hyperoxic treatment groups ($P = 0.002$).

Determination of oxidative DNA damage

Both hyperoxic and hypoxic conditions showed strongly significant ($P < 0.00005$) increase for oxidative DNA damage compared to normoxic condition. Oxidative DNA damage was relatively low in normoxic compared to the treatment groups. Conversely, the highest degree of

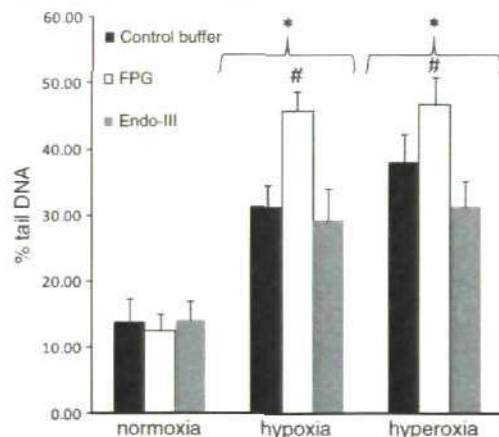


Fig. 2 Induction of DNA single strand breaks (represented as percentage tail DNA) in *C. carpio* erythrocytes following 30 days exposure to normoxia, hypoxia and hyperoxia (7, 1.8 and 12.3 mg l^{-1} respectively). Values are average median \pm S.E. * Statistically significant different versus normoxia, # Statistically significant different versus buffer and Endo-III at $P < 0.05$; $n = 6$

oxidative DNA strand breaks was seen in the presence of Fpg enzyme (approx. 25% higher) in both the treatment groups compared to the normoxic condition. This enzyme showed a statistically significant difference compared to buffer control and Endo-III treatments using two ways ANOVA (Fig. 2).

Determination of haematological parameters

The results obtained for various haematological parameters are summarised in Table 1. There was a significant difference for Hct values among the groups (ANOVA, $P = 0.001$); the hypoxic group showed 25% higher values than the normoxic and the hyperoxic groups. The highest Hb concentration was observed in hypoxic group, approximately 40% higher than in the normoxic group (ANOVA, $P = 0.03$). The Hb concentration in the hyperoxic group was

Table 1 Haematological parameters in *Cyprinus carpio* exposed to normoxic, hypoxic and hyperoxic conditions for 30 days

Parameters	Normoxia	Hypoxia	Hyperoxia
Hct (%)	31.16 \pm 1.24 ^a	38.00 \pm 0.80 ^b	30.83 \pm 1.44 ^a
Hb (g/dl)	6.76 \pm 0.60 ^a	9.57 \pm 0.66 ^b	7.41 \pm 0.48 ^{ab}
RBC (cells $\times 10^6/\mu l$)	1.82 \pm 0.20 ^a	3.42 \pm 0.30 ^b	2.70 \pm 0.08 ^a
WBC (cells $\times 10^3/\mu l$)	14.70 \pm 0.43 ^a	14.32 \pm 0.51 ^a	15.11 \pm 0.93 ^a

Data are mean \pm S.E. Groups with different alphabetic superscripts indicate significant difference at $P < 0.05$, ($n = 6$)

marginally higher than the normoxic group, but was not significantly different from either normoxic or hypoxic groups. On the other hand, RBC count increased by approximately 90% in hypoxic group and by approximately 50% in the hyperoxic group compared to the normoxic group (Kruskal-Wallis, $P = 0.0003$), multiple range tests detected significant differences between hypoxic and the hyperoxic groups. No differences were found among the groups for total leukocyte counts.

Histopathological and transmission electron microscopic studies

The liver sections of control (normoxic) group exhibited normal morphological structures with no abnormalities in the hepatocytes. It showed a homogenous cytoplasm around a centrally located spherical nucleus (Fig. 3a). Microscopic examination of hepatocytes and their nuclei from hypoxic group areas indicated histopathological changes after 30 days of exposure compared to the normoxic group. Hepatocytes in 4 fish (out of 6) lost their normal boundaries. There were cellular and nuclear degeneration, cytoplasmic vacuolation in most regions of the liver sections (Fig. 3b). Livers obtained from the hyperoxic treatment did not show evidence of any histopathological changes under the light microscopy (Fig. 3c).

Gill morphology in the control (normoxic) group had normal morphological structures in which lamellae were lined by squamous epithelium composed of non differentiated cells (Fig. 3d). Gills from hypoxic condition showed several histological alterations including lifting of lamellar epithelium and enhanced presence of goblet cells on the lamellae compared to normoxic group. In addition, in some cases aneurysm resulted in the fusion of some secondary lamellae (Fig. 3e). Gills from hyperoxic group showed lifting of the lamellar epithelium and curling of secondary lamellae. The extent of the damage was however not severe compared with hypoxic condition (Fig. 3f). Quantitative analysis using ANOVA suggested that most of these changes were significantly different from the normoxic group (data not shown).

For TEM, liver from normoxic carp showed normal organelles (e.g. cell membranes, nuclei, mitochondria, rough endoplasmic reticulum; Fig. 4a), hypoxic specimens revealed significantly increased number of lipid droplets in the cells (homogeneous semi-electron dense vacuole) of varying sizes ($17.3 \mu\text{m} \pm 0.4$) compared with normoxic and hyperoxic specimens (2.50 ± 0.61 and 6.20 ± 0.90) respectively (ANOVA, $P = 0.03$). In hypoxic condition, nucleus showed areas which were relatively clear and occupied by dense heterochromatin within nuclear envelope (Fig. 4b). On the other hand, liver from hyperoxic

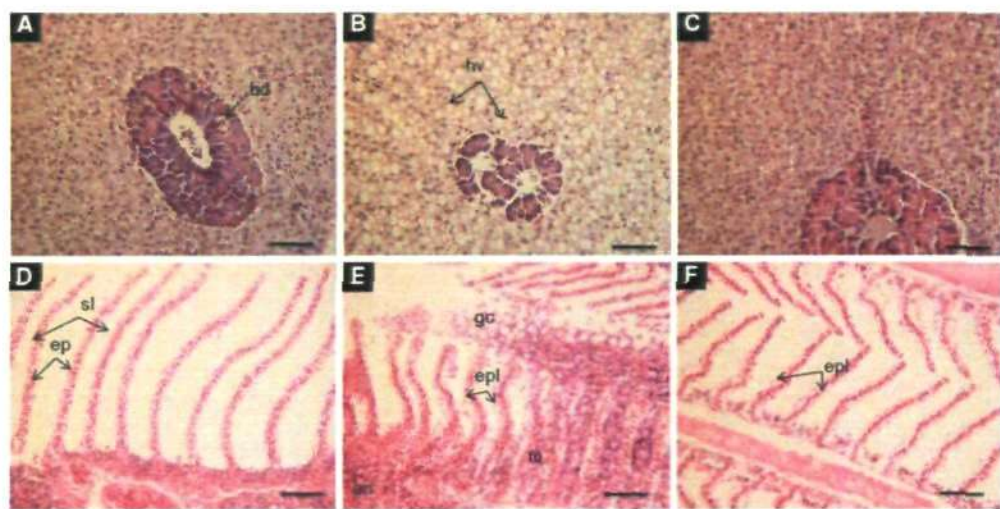


Fig. 3 Light micrographs of sections through liver and gill of *C. carpio* showing histological structures of normoxic, hypoxic and hyperoxic treatments stained with H&E at 5 μm thickness. **a** normoxic liver, **b** hypoxic liver, **c** hyperoxic liver, **d** normoxic gill, **e** hypoxic

gill and **f** hyperoxic gill. *bd* bile duct, *hv* hydrobic vacuolation, *sl* secondary lamellae, *ep* epithelial cell, *epl* epithelial cell lifting, *gc* goblet cell, *fu* fusion, *an* aneurysm. Scale bars 50 μm .

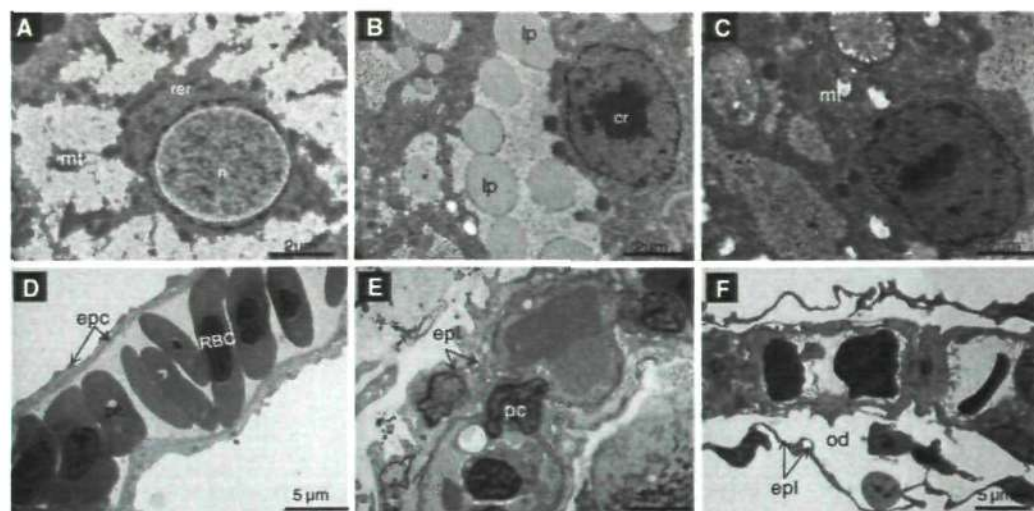


Fig. 4 Transmission electron microscopy images. **a** normoxic liver. **b** hypoxic liver, showing lipid droplets. **c** hyperoxic liver, the mitochondria are large and numerous. **d** secondary lamellae of gill from normoxic condition. **e** hypoxic secondary lamellae and **f** hyperoxic secondary lamellae. *n* nucleus, *nu* nucleolus, *mt* mitochondria, *rer* rough endoplasmic reticulum, *lp* lipid droplets, *pc* pillar cell, *RBC* red blood cell, *ep* epithelial cell, *epl* epithelial cell lifting, *od* oedema

treatment showed increased number of the mitochondria (23.40 ± 0.44) which was significantly different (ANOVA, $P = 0.03$) from normoxic and (8 ± 0.02) hypoxic conditions (11.30 ± 0.51) (Fig. 4c). The nucleus of the hepatocytes also showed irregular shape occupied by dense heterochromatin in hyperoxic condition, which was not apparent while conducting light microscopic studies. TEM images in secondary lamellae of normoxic gill exhibited normal organelles with epithelial and pillar cells (Fig. 4d). Hypoxic specimens showed lifting of the epithelial cells. There was also a breakdown of pillar cells and disorganisation of blood spaces (Fig. 4e). The secondary lamellae of hyperoxic gill also revealed separation of epithelial cells and intracellular oedema (Fig. 4f).

Table 2 Growth performance of carp exposed to normoxic, hypoxic and hyperoxic conditions for 30 days

Variables	Normoxia	Hypoxia	Hyperoxia
Initial weight (g)	98.3 \pm 1.73 ^a	97.3 \pm 2.41 ^a	98.6 \pm 2.09 ^a
Final weight (g)	165.2 \pm 4.61 ^a	139.8 \pm 7.08 ^b	146.3 \pm 4.24 ^{ab}
Weight gain (g)	66.7 \pm 3.52 ^a	42.2 \pm 6.43 ^b	47.7 \pm 3.75 ^{ab}
SGR (% g ⁻¹)	1.73 \pm 0.01 ^a	1.23 \pm 0.10 ^b	1.30 \pm 0.09 ^{ab}
FCR	1.01 \pm 0.21 ^a	1.07 \pm 0.11 ^b	1.02 \pm 0.08 ^{ab}
Survival rate (%)	100.0 \pm 0.00	100.0 \pm 0.00	100.0 \pm 0.00

Data are mean \pm S.E. Groups with different alphabetic superscripts indicate significant difference at $P < 0.05$; ($n = 6$)

Determination of growth performances

No mortalities occurred during the experimental period. SGR after 30 days exposure (hypoxic and hyperoxic conditions) was significantly lower in the hypoxic group by approximately 30% compared to fish exposed to normoxic condition (ANOVA, $P = 0.03$). There was no significant difference for SGR between hypoxic and hyperoxic conditions (Table 2). The result suggested that the SGR was significantly affected by the level of dissolved oxygen as evident by significant growth depression in the hypoxic group.

Discussion

Several carp species (e.g. Crucian carp: *Carassius carassius*; gold fish: *Carassius auratus*; the mirror or common carp: *C. carpio*) are highly tolerant to hypoxic and even to anoxic conditions. This adaptive capability is critically important to allow them to occupy specific environmental niches where oxygen level can drop down to low concentrations (van den Thillart and van Waarde 1985). Therefore, species that routinely tolerate hypoxic status need a defensive strategy to cope with oxygen limiting conditions. This strategy could include changes in tissue-specific activities of antioxidant enzymes (Lushchak et al. 2001;

Lushchak et al. 2005; Lushchak and Bagnyukova 2006; Sevgi Kofayli 1999). In this context, GPx activity has been used as indices of oxidative stress, since this is considered to be the most important enzyme providing protection against this stress (Livingstone 2001; Valavanidis et al. 2006). Our results suggest that in the liver, hyperoxia induced a marked decrease in GPx activity compared to normoxic condition. Decreased activity of liver GPx in hyperoxic condition is possibly related with inactivation under enhanced ROS levels (Halliwell and Gutteridge 1999). This decrease was not significantly different in hypoxic compared with normoxic group. Although not significant at the end of exposure period, decreased activity of this enzyme under hypoxic condition may reflect a general depression of metabolic activities that may affect both xenobiotic processing and protein synthesis (Lushchak et al. 2005). In contrast, significant increased GPx activity in blood plasma in the hyperoxic compared with normoxic and hypoxic groups indicates increased oxidative stress in this treatment group. It is possible that exposure to hyperoxia can stimulate ROS production which acts as upstream signaling molecules to enhance oxidative stress. Such a response has previously been reported in rats exposed to hyperoxia (Buccellato et al. 2004). In fish, a previous study with rainbow trout has also demonstrated an elevation of GPx activity following exposure to ozonized water. This also increased the level of lipid peroxidation indicating that these fish were subjected to oxidative stress (Ratola et al. 2002). The decreased GPx activity in blood plasma in hypoxic compared with normoxic and hyperoxic groups probably indicates that the activity of this enzyme was not sufficient to deal with oxidative stress arising under hypoxic condition.

For the Comet assay, significant increase for DNA strand breaks observed under hyperoxic condition is not surprising. Hyperoxic condition is known to elevate the production of ROS leading to oxidative stress (Lushchak and Bagnyukova 2006). In contrast, the observed increase for DNA damage under hypoxic condition compared to normoxic condition is more intricate to explain. Liepelt et al. (1995) reported that highest rates of DNA strand breaks in the gills occur when the rainbow trout were kept under hypoxic condition ($3.3 \text{ mg O}_2 \text{ l}^{-1}$; 5 h exposure) followed by a rapid increase of the oxygen concentration. It is however not clear why hypoxic condition could lead to oxidative damage. Given that under hypoxic, opposed to anoxic condition, some degree of molecular oxygen is still available, ROS level could increase due to reduction of mitochondrial electron transport chain and their subsequent leakage to residual oxygen molecules leading to oxidative stress (Dirmeier et al. 2002). It has also been speculated that under hypoxic condition, xanthine dehydrogenase can be converted into xanthine oxidase which produces ROS as

products (Lushchak and Bagnyukova 2007; Lushchak 2011). Under hypoxic condition, limited proteolysis or oxidation could lead to the production of efficient ROS generating metabolites (Lushchak 2011). In addition, hypoxia may result in inactivation of carriers of the electron transport chain and this process could increase the chance of electrons to 'escape' and reduce oxygen via one-electron mechanisms (Lushchak and Bagnyukova 2007). Furthermore, it has been suggested that repair of DNA strand breaks under hypoxic condition is less effective compared to normoxic condition (Modig et al. 1974). It could therefore be assumed that spontaneous DNA strand breaks could accumulate under chronic hypoxic condition as a result of inefficient DNA repair capability. Our results show that both hypoxic and hyperoxic conditions have considerable impact on the level of DNA strand breaks in fish erythrocytes. These results are consistent with previous studies where fish erythrocytes have been shown to be sensitive for measuring the genotoxic effects either in laboratory or in field studies (Belpaeme et al. 1998; Frenzilli et al. 2004; Theodorakis et al. 1994; Li et al. 2005; Jha 2004, 2008).

A significant increase in haemoglobin concentration in response to hypoxia compared with normoxic conditions (approximately 40%) is consistent with a number of studies in fish chronically exposed to hypoxic condition (Killifish: Greaney and Powers 1978; rainbow trout: Soivio et al. 1980). However, carp have not been shown to demonstrate significant increases when exposed in a similar way (Lykkeboe and Weber 1978; Jensen and Weber 1985). This suggests that increasing haemoglobin concentration possibly improves preserving oxygen delivery during hypoxic challenge by protecting oxygen diffusion gradient from blood to tissues. Besides, there was a steep increase for the haematocrit value which was significantly different (approx. 25%) relative to normoxic and hyperoxic conditions, resulting possibly from a significant increase in number of red blood cells. This response has been observed in many marine and freshwater fish species (Muusze et al. 1998; Smit and Hattinck 1978; Soldatov 1996). The increase in haemoglobin and haematocrit values were however not found to be closely linked (Hct 25% vs. Hb 40%). Both Hb and Hct values could be affected by a number of biological (e.g. age, sex etc.) factors influencing erythropoiesis and metabolic processes in addition to procedural factors employed to estimate the values accurately (Quintó et al. 2006). The processes responsible for the increased numbers of RBCs in hypoxic condition however are not clear. Perhaps, this increase is associated with both their release from blood storing organ (e.g. spleen) and the activation of the erythropoiesis in blood forming tissues concentrated in head kidney (Estebani et al. 1989). Both mammalian and fish studies have suggested that hypoxia

inducible factor 1 (HIF-1 α) is also responsible for activation of erythropoietin (EPO) gene transcription for enhancement of red blood cell production (Soitamo et al. 2001; Okino et al. 1998; Guillemín and Krasnow 1997). The overall effect of differential gene expression has been suggested to lead to a series of biochemical and physiological responses, allowing the organisms to survive under hypoxic conditions with a net decrease in metabolic rate and protein synthesis (Wu 2002).

For histopathological and ultrastructural studies, the high accumulation of lipid droplets observed in hypoxic liver cells has been suggested to be associated with increased elongation of fatty acid and inhibition of lipolysis (van den Thillart et al. 2002). Increased synthesis or decreased catabolism and mobilization of lipid could account for lipid accumulation during hypoxia. Reduction in molecular available oxygen is known to decrease the intensity of oxidative phosphorylation occurring in mitochondria. This could lead to reduction in the formation of adenosine triphosphate (ATP) which are needed for lipolysis (van Raaij et al. 1994). Our results are in line with previous study by Poon et al. (2007) who reported increased lipid content in the liver after 42 days exposure of common carp to hypoxia. Furthermore, ultrastructural study of flat fish (*Plathichthys flesus* L.) collected from highly contaminated sites with organochlorines and heavy metals have been shown to contain increased lipid droplet (Kohler 1990). For hyperoxic condition, liver didn't show

any significant histopathological changes, however, under the TEM, mitochondria were relatively larger in size and higher in number. This finding is consistent with observed increase in mitochondrial number per alveolar epithelial cells in hyperoxically exposed rat (Khazanov and Poborskii 1991). This confirms that increased number of mitochondria is a generalised response to oxidative stress.

The gills showed alterations in hypoxic conditions such as epithelial lifting, aneurysms, increased numbers of goblet cells, besides fusion of some secondary lamellae. These could possibly be examples of defense mechanisms. Similar histological changes in gills were common in a channel catfish, *Ictalurus punctatus*, exposed to sublethal hypoxic condition (Scott and Rogers 1980). The epithelial lifting have also been reported in gills of sea bass *Dicentrarchus labrax* exposed for 3 months to hypoxic and hyperoxic conditions (Rinaldia et al. 2005). These histological alterations are non specific and common to different environmental stresses and a range of contaminants (Mallatt 1985).

Our study confirms that mirror carp demonstrate high tolerance to long term hypoxia as no mortalities occurred over the exposure period. There was however significantly decreased SGR in fish exposed to hypoxic compared to normoxic condition. The lower SGR and growth reduction are accordance with previously reported investigations in other fish species showing a decline in growth and feed utilisation performance under a reduced oxygen or hypoxic

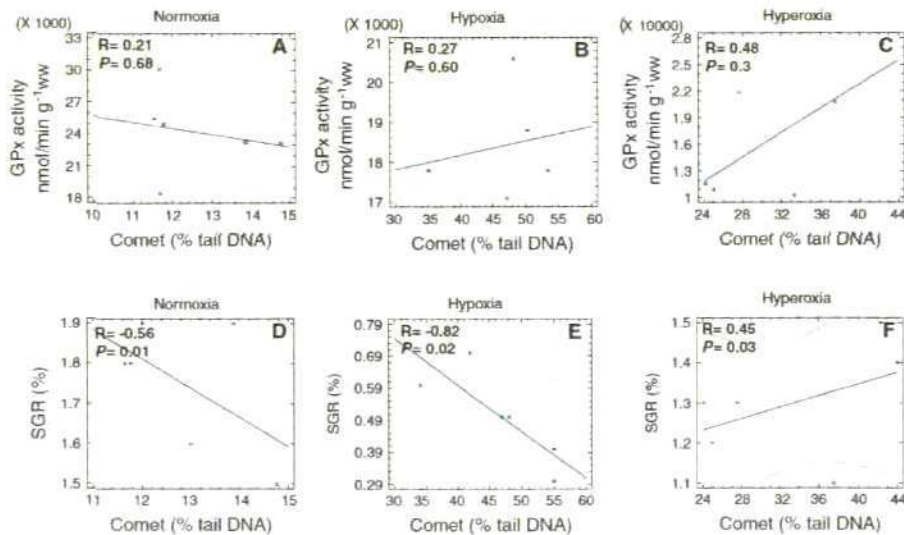


Fig. 5 Linear regression analysis illustrating correlations between the comet assay and the GPx activity (a c), correlations between the comet assay and the SGR (d f) in *C. carpio* following 30 days

exposure to normoxia, hypoxia and hyperoxia. The solid line is a linear regression and the dashed lines represent 95% confidence limits

environment (Chabot and Dutil 1999; Dabrowski et al. 2004; Thetmeyer et al. 1999). As mentioned earlier, this probably results as a consequence of down regulation of maintenance (basal) energy expenditure (Miller 2005), which could also affect voluntary food intake and consequent 'scope' for growth (Glencross 2009). In this context, correlation between oxygen consumption and protein synthesis in fish cell lines has also been reported (Smith and Houlihan 1995).

It is interesting to note that induction of oxidative DNA damage showed no correlation with GPx activities in liver under hyperoxic and hypoxic conditions in the present study (Fig. 5a-c). Furthermore, SGR showed a significant negative correlation with oxidative DNA damage under hypoxic compared to hyperoxic and normoxic conditions (Fig. 5d-f). Such chronic conditions in the natural environment or in aquaculture would have profound knock-on effects on the Darwinian fitness of the organism.

In conclusion, our study suggests that compared to normoxia, both chronic hypoxia and hyperoxia induce oxidative DNA damage, oxidised purines showing higher levels of damage compared to pyrimidines in a carp species. Hypoxia also induced a significant increase in most haematological parameters along with ultrastructural changes in both liver and gills. Different exposure conditions also affected the specific growth rates of the fish, which was observed to correlate with oxidative DNA damage. Given the increasing number of 'dead zones' in different parts of the world, we need to better comprehend the hypoxic conditions on the biota either alone or in combination with other contaminants and environmental stressors. Additionally, the intensive aquaculture or experimental rearing of new fish within recirculation systems with high aeration and varying sensitivity to ROS could influence production efficiency and biological responses which will also warrant further investigations for this globally expanding industry.

Acknowledgments SAM is funded by the Ministry of Higher Education and Scientific Research, Republic of Iraq. ANJ would like to acknowledge the support received from European Regional Development Fund, INTERREG IVA (Grant No. 4059). We are thankful to Professor Andrew Collins, University of Oslo, Norway, for providing bacterial enzymes used for the modified Comet assay. Thanks are also due to Mr. Peter Russell and Mr. Benjamin Eynon for technical assistance and to Mr. Glenn Harper for help in electron microscopic studies.

References

- Au DWT, Wu RSS, S ZB, Lam PKS (1999) Relationship between ultrastructural changes and EROD activities in liver of fish exposed to Benzo[a]pyrene. *Environ Pollut* 104:235-247
- Azqueta A, Shaposhnikov S, Collins AR (2009) DNA oxidation: investigating its key role in environmental mutagenesis with the comet assay. *Mutat Res* 674:101-108
- Belpaeme K, Cooreman K, Kirsch-Volders M (1998) Development and validation of the in vivo alkaline comet assay for detecting genomic damage in marine flatfish. *Mutat Res* 415:167-184
- Buccellato LJ, Tso M, Akinci OI, Chandel NS, Budinger GS (2004) Reactive oxygen species are required for hyperoxia-induced bax activation and cell death in alveolar epithelial cells. *J Biol Chem* 279:6753-6760
- Cacciatolo MA, Trinh L, Lumpkin JA, Rao G (1993) Hyperoxia induces DNA damage in mammalian cells. *Free Radic Biol Med* 14:267-276
- Camargo MMP, Martinez CBR (2007) Histopathology of gills, kidney and liver of a Neotropical fish caged in an urban stream. *Neotrop Ichthyol* 5:327-336
- Cech JJ, Mitchell SJ, Wragg TE (1984) Comparative growth of juvenile white sturgeon and striped bass: effects of temperature and hypoxia. *Estuaries Coasts* 7:12-18
- Chabot D, Dutil JD (1999) Reduced growth of Atlantic cod in non-lethal hypoxic conditions. *J Fish Biol* 55:472-491
- Dabrowski K, Lee KJ, Guz L, Verlhac V, Gabaudan J (2004) Effects of dietary ascorbic acid on oxygen stress (hypoxia or hyperoxia), growth and tissue vitamin concentrations in juvenile rainbow trout (*Oncorhynchus mykiss*). *Aquaculture* 233:383-392
- Diaz RJ, Rosenberg R (2008) Spreading dead zones and consequences for marine ecosystems. *Science* 32:926-929
- Dirmeyer R, O'Brien KM, Engle M, Dodd A, Spears E, Poyton RO (2002) Exposure of yeast cells to anoxia induces transient oxidative stress: implications for the induction of hypoxic genes. *J Biol Chem* 277:34773-34784
- Esteban MA, Meeguer J, Garcia AA, Agulleiro B (1989) Erythropoiesis and thrombopoiesis in the head-kidney of the sea bass (*Dicentrarchus labrax* L.), an ultrastructural study. *Arch Histol Cytol* 52:407-419
- Frenzilli G, Scarcelli V, Barga ID, Nigro M, Forlin L, Bolognesi C, Sturve J (2004) DNA damage in eelpout (*Zoarces viviparus*) from Göteborg harbour. *Mutat Res* 552:187-195
- Glencross BD (2009) Reduced water oxygen levels affect maximal feed intake, but not protein or energy utilization efficiency of rainbow trout (*Oncorhynchus mykiss*). *Aquac Nutr* 15:1-8
- Gozal E, Sachleben LR Jr, Rane MJ, Vega C, Gozal D (2005) Mild sustained and intermittent hypoxia induce apoptosis in PC-12 cells via different mechanisms. *Am J Physiol* 288:C535-C542
- Greaney SG, Powers AD (1978) Allosteric modifiers of fish hemoglobins: in vitro and in vivo studies of the effect of ambient oxygen and pH on erythrocyte ATP concentrations. *J Exp Zool* 203:339-349
- Guillemin K, Krasnow MA (1997) The hypoxic response: huffing and puffing. *Cell* 89:9-12
- Halliwell B, Gutteridge JMC (1999) Free radicals in biology and medicine. Clarendon Press; Oxford University Press, Oxford New York
- Handy H, Depledge MH (1999) Physiological responses: their measurement and use as environmental biomarkers in ecotoxicology. *Ecotoxicology* 8:329-349
- Jensen FB, Weber RE (1985) Kinetics of the acclimational responses of tench to combined hypoxia and hypercapnia. *J Comp Physiol B Biochem Syst Environ Physiol* 156:197-203
- Jha AN (2004) Genotoxicological studies in aquatic organisms: an overview. *Mutat Res* 552:1-17
- Jha AN (2008) Ecotoxicological applications and significance of the comet assay. *Mutagenesis* 23:207-221
- Khazanov VA, Poborski AN (1991) Respiration of rat brain mitochondria during hyperoxia and normoxia. *Bull Exp Biol Med* 112:1258-1261

- Köhler A (1990) Identification of contaminant induced cellular and subcellular lesions in the liver of flounder (*Platichthys flesus* L.) caught at differently polluted estuaries. *Aquat Toxicol* 16:271–293
- Kumaravel TS, Jha AN (2006) Reliable Comet assay measurements for detecting DNA damage induced by ionising radiation and chemicals. *Mutat Res* 605:7–16
- Li CS, Wu KY, Chang-Chien GP, Chou CC (2005) Analysis of oxidative DNA damage 8-hydroxy 2'-deoxyguanosine as a biomarker of exposures to persistent pollutants for marine mammals. *Environ Sci Tech* 39:2455–2460
- Liepert A, Karbe L, Westendorf J (1995) Induction of DNA strand breaks in rainbow trout *Oncorhynchus mykiss* under hypoxic and hyperoxic conditions. *Aquat Toxicol* 33:177–181
- Livingstone DR (2001) Contaminant-stimulated reactive oxygen species production and oxidative damage in aquatic organisms. *Mar Pollut Bull* 42:656–666
- Livingstone DR (2003) Oxidative stress in aquatic organisms in relation to pollution and aquaculture. *Revue Méd Vet* 154:427–430
- Lushchak VI (2011) Environmentally induced oxidative stress in aquatic animals. *Aquat Toxicol* 101:13–30
- Lushchak VI, Bagnyukova TV (2006) Effects of different environmental oxygen levels on free radical processes in fish. *Comp Biochem Physiol B Biochem Mol Biol* 144:283–289
- Lushchak VI, Bagnyukova TV (2007) Hypoxia induces oxidative stress in tissues of a goby, the rotan *Percottus glenii*. *Comp Biochem Physiol B Biochem Mol Biol* 148:390–397
- Lushchak VI, Lushchak LP, Mota AA, Hermes-Lima M (2001) Oxidative stress and antioxidant defenses in goldfish *Carassius auratus* during anoxia and reoxygenation. *Am J Physiol* 280:R1100–R1107
- Lushchak VI, Bagnyukova TV, Lushchak OV, Storey JM, Storey KB (2005) Hypoxia and recovery perturb free radical processes and antioxidant potential in common carp (*Cyprinus carpio*) tissues. *Int J Biochem Cell Biol* 37:1319–1330
- Lykkeboe G, Weber RE (1978) Changes in the respiratory properties of the blood in the carp, *Cyprinus carpio*, induced by diurnal variation in ambient oxygen tension. *J Comp Physiol B* 128:117–125
- Mallatt J (1985) Fish gill structural changes induced by toxicants and other irritants: a statistical review. *Can J Fish Aquat Sci* 42:630–648
- Martincovic D, Villeneuve DL, Kahl MD, Blake LS, Brodm JD, Ankley GT (2009) Hypoxia alters gene expression in the gonads of zebrafish (*Danio rerio*). *Aquat Toxicol* 95:258–272
- Miller AT (2005) The role of oxygen in metabolic regulation. *Helgoland Mar Res* 14:392–406
- Modig HG, Edgren M, Révész L (1974) Dual effect of oxygen on the induction and repair of single-strand breaks in the DNA of X-irradiated mammalian cells. *Int J Radiat Biol* 26:341–353
- Musze B, Marconi J, van den Thillart G, Almeida-Val V (1998) Hypoxia tolerance of Amazon fish: respirometry and energy metabolism of the cichlid *Astronotus Ocellatus*. *Comp Biochem Physiol A Mol Integr Physiol* 120:151–156
- Myers MS, Johnson LL, Hom T, Collier TK, Stein JE, Varanasi U (1998) Toxicopathic hepatic lesions in subadult English sole (*Pleuronectes vetulus*) from Puget Sound, Washington, USA: relationships with other biomarkers of contaminant exposure. *Mar Environ Res* 45:47–67
- Nikimaa M (2002) Oxygen-dependent cellular functions: why fishes and their aquatic environment are a prime choice of study. *Comp Biochem Physiol A Mol Integr Physiol* 133:1–16
- Okino ST, Chachester CH, Whitlock JP (1998) Hypoxia-inducible mammalian gene expression analyzed in vivo at aTATA driven promoter and at an initiator-driven promoter. *J Biol Chem* 273:23837–23843
- Poon WL, Hung CY, Nakano K, Randall DJ (2007) An in vivo study of common carp (*Cyprinus carpio* L.) liver during prolonged hypoxia. *Comp Biochem Physiol D* 2:295–302
- Quintó L, Aponso JJ, Menéndez C, Sacartal J, Aude P, Espasa M, Mandomando I, Guinovart C, Macete E, Hirt R, Urassa H, Navia MM, Thompson R, Alonso PL (2006) Relationship between haemoglobin and haematocrit in the definition of anaemia. *Trop Med Int Health* 11:1295–1302
- Reeves JF, Davies SJ, Dodd NJF, Jha AN (2008) Hydroxyl radicals (OH) are associated with titanium dioxide (TiO₂) nanoparticle-induced cytotoxicity and oxidative DNA damage in fish cells. *Mutat Res* 640:113–122
- Rinaldia L, Patrizia B, Tettamantia G, Grimaldia A, Terovaa G, Sarogliaa, Eguileor Md (2005) Oxygen availability causes morphological changes and a different VEGF/Flk-1/HIF-2 expression pattern in sea bass gills. *Ital J Zool* 72:103–111
- Ritola O, Livingstone DR, Peters LD, Lindström-seppä P (2002) Antioxidant processes are affected in juvenile rainbow trout (*Oncorhynchus mykiss*) exposed to ozone and oxygen-supersaturated water. *Aquaculture* 210:1–19
- Scott AL, Rogers WA (1980) Histological effects of prolonged sublethal hypoxia on channel catfish *Ictalurus punctatus* (Rafinesque). *J Fish Dis* 3:305–316
- Sevgi Kolaylı EK (1999) A comparative study of antioxidant enzyme activities in freshwater and seawater-adapted rainbow trout. *J Biochem Mol Toxicol* 13:334–337
- Singh NP, McCoy MT, Tice RR, Schneider EL (1988) A simple technique for quantitation of low levels of DNA damage in individual cells. *Exp Cell Res* 175:184–191
- Smith GL, Hatching J (1978) The effect of respiratory stress on carp haemoglobin. *Comp Biochem Physiol A* 59:369–374
- Smith RW, Houlihan DF (1995) Protein synthesis and oxygen consumption in fish cells. *J Comp Physiol B* 165:93–101
- Sotiano AJ, Rabergh CMI, Gassmann M, Sistonen L, Nikimaa M (2001) Characterization of a hypoxia-inducible factor (HIF-1 α) from rainbow trout. Accumulation of protein occurs at normal venous oxygen tension. *J Biol Chem* 276:19699–19705
- Soivio A, Nikimaa M, Westman K (1980) The blood oxygen binding properties of hypoxic *Salmo gairdneri*. *J Comp Physiol B* 136:83–87
- Soldatov AA (1996) The effect of hypoxia on red blood cells of flounder: a morphologic and autoradiographic study. *J Fish Biol* 48:321–328
- Theodorakis CW, D'Surney SJ, Shugart LR (1994) Detection of genotoxic insult as DNA strand breaks in fish blood cells by agarose gel electrophoresis. *Environ Toxicol Chem* 13:1023–1031
- Thetmeyer H, Waffer U, Black KD, Insefmann S, Rosenthal H (1999) Growth of European sea bass (*Dicentrarchus labrax* L.) under hypoxic and oscillating oxygen conditions. *Aquaculture* 174:355–367
- Thomas P, Rahman MS (2010) Region-wide impairment of Atlantic croaker testicular development and sperm production in the northern Gulf of Mexico hypoxic dead zone. *Mar Environ Res* 69:S59–S62
- Valavandis A, Vlahogiann T, Dassenakis M, Scoullas M (2006) Molecular biomarkers of oxidative stress in aquatic organisms in relation to toxic environmental pollutants. *Ecotoxicol Environ Saf* 64:178–189
- van den Thillart G, van Waarde A (1985) Teleosts in hypoxia: aspects of anaerobic metabolism. *Mol Physiol* 8:393–409
- van den Thillart G, Vrienen G, Zaagsma J (2002) Adrenergic regulation of lipid mobilization in fishes: a possible role in hypoxia survival. *Fish Physiol Biochem* 27:189–204
- van Raaij MTM, Breukel BJ, van den Thillart JM, Addink ADF (1994) Lipid metabolism of goldfish, (*Carassius auratus* L.)

- during normoxia and anoxia: Indications for fatty acid chain elongation. *Comp Biochem Physiol B Biochem Mol Biol* 107:75-84
- Wedemeyer GA (1997) Effects of rearing conditions on the health and physiological quality of fish in intensive culture. In: Dwana GK, Pickering AD, Sumpter JP, Schreck CB (eds) *Fish stress and health in aquaculture*. Cambridge University Press, Cambridge, pp 35-71
- Wu RSS (2002) Hypoxia: from molecular responses to ecosystem responses. *Mar Pollut Bull* 45:35-45

Appendix II

Poster presentation

The level of glutathione in the cell-free haemolymph of the blue mussel, *Mytilus edulis*

A. John Moody, Sherain Al-Subial and Awadhesh Jha

Ecotoxicology and Stress Biology Research Centre, School of Biological Sciences, University of Plymouth

Introduction

In rats oxidative stress induced by exposure to reactive oxygen species (ROS) (e.g. hydroxyl hydroperoxide), or ROS generators (e.g. diesel) causes an increase in plasma glutathione levels through excretion of oxidized glutathione by the liver (Adams *et al.*, 1993). In contrast acetaminophen or diethyl maleate, which cause oxidative stress by depletion of hepatic glutathione, cause a decrease in plasma glutathione. We have investigated whether, in *Mytilus edulis*, glutathione in the cell-free component of the haemolymph could be used in an analogous way as an indication of 'global' oxidative stress in this organism.

Materials & Methods

Mussels (*Mytilus edulis*) of similar shell length (51–58 mm) were collected from the Port Cuan, North Cornwall, a reference site. After collection they were immediately transported to the laboratory (<2 h), and placed in highly aerated tanks with filtered sea water (1.5 animals/l) at 15 °C. They were fed daily with a suspension of microalgae (*Isocrysis galbana*, Lipidify, Ipswich, Dorset, UK), and allowed to acclimatise for at least 3 days before use in experiments.

Extraction of haemolymph

Haemolymph was extracted from the mussels via the posterior adductor muscle. To access the adductor muscle the valves were pried apart approximately midway towards the posterior from the byssus. A 1 ml hypodermic syringe fitted with a 21 gauge needle was used to withdraw the haemolymph (Figure 1). The needle was then removed and the haemolymph gently expelled into an Eppendorf tube. Haemocytes were then removed by centrifugation (1 min at 13,000–15,000 g), the cell-free fraction was stored on ice or at -20 °C until use.

Measurement of total glutathione in cell-free haemolymph

Total glutathione was measured essentially as described by Owens & Belcher (1985).

Measurement of lysine dehydrogenase activity in cell-free haemolymph

Lysine dehydrogenase activity (Figure 2) was measured essentially according to the Sigma-Aldrich protocol for aspartate dehydrogenase (Gade & Grieshaber, 1975) except that the assay pH was 7.5 rather than 8.0 (to increase the background rate of autooxidation of NADH) and the L-lysine was replaced with L-lysine.

Exposure of mussels to hydrogen peroxide

For exposure to H₂O₂, mussels were maintained in well-aerated seawater in 2 l glass beakers (3 per beaker). The exposure was carried out in triplicate for 6 h, using a nominal concentration of 17.6 µM (i.e. 4 µl of 30% (w/v) H₂O₂ was added to each beaker). However, an experiment, the concentration of H₂O₂ rapidly decreased (0% to 10% Figure 5), and a further 4 µl of 30% H₂O₂ was added at 3 h to replenish it. Controls were also carried out in triplicate: in these distilled water was added in place of H₂O₂.

Measurement of hydrogen peroxide concentrations in sea water

Hydrogen peroxide was measured using a modification of horvonnic acid-haematein peroxidase (HAAHRP) fluorescent method of Starik & Nehl (1999). Figure 6 shows a calibration using this system.



Figure 1 extraction of haemolymph from the posterior adductor muscle. Mussels were held with the posterior upwards to allow sealer to drain away.

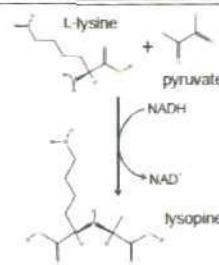


Figure 2: the reaction catalysed by lysine dehydrogenase.

Other dehydrogenases, which catalyse NADPH-dependent reductive decarboxylation of various amino acids to pyruvate have a similar role to that of α - and γ -lactate dehydrogenase (Gade & Grieshaber, 1975). There is little LDH activity in *Mytilus* adductor muscle.

References

- Adams JD, Lauterburg BH and Mitchell JR (1993) Plasma glutathione and glutathione disulfide in the rat: regulation and response to oxidative stress. *J Pharmacol Exp Ther* 277, 749–754.
- Gade G and Grieshaber M (1975) A rapid and specific enzymatic method for the estimation of L-lysine. *Anal Biochem* 68, 363–369.
- Gade G and Grieshaber M (1986) Pyruvate reductases catalyze the formation of lactate and pyruvate in aerobic invertebrates. *Comp Biochem Physiol* 83B, 255–272.
- Owens CW and Belcher RW (1985) A colorimetric micro-method for the determination of glutathione. *Biochem J* 24, 703–711.
- Starik K and Nehl H (1999) H₂O₂ detector from intact mitochondria as a measure for one-electron reduction of oxygen requires a non-invasive assay system. *Biochim Biophys Acta* 1413, 70–80.

Results

Glutathione was detectable in the cell-free component of samples of haemolymph extracted via the posterior adductor muscle. However, the values obtained were extremely variable (3.2 ± 1.8 µM; mean ± S.D., n = 28).

To test whether this variability was in part due to variable contamination by intracellular glutathione during haemolymph extraction, we measured NAD-dependent D-lysine dehydrogenase (LyDH; EC 1.5.1.18) activity in the same samples. The assumption is that LyDH is an exclusively intracellular enzyme in this organism.

There was a significant (P < 0.0001) linear correlation (Figure 3) (slope = 0.0280 ± 0.0028 µM/nmol min⁻¹ ml⁻¹; ± S.E.) between glutathione levels and LyDH activity, indicating that much of the supposed haemolymph glutathione was artefactual.

Extrapolation to zero LyDH activity gave a basal value for cell-free haemolymph glutathione (0.74 ± 0.29 µM; ± S.E.) which though low is significantly greater than zero (P = 0.0169).

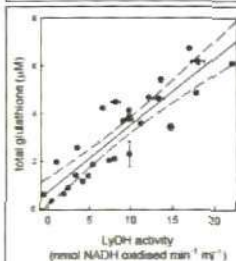


Figure 3 correlation between the glutathione content of cell-free haemolymph and lysine dehydrogenase activity.

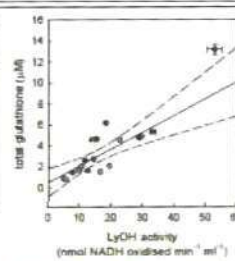


Figure 4 effect of H₂O₂ exposure on the glutathione content of cell-free haemolymph.

After exposure of mussels normally to 17.6 µM H₂O₂ (see Materials & Methods and Figure 5) both glutathione and LyDH activity were measured. Haemolymph samples were taken and both in 20 different samples of cell-free haemolymph glutathione and LyDH activity measured (● control, ○ H₂O₂). The dashed lines represent 95% confidence limits. The solid line is a linear regression (95% confidence limits). The error bars indicate the variability of the measurements (± S.E., n = 3).

Exposure of mussels to hydrogen peroxide (17.6 µM nominal concentration, see Materials & Methods and Figure 5) for six hours did not significantly change the level of cell-free haemolymph glutathione (GLM with LyDH activity as a quantitative factor and H₂O₂ exposure as a categorical factor; P = 0.746, n = 9).

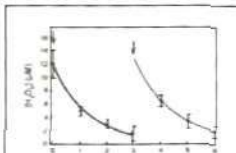


Figure 5 concentrations of H₂O₂ in the seawater during the exposure of the mussels.

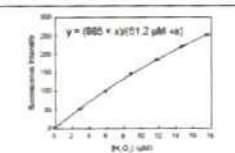


Figure 6 calibration of the HAAHRP H₂O₂ determination method.

Seawater (5 ml) was mixed with 2.5 (µM) HRP in 50 mM potassium phosphate, pH 7.5, containing 1 mM potassium EDTA. HAAHRP (50 µl of 10 mM) was then added. Three millilitres of the mixture was transferred to a cuvette and H₂O₂ (0.36 mM stock) was added. The fluorescence intensity was measured when it had stabilised after each addition (λ_{exc} = 312 nm, λ_{em} = 420 nm).

Conclusion

It is clear that care must be taken when measuring biochemical parameters associated with cell-free haemolymph from *M. edulis* either to avoid contamination by intracellular material or to allow for it by simultaneously measuring an intracellular marker such as LyDH activity.



Contamination of bivalve haemolymph samples by adductor muscle components: implications for biomarker studies

Sherain Al-Subial, Awadhesh N. Jha and A. John Moody

Ecotoxicology and Stress Biology Research Centre, School of Biological Sciences,
University of Plymouth, Plymouth, PL4 8AA, UK



Introduction

- Haemolymph samples from bivalve molluscs extensively used in ecotoxicological studies
- Withdrawal of haemolymph via the posterior adductor muscle, may lead to contamination with the intracellular contents of adductor myocytes
- Lysine dehydrogenase (LyDH) activity, an adductor myocyte marker used to investigate the impact of this potential contamination on levels of total glutathione, glutathione peroxidase (GPx) and acetylcholinesterase (AChE) measured in cell-free haemolymph

Materials & Methods

- Mussels (*Mytilus edulis*) collected from reference site and allowed to acclimatize for at least one week
- Measurement of total glutathione content, lysine dehydrogenase, glutathione peroxidase and acetylcholinesterase activities
- Haemolymph extracted from the mussels via the posterior adductor muscle with the help of syringe (1 ml) and needle (21 gauge)
- Haemocytes removed by centrifugation
- Cell-free fraction either placed on ice until use, for lysine dehydrogenase and glutathione peroxidase measurements, or stored at -80°C for total glutathione and acetylcholinesterase measurements
- Total glutathione content measured essentially as described by Owens & Belcher (1965)
- Lysine dehydrogenase activity measured as per the Sigma-Aldrich protocol for opine dehydrogenase (Gaede & Grieshaber, 1975) except that the assay pH was 7.5 rather than 6.5 and the L-arginine was replaced with L-lysine
- Glutathione peroxidase measured as described by Tran *et al.* (2007)
- Acetylcholinesterase determined according to Galloway *et al.* (2002)

Results

- Glutathione values obtained were extremely variable; $3.2 \pm 1.8 \mu\text{M}$, (mean \pm S.D., $n = 28$)
- To test whether this variability in part due to variable contamination by intracellular glutathione during haemolymph extraction, NAD-dependent D-lysine dehydrogenase activity measured in the same samples (LyDH is an exclusively intracellular enzyme in this organism)
- A significant ($P < 0.0001$) linear correlation (Fig. 1) between glutathione levels and LyDH activity, indicating that much of the supposed haemolymph glutathione artefactual
- GPx showed a significant linear relationship ($P = 0.025$) with LyDH levels consistent with both enzymes originating from the myocytes (Fig. 2A). This is further demonstrated in Fig. 2B where the GPx and LyDH data are plotted against the protein content
- AChE and LyDH activities showed a hyperbolic relationship (Fig. 3A), a significant ($P = 0.136$) non-linear relationship found between AChE and protein (Fig. 3B). It appears that AChE originates from a different compartment

Conclusion

- Using a biomarker in cell-free haemolymph, it may be prudent to check whether contamination could be an issue (e.g. by looking for a correlation with a myocyte marker such as opine dehydrogenase activity)
- Adductor muscle may be a more generally useful tissue in which to determine biomarker responses (e.g. in the glutathione/glutathione peroxidase system)

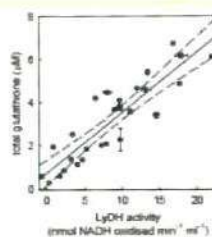


Figure 1: relationship between the glutathione content of cell-free haemolymph and lysine dehydrogenase activity

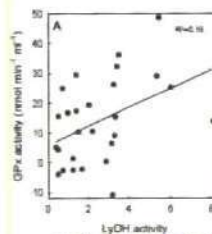


Figure 2A: relationship between the GPx activity and LyDH activity

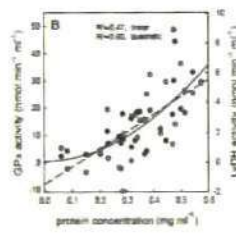


Figure 2B: relationships between the GPx activity, LyDH activity and protein content of cell-free haemolymph

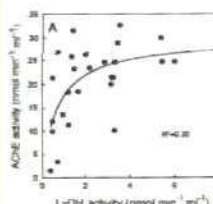


Figure 3A: relationship between the AChE activity and LyDH activity

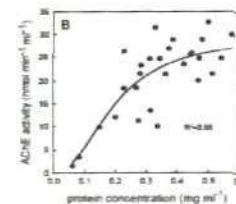


Figure 3B: relationship between the AChE activity and the protein content

References

- Gaede G and Grieshaber M (1975) A rapid and specific enzymatic method for the estimation of L-arginine. *Anal. Biochem.* 66, 393-399.
- Galloway TS, Millard N, Broome MA, Depledge MH (2002) Rapid assessment of organophosphorus/carbamate exposure in the bivalve mollusc *Mytilus edulis* using contained esterase activities as biomarkers. *Aquat. Toxicol.* 61, 169-180.
- Owens CW and Belcher RV (1965) A colorimetric micro-method for the determination of glutathione. *Biochem. J.* 94, 705-711.
- Tran D, Moody AJ, Fisher AS, Foulkes ME, Jha AN (2007) Protective effects of selenium on mercury-induced DNA damage in mussel haemocytes. *Aquat. Toxicol.* 84, 11-18.

Photo-induced toxicity of aged C₆₀ fullerenes in a marine invertebrate model

Al-Subiai SN¹, Kadar E², Readman J², Moody JA¹ and Jha AN¹

¹School of Biological Sciences, University of Plymouth, Plymouth, UK, PL4 8AA
²Plymouth Marine Laboratory, Plymouth, UK, PL1 3DH



PML Plymouth Marine Laboratory



Background

- Growing concerns over the potential detrimental impact of engineered nanoparticles (ENPs) on the human and environmental health; little known about their fate and behaviour in the environment¹
- Several recent reports have described their toxicity, none have reported the potential toxicity resulting from photochemical transformation of C₆₀ fullerenes (C₆₀) in aquatic organisms

Aims & objectives

- To study the genotoxic effects following *in vitro* exposure of *M. edulis* sperm to fresh C₆₀ (FC₆₀) and aged C₆₀ (AC₆₀), and the developmental consequences at early life stages
- To study the biological responses of adult mussels to the *in vivo* exposure of FC₆₀ and AC₆₀ to better understand the adverse effects of potentially degraded C₆₀ particles

Experimental design & methodologies

- The stock suspension of 1.0 mg l⁻¹ C₆₀ in sea water ultrasonicated for 2h, and then exposed to natural sunlight for 30 days at room temperature, Fig. 1
- Spawning induced by injected posterior adductor muscle with 1 ml of 0.50 M KCl combined with heat shock²
- Sperm collected and exposed for 2h and fertilisation was conducted in 1:10⁴ ratio, Fig. 2A
- Adult mussels were exposed *in vivo* to aged sea water (ASW), FC₆₀ and AC₆₀, and two exposure periods were considered: (a) 3 days exposure and (b) 3 days post-exposure, Fig. 2B



Fig 1 C₆₀ suspensions (1.0 mg l⁻¹) in sea water at concentration (A) FC₆₀ & (B) AC₆₀

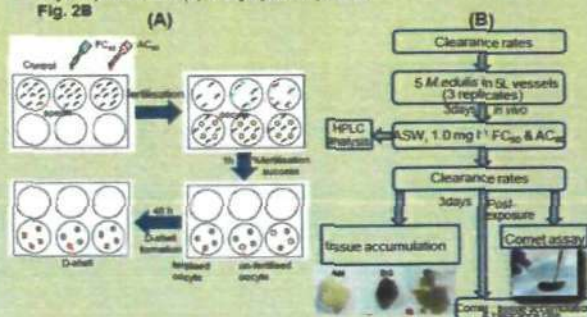


Fig 2 Experimental design (A) *in vitro* (B) *in vivo* for exposure condition. AM= adductor muscle, DG= digestive gland, Gr= gills

Results

Table 1 C₆₀ characterisation measurements performed with FC₆₀ and AC₆₀ using multi-methods³. Values are mean ± S.E, n = 3.

Particles characterisation	Method	Fresh C ₆₀	Aged C ₆₀
Z-average diameter (nm)	DLS	675.37 ± 19.06	911.8 ± 98.68
Polydispersity	DLS	0.57 ± 0.018	0.667 ± 0.06
Zeta potential	Zeta-sizer	-12.73 ± 1.18	-8.832 ± 0.90
Mean particle size (nm)	AFM	121.9 ± 6.13	18.80 ± 1.29

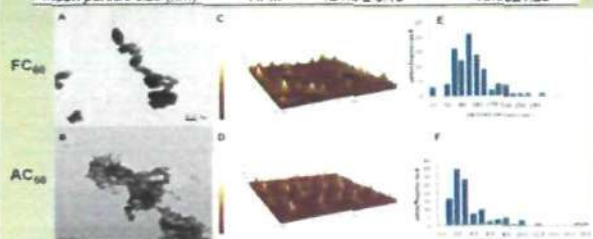


Fig 3 Characterisation of FC₆₀ versus AC₆₀ particles (A & B) TEM; (C & D) 3-D AFM image; (E & F) particles size-distribution.

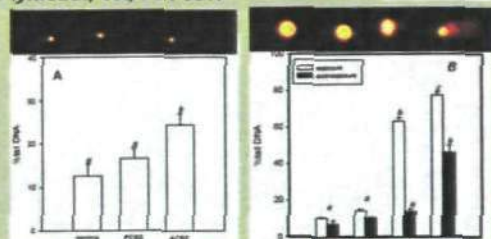


Fig 4 DNA single strand break in *M. edulis* following *in vitro* and *in vivo* exposures: (A) sperm; (B) haemocytocytes. Values are mean ± S.E, n = 3. Bars with the same letters are not significantly different according to the multiple range test (LSD).

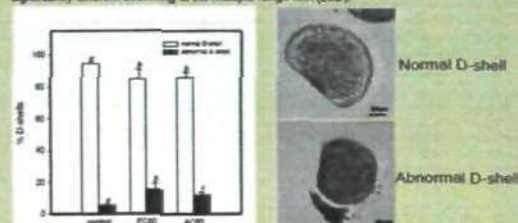


Fig 5 Percentages of normal D-shell stage larvae after 48h fertilisation. Values are mean ± S.E, n = 3, bars with the same letters are not significantly different according to the multiple range test (LSD).

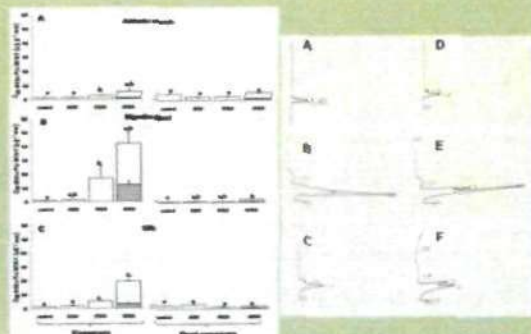


Fig 6 C₆₀ accumulation pattern in *M. edulis* tissues as analysed by HPLC. Values are mean ± S.E, n = 3, bars with the same letters are not significantly different according to the multiple range test (LSD). HPLC chromatogram results (A-C) FC₆₀, (D-F) AC₆₀

Conclusion

- *In vitro* exposure to sperm and *in vivo* exposure of adult *M. edulis* to AC₆₀ impaired development in the early life stages and enhanced toxicological injury in adult stage
- Evidence for the instability of photochemically transformed C₆₀ under environmental relevant condition and toxicity of AC₆₀ at different life stages of *M. edulis*
- Additional toxicological assessments (isolation, identification and characterisation) of the breakdown products of AC₆₀ needed to develop a more conclusive understanding of the toxic mechanism

References

- USEPA. 2010. New nano-specific regulations forthcoming from U.S.EPA, USA.
- ASTM. 1997. Standard guide for conducting bioconcentration tests with fishes and saltwater bivalve molluscs E-1022-94. Philadelphia, PA: American Society for Testing of Materials.
- Domingos et al. 2009. Characterizing manufactured nanoparticles in the environment: multimethod determination of particle sizes, Environmental Science & Technology 43: 7277-7284

Dead zones, hypoxia and fish health: an integrated study to determine impact of oxidative stress in fish



Sanaa A. Mustafa, Sherain N. Al-Subiai, Simon J. Davies and Awadhesh N. Jha

School of Biological Sciences, University of Plymouth, Plymouth, PL4 8AA

Background

- ❖ Oxidative stress may lead to pathophysiological conditions and could severely affect health and fitness of humans and natural organisms¹
- ❖ Hypoxia and hyperoxia are potential environmental stressors in the aquatic environment, particularly in intensive aquaculture²
- ❖ No scientific studies have evaluated the impact of different levels of oxygen concurrently at different levels of biological organisation

Aims & objectives

- ❖ Investigate the effects of chronic hypoxia and hyperoxia on a model fish species, *Cyprinus carpio* (mirror carp) at different levels of biological organisation (viz. biochemical, DNA and tissue levels)
- ❖ Compare the degree of biological responses under different exposure conditions
- ❖ Link and correlate the responses with 'fitness' and growth of carp

Experimental design & methodologies

- ❖ 36 carp (118 ± 2.4 g) distributed and acclimatised in 6 tanks in duplicate (i.e. 6 fish tank⁻¹ in duplicate)
- ❖ Fish exposed to three oxygen levels: 7.1 ± 0.4 mg l⁻¹ (normoxia); 1.8 ± 0.1 mg l⁻¹ (hypoxia- by lowering the dissolved oxygen level using nitrogen gas; purity 99.99%), and 12.3 ± 0.2 mg l⁻¹ (hyperoxia- by oxygen enrichment; purity 99.95%) for 30 days (Figure. 1)
- ❖ Following 30 days exposure period:
 - Blood samples collected to study the induction of DNA strand breaks applying modified comet assay using two bacterial enzymes: Formamidopyrimidine DNA glycosylase (FPG) and Endonuclease III (Endo III) to determine oxidative DNA damage in the erythrocytes³
 - Glutathione peroxidase (GPx), an anti-oxidative enzyme activity measured in liver and plasma²
 - Ultrastructural changes in the tissues (e.g. liver, gill) using TEM⁴



Figure 1. Experimental setup

Results

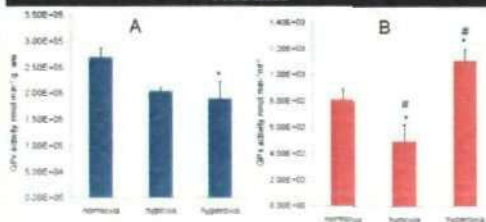


Figure 2. Activity of GPx (A) in liver (B) in plasma, following 30 days of exposure to normoxia, hypoxia and hyperoxia. Values are mean ± S.E. (*) significant differences from normoxic group (K) indicates significant differences between groups.

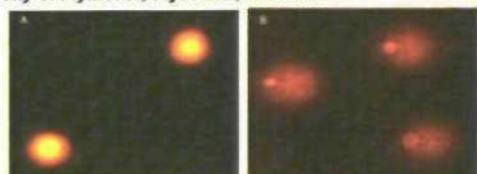


Figure 3. Comet response in erythrocytes of carp: (A) normal cell (B) damaged cell.

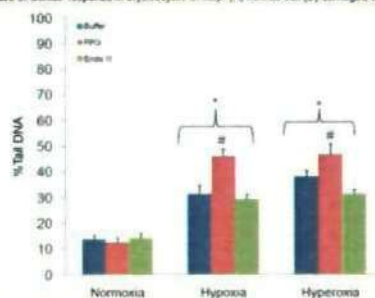


Figure 4. DNA single strand break in mirror carp erythrocytes following 30 days exposure to normoxia, hypoxia and hyperoxia. Values are mean ± S.E. n = 5. (*) statistically significant different versus normoxia, (K) statistically significant different versus buffer and EndoIII.

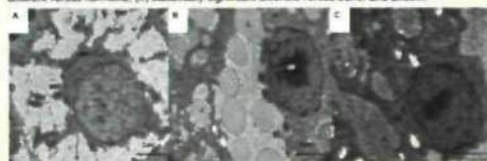


Figure 5. Transmission electron microscopy (TEM) images of liver: (A) normoxic: nucleus (n), mitochondria (mt), rough endoplasmic reticulum (rer) (B) hypoxic: increased number of lipid droplets (L) and condensed chromatin (ct) (C) hyperoxic: large and increased number of mitochondria and condensed chromatin.

Conclusions

- ❖ Compared to normoxia, both hypoxia and hyperoxia induced DNA damage; oxidised purines showing higher levels of damage compared to pyrimidines; no significant difference observed between oxidised pyrimidine and controls for hypoxic and hyperoxic conditions
- ❖ GPx activity significantly decreased in the hyperoxic liver compared to the normoxic conditions; in the plasma compared to controls, the levels decreased in hypoxic conditions and increased in hyperoxic condition, indicating some compensatory response mechanism
- ❖ TEM studies revealed ultrastructural changes in different tissues (i.e. liver and gill)
- ❖ Different exposure conditions also affected the specific growth rate (SGR) of the fish

References

- Barker GF *et al* (2006) *Am J Respiratory Cell and Molec Biol* 35, 277-288.
- Lushchak V & Bagryukova TV (2006) *Comp Biochem and Physiol Part B* 144, 283-289.
- Frenzel G *et al* (2004) *Mutation Res* 552, 187-195.
- Au DWT *et al* (1999) *Environ Pollut* 104, 235-247.